MODELING OF HIGH SOLID FLUX CIRCULATING FLUIDIZED BED REACTORS

A

THESIS SUBMITTED

TO THE

UNIVERSITY OF MUMBAI

FOR THE

Ph. D. (TECH.) DEGREE

IN

CHEMICAL ENGINEERING

SUBMITTED BY

NAREN P. R.

UNDER THE GUIDANCE OF

PROFESSOR ARVIND M. LALI

INSTITUTE OF CHEMICAL TECHNOLOGY,

MATUNGA, MUMBAI-400 019.

NOVEMBER 2009

STATEMENT TO BE INCORPORATED BY THE CANDIDATE IN THE THESIS AS REQUIRED UNDER ORDINANCE O.770 FOR THE Ph.D. DEGREE

STATEMENT BY THE CANDIDATE

As required by the University Ordinance O.770, I wish to state that the work embodied in this thesis titled "**MODELING OF HIGH SOLID FLUX CIRCULATING FLUIDIZED BED REACTORS**" forms my own contribution to the research work carried out under the guidance of **Professor Arvind M. Lali** at the Institute of Chemical Technology. This work has not been submitted for any other degree of this or other university. Wherever references have been made to previous work of other, it has been clearly indicated as such and included in the bibliography.

P. R. Naren

Naren, P.R.
(Research Scholar)

Certified by

Professor Arvind M. Lali
Research Supervisor,
Department of Chemical Engineering,
Institute of Chemical Technology
Mumbai 400 019

Date: 25th Nov 2009
Place: Mumbai.

CERTIFICATE

The research work described in this thesis has been carried out by Naren, P.R. under my supervision. I certify that this is his bonafide work. The work described is original and has not been submitted for any other degree of this or any other university. Further that he was a regular student and has worked under my guidance as a full time student at Institute of Chemical Technology until the submission of the thesis to the University of Mumbai.

Professor Arvind M. Lali
(Research Supervisor)

Date: 25th Nov 2009
Place: Mumbai.

"Entia non sunt multiplicanda praeter necessitatem" that translates to "Entities must not be multiplied beyond necessity"

- **William of Ockham**

Acknowledgement

Acknowledgement – The most difficult job in research documentation

In expressing my intangible gratitude to two iconic research supervisors – Prof. Arvind M. Lali (AML) of Institute of Chemical Technology (ICT) and Dr. Vivek V. Ranade (VVR) of National Chemical Laboratory (NCL) in tangible words, I realize the full meaning of the couplet of Sant Kabir:

सब धरती कारज करूँ, लेखनी सब बनराय ।
सात समुद्र की मसि करूँ गुरुगुन लिखा न जाय ॥

I thank AML for the freedom and faith that he bestowed onto me in these 4+ years of Phd career at ICT. He has taken every sincere efforts and pains to make this journey of mine enjoyable at ICT. This made me to concentrate on to my research problem with full zeal.

I thank VVR – for without his noble touch and guidance, the research work wouldn't have taken the shape of a dissertation thesis. He bestowed sound technical knowledge and imparted all requisite skills to handle the research facility. His mind is like a parachute, it's always open for discussion of all sorts and he has practical solutions to all problems that I confronted with.

I owe due credit to all my teachers and departmental fraternity at ICT and at NCL, for providing me with this excellent research opportunity. I sincerely thank Council of Scientific and Industrial research (CSIR), India, for the financial support received through GATE-JRF-SRF research fellowship program.

My lab mates and colleagues at AML's Lab – DAE Center, ICT, iFMG and at NCL have been a good source of energy all through this period. My labmates at ICT have never turned down any request of mine and have always been helpful in processing all papers that I pass onto them and would get things done on my behalf from ICT. I take this golden opportunity to thank them all – the list goes like: Abijar, Amit Naik, Amol Mahulkar, Amritraj, Annamma, Anoop, Anupama, Archana, Aruna, Bidisha, Chaitali, Deepak, Dillip Rana, Ganesh, Jagdish, Kishore, Manish, Mahendra, Monica, Nilesh, Pooja, Pratap, Pravin, Rashmi, Sagar, Sameer, Sandeep, Sohel, Umesh, Vinod, Yogesh, Yogesh Misra and its incomplete as well. Apart from my own lab mates, the stay at ICT is made pleasant by the good association that I enjoyed with many other friends - Amit Mahulkar, Amit Sharma, Ankit, Arijit, Chellani, Jothir, Kumaresan, Mayur Sathe, Piyush, Prashanth Sakharkhar, Sachin Jangam, Sachin Mathpathi, Suresh etc. and are worth mentioning here.

A whole lot of things are learnt from being amongst my iFMg fraternity. I sincerely thank each one of this iFMg family – Aditi, Ajay, Ajith Joshi, Akshay, Amey, Amit Chaudhari, Amit Kanashetti, Amol, Anil, Ashish, Avinash, Bharath, Chaitanya, Chandrasekhar, Dev, Ganesh, Kaustubh, Latif, Madhavi, Manish, Manoj Bagade, Mohan, Mukesh, Munshi, Nayana, Nitin, Parag, Pawan, Prashanth Gunjal, Prashanth Durge, Rahul Kharat, Rahul

Rayaprolu, Ranjeet, Ravi, Sampada, Sarita, Sanjesh, Sashi, Vikranth, Vishwanath, Yogesh etc., for their support, guidance and assistance rendered in all situations through these 4+ years. My iFMg and NCL days would always be adorned with the rich acquaintance and moments I shared with all these people.

I also take this chance to mention the support received from my BTech friends – Aarthi, Antony, Mahendran, Mani, MK, Murali, Santhosh and Sivakumar.

During this tenure, I also got good opportunity to interact with other research groups and like minded people like Prof. Shantanu Roy of IITD, Dr. Pant from BARC, Prof. Datta Dandge of MIT, Pune, Dr. Sanjay Danao of AISSMS, Pune, Dr. Savithri of NIIST, Trivandrum. I thank them for their valuable interactions and the interest they showed in this work.

Outcome of PhD research also needs good rapport from the technical and administrative support system. I am fortunate to have good support staff from ICT and NCL. Specifically, I thank Mr. Subash Wanjale for setting up the cold flow CFB setup at NCL and Mr. Hasmukh Raheja for providing the necessary support from departmental office.

My aunt's family (Amba athai, Athimbair, Paati & Prasad) and Shri Krishnan mama's family (esp. Mami) needs special mention. They provided homely atmosphere in the absence of my Amma – Appa and I am like their own son in all its true sense. Their home is like my extended Chennai home, where I go and relax freely without any second thoughts.

Needless to mention, my family comprising right from Amma, Appa, Patiamma, Chitappas and Chithis, Vidya, Chuchi, Parchu and Sanju, who are all part and parcel of me, kept me going and glowing and provided the best support one can think of from home. This work is a miniscule offering to the boundless love they shower on me.

I wish to end this acknowledgement note on a noble saying from Rig ved:

May powers auspicious come to us from every side, never deceived, unhindered, and victorious, (1.89.1)

And I realize this with all noble people around me and good guidance I received from my research guides – VVR and AML.

Table of Contents

List of Figures

List of Tables

CHAPTER 1

INTRODUCTION

The chapter briefly discusses salient features and applications of circulating fluidized bed riser reactors. Subsequently, the motivation for taking up the research work is presented. The objectives identified for the work are then discussed. Thesis organization based on the adopted methodology is presented at the end of the chapter.

1.1. INTRODUCTION

Circulating fluidized bed (CFB) refers to the state of gas solid fluidization system wherein the solids are entrained out of the system by the flowing gas. The gas velocities in CFB are far greater than particle terminal settling velocity. The solid flow into the system, in principle must be maintained externally to counterbalance the entrainment out of the system. Typical circulating fluidized bed rector consists of four principal components – riser, cyclone separator, downcomer and solid flow control device (Figure 1.1). Gas is introduced at the bottom section of the riser and carries with it the solids fed from the down comer through the flow control device. CFBs are also operated in down flow mode of operation (Cheng *et al.*, 2008; Wu *et al.*, 2007). This work is devoted to the up flow mode of CFB reactors owing to its commercial relevance in process industries. The solids flowing along the gas gets separated at the cyclone separators and solids are collected into the downcomer. Downcomer serve as solid storage device and also provides the necessary head to main the pressure balance for steady operation of CFB system. The solid control device can either be a mechanical seal or a non mechanical loop seal like L valve, J valve. The function of solid loop seal is to prevent the backflow of fluidizing gas into the downcomer and to independently control the solid circulation rate into the CFB system. The inlet and exit configuration of the CFB system also affect the prevailing flow structure in the CFB system. CFB systems operate under fast fluidization regime to dense conveying regime with both superficial gas velocity and solid circulation being the control parameters.

1.1.1. Applications

Circulating fluidized bed applications may be broadly grouped into low density and high density circulating fluidized bed processes (Zhu and Bi, 1995). Well known commercial applications include fluid catalytic cracking (FCC) process, Synthol reactor for Fischer Tropsch synthesis (Contractor and Chaouki, 1991) and calcination of aluminum trihydrate to high purity alumina (Reh, 1986). Industrial processes involving CFB reactor as key element are well documented in literature (Koornneef, 2007; Berruti *et al.*, 1995; Zhu and Bi, 1995; Reh, 1986). Various new technologies are being developed based on circulating fluidized beds such as chemical looping combustion, CO_2 absorption by lime, methanol to olefins, hot gas cleaning, direct

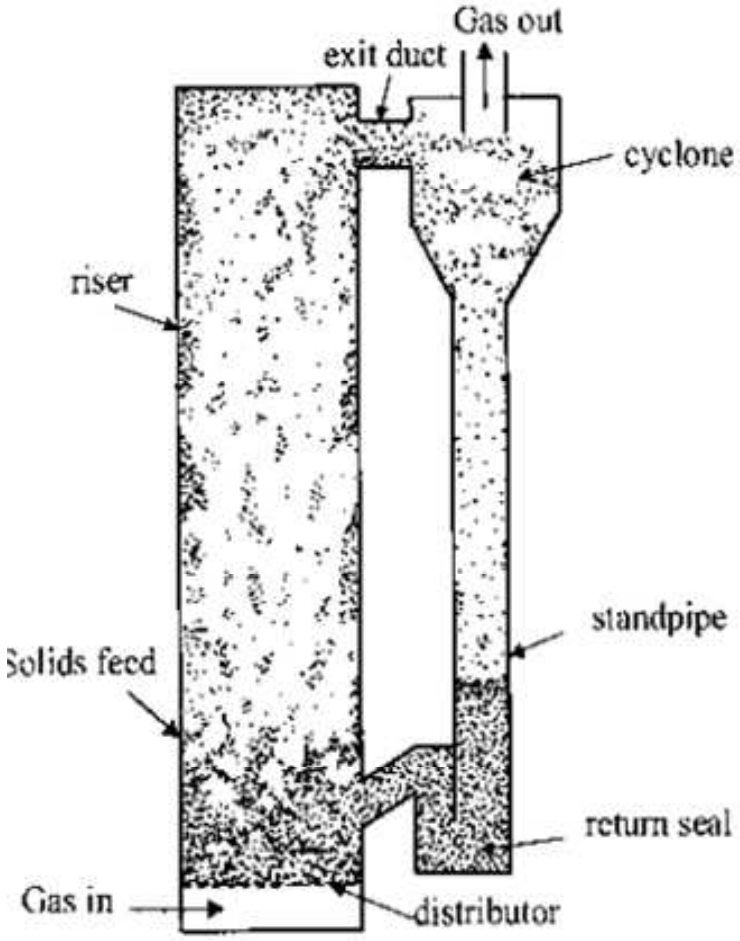

Figure 1.1: A typical circulating fluidized bed system (Yang, 2003)

oxidation of propane to acrylic acid process etc. Brief explanations of some of them are given below.

DuPont has commercialized the use of circulating fluidized bed technology for maleic anhydride production from n-Butane oxidation (Contractor, 1999). Main consumption of maleic anhydride is in production of polyester resins for boat building, automotive and electrical industries as reinforced plastics. Oxidation of n-Butane over Vanadium Phosphorus Oxide (VPO) catalyst is a typical redox reaction with high oxygen requirement of 3.5 moles of oxygen per mole of n-Butane. Commercially, reaction is carried out in fixed bed tubular reactors. Owing to high exothermic nature of reaction and hazards from explosive mixtures, n-Butane inlet feed concentration is limited to 2 mol% in air. This requires use of specialized cooling equipments. Fluidized bed technology is developed as suitable alternative to fixed bed process. Fluid bed process reduced the problem of hot spots and subsequent activity loss. Inlet feed concentration as high as 4 mol% could be used with the fluidized bed technology. However, rapid axial mixing of catalyst and gas phase back mixing in fluidized bed reactors resulted in selectivity loss with degradation to combustion products. Attempts to reduce degradation products by limiting oxygen concentration resulted in catalyst over-reduction. Circulating fluidized bed technology offers the advantage of carrying out oxidation (in riser) and catalyst regeneration (in regenerators) in separate reactor units. Near plug flow of gases in CFB limits the further degradation of maleic anhydride and butane to CO_2. Contractor (1999) discussed the salient features of development of CFB technology for maleic anhydride from inception to pilot scale operation. Demonstration plant of 0.152 m i.d. and 27 m height riser was successfully operated for over 18 months to demonstrate use of CFB technology. The operation was carried out at high solid flux condition up to 1000 kg/m^2s and at temperature range of 360^o – 420^oc and 2 bar pressure. CFB technology offered high selectivity to maleic anhydride with high butane conversion rates than fluidized bed reactors. Further concentrated products were obtained as riser was operated at very low oxygen concentration. High throughputs were realized with riser operated at high inlet feed concentration of upto 25mol% of butane. Based on success of demonstration plant, DuPont (Contractor, 1999) commercialized 81 thousand tons per annum plant in 1996 for its Tetrahydrofuran (THF) plant.

Chemical looping combustion (CLC) offers promising alternative of combustion with inherent CO_2 separation (Kolbitsch *et al.*, 2009; Kronberger *et al.*, 2005; Lyngfelt *et al.*, 2001). The CLC technology consists of a fuel reactor and an air reactor. The metal-oxide catalyst recirculating between these reactors provide oxygen needed for combustion process. In the fuel reactor, the metal-oxide is reduced and the fuel gas undergoes combustion to give primarily carbon di-oxide and water. Water is condensed to obtain pure CO_2. The reduced metal-oxide catalyst is then oxidized in the air reactor. Circulating fluidized bed reactor technology is being looked upon for commercializing the CLC systems on industrial scale. Laboratory and pilot plant studies demonstrated successful operation of CLC operation in CFB's. The CFB based CLC system consists of riser reactor operating as air reactor and a bubbling reactor for the fuel combustion. Ni, Co, Fe, Cu based metal-oxide catalysts are being investigated as probable metal-oxide catalysts. Typical size range of catalyst varies from 7μm to 2000 μm.

Acrylic acid is one of the primary intermediate for manufacture of dyes, paints and polymers. Direct oxidation of propane to acrylic acid is looked upon as an alternative to the existing propylene route. Godefroy *et al.* (2009) briefly discussed various available alternatives for acrylic acid production employing fixed, turbulent and CFB technology. Preliminary process economics showed that turbulent and CFB technology offer an edge over employing fixed bed route, which is limited by available heat transfer area. However, they reported that capital costs might prevent adoption of CFB technology over turbulent fluidized bed reactor. In future, with the advent of newer catalysts that offer greater conversion and/or selectivity, the investment costs for CFB technology would be competitive with the fluidized bed technology. Moreover, their study also identified the inherent difficulty in scaling up of CFB reactor systems.

Thus, the operating conditions and the prevailing flow structure of the CFB processes briefed above differ significantly from each other. The circulating fluidized bed can be operated in dense, fast fluidized and dilute flowing regime (Figure 1.2) as reviewed by Qi *et al.* (2009), Mei *et al.* (2007) and Bai *et al.* (1993) etc. For instance, in coal combustion, the gas velocity and solid flow rate are typically 5 – 8 m/s and less then

40 kg/m^{2}s respectively, whereas in the fluid catalytic cracking process, its 15 – 20 m/s and greater than 300 kg/m^{2}s respectively (Fan and Zhu, 1998). This work focuses on high density CFB processes. Typical high density CFB operates at superficial gas velocity ranging from 5 to 20 m/s with solid circulation flux greater than 100 kg/m^{2}s. The motivation behind selecting to simulate high solid flux CFB reactors systems is discussed in the next section.

1.2. MOTIVATION

The study of hydrodynamics of high solid flux circulating fluidized bed reactor assumes significance in the context of understanding the fundamentals of high flux gas – solid flow and also driven by developments in current CFB technologies. The fluid catalytic cracking technology is continuously being improved to cater market needs and other environmental implications. FCC units are required to operate with heavier feedstock having higher sulphur content. Stringent environmental legislations require that FCC cracker products have low sulphur content. Developments in FCC technologies are aimed to produce Ultra Low Sulphur Gasoline (ULSG) and Ultra Low Sulphur Diesel (ULSD) from heavier crude fractions. Few refineries are looking to make the FCC's produce high value petrochemicals like propylene without compromising the fuel output mode. For example the MAXOFIN^{TM} technology of Kellogg Brown and Root, Inc, offers operational flexibility to operate FCC either in maximum propylene yield mode or in the gasoline yield mode depending on the market needs (Corma *et al.*, 2004; Gilbert *et al.*, 2002). Such process improvements in FCC technology call for severe operating conditions and hardware requirements of the FCC units. Cracking of heavier crude require large heat supply and hence high solid circulation flux are required. Higher reactor temperature and high catalyst to oil ratio further requires efficient feed distribution system. The milli-second riser reactors also require high catalyst/oil ratio. Increase of solid circulation flux and suspension density will be very useful for other applications requiring even higher solids/gas feed ratios and higher solid concentration. Novel reactor technology based on two stage riser process and improved riser design to maximize FCC yields are already undertaken. Reports stating eight commercial units in operation with the two stage riser technology are available (Shan *et al.*, 2006; Wang *et al.*, 2004). Thus, there is significant scope for development of new processes and realizing improvements in

existing process technologies through thorough investigation and understanding of high solid flux risers.

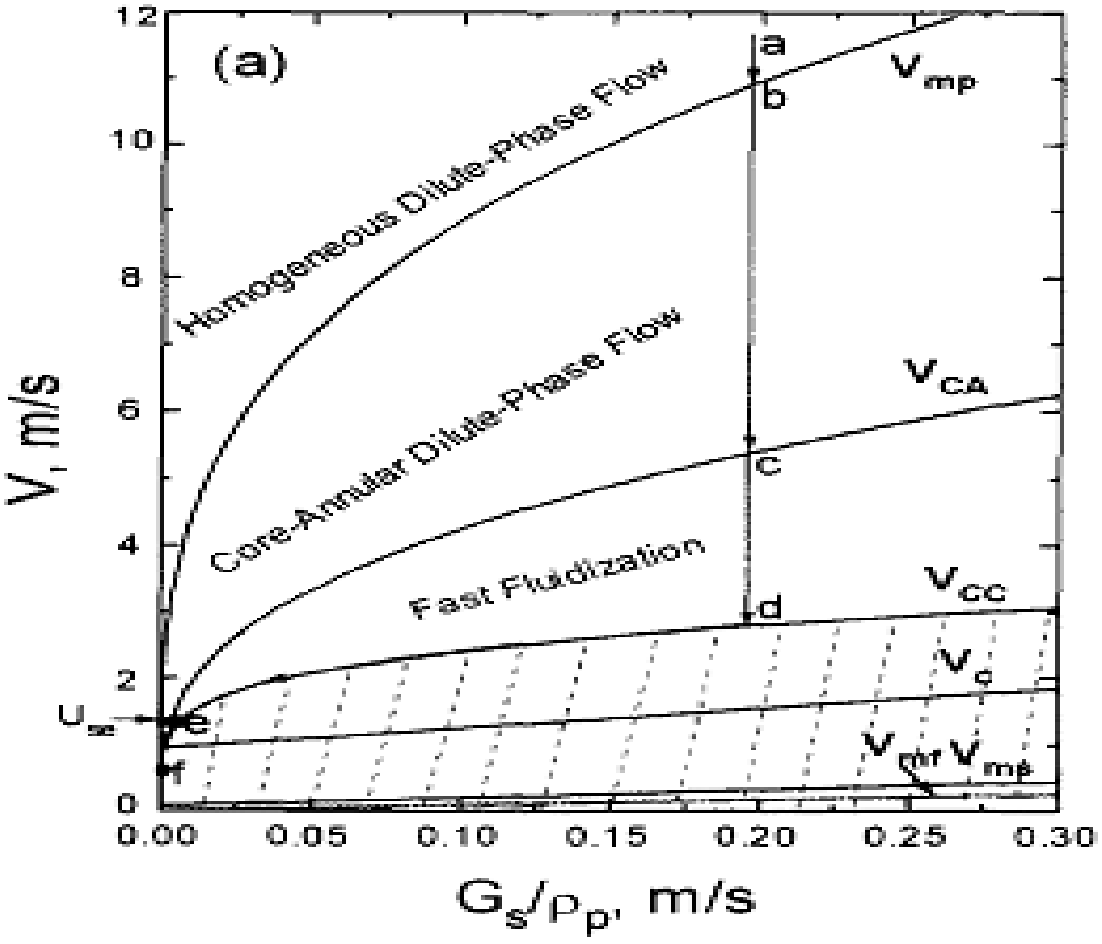

Figure 1.2: Flow regime map for as gas solid upward transport for a typical Geldart A system of ρ_p 1500 kg/m^3 and d_p 60 μm through 0.15m pipe. (Bi and Grace, 1995).

Quantitative understanding and predicting the performance of CFBs rely on the ability to capture and model inherently complex hydrodynamics of gas – solid flow in these systems (Gauthier, 2009). Gauthier (2009) listed the complex flow phenomena occurring in industrial CFB reactors and highlighted the need for further research and development in such systems. Lack of generalized scaling laws and fluid-particle interactions at larger scales accompanied by chemical reaction, mass and heat transfer was also briefed in the work. For instance, commercialization of n-butane to maleic anhydride based on CFB technology (Contractor, 1999) was not commercially successful owing to the scaling issues (Gauthier, 2009). Therefore there is a greater need to improve our understanding of gas solid flow in CFB systems and develop reliable scaling methods to commercialize new CFB technologies.

Computational fluid dynamics (CFD) facilitates and shortens development time cycles of new and/or improvements of existing process know-how to cater future demands. Recent years saw increasing usage of CFD models to understand fluid dynamics of high solid flux systems like those in commercial FCC riser etc. and to evaluate alternate hardware configuration for better process output.

Several attempts were made in the past to understand the hydrodynamics of gas – solid flows in vertical pipes or risers and channels. Models of varying degree of complexity like two-fluid models (the Eulerian-Eulerian framework), the Eulerian-Lagrangian framework and direct numerical simulations were attempted in the past to understand the underlying dynamics of gas solid flows (Curtis and van Wachem, 2004; van Wachem and Almstedt, 2003; Loth, 2000; Peirano and Leckner, 1998). However, the two-fluid based continuum models offer computational edge over other models especially in case of systems operating with high solid holdup and with those involving large industrial/ complex geometry (Zhu *et al.*, 2007).

The two-fluid continuum model description for fluidized bed is based on the mass, momentum and energy conservation law as given by Anderson and Jackson (1967). These models can be broadly classified into CFD based computational models (Benyahia, 2009; Lu *et al.*, 2009; Igci *et al.*, 2008; Almuttahar and Taghipour, 2008; Vaishali *et al.*, 2007; Cruz *et al.*, 2006; Huilin *et al.*, 2003; de Wilde *et al.*, 2003; Sun and Gidaspow, 1999; Nieuwland, 1994; Dasgupta *et al.*, 1993 and 1994; Sinclair and

Jackson, 1989; etc) and semi-empirical based hydrodynamic models (Godfroy *et al.*, 1999; Nieuwland, 1994; Pugsley *et al.*, 1993; Nakamura and Capes, 1973). The computational models require less ad-hoc adjustments and/or facilitate in generalization of the empirical/semi-empirical correlations developed through actual physical experiments to wide operating conditions (Ranade 2002; Sun and Gidaspow, 1999).

The solid phase is modeled as a fluid continuum with shear stress tensors computed using kinetic theory of granular flows (KTGF). The KTGF, analogous to the kinetic theory of gases, is characterized by the granular temperature. The solid phase pressure and the viscosity, which resists the motion of the particles, are defined in terms of granular temperature. The models based on KTGF require less ad- hoc adjustments and are widely used (Ranade, 2002 and references therein).The constitutive expressions of the KTGF model involves number of parameters like specularity coefficient, particle – particle restitution coefficient, angle of internal friction etc. In addition, prediction of high solid holdup near the walls requires appropriate specification of the wall boundary conditions for the solid phase. The shear at the wall for the solid phase is specified through an adjustable specularity coefficient parameter in the KTGF model.

Several attempts were made in the past to simulate, understand and develop state of art computational two-fluid models for gas solid riser flows. In spite of such sustained efforts, most of these works that dealt with the gas solid riser flows were faced with issues like:

a) Approximating the gas solid flow in cylindrical risers as flow through channels and simulating the flow in 2D Cartesian domain.
b) Most studies addressed the effects of model parameters on few selected quantities like either holdup or solid velocity or only turbulent quantities. Consistent and complete experimental data measured on a single riser system is rarely available.
c) Simulations were mainly concerned at low solid flux conditions or low mass loadings

d) Parametric analysis in some cases was coupled with complex flow geometry like risers with two inlets, abrupt exit etc and hence pose difficulty in independent parametric evaluation.

Thus, there is a need to evaluate the two-fluid model for simulating gas solid riser flow operating at high solid flux conditions and bring out the salient features and capabilities of the constituent closures in predicting the riser flow features.

1.2.1. Objectives of Present Work

The objectives of the present work are

1. To develop and use the Eulerian – Eulerian two fluid computational models for simulating flow in gas solid riser reactors and simulate gas solid flow profiles at typical high solid flux flow conditions.
2. Evaluate the model closures for simulating gas solid flow. More specifically, evaluation of multiscale based drag model for interphase exchange coefficient, boundary condition for solid phase etc. will be focused as part of the work.
3. Extend the simulated CFD model from lab scale systems to pilot scale systems and look into the scale up of predicted flow profiles.

Although, the work lays more emphasis on the numerical experiments pertaining to gas solid riser flows, comparisons with available experimental data were also made and meaningful conclusions drawn thereof. Overall methodology followed and the thesis organization is given in the following section.

1.2.2. Methodology

In conjunction with the aforementioned objectives, the research work is divided into three parts each targeted to address a specific issue described as follows:

Part 1: Evaluation of structure dependent drag model

The flow in riser at high solid flux conditions is accompanied by pronounced radial segregation and cluster formation (Lackermeier *et al.*, 1994; Horio and Kuroki, 1994; Yerushalmi and Squires, 1977). The clusters are dynamic entities and result in enhanced slip velocities observed in riser flows. The cluster formation results in decreased inter phase momentum drag experienced by the particles. Modeling the

interphase momentum exchange coefficient assumes significances in capturing these key features of gas solid flows. Further, the interphase momentum exchange provided by drag plays an important part than the solid phase stress tensor (Ranade, 2002; Agrawal *et al.*, 2001; Yasuna *et al.*, 1995 and references cited therein).

Attempts were made in the past to evaluate the momentum exchange closures in modeling the gas solid flow in high flux risers. The drag correction factors based on empirical correlations were seldom valid for range of high solid conditions existing in riser reactors and were not able to predict the observed increase in slip velocities in these systems. Nieuwland (1994) developed empirical correlation to correct the slip velocity at high solid flux flows from the data of van Breugel *et al.* (1969). At solid holdup greater than 10%, the correction factor was about 30. The correlation of Nieuwland (1994) showed improved predictability of the model with experimental data of van Breugel *et al.* (1969). But evaluation with Yang *et al.* (1992) showed not so good results. O'Brien, and Syamlal (1994) used experimental solid volume fraction data to empirically adjust the drag coefficient in simulating gas solid riser flows. However, the model had serious limitation, as the proposed relation was not generalized for all operating conditions.

Sundaresan's research group (Igci *et al.*, 2008; Andrews *et al.*, 2005; Agrawal *et al.*, 2001.) showed that coarse grid simulations with sub grid closure can predict the occurrence of clusters and radial segregation in gas solid flows. The sub grid closure was either a simple time average closure or a filtered closure based on arbitrarily chosen filter size or a stochastic closure. Their work highlighted that inclusion of sub grid closures to account for unresolved flow structures or clusters significantly affected the predicted results from two-fluid models.

To overcome the shortcomings of the conventional drag correlation, Li (2000) developed Energy Minimization Multiscale Model (EMMS), a structure specific model to represent interaction between gas and solid phases. The model addressed the heterogeneity at different scales existing in gas solid flows and the average drag coefficient was obtained as sum contribution of the component drags at different scales of interaction. The EMMS model accounts for cluster formation and captures the effective increase in slip velocity. The model was further extended to incorporate

inertial effects by Wang and Li (2007). The EMMS framework appears to be a promising approach for simulating high solid flux riser flows. However, the use of the EMMS model at high solid flux conditions existing in FCC riser systems is yet to be ascertained. There is a lacuna in the literature regarding the applicability of EMMS approach to high flux flows.

In the first part of this work, the EMMS based drag model for interphase momentum transfer was simulated for typical high solid flux flow conditions and improvements of existing EMMS framework in terms of predicting published pressure drop data was investigated.

Unlike earlier studies wherein EMMS drag correlation was incorporated into CFD and results from computational model was compared with experimental data, direct comparison of EMMS model output with available data was attempted in this work. This assumes significances as it enables evaluation of constituent expressions of computational models. Prediction of explicit occurrence of minimum energy consumption conditions, comparison of predicted cluster size with reported values from literature, sensitivity of predicted drag with EMMS parameters etc were also addressed as part of this exercise.

Part 2: 3D Periodic computational model for simulating fully developed riser flows

Developing state of art engineering model with reactions requires basic flow information such as time averaged fully developed flow profiles (velocity and solid volume fraction) and/or dispersion coefficients etc. Though empirical correlations are available, they do not offer predictive flexibility over wide operating conditions. This necessitates development of hydrodynamic model for gas solid riser flows to predict time averaged fully developed flow profiles. Moreover fully developed flow was observed in typical risers with large H/D ratios (Monazam and Shadle, 2008; Huang et al., 2006). Simulation of actual risers with H/D > 50, without jeopardizing the spatial resolution, demands enormous computational cost and time. One-way to alleviate huge computational requirement without compromising on the spatial resolution is by use of periodic flow domains to simulate fully developed flow profiles. Such attempts were made in the past to analyze the predictive capability of

two-fluid model approach in simulating gas solid vertical flows (See for example Igci *et al.*, 2008; Benyahia *et al.*, 2007; Zhang and Reese, 2003 etc.). Agrawal *et al* (2001) performed highly resolved simulations in 2D and 3D periodic computational domain with domain size equivalent to typical grids used in coarse simulations of large systems. They showed that the two-fluid model is capable of predicting the unstable transient clusters/strands provided the grid size employed is of the order of $10d_p$. Computational tools like FLUENT^{TM}(Version 6.3.26), CFX^{TM}(Version 10, both from Ansys Inc, USA) do not have in-built periodic model for simulating fully developed flows for multiphase systems with specified mass flow rates for each phase. This can be overcome by use of user-defined functions (UDF) to make the computational domain translationally periodic along the flow direction explicitly.

In this research work, periodic 3D CFD model based on two-fluid approach was developed for simulating fully developed hydrodynamic flow profiles (holdup, local velocities) through external user defined functions. Numerical experiments were performed with this periodic computational model and conclusions drawn accordingly on the effect of various model closures and tuning parameters like specularity coefficient, granular model formulation and so on. The results from the UDF based 3D periodic model were also compared with the 2D axis-symmetric and 2D full riser domain simulations.

Part 3: Numerical simulation of scaling laws for riser flow

Successful design of such systems from lab scale to industrial scale necessitates scaling parameters that ensure proper hydrodynamic similarity between reactors at various scales or across operating conditions. Extensive efforts have gone into establishment of scaling laws based on governing equations of continuity and momentum of Anderson and Jackson (1967). Different sets of scaling laws established involves dimensionless groups such as Reynolds number, Froude number, flow rate ratio, particle diameter to column diameter ratio etc. Knowlton *et al.* (2007), Xu and Gao (2003), van der Meer *et al.* (1999), Glicksman *et al.* (1993), Chang and Louge (1992), Glicksman (1984), had dealt with these scaling parameters under different flow assumptions.

Recently Qi *et al.* (2008) analyzed the available literature and own experimental data and suggested an empirical scaling parameter based on Froude number and flow rate ratio to ensure local and global hydrodynamic similarity in riser reactors. This empirical scaling parameter was shown to ensure both local and global hydrodynamic similarity under different operating conditions. For the same Qi scaling ratio (Qi *et al.*, 2008) radial profiles of solid concentration, particle velocity and cluster voidage exhibited similar profile in the fully developed flow region. The average solid holdup was shown to vary linearly with respect to the $Fr_D^{-0.3} G_s / (\rho_p u_g)$ scaling ratio.

This looks promising as a single scaling parameter ensuring hydrodynamic similitude in riser systems at both, local and global, levels. Nevertheless, this empirical parameter cannot guarantee hydrodynamic scaling in risers beyond their range without rigorous validation. The parameter was tested with most of data sets obtained with air as fluid medium at ambient conditions. The proposed scaling parameter did not consider the effect of fluid density. Further, the ratio of particle size to column diameter may be significant in small diameter risers and affect the relative contribution of particle shear at wall to the overall pressure gradient (Pita and Sundaresan, 1991 and references therein). Further validation of the scaling parameter requires extensive experimental data sets of good reliability.

This can be avoided to an extent, with the use of computational models, wherein the simulated profiles at different conditions can be compared to draw meaningful conclusions on scaling analogies. The periodic computational model with UDF developed earlier was employed to address this issue. A set of operating conditions, all having the same Qi scaling ratio (Qi *et al.*, 2008) was simulated following the periodic 3D computational model. The work was oriented towards numerical prediction of hydrodynamic similarity at high solid flux operating conditions. A comprehensive collection of all available data on pressure drop and solid holdup in gas solid riser flows was done and observed discrepancies in development of scaling laws based on experimental set up were highlighted.

1.2.3. Thesis organization

The thesis is organized into four chapters and appendix section as mentioned below. The thesis is further provided with the nomenclature and reference section complete with all necessary bibliographic information.

Chapter 1 discusses on the background for taking up this research work and the motivation behind the work. The objectives and methodology are discussed therein.

Chapter 2 is on Energy Minimization Multiscale (EMMS) model and evaluation of EMMS for high solid flux riser flows.

Chapter 3 is on development of computational models based on two-fluid approach. The mathematical model is discussed briefly at the beginning of the chapter and equations employed are tabulated for the reference of the reader. Followed by 3D periodic model based on user defined sub routine, the 2D axis symmetric and 2D full domain simulations are discussed.

Chapter 4 is on the use of developed periodic 3D computational model to evaluate the scaling in riser flows. Experimental data on pressure drop and solid hold up are consolidated and presented therein with the systematic analysis.

Annexure are provided at the each of each chapter, wherever applicable.

Appendix provided at the end of the thesis gives details of the two fluid CFD model studies on gas solid riser systems and the user defined function used for the periodic flow simulation.

CHAPTER 2

MUTLISCALE DRAG MODEL FOR GAS SOLID RISER FLOWS

The chapter briefly outlines the importance of multiscale model for gas solid flows and the energy minimization muti-scale (EMMS) based drag coefficient model for the gas solid riser flows. The EMMS model was simulated for high solid flux conditions. The model was tested for implicit minimum in the energy consumption for suspension and transport of particles. Sensitivity analysis of model parameters was performed and the EMMS model output were compared with available experimental data outside the CFD domain. Attempts made to improve the existing lacunae in the EMMS framework keeping intact the energy minimization postulate were also discussed and conclusion drawn accordingly.

2.1. BACKGROUND

2.1.1. Importance of Interphase Drag Closures in Modeling Gas Solid Flows

Quantitative understanding and predicting the performance of CFBs rely on the ability to capture and model the inherent complex hydrodynamics of gas – solid flow in these systems. In recent years, computational fluid dynamics (CFD) based models are increasingly used to understand and to quantitatively predict gas-solid flows in risers

Most of the CFD models of high solid flux risers are based on the Eulerian-Eulerian approach (Ranade, 2002). In this approach, gas – solid flow is modeled as interpenetrating continua. These models require appropriate formulation of inter phase momentum exchange for coupling between the phases. It has been shown that inter phase drag force formulation is the critical closure for simulating gas-solid riser flows with adequate accuracy (Ranade, 2002; Agrawal *et al.*, 2001; Qi *et al.* 2000 and so on). Agrawal *et al.* (2001) reported that the contribution of solid stress obtained from KTGF was negligible and the effect of particle clusters played a dominant role in simulation.

Conventionally Wen and Yu (1966) and/or Ergun (1952) correlations are used in estimating inter phase drag. These correlations predict the drag correction factor to be dependent only on the overall solid holdup and shows increased drag with solid concentration. It is note worthy to mention that these correlations were derived based on experiments done on particulate fluidized bed and/or fixed bed. In the fast fluidization regime operating at high solid flux, radial segregation of particles occurs in riser and occurrence of strands of particles (clusters) becomes more pronounced (Muller and Reh, 1994). The strands of particles or clusters are dynamic entities and affect the flow structure and the performance of the CFB system. Because of formation of such clusters, solid particles exhibit slip velocity many times higher than their terminal settling velocity. Such high velocity leads to possibility of down flow of particles near the wall (Derouin *et al.*, 1997; Nieuwland, 1996). The pronounced lateral segregation and solids down flow near the wall with the velocities much higher than the terminal settling velocities may occur due to the formation of clusters. The experimental results of Muller and Reh (1994) showed too, that the formation of

stands of particles resulted in considerable drag reduction, leading to longer acceleration region in risers. Qi *et al.* (2000) reported that the particles fed into the riser got elutriated immediately and the simulated flow became rather dilute as a whole if the drag correlation derived from Ergun equation was employed. They claimed that the current drag correlations were only suitable for low gas velocity and coarse particles, in which case the terminal velocity was equal to the superficial gas velocity. It has been observed that it was not possible to simulate the down flow near the riser wall without modifying the underlying interphase momentum exchange model. None of the correlations mentioned above account for formation of clusters and increase in effective slip velocity and therefore none were able to capture the key flow characteristics of high solid flux risers (for example, Makkawi and Wright, 2003; Ranade, 1999). Hence, it is essential that any computational model developed to predict the flow dynamics in gas-solid riser must account for the formation of clusters and hence for the observed increase in slip velocities.

2.1.2. Modification of Interphase Momentum Exchange in Two-fluid Models

Efforts are taken in the past to empirically develop and incorporate drag coefficient correction factors tuned to fit given set of experimental data. For instance, O'Brien and Syamlal (1994) investigated the data of Bader *et al.* (1988) and empirically corrected the drag coefficient to match the experimental data. Bai *et al.* (1991) and Li *et al.* (1982) proposed an empirical correlation for the drag coefficient based on their own experimental results. Their correlation was based on average solid hold values over the entire cross section and thus the drag coefficient did not reflect the dependence on local heterogeneous structure and/or radial heterogeneity. Matsen (1982) proposed a correlation to estimate the slip velocity of clusters as a function of single particle terminal settling velocity and volume fraction of solids. The ratio of slip velocity to terminal settling velocity at 10% solids volume concentration was about 5. Similarly, Nieuwland (1994) proposed an empirical correlation to correct the drag coefficient in gas-solid riser flows. They observed that experimental slip velocities were as high as 30 times as that of the terminal settling velocity of the particles. Recently, Helland *et al.* (2007) employed two quadratic type correction functions, to account for the formation of clusters and for the observed decrease in drag coefficient with solid holdup. These voidage functions had minimum drag

coefficient at solid holdup of 0.023 and 0.042 for lower and higher particle Reynolds number respectively. This gave settling velocity of the particle as two and three times the terminal settling velocity of an isolated particle.

It is clearly evident that empirical correlations used to account for the influence of clusters on the interphase drag force term differed significantly in their predicted slip velocities. Moreover, such correlations were found not be very useful for all experimental data sets and lacked generality. The correction factors for the drag coefficient cannot be employed for experimental conditions, other than those used to develop or test these developed relations, with confidence. It appears that cluster formation, their size and slip velocity may be functions of more parameters other than just the solids volume fraction and terminal settling velocity. Corrections to the drag coefficient to include the cluster formation have to be done with more insight into the physics of the system rather than correlations based on average experimental quantities. Recently Makkawi and Wright (2003) pointed out that it was far from inaccurate to assume that the exponent of the correction factor for the drag coefficient was a constant and proposed several correlations of the exponent of the correction factor for the wall and for the center region of a fluidized bed on the basis of own experimental results.

Yang *et al.* (2004) have briefly reported on the schemes to correct the inter phase drag correction factor to include the effect of flow structures. These are discussed in the foregoing sections.

Interface tracking between gas and particles

Direct numerical simulation (DNS), pseudo – particle modelling (PPM) and Lattice – Boltzmann method (LBM) approaches track the interface between each particle and the surrounding gas. The interactions between the phases need not be described explicitly. DNS approaches are based on solving Navier - Stokes equation for the all the concerned particles of the gas – solid system. The influence of particles on fluid was reflected by the nonslip boundary condition of fluid flow field and was then computed by solving the Navier – Stokes equation, whereas the influence of fluid on particles was reflected by the integration of the stress on each element around the surface of particles. In PPM and LBM approaches, the fluid is resolved into pseudo –

particles of length scales smaller than the constituent particle size and then the drag force is calculated by the collision process between pseudo particles and real particles.

Refinement of computational grids

Zhang and van der Heyden (2001) and Agrawal *et al.* (2001) have indicated that simulations of the gas-solid two-phase flow with high grid resolution using the conventional correlations for the average drag coefficient or even using correlations for the standard drag coefficient for a single particle is capable of simulating the meso-scale structures. This is due to fact that heterogeneity is weakened as the grid size is reduced.

Structure specific model or multi-scale models

Another approach in developing drag correlations to represent the physical flow structure existing in gas – solid flow is to assume a structure for each control volume and then solve the pertinent force balance equations and obtain information regarding the interaction at different scales. This is referred to as sub-scale or meso-scale modeling approach, wherein appropriate models are developed to capture the cluster and its influence on the flow. Li (2000, 1994) developed the structure specific model to represent interaction between gas and solid phases. He represented the heterogeneity at different scales existing in gas solid flows and obtained the average drag coefficient as sum contribution of the component drags at different scales of interaction. Yang *et al.* (2003a, 2003b) employed the approach of energy minimization multi scale modeling (EMMS) of Li (2000) to obtain effective drag coefficient for typical low solid flux riser flow. They showed that the effective drag from the EMMS model was less than that predicted by conventional drag closures. The EMMS model accounts for cluster formation and captures the effective increase in slip velocity. This appears to be a promising approach for simulating high solid flux riser flows. The significance of the structure based model for drag coefficient is discussed in the following section.

2.1.3. Need for Multi Scale Modeling Approach

The need for drag correction factors based on multi scale approach arises from the experimental observations, as discussed earlier, that the presence of meso scale

structures (clusters or stands of particles) results in decreased drag than that predicted by the conventional drag correlations.

Figure 2.1 shows the possibility of the two possible flow structures with the same overall solid holdup. Essentially the drag in these two flow structures and the transport characteristics are different and thus modeling such flow structures with the correlations based on average cross sectional values are not justified. Further more Figure 2.2 signifies that drag coefficient is sensitive to the prevailing structures in the flow and stresses the need to modify the drag correlations with a more insight in to the prevailing structures in the flow field rather than based on average values.

Moreover the drag modification approaches based on grid refinement and those based on direct numerical simulation, though can themselves provide all the necessary closures laws for the flow models, are computationally more intensive. These can be used to understand the issues like cluster formation, their characterization and segregation with few hundreds or thousands particles. But for simulation of practical high solid flux flows it is evident that these results are either directly or indirectly be coupled with other models to derive a meaningful conclusion. The structure specific model of Li (2000), on other hand looks promising to develop the drag closure relations for the practical operating conditions with ease.

The earlier works on EMMS (Ge and Li, 2003; Yang *et al.*, 2003a, 2003b; Xu and Li, 1998; etc) involved development of drag coefficient correction factor following EMMS approach and incorporating the effective drag from EMMS model into the two fluid CFD model. The earlier work validated the results from CFD simulation against the experimental quantities. It is strongly recommended that development of state of art CFD model requires usage of appropriate constituent relations that represent the physics of the system. Such constituent relations are needed to be thoroughly investigated and evaluated prior to their inclusion in the CFD framework. In the earlier work, no attempts have been made to compare the EMMS model outputs (cluster size) with available experimental data/correlation. This could disguise the efficient usage and development of drag correlation for the CFD model. Further, in the EMMS framework, cluster voidage is assumed at constant value independent of operating conditions. In contrast, the observed experimental data (Harris *et al.*, 2002)

shows cluster voidage as a function of overall solid holdup. This issue is studied in the present work.

The earlier attempts have restricted to usage of EMMS model for low solid flux operating conditions. Recently Jiradilok *et al.* (2006) used the EMMS model to simulate their riser flow at high flux condition of 98 – 167 kg/m^{2}s. However Jiradilok *et al.* (2006) incorporated the drag coefficient correction factor from the EMMS results of Yang *et al.* (2004), to their simulate riser flow. It should however be noted that drag coefficient correction factors need to be obtained from the EMMS model for each specific case (Yang *et al.*, 2004). The correction factor as reported by Yang *et al.* (2004) is not a generalized correlation and is applicable only for the system studied by Yang *et al.* (2004). The system and the simulated operating conditions of Yang *et al.* (2004) and Jiradilok *et al.* (2006) are quite different. The simulation results and subsequent conclusions drawn by Jiradilok *et al.* (2006) cannot be generalized. More recently Qi *et al.* (2008) employed drag coefficient developed from EMMS approach to simulate gas solid flow at solid flux of 53 kg/m^{2}s and 489 kg/m^{2}s. However, their work did not provide evaluation of the EMMS approach outside the CFD domain. Comparison of predicted cluster size with reported values from literature, sensitivity of predicted drag with EMMS parameters etc were not discussed in their work. The use of the EMMS model at high solid flux conditions existing in FCC riser systems are yet to be ascertained. Very few works employed EMMS model for simulating the gas-solid flows in high flux risers. Hence, in this research work, EMMS model was evaluated outside the CFD domain and parametric sensitivity of the model was carried out to draw meaningful conclusions.

In the section to follow, the basic structure of the EMMS model and its mathematical formulations are discussed in brief.

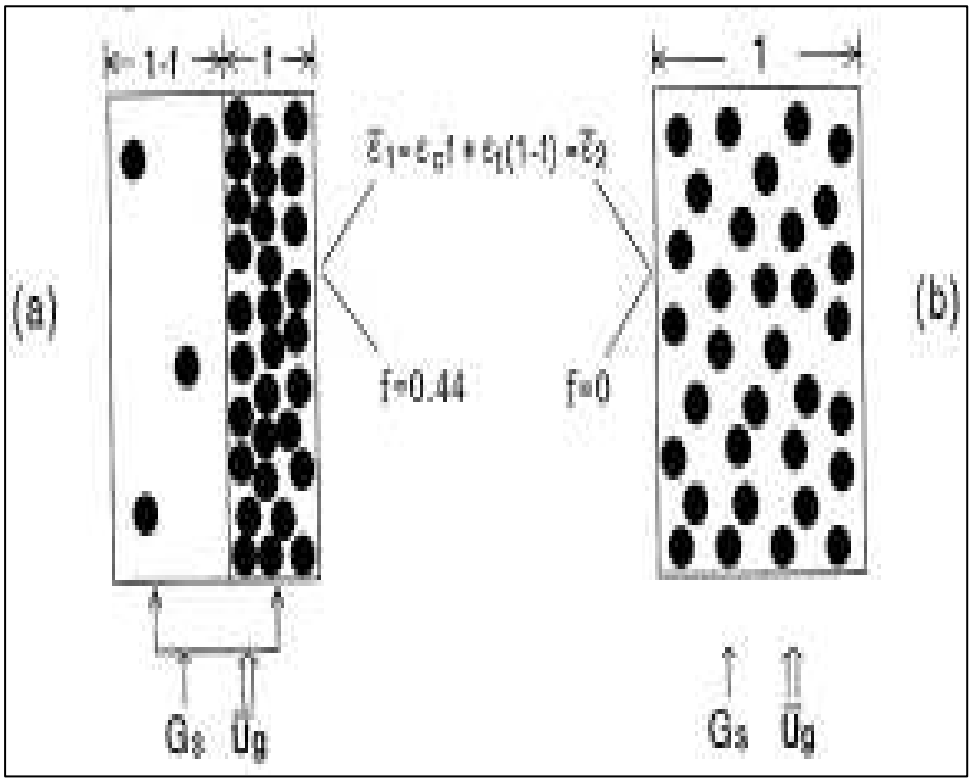

Figure 2.1: Structure resolution with same average solid holdup (Li *et al.*, 1998)

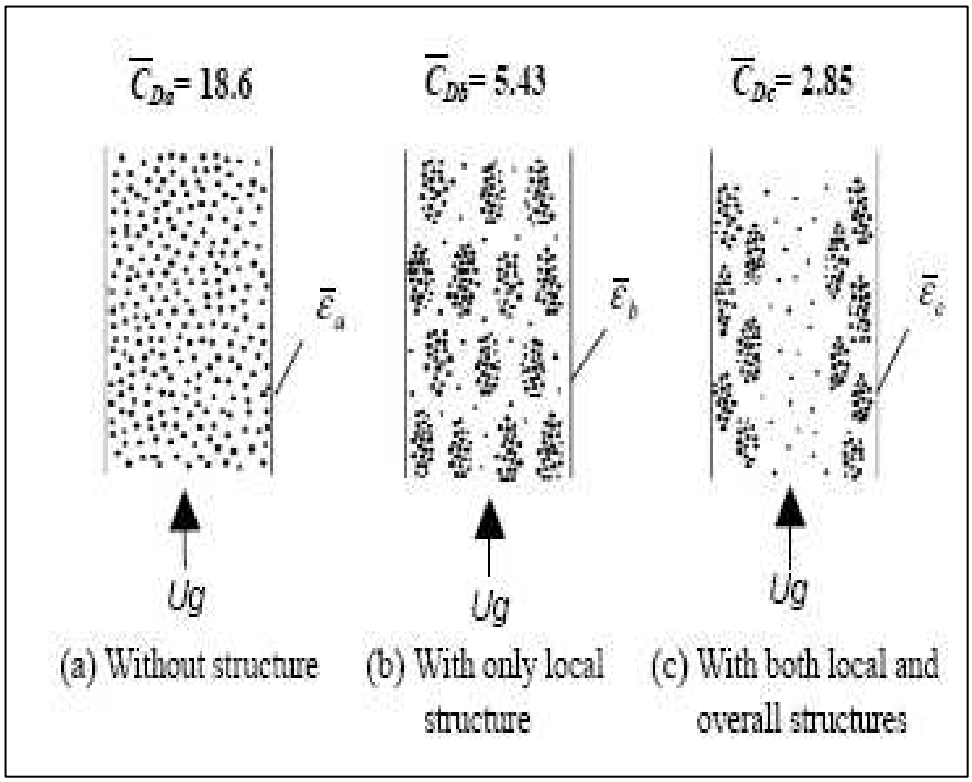

Figure 2.2: Sensitivity of drag coefficients to flow structures. (Li and Kwauk, 2003)

2.2. ENERGY MINIMIZATION MULTI SCALE (EMMS) MODEL

The energy minimization multiscale modeling was proposed by Li *et al.* (1998) and subsequently investigated by number of researchers mainly from the Chinese Academy of Science and their collaborators (Yang *et al.*, 2003a, 2003b, 2004; Xu and Li, 1998 etc.). The model was proposed with the primary objective to focus on observed drag in two-phase gas solid flow accompanied by clustering phenomena. The gas solid flow possesses spatial and temporal heterogeneity. This spatial and temporal heterogeneity was addressed by modeling the gas solid flow consisting of two phases namely the dense or the cluster phase and the dilute or the lean phase. The flow mechanism occurring in these phases depend upon the scale of observation, which leads to rather heterogeneity in terms of drag. The total effective drag for the gas solid flow was expressed in terms of sum contribution of the component drag from the cluster and the dilute phase. Much of the material described in this section follows Li and Kwauk (2003).

2.2.1. Flow Mechanisms in Gas Particle Flow

Gas and particle exhibits their own individual movement tendencies. Particles, by virtue of their higher inertia, tend to accumulate with minimum potential energy. Gas tends to move through the least resistance path. Depending on the relative dominance of the gas or the particle nature of the flow, characteristics of the two-phase gas solid flow in risers fall into different flow regimes from fixed to the pneumatic transporting flow. The prevailing mechanisms in gas solid flow is classified accordingly into three types (Li and Kwauk, 2003) described below

Particle dominance (PD)

The gas solid flow governed by particle dominance realizes distinct particle motion and the motion of the fluid has negligible effect in dictating the motion of the particles and on the other hand the fluid motion is dictated by the particle. This corresponds to fixed bed regime (Figure 2.3).

Fluid dominance (FD)

In this mechanism the distinctive motion of the fluid is recognized and the particle motion is governed by the fluid flow around the particle. This corresponds to the transport regime in gas solid flow wherein the particles are simply carried away by the fluid domain along in their direction (Figure 2.3).

Particle fluid compromise (PFC)

The gas solid flow in fluidized bed is neither of fluid dominance nor of particle dominance. There exists balance between the two prevailing mechanisms and the resultant flow is due to the compromise between the particle and the fluid dominance mechanisms (Figure 2.3).

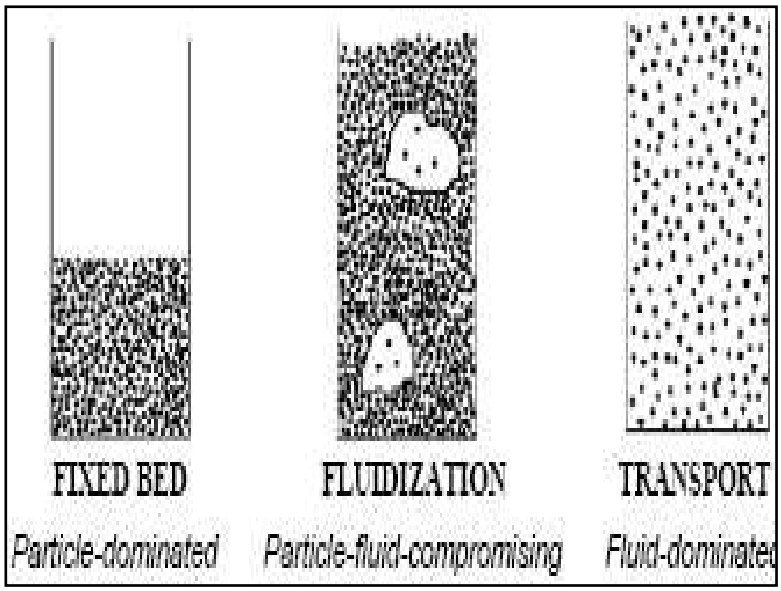

Figure 2.3: Mechanisms of interaction in gas solid flow (Li and Kwauk 2003)

2.2.2. Fluid – Particle Scales of Interaction

The gas solid flow exhibits three scales of interaction depending upon the scale of observation. Depending upon these scales of observation the flow mechanisms existing in these are also different. In the structure specific model (Li and Kwauk, 2003) three scales of fluid – particle interactions are identified as micro, meso and macro scale.

Micro scale or particle scale of interaction

The micro scale is at the scale of observation of particle size, which is about 100 – 500 microns. The constituent particles of the gas solid flow can be at the cluster phase or/and in the dilute phase. In the cluster phase (Figure 2.4) the particle is under the influence of the surrounding particles and experiences the particle dominance mechanism. In the dilute phase, the particle is surrounded by the fluid and is under the fluid dominance mechanism. Thus depending on the phase in which the particle has its presence it experiences either particle or the fluid dominance mechanism.

Meso scale of interaction

Meso scale of interaction is concerned with the interaction between the cluster as a whole entity and the dilute phase surrounding it (Figure 2.4). This is at the cluster scale of observation, which is about 10 to 500 times the particle scale (particle size). The particles along the cluster boundary which defines the cluster as an entity is experiencing the fluid-particle compromise mechanism, as it is under the effect of neighboring particles from inside the cluster and also the surrounding fluid of the dilute phase which encircles it. For simplicity it is inherently assumed that the cluster is surrounded by only the fluid and that particle –particle interaction between the cluster and the dilute phase are hence not accounted and considered. This also eliminates the possibility of cluster – cluster interaction that is not accounted in the model.

Macro scale of interaction

The macro scale is at the system level (Figure 2.4). It deals with the interaction between the gas solid flow as a whole and the system boundaries, which result in macro heterogeneity. The macro heterogeneity has radial and axial components as well. The wall-effect results in radial distribution patterns in the hydrodynamic parameters. Axial macro scale interaction results from the pressure drop considerations and inlet and outlet effects. The macro scale of interaction governs the dependence of local hydrodynamic flow structures on location.

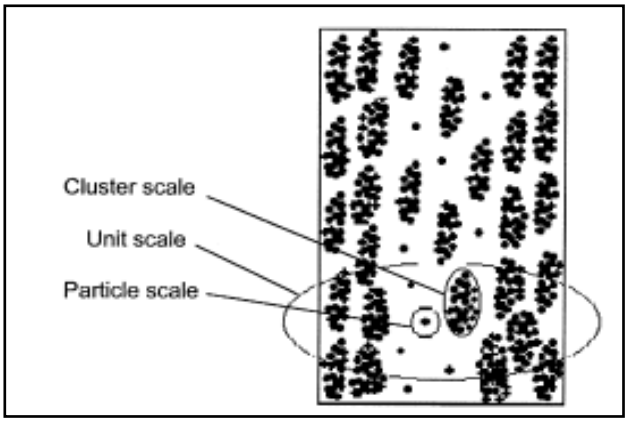

Figure 2.4: Scales of interaction in gas solid flow. (Li 2000)

2.2.3. Energy Resolution and Concept of Energy Minimization

The total energy associated with fluid – particle system, expressed as specific energy consumption rate, N_T, consist of two components – energy consumed for suspension and transport of particles, N_{st}, and energy dissipated in the particle – fluid flow, acceleration etc, N_d. N_{st} is further slit into the energy required for suspension, N_s and energy required for transport, N_t.

$$N_T = N_{st} + N_d \quad (2.1)$$

$$N_{st} = N_s + N_t \quad (2.2)$$

The energy term, N_s, results from the slip between the fluid and the particles is also dissipated because it does not contribute to the upward motion of the particles, making the total dissipated energy as $N_s + N_d$. However, this portion of energy is responsible for retaining the potential energy of the particles, which are suspended in the system that is, keeping the system expanded, and is therefore different from the purely dissipated energy N_d. These energies are quantified by respective pressure heads, neglecting the wall friction effects. The energy N_{st} is given as sum of the respective pressure heads times slip velocity in the cluster, dilute phase and in the interphase. The term N_{st} characterizes the intrinsic tendency of particles toward an array of the lowest interaction with the fluid or simply the movement capability of the particles.

Energy consumption is also expressed in terms of energy consumed per unit volume of the system, W_T, W_{st}, and W_d as given by Equation 2.3.

$$W_T = N_T(1-\varepsilon)\rho_p$$
$$W_{st} = N_{st}(1-\varepsilon)\rho_p \qquad (2.3)$$
$$W_d = N_d(1-\varepsilon)\rho_p$$

The energy term, W_{st}, expresses the intrinsic tendency or capability of the fluid to move through lowest resistance path.

The total energy, N_T, is thus resolved and used in characterizing the flow regimes of gas solid flow – fixed to transport regime. For the gas solid flow corresponding to fluidization, at velocities between the minimum fluidization velocity, and the transport velocity, neither the particles dominate nor can the fluid dominate the other in displaying either's tendency exclusively. The PFC flow mechanism is thus said to exist. In the lower end of this regime or velocity range, the particles tend to accumulate as continuous dense phase emulsion admitting excess gas to pass through as bubbles. At the higher end of this velocity range, the particles in the continuous emulsion shred themselves to form clusters or strands and form discontinuous dense phase, distributed in a dilute broth of sparsely distributed particles, called the dilute continuous phase. Particles in the dense phase tend to form clusters along the walls giving rise to gradient across the flow section. This regime as postulated by Li (2000) is characterized by minimal energy per unit mass of particles, N_{st}, (Equation 2.4) at which the particles aggregate to form clusters and stands.

At the fluid dominant flow mechanism, when the fluid velocity exceeds the transport velocity, all particles are freely flown through the fluid media and all the energy is spent in breaking the particle clusters as small as closer to individual particles and in distributing them through the flow section. Maximal particle dispersion corresponds to maximal energy expenditure per unit mass of particles, which is mathematically stated in Equation 2.4.

$$\begin{aligned} N_{st} &= \text{Min}, \quad \text{PFC} \quad \text{mechanism} \\ &= \text{Max}, \quad \text{FD} \quad \text{mechanism} \end{aligned} \qquad (2.4)$$

2.2.4. Mathematical Framework of EMMS Model

According to the energy minimization multi scale model, the gas particle interaction (fluid – solid interaction) occurs not only between single particle and the surrounding fluid in the dense and/or the dilute phase (micro scale) but also between the clusters

and the surrounding dilute broth (meso scale). The fluid tends to move upwards with minimal resistance while the particles tend to array themselves with minimal potential energy and consequently the compromise between the respective movement tendencies leads to the minimization of energy consumption rate for suspension and the transport of particles. The gas solid two phase flow is modeled in cluster – dilute phase framework. Eight variables are defined to describe the two phases (Figure 2.5). The cluster phase is characterized by homogeneous clusters of uniform size d_{cl}, and voidage ε_c. The cluster phase fraction in a given volume is characterized by f. Dilute phase is assumed to be consisting of discrete particles of uniform size d_p, with voidage of ε_f. The superficial gas and particle velocity in the cluster and dilute phase are characterized by u_{gc}, u_{pc}, u_{gf} and u_{pf} respectively. Force balance for the cluster and dilute phase, pressure balance equations and continuity equation for the gas and particle are shown in Table 2.1.

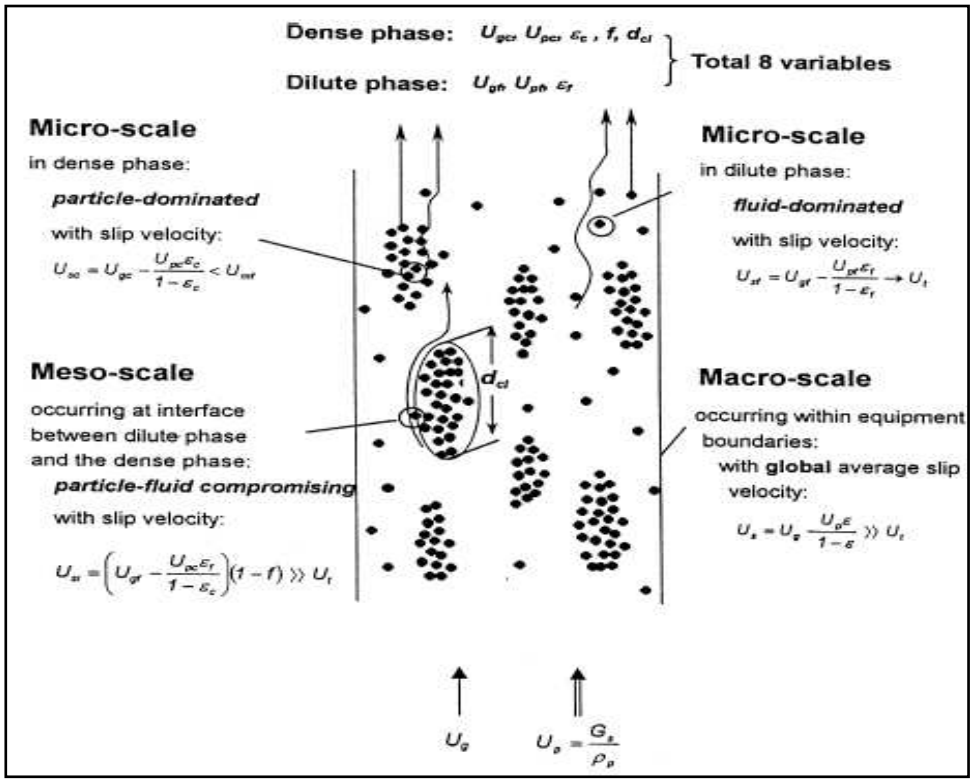

Figure 2.5: Eight structure specific parameters of the model. Li (2000)

Table 2.1: Basic equations of EMMS model

Sno	Equation	Expression
1	Force balance in cluster phase	$m_c F_c f + m_i F_i - f(1-\varepsilon_c)(\rho_p - \rho)g = 0$
2	Force balance in dilute phase	$m_f F_f (1-f) - (1-f)(1-\varepsilon_f)(\rho_p - \rho)g = 0$
3	Pressure balance between cluster and dilute phase	$m_f F_f + \frac{m_i F_i}{(1-f)} - m_c F_c = 0$
4	Continuity equation for gas	$u_g = u_{gf}(1-f) + u_{gc} f$
5	Continuity equation for particles	$u_p = u_{pf}(1-f) + u_{pc} f$
6	Overall continuity equation	$\varepsilon = \varepsilon_f (1-f) + \varepsilon_c f$

Table 2.2: Degree of freedom analysis for the basic and extended EMMS

Primary variables	Known u_g, G_s, d_p, Unknown u_{gc}, u_{gf}, u_{pc}, u_{pf} ,ε_c, ε_f, ε, f, d_{cl} , a_c, a_f, a_i	3 **12** *(9)*
Primary equations	Force balance equation (2), pressure balance equation (1) Pressure balance equation in terms of inertial terms (1) and continuity equation (3)	**7** *(6)*
Secondary variables	F_c, F_f, F_i, C_{Dc}, C_{Df}, C_{Di}, C_{D0c}, C_{D0f}, C_{D0i}, Re_c, Re_f, Re_i, u_{sc}, u_{sf}, u_{si}, m_c, m_f, m_i	18
Secondary equations	Drag force expression (3), Drag coefficient relation (6), Reynolds number expression (3), Slip velocity definition (3) , Expression for number of particles/cluster per unit volume (3)	18
Degree of freedom	= Total no of unknown variables –Total no of equations = (**12**+18) – (**7**+18)	**5** *(3)*

*Italicized numbers in brackets are for the basic EMMS model without inertial terms

EMMS model has three degrees of freedom to arrive at the solution (Table 2.2) corresponding to the point of minimal energy consumption for suspension and transport. The EMMS model employs cluster size correlation based on energy consumed for suspension and transport as given by Equation 2.5. The cluster size correlation is based on the assumption that cluster size is inversely proportional to the energy consumed for suspension and transport. As voidage tends to maximum value ($\varepsilon \rightarrow \varepsilon_{max}$), all input energy is utilized for transport of particles and d_{cl} tends to d_p (Li, 1994).

$$d_{cl} = \frac{d_p\left[\frac{u_p}{(1-\varepsilon_{max})} - \left(u_{mf} + \frac{u_p\varepsilon_{mf}}{1-\varepsilon_{mf}}\right)\right]g}{\frac{N_{st}\rho_p}{(\rho_p - \rho)} - \left(u_{mf} + \frac{u_p\varepsilon_{mf}}{1-\varepsilon_{mf}}\right)g} \qquad (2.5)$$

With cluster diameter defined by Equation 2.5, the two other parameters are needed such that the energy required for suspension and transport, is minimum. Li and Kwauk (2003) postulated that for the fluidization regime, the fluid particle compromise mechanism prevails and the energy spent for suspension and transport was minimized as cluster voidage reduces to minimum fluidization voidage and the dilute phase voidage reaches the upper bound, which is the maximum voidage attainable in the gas solid system. The necessary closures are given by Equation 2.6.

For the case of fluidization with particle – fluid compromise PFC, the EMMS model postulates, mathematically, the occurrence of minimal N_{st} at

$$\begin{aligned} \varepsilon_c &= \varepsilon_{mf} \\ \varepsilon_f &= \varepsilon_{max} \end{aligned} \qquad (2.6)$$

With the additional constraints for cluster voidage and dilute phase voidage, satisfying minimal energy consumption (Equation 2.4), the EMMS model equations give a unique solution for the given operating conditions G_s and u_g. The derivation of model equations can be found in Annexure 2A.

Extended EMMS Model

Recently Wang and Li (2007) incorporated three additional inertial terms "a_c, a_i and a_f" in the force balance equations for the cluster phase, interphase and dilute phase respectively. Following the approach of Xu and Li (1998), the set of equations was iteratively solved to arrive at the solution. With incorporation of additional terms in the EMMS framework, the model has 5 degrees of freedom (Table 2.2). The inertial phase term for the interphase a_i is calculated from the pressure balance between the constituent phases. Detailed model description can be found from Li (1994) and works therein.

Solution of EMMS model equations

The solution of the EMMS model equations was based on suitable expressions for the component drag force terms, F_c, F_f, F_i and slip velocity u_{sc}, $u_{sf,}$ and u_{si}. Appropriate expression for drag coefficients have to be incorporated in the expressions for the drag force. EMMS model solution is based on the following assumptions –

(1) The cluster and the dilute phase were considered to be homogeneous and also the clusters were homogeneously distributed in a given volume section. Hence Wen and Yu (1966) correlation was applied to determine the drag in the cluster phase, dilute phase and for the particles in the interface between the clusters and dilute phase.

(2) Only drag and gravity forces were considered.

(3) The cluster voidage was set equal to the minimum fluidization voidage and the dilute phase voidage was set at the maximum value of 0.9997 as given by Matsen (1982). This was in line with equation (2.6)

Apart from the three assumptions mentioned earlier, Xu and Li (1998) simplified the original equations of the EMMS model by usage of power law form of drag expression for the standard drag coefficient in place of Wen and Yu (1966) expression. The equations (Annexure 2A) were solved for the given operating conditions (input parameters) employing bisection search algorithm. The solution was initiated with guess value for the cluster fraction and iterations were continued until cluster fraction converges satisfying the criteria given by Equation (2.7). Tolerance value was set as 10^{-6}.

$$\left|f_i - f_{i-1}\right| \leq \text{tolerance} \qquad (2.7)$$

where i is the iteration number

From the knowledge of the eight parameters of the structure specific model, the component drag coefficients and the total effective drag coefficient were calculated. The correction factor for the drag coefficient was calculated taking the Wen and Yu (1966) drag expression as a reference.

Model equations were solved in MATLAB 7. The MATLAB code was tested by comparison of the results from the present work with reported simulation results for air- FCC system (929.5 kg/m^3 and 54 μm) at G_s = 50 kg/m^{2}s (Xu and Li, 1998). Good agreement was seen for all the reported profiles (Figures 2.6a – 2.6c). This ensured that the model equations and the code used were in consistence with the results published earlier. The model and its MATLAB implementation were then used for further investigation of the EMMS model. All simulation studies were done with air – sand system of particle diameter 129 μm and particle density 2540 kg/m^3. Typical high solid flux condition of solid circulation flux of 100 – 500 kg/m^{2}s and superficial gas velocity in the range 5 – 20 m/s was used.

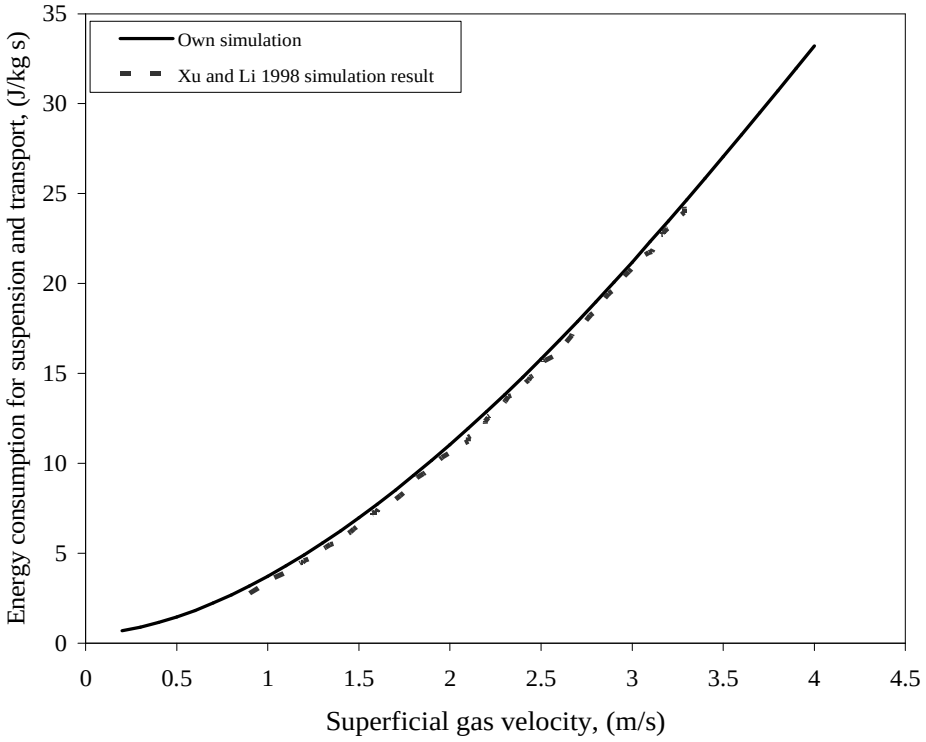

Figure 2.6a: Variation of energy consumed for suspension and transport with superficial gas velocity

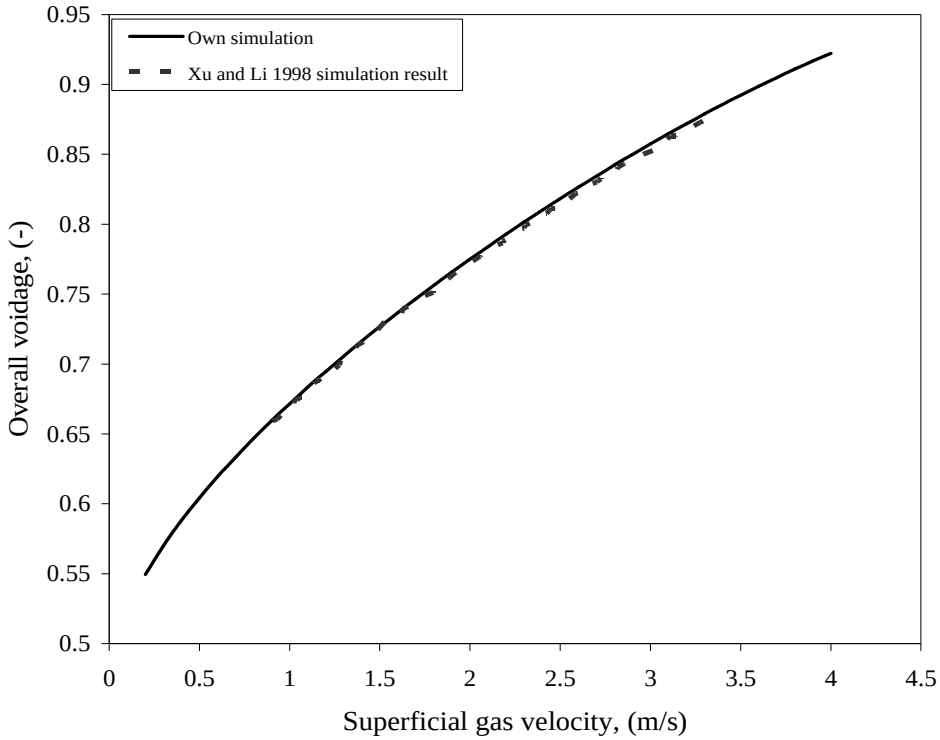

Figure 2.6b: Variation of overall voidage with superficial gas velocity

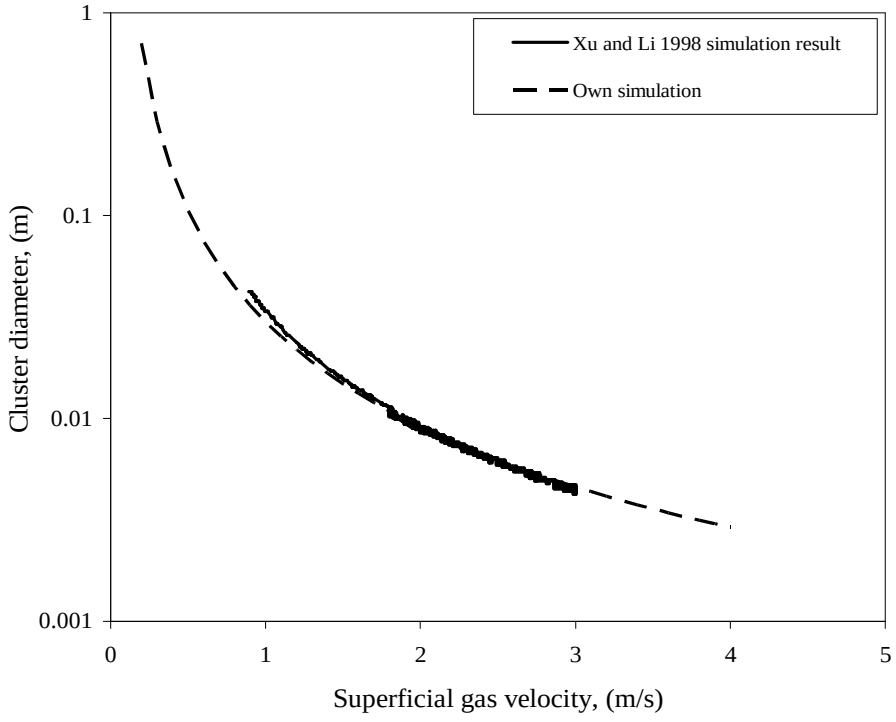

Figure 2.6c: Variation of cluster size with superficial gas velocity

2.3. RESULTS AND DISCUSSION

2.3.1. Criterion of Minimum Energy Consumption Solution

EMMS model is based on the postulate that for given operating condition the gas solid system attains the state of minimum energy consumption for suspension and transport (N_{st}). The extended EMMS model has five degrees of freedom (Table 2.2). Hence, the EMMS model solution corresponds to the global minimum in the N_{st} in the five-dimensional space. Ge and Li (2003) discussed the existence of different regimes of gas – solid fluidized bed with the possibility of two minima for the N_{st} – one at $\varepsilon_c = \varepsilon_{mf}$ and the second at higher value of around 0.96 – 0.997. They varied the cluster voidage over the range from ε_{mf} to ε_{max}. The existence of minima at cluster voidage of ε_{mf} needs to be ascertained on the grounds of increase in energy consumption as ε_c tends to (or becomes lower than) ε_{mf}. Though in principle the cluster voidage ranges from ε_{min} to ε_{max}, it was varied from 0 to 1 to understand the mathematical behavior of the EMMS system of equations and the nature of solution obtained beyond acceptable limits. Contour plots of N_{st} were analyzed, keeping all but variable fixed, to infer the local minimum N_{st} with respect to the variable under consideration. The locus of local-minimum N_{st} was further analyzed for the global minima in the energy consumption profile with reference to cluster inertial term a_c, cluster voidage ε_c and cluster size d_{cl}. The base case simulation was done for air – sand 129μm - 2540 kg/m^3 system and drag coefficient for the constituent phases was calculated from Wen and Yu (1966). To maintain consistency with previous reported works on EMMS, Li (1994) cluster size was taken for base case simulations and dilute phase voidage was kept as 0.9997 in this study. The force balance equation for the dilute phase was simplified with a_f value as 2g. It should be noted that keeping all inertial terms as 2g corresponded to the basic framework of the EMMS model.

The variation of energy consumption ratio (N_{st}/N_t) with dimensionless cluster phase inertia (a_c/g) for superficial gas velocity 10m/s and solid flux 300 kg/m^{2}s is shown in Figure 2.7. The simulation was done at different assumed values of cluster phase voidage. Occurrence of local minima in the energy consumption with cluster phase inertial term was inferred at all assumed values of cluster voidage up to certain value (say ~0.97 in Figure 2.7). At still higher values of cluster voidage, energy consumption ratio increases with cluster phase inertial term.

The plot is re-drawn in terms of cluster voidage and shown in Figure 2.8. At lower values of a_c, minimum N_{st} is observed at higher values of cluster voidage with lowest possible cluster voidage assumed at 0.4. At higher values of a_c, distinct minimum with respect to cluster voidage was not observed (Figure 2.7 and 2.8). The minimum N_{st} shifts to lowest possible cluster voidage. For example at a_c > 10g, there was no distinct minimum N_{st} with cluster voidage for u_g = 10m/s and G_s = 300 kg/m^{2}s.

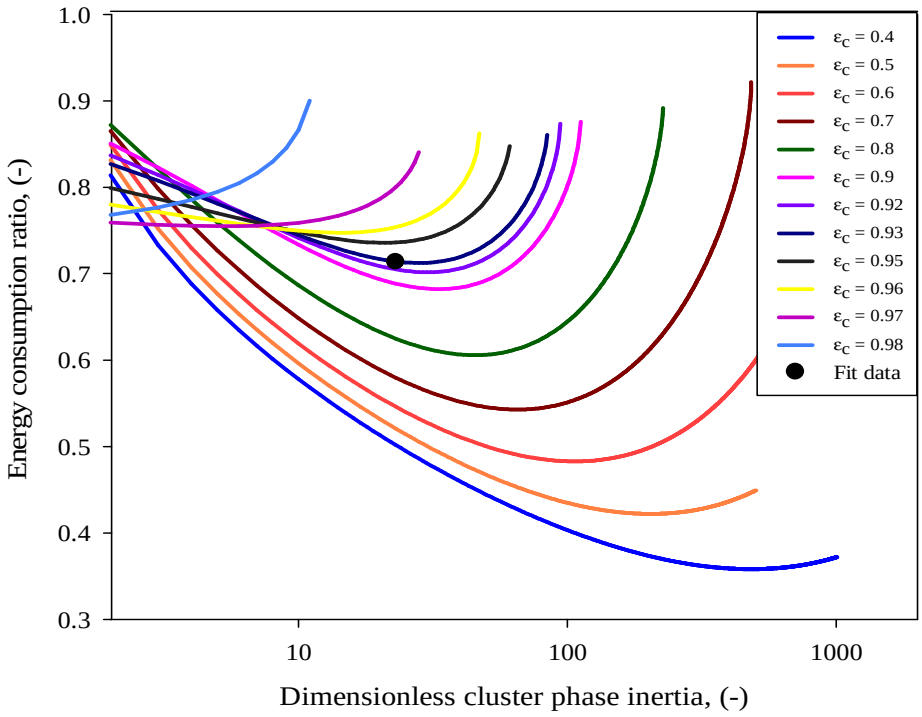

Figure 2.7: Variation of energy consumption ratio with dimensionless cluster phase inertia at different cluster voidage for u_g = 10 m/s and G_s = 300 kg/m^{2}s and at ε_f = 0.9997 and Li (1994) cluster size

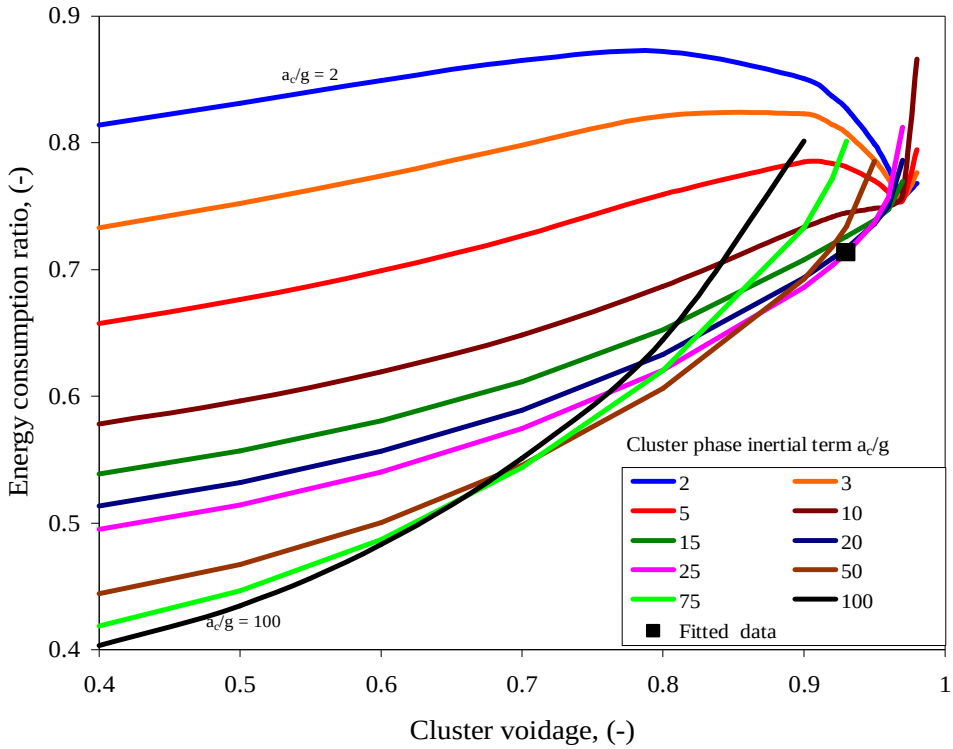

Figure 2.8: Variation of energy consumption ratio with cluster voidage at different dimensionless cluster phase inertia for u_g = 10 m/s and G_s = 300 kg/m^{2}s and at ε_f = 0.9997 and Li (1994) cluster size

Further, this local minimum N_{st} solution with cluster voidage was found to depend on the arbitrarily assumed value of lowest possible cluster voidage. To illustrate the same, the basic framework of the EMMS model with cluster inertia fixed at 2g was simulated. It was observed that the local minimum in the N_{st} with cluster voidage was found to be depended on the lowest minimum cluster voidage. A small shift in the lowest minimum cluster voidage, say from 0.4 to 0.5, (or called as choking point transition voidage in EMMS literature) would result in shifting of occurrence of the minimum N_{st} (Figure 2.9). For instance a change of lowest possible cluster voidage from 0.5 to 0.6 would shift in the critical choking solid circulation flux from G_s ~500 kg/m^2s to G_s ~ 600 kg/m^2s. Thus, with ambiguity in determination of this choking point transition or in EMMS terminology the particle-fluid compromise (PFC) to fluid dominance (FD), determination of critical solid flux remains an academic exercise. In the FD regime, the EMMS solution would correspond to the point of local minimum N_{st} with cluster voidage and in the PFC the EMMS solution would correspond to the lowest possible cluster voidage arbitrarily assumed in the model. Thus, the basic framework of the EMMS model without the inertial terms did not exhibit a distinct and explicit minimum in the N_{st} with cluster voidage.

In contrast, for a given value of cluster voidage, the extended model predicts explicit local minimum in N_{st} with respect to cluster phase inertial term (Figure 2.7). The points of minimum energy consumption correspond to the EMMS solution for the given operating condition. Further this did not require prior determination of choking point as the case with the basic EMMS framework. The dilute phase inertial term was found not to have very significant change in the result obtained and the point of local minimum N_{st} with cluster inertia was not affected by order of magnitude change in dilute phase inertial term. Hence for sake of simplicity, dilute phase inertial term was assumed at value of 2g for all further simulations (Figure 2.10).

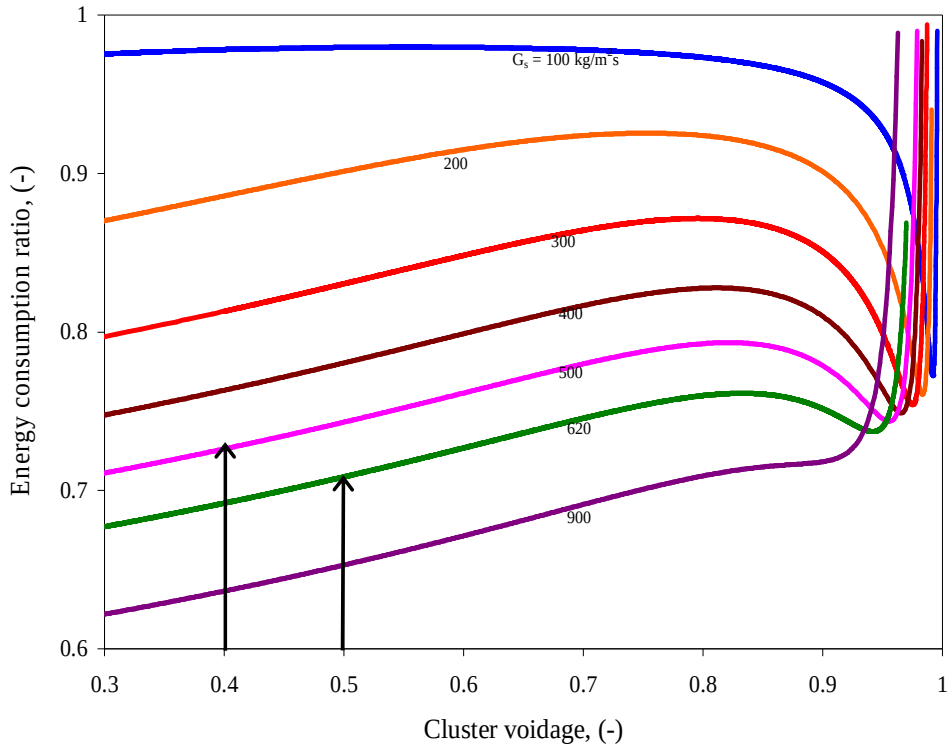

Figure 2.9: Variation of energy consumption ratio with cluster voidage at different solid circulation flux for u_g = 10m/s and Li (1994) cluster size, ε_f = 0.9997 and a_c = 2g

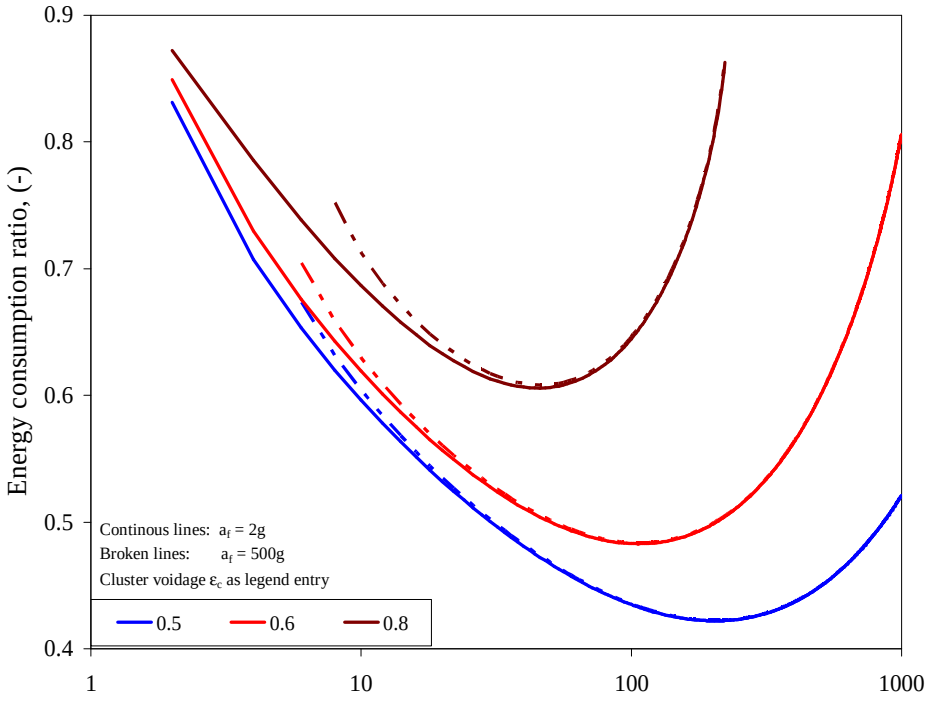

Figure 2.10: Variation of energy consumption ratio with dimensionless cluster phase inertia showing the effect of dilute phase intertial term (a_f): u_g = 10 m/s and G_s = 300 kg/m^{2}s and ε_c= 0.5-0.8, ε_f = 0.9997 and Li (1994) cluster size

To ascertain the global minima in the energy consumption, simulation was done for cluster voidage range from 0.3 – 0.8 and cluster size ratio (d_{cl}/d_p) of 25 – 1000. At each value of cluster size ratio and cluster voidage, local minimum in the energy consumption with respect to cluster phase inertia was determined. The variation of the cluster phase inertia corresponding to local minimum N_{st} ($a_c\big|_{Nst_{min}}$) is shown in Figure 2.11. For any set value of ε_c, the global minimum occurs at highest possible cluster size, not explicitly predicted from the EMMS model. The energy consumption ratio decreased monotonically with decrease in cluster voidage in the range 0.3 – 0.8. Further this observation was not affected by the operating condition (Figure 2.12). Thus, inclusion of an additional inertial term (a_c) showed improvement towards attainment of distinct energy minimization locally but not on global scale. Minimum energy consumption was observed only with a_c and not with ε_c and/or d_{cl}. The global minimum in the energy consumption occurs at the lowest possible cluster voidage and highest cluster size assumed in the EMMS framework.

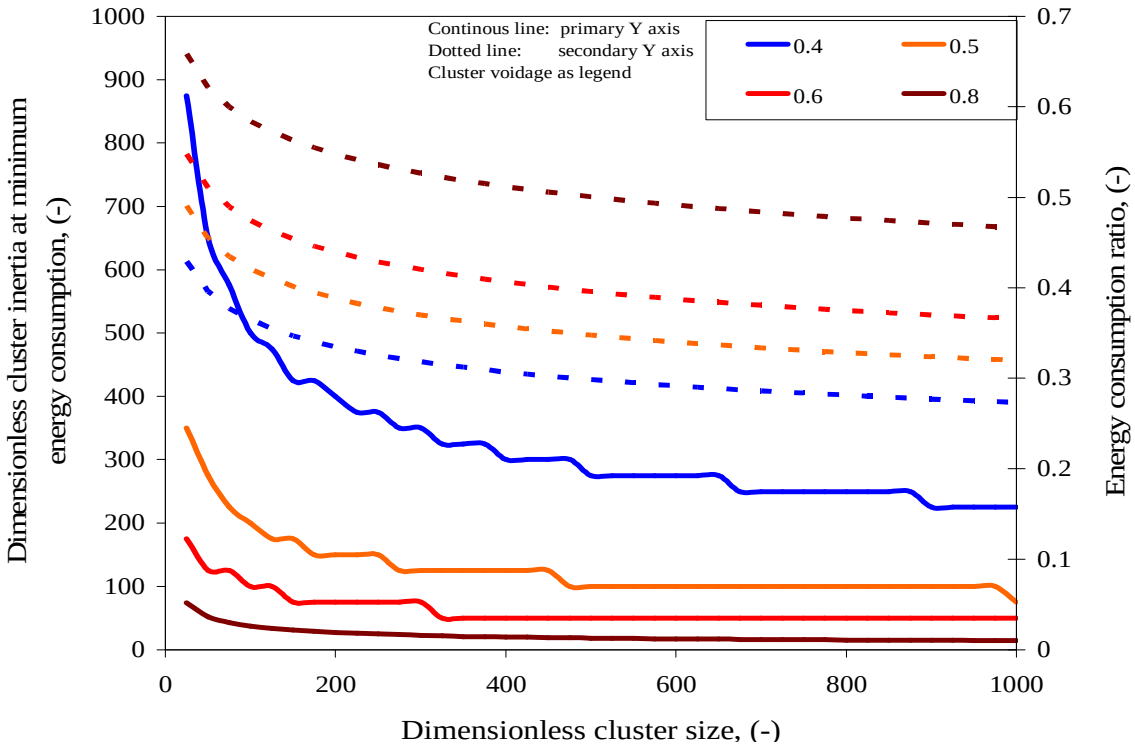

Figure 2.11: Variation of cluster inertia and corresponding minimum energy consumption ratio with cluster size at different cluster voidage for u_g = 10m/s and G_s = 300 kg/m^{2}s

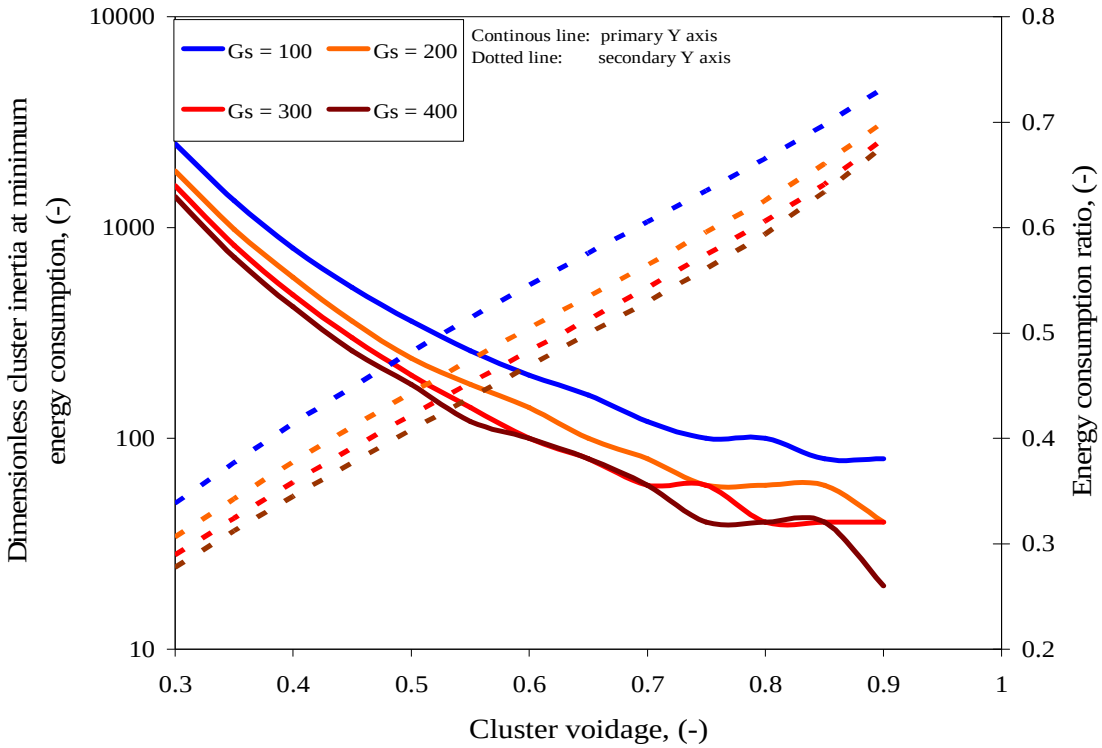

Figure 2.12: Variation of cluster inertia and corresponding energy consumption ratio with cluster voidage at different solid circulation flux and u_g = 10 m/s and Li (1994) cluster size

2.3.2. Sensitivity of Results with Dilute Phase Voidage

The EMMS framework sets the dilute phase voidage at the value of maximum voidage, stated as 0.9997. To ascertain the sensitivity of dilute phase voidage, the basic framework of EMMS model was simulated for air – solid riser system (ρ_p 2540 kg/m^3 and d_p 129μm) operated at solid circulation flux of 300 kg/m^{2}s and cluster phase inertia (a_c/g) set to 2. The dilute phase voidage was varied in the range from 0.999 – 0.9999. The effect of small perturbation in this value on the EMMS model was found to significantly affect the drag coefficient correction factor. For a 0.02% change in dilute phase voidage the effective drag coefficient correction factor increased by a factor of 2 (Figure 2.13a). The model is unstable with small perturbations in dilute phase voidage. The extreme sensitivity with respect to the assumed value of dilute phase voidage is certainly undesirable. Such extreme sensitivity of the EMMS model with the dilute phase voidage was due to the cluster size correlation employed in the EMMS approach. The sensitivity of the predicted cluster size following Li (1994) correlation with the dilute phase voidage is shown in Figure 2.13b. It was therefore essential to examine possibility of using alternative

correlations for estimating cluster sizes. This was examined and discussed in the following section.

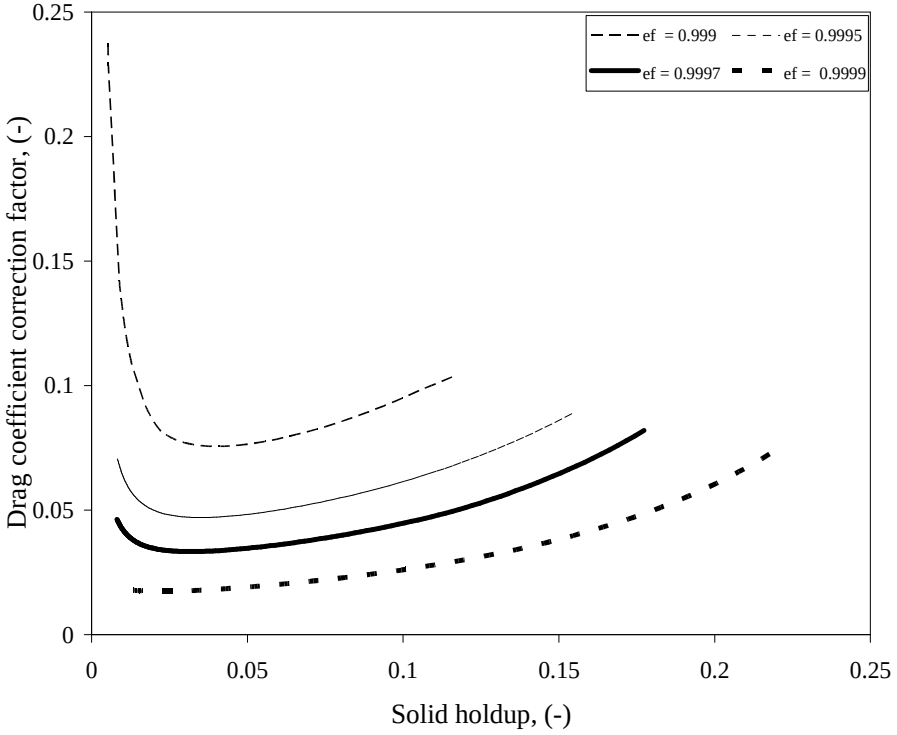

Figure 2.13a: Variation of drag coefficient correction factor with solid holdup for G_s = 300 kg/m^{2}s at different values of dilute phase voidage with Li (1994) cluster size and ε_c = 0.5, a_c = 2g

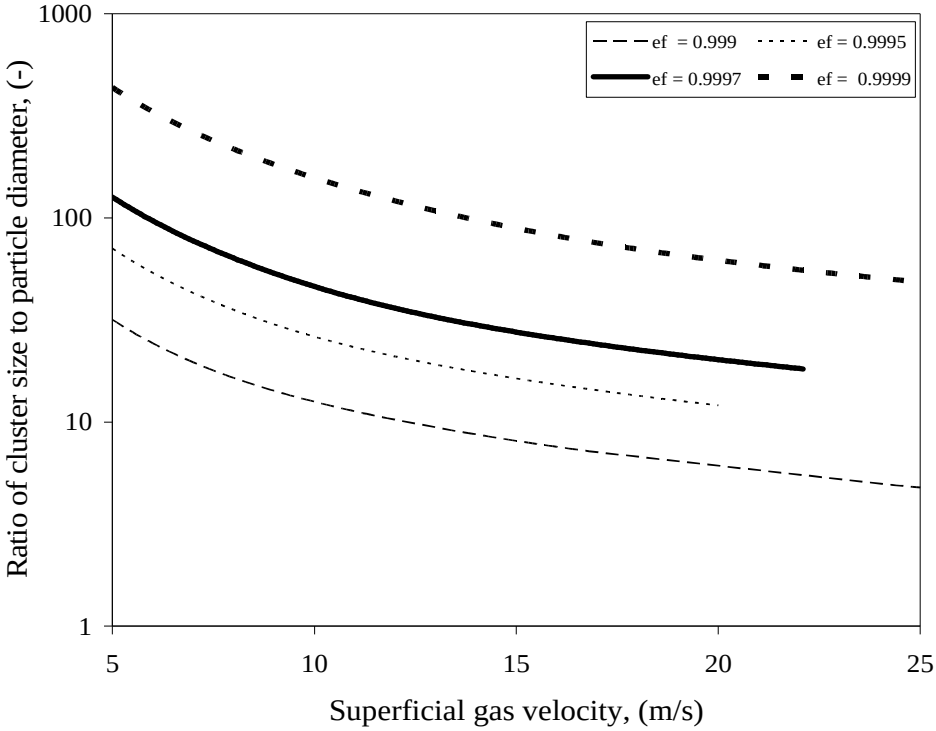

Figure 2.13b: Variation of cluster size as function of superficial gas velocity at G_s = 300 kg/m^{2}s at different values of dilute phase voidage with Li (1994) cluster size and ε_c = 0.5, a_c = 2g

2.3.3. Comparison of Cluster Size Predicted with EMMS Model with Reported Correlations

The cluster size correlation employed in EMMS model was based on empirically relating the cluster size with energy consumed for suspension and transport (Li, 1994). Several other cluster size correlations are available. For example, Harris *et al.* (2002) developed a set of correlations for mean cluster solids concentration (Equation 2.8), and cluster size (Equation 2.9), in terms of mean cross sectional averaged solids concentration as:

$$\overline{\varepsilon_{cl}} = \frac{0.58\overline{\varepsilon_s}^{1.48}}{0.013 + \overline{\varepsilon_s}^{1.48}} \tag{2.8}$$

$$\overline{d_{cl}} = \frac{\overline{\varepsilon_s}}{40.8 - 94.5\overline{\varepsilon_s}} \tag{2.9}$$

The cluster size in Equation (2.9) denotes the mean vertical cluster length in the near wall region of risers. Wei *et al.* (1995) have reported an empirical relation (Equation 2.10), for the radial cluster size, based on their own experimental data, in terms of local bed voidage and Reynolds number based on riser diameter. The experiments were carried out with air and FCC catalyst of 54μm and 1398 kg/m^3 on riser of 8m height and 0.186m inner diameter. The cluster size was determined by cross correlation technique on the data obtained from optical fiber image sensor. The experiments were done for the superficial gas velocity range of 1.2 to 8.5 m/s and solid circulation flux of 18 to 215 kg/m^{2}s.

$$\begin{aligned} r_{cl} &= A(1-\varepsilon)^B \, Re^{-C} \\ A &= 34.4 \pm 1.9 \\ B &= 0.61 \pm 0.02 \\ C &= 0.075 \end{aligned} \tag{2.10}$$

Zou *et al.* (1994) obtained an empirical correlation for dimensionless cluster size based on image analysis. The experiments were performed with air – FCC system (d_p 54 μm and ρ_p 929.5 kg/m^3) on 0.09 m diameter and 10 m height riser operated at superficial gas velocity of 1.3 – 3.5 m/s and solid circulation flux of 9 – 65 kg/m^{2}s. The Zou *et al.* (1994) correlation is given in Equation 2.11.

$$\frac{\overline{d_{cl}}}{d_p} = 1.8543\left[\frac{(1-\varepsilon)^{0.25}\ \varepsilon^{-1.5}}{(\varepsilon-\varepsilon_{mf})^{2.41}}\right]^{1.3889} + 1 \qquad (2.11)$$

Gu and Chen (1998) [as reported in Bi, 2002] gave the expression for cluster size as

$$d_{cl} = 1 + \left[\frac{0.027}{d_p} - 10\right](1-\varepsilon) + \frac{32}{d_p}(1-\varepsilon)^6 \qquad (2.12)$$

It is obviously evident that these cluster size correlations do not depend on dilute phase voidage and hence not sensitive to the dilute phase voidage. For instance, drag coefficient correction factor computed with Harris *et al.* (2002) and Wei *et al.* (1995) did not exhibit sensitivity with dilute phase voidage (Figure 2.14 and 2.15). The dilute phase voidage was found not to affect the predicted overall solid holdup/cluster fraction. Usage of appropriate correlations for the cluster size in the EMMS framework was therefore critical. The observed sensitivity with dilute phase voidage (discussed in the previous section) was not inherent of the model but was because of the choice of the cluster correlation of Li (1994).

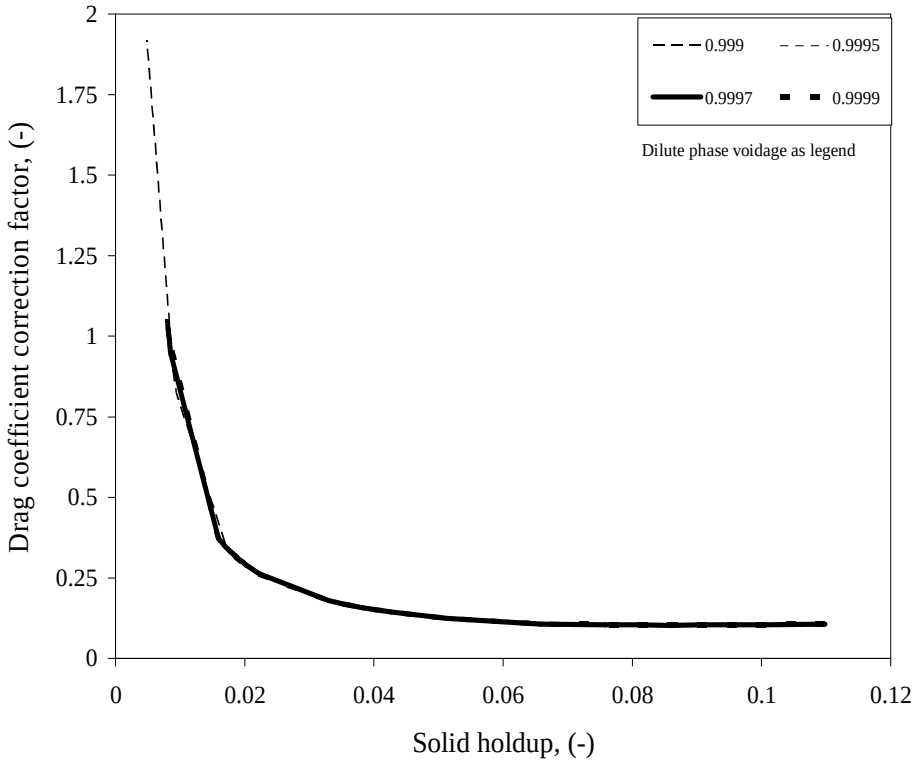

Figure 2.14: Variation of drag coefficient correction factor with solid holdup for G_s = 300 kg/m^{2}s at different values of dilute phase voidage with Harris *et al.* (2002) cluster size and ε_c = 0.5, a_c = 2g

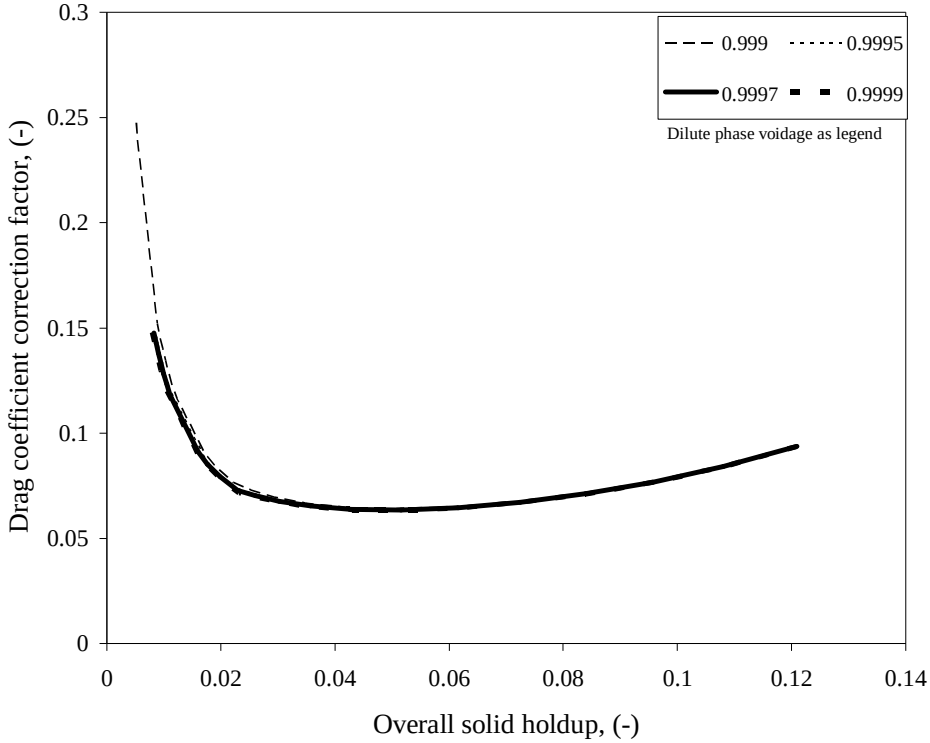

Figure 2.15: Variation of drag coefficient correction factor with solid holdup for G_s = 300 kg/m^{2}s at different values of dilute phase voidage with Wei *et al.* (1995) cluster size and ε_c = 0.5, a_c = 2g

2.3.4. Comparison of EMMS Model Pressure Drop with Experimental Pressure Drop Values

Comparison of reported experimental fully developed pressure drop values in gas – solid CFB with the pressure drop value from EMMS model was done to assess the EMMS approach. The literature data used for pressure drop evaluation were selected to see that location of pressure drop measurement was in the fully developed region. For data wherein axial pressure gradient profile was reported in the literature, the pressure drop corresponding to the fully developed region was considered in this study. The details of the reported experimental pressure drop data is tabulated in Table 2.3.

The extended EMMS model was simulated with set value of cluster voidage and cluster size given by Li (1994) to obtain local minimum in the energy consumption with cluster phase inertial term. From the knowledge of cluster fraction computed from extended EMMS model (solution point corresponding to minimum energy consumption with respect to cluster phase inertia), the solid holdup was determined from overall mass balance. Subsequently the pressure drop was computed from the overall solid holdup value, ignoring the frictional resistance. The pressure drop from the solution corresponding to minimum energy consumption was compared against the reported data (Figure 2.16a and 2.16b) of Nieuwland (1994). The EMMS solution corresponds to minimum N_{st} against a_c for each ε_c (minimum point on each curve of Figure 2.7). The extended model was found to poorly predict the experimental pressure drop at any assumed value of cluster voidage. This shows that cluster voidage cannot be set at constant value independent of operating conditions. This was in agreement with the correlation of Harris *et al.* (2002) that showed cluster voidage to be function of overall solid holdup.

The basic framework of the EMMS model with $a_c = 2g$ also suffered from poor prediction of literature pressure drop value (Figure 2.17). It must be note worthy to recollect that the basic framework of the EMMS model do not signify the minimum N_{st} and depend of the arbitrarily set value of lowest cluster voidage (0.5 for this case).

Table 2.3: Literature data used for EMMS model evaluation

Sno	Reference	Riser Dimensions	Particle Properties	Superficial gas velocity m/s	Solid circulation flux, kg/m^{2}s
1.	Nieuwland (1994)	H = 3m i.d. = 0.03 m D/d_p = 45.8	Glass beads ρ_p = 2900 kg/m^3 d_p = 655 μm Ar = 30.0439 u_{ter} = 5.288 m/s	12.3	105 – 300
2.	Nieuwland$^+$ (1994)	H = 8m i.d. = 0.054m D/d_p = 418.6	FCC ρ_p = 2540 kg/m^3 d_p = 129 μm Ar = 5.7534 u_{ter} = 0.77 m/s	10	100 – 400
3.	Monceaux *et al.* (1986) [as reported in Dasgupta *et al.*, 1998]	H = N.A. i.d = 0.144m D/d_p = 2441	FCC ρ_p = 1385 kg/m^3 d_p = 59 μm Ar = 2.12 u_{ter} ~ 0.133 m/s	4.6	50 – 250
4.	Yerushalmi (1986) [as reported in Dasgupta *et al.*, 1998]	H = N.A. i.d = 0.152 m D/d_p = 3102	FCC ρ_p = 1070 kg/m^3 d_p = 49 μm Ar =1.6168 u_{ter} = 0.073177	2.2 and 4	50 – 250
5.	Bader *et al.* (1988). [as reported by Obrien and Syamlal, 1994]	H = 12.2 m i.d. = 0.305 m D/d_p = 4013	Sand ρ_p = 1714 kg/m^3 d_p = 76 μm Ar = 3.404548 U_{ter} ~ 0.236 m/s	3.7 – 10	98 and 147
6.	Yerushalmi *et al.* (1976)	H = 7.0104 m i.d. = 0.0762 m D/d_p = 1270	FCC ρ_p = 881 kg/m^3 d_p = 60 μm Ar = 2.2 u_{ter} ~ 0.086 m/s	1.8 -4.5	20 – 220
7.	Herbert *et al.*$^+$ (1998)	Downer H = 4.6 m i.d. = 0.05 m D/d_p = 667	FCC ρ_p = 1400 kg/m^3 d_p = 75 μm Ar = 2.71 u_{ter} = 0.203 m/s	0.4 – 6.1	79 and 92
8.	Huang *et al.* (2007)	H = 15.1 m i.d. = 0.1 m D/d_p = 1493	FCC ρ_p = 1500 kg/m^3 d_p = 67 μm Ar = 2.474 u_{ter} = 0.179	2.5 - 10	38 – 220
11.	Qi *et al.* (2008)	H = 15.1 m i.d. = 0.1 m D/d_p = 1493	FCC ρ_p = 1500 kg/m^3 d_p = 67 μm Ar = 2.474 u_{ter} = 0.179	3 – 12	24 – 225
N.A.	Not Available				
+	Pressure drop obtained from axial pressure gradient profile at fully developed region.				

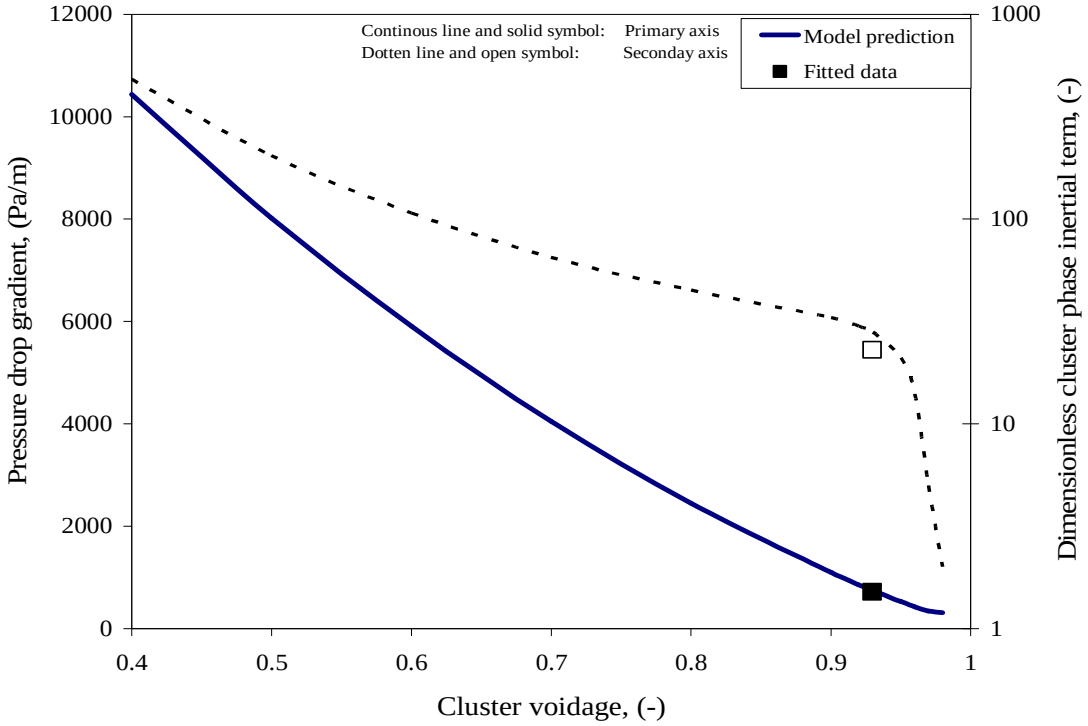

Figure 2.16a: Variation of pressure drop gradient and dimensionless cluster phase inertia at minimum energy consumption with cluster voidage at u_g = 10m/s and G_s = 300 kg/m^{2}s with Li (1994) cluster size and ε_f = 0.9997. Symbols show model fitted to data of Nieuwland (1994)

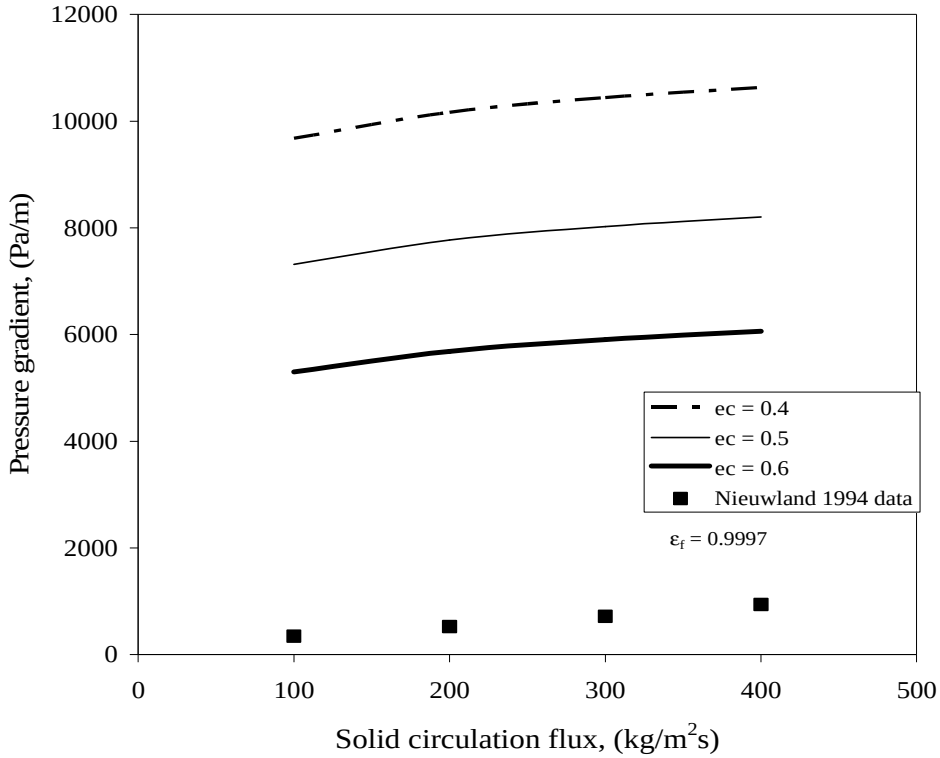

Figure 2.16b: Comparison of predicted pressure gradient at minimum N_{st} with Li (1994) cluster size, ε_f = 0.9997 and at different cluster voidage for Nieuwland (1994) data at u_g = 10 m/s

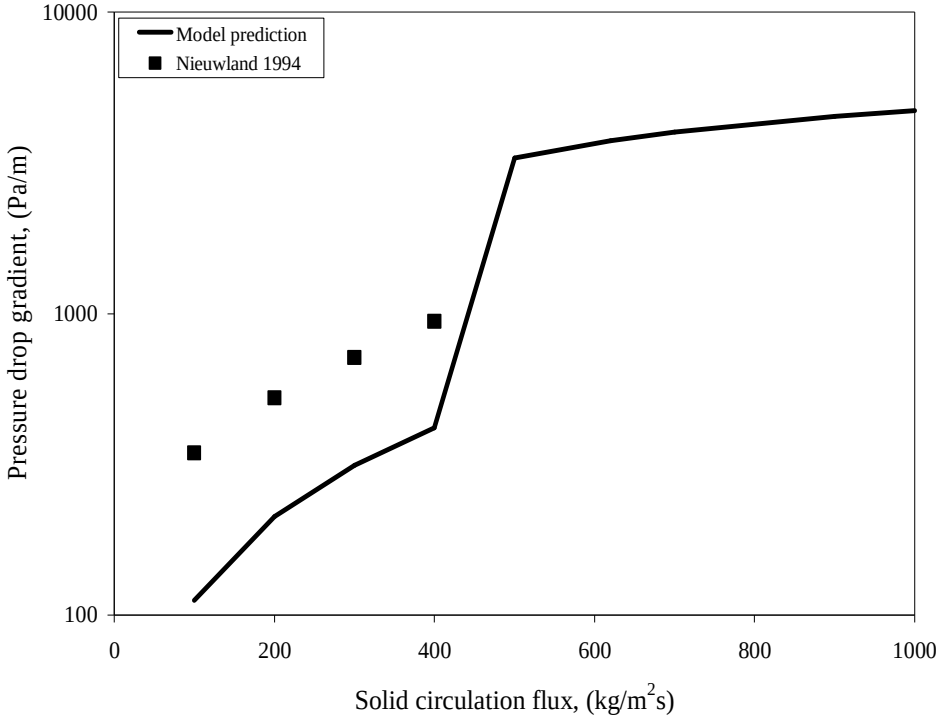

Figure 2.17: Pressure drop gradient as function of solid circulation flux with EMMS model predictions with Li (1994) cluster size, $\varepsilon_f = 0.9997$ and $a_c = 2g$ for Nieuwland (1994) data at $u_g = 10m/s$

While interpreting these results, it should be noted that the gas-solid flow in riser exhibits significant radial heterogeneity at high solid fluxes. To account for such radial heterogeneity, the EMMS model was applied with a core-annulus framework for simulating gas-solid flows in risers. The details of core-annulus framework are discussed in Annexure 2B. However, even with the core – annulus framework which accounts for radial heterogeneity, the predictions of the EMMS model did not change significantly and therefore could not successfully predict the experimental data of pressure drop.

The EMMS model was further tested by comparing predicted results for the downward gas-solid flows. Downers exhibit nearly uniform radial profile with minimal boundary effects. The comparison of the predicted pressure drop from the basic EMMS framework with $a_c = 2g$ with experimental downer data of Herbert *et al.* (1998) is shown in Figure 2.18a and Figure 2.18b. It can be seen that despite the radial uniformity in downers, the predicted pressure drop was significantly higher than the experimental data. It is known that effect of skin friction in downer flows is

larger than in riser. However its contribution in predicting pressure drop was negligible (less than 10% up to superficial gas velocity of 5m/s) in comparison with the order of magnitude difference observed between the predicted and reported values. Direct comparison of predicted overall solid holdup with the reported values of Herbert *et al.* (1998) also showed significant difference. These observations supported the conjecture that methodology of fixed cluster parameters like voidage or size required to be investigated in the EMMS framework.

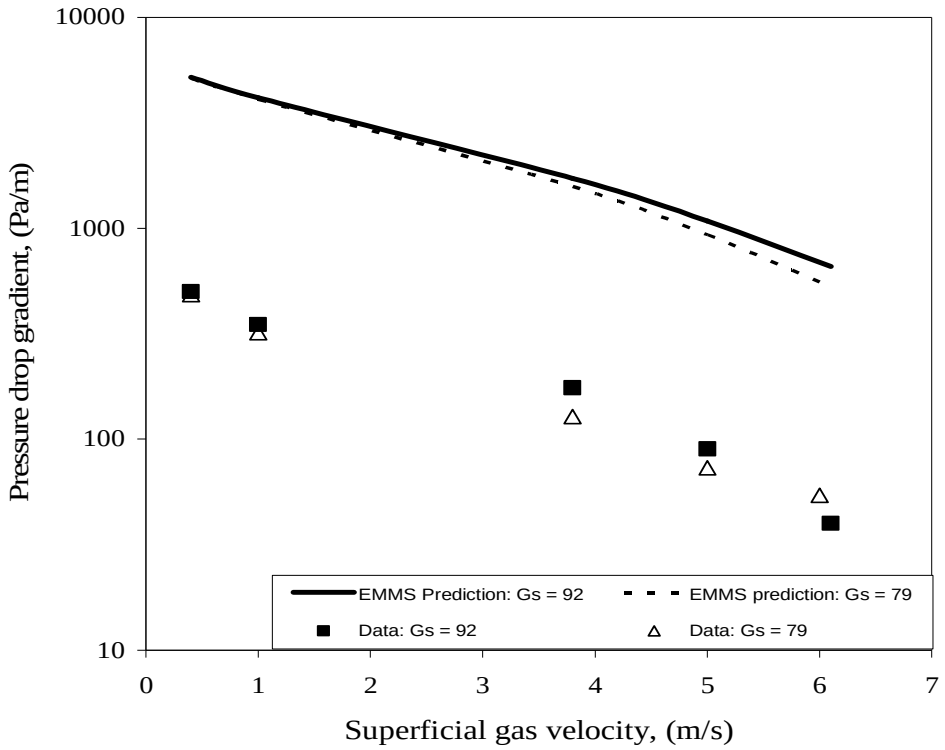

Figure 2.18a: Pressure drop gradient as function of superficial gas velocity with EMMS model predictions for Herbert *et al.* (1998) downer system with $a_c = 2g$, $\varepsilon_c = 0.5$ and $\varepsilon_f = 0.9997$

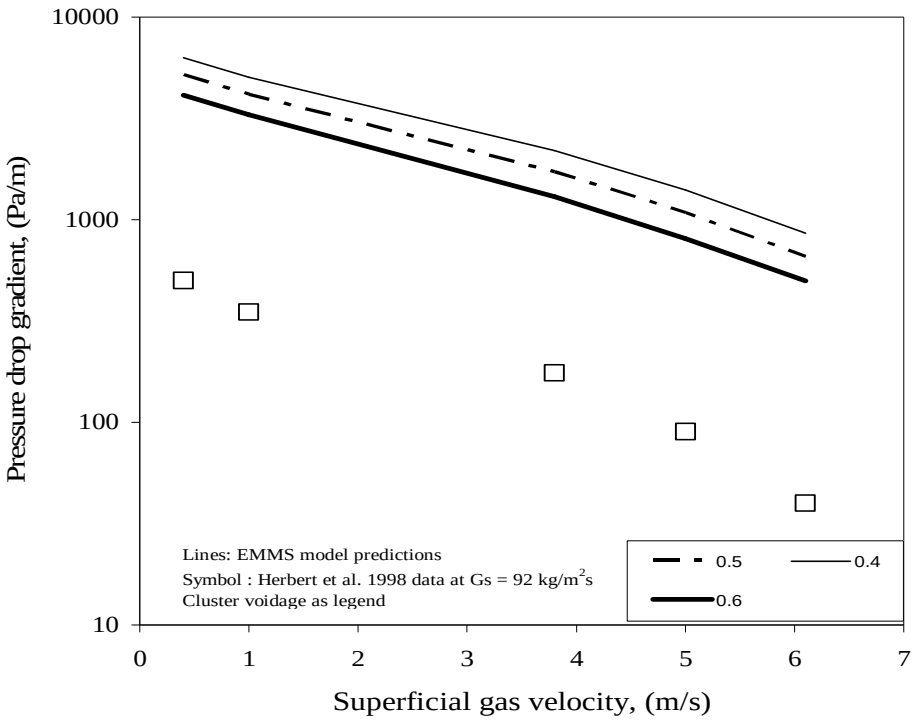

Figure 2.18b: Pressure drop gradient as function of superficial gas velocity with EMMS model predictions for Herbert *et al.* (1998) downer system at G_s = 92 kg/m^{2}s and with a_c = 2g, ε_f = 0.9997 and Li (1994) cluster size

The poor prediction of EMMS pressure drop with literature data, motivated to adjust one of the model parameters to match the literature data. The extended EMMS model has 5 degrees of freedom to arrive at the solution corresponding to minimum energy consumption. For the given operating condition of superficial gas velocity and solid circulation flux, dilute phase voidage (ε_f) was assumed. The dilute phase inertial term (a_f) was fixed at value of 2g for brevity as it was found not significantly alter the solution. Eventually, 3 degrees of freedom (ε_c, d_{cl} and a_c) could be fitted to arrive at EMMS solution of minimum energy consumption that fits the literature pressure drop.

In the first case, the cluster voidage was fitted to match the literature pressure drop and cluster size was determined from Li (1994) relation. The exercise of fitting the cluster voidage to match the experimental pressure drop also guaranteed the energy minimization criteria of the EMMS framework. At given overall solid holdup, the fitted cluster voidage correspond to minimum N_{st} as shown in Figure 2.19. It should that attempt of fitting cluster voidage with experimental data, for the EMMS model without the inertial term (a_c = 2g) destroyed the energy minimization framework of the EMMS model as shown by the fitted data in Figure 2.20. The fitted curve does not guarantee the minimum in N_{st}. The extended EMMS model with additional degrees of freedom guaranteed energy minimization in conjure with prediction of experimental data. The fitted data point ensured local minima in N_{st} with a_c as shown in Figure 2.19.

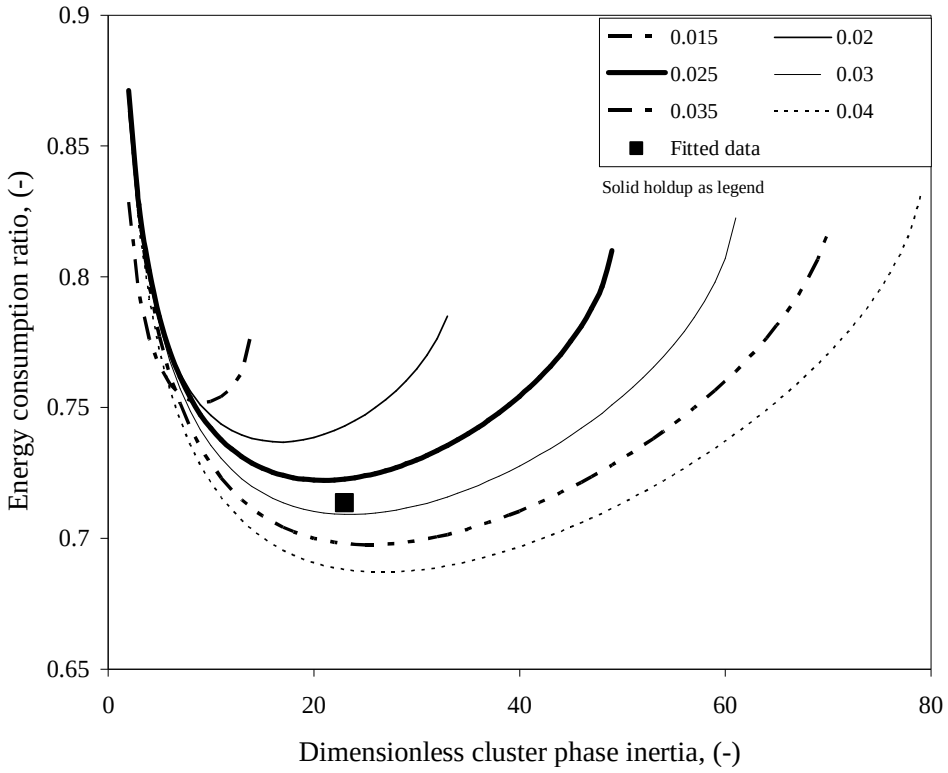

Figure 2.19: Variation of energy consumption ratio with cluster phase inertial term at different solid holdup with Li (1994) cluster size for Nieuwland (1994) data at u_g = 10 m/s and G_s = 300 kg/m^{2}s

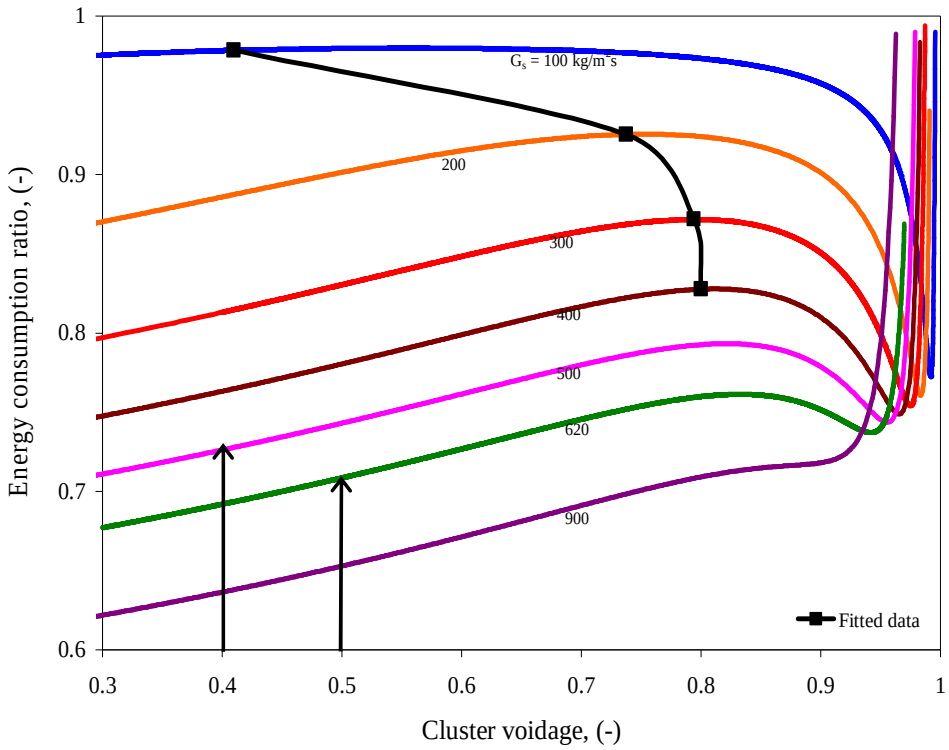

Figure 2.20: Variation of energy consumption ratio with cluster voidage at different solid circulation flux for u_g = 10m/s and Li (1994) cluster size, ε_f = 0.9997 and a_c = 2g and the data fitted to Nieuwland (1994) system

The procedure of fitting cluster voidage was sensitive to the dilute phase voidage owing to the cluster size correlation (Li, 1994) employed in the EMMS model (Figure 2.21). Hence, appropriate correlations for cluster size needs to be used in the EMMS framework that avoids such undue sensitivity with dilute phase voidage. Following discussions made earlier, Harris *et al.* (2002) correlation was also used to correlate cluster size with solid holdup in the EMMS model. Before this, an exercise was carried out to ensure that the method of fitting cluster voidage guaranteed local minimum N_{st} at all values of cluster size. The effect of cluster size on the fitted cluster voidage and the energy consumption ratio is shown in Figure 2.22 and Figure 2.23. At each cluster size ratio, the overall solid holdup was held constant at reported experimental value (solid holdup or pressure drop). The cluster voidage was fitted for various assumed a_c values. The EMMS solution would correspond to point of minimum N_{st} with a_c. For any given cluster size value, explicit minimum energy consumption with a_c was observed, but the global attainment of minimum energy

consumption was observed at highest possible cluster size. Thus, the cluster size retains its key significance in model predictions.

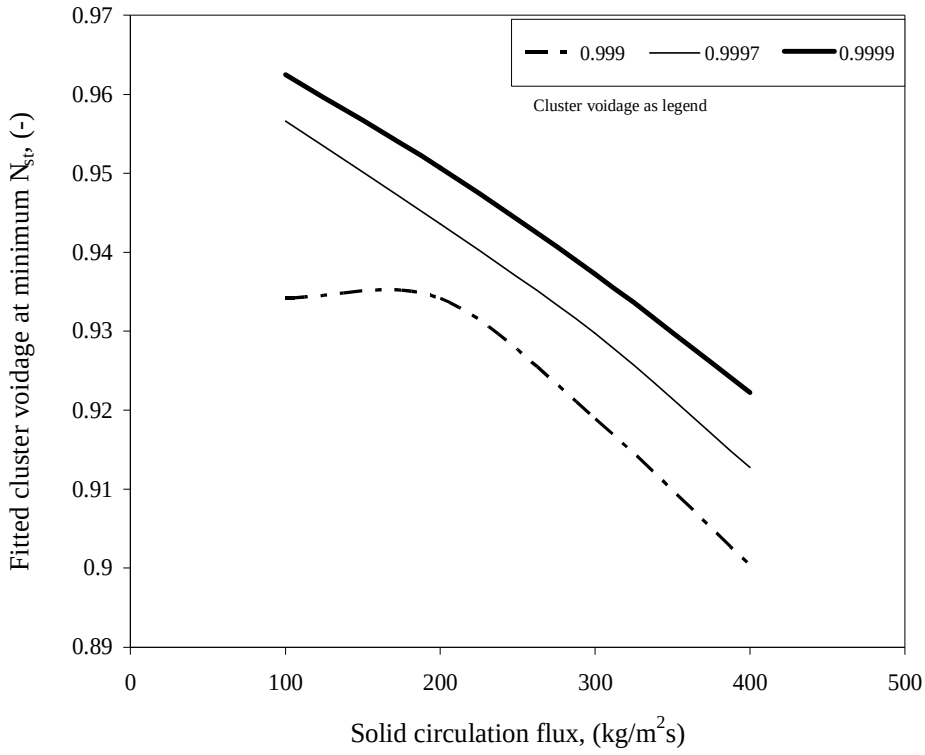

Figure 2.21: Variation of fitted cluster voidage at minimum N_{st} with solid circulation flux for Nieuwland (1994) data at u_g = 10m/s with Li (1994) cluster size and different values of dilute phase voidage

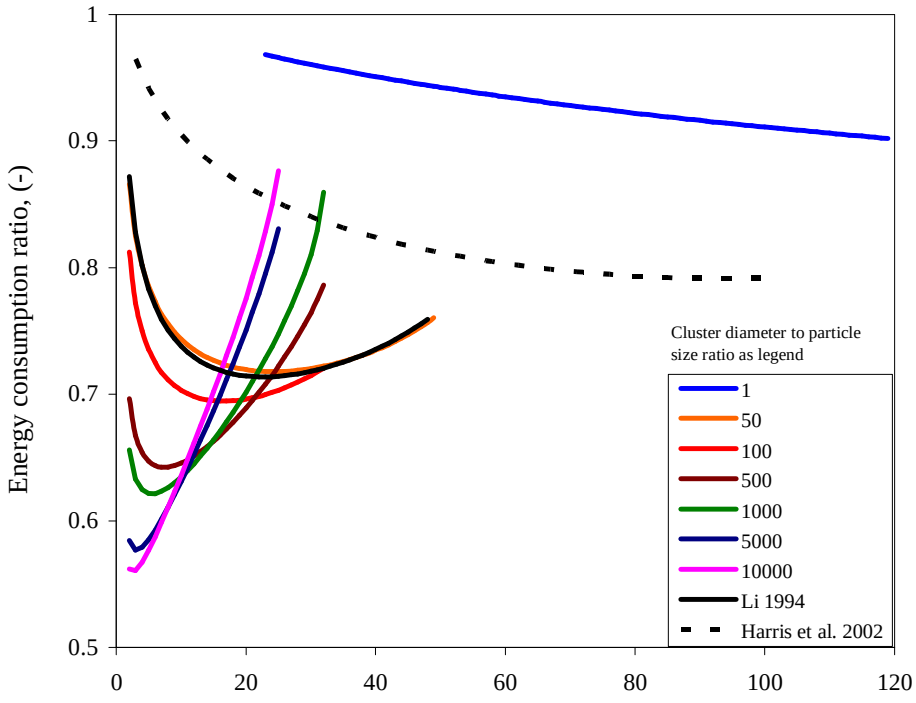

Figure 2.22: Variation of energy consumption ratio at fitted cluster voidage with dimensionless cluster phase inertia at different cluster size ratio for Nieuwland (1994) data at u_g = 10m/s and G_s = 300 kg/m^{2}s

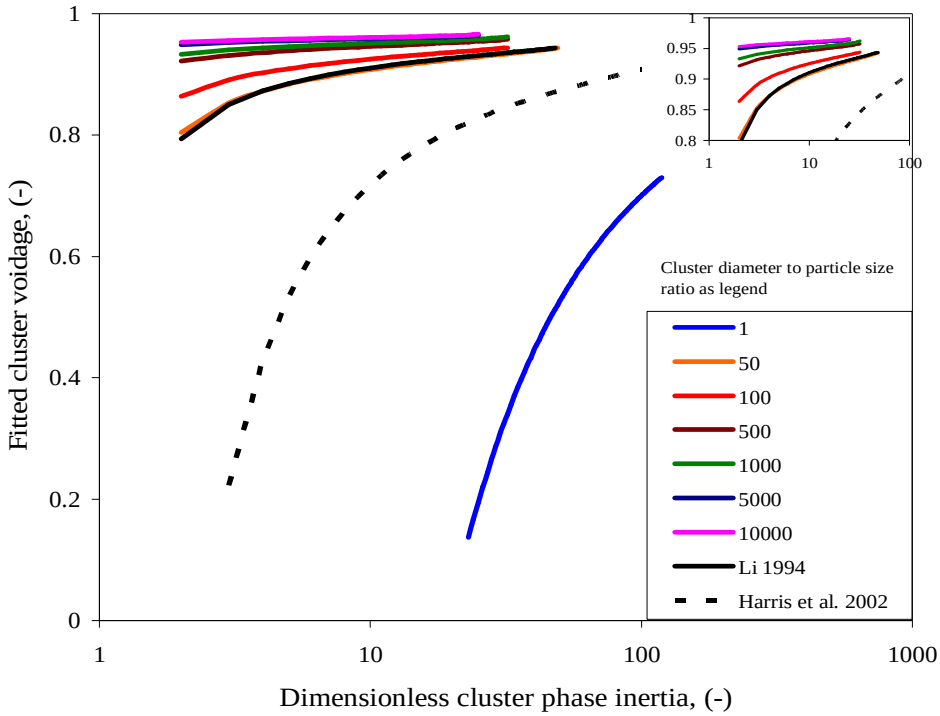

Figure 2.23: Variation of fitted cluster voidage with dimensionless cluster phase inertia at different cluster size ratio for Nieuwland (1994) data at u_g = 10m/s and G_s = 300 kg/m^{2}s

In the second attempt, the cluster size was fitted to match the experimental pressure drop data for assumed cluster voidage value. For given cluster voidage, the energy consumption profile did not show occurrence of minimum value with a_c (Figure 2.24). There was no significant change in N_{st} with the fitted cluster size. This was obvious as a_c affects the force balance of particles within a single cluster rather than that of cluster as whole. Also at large values of a_c (say ~45 for ε_c of 0.5), the fitted cluster size ratio was less than 1, which is physically not realistic. Thus fitting cluster size to match with experimental pressure drop at assumed cluster voidage proved to be not very useful. For the same reasons, optimizing all three parameters to obtain minimum energy consumption solution that fits the experimental data was also not possible. Hence all further results were obtained by adjustment of cluster voidage for pre-specified cluster size values.

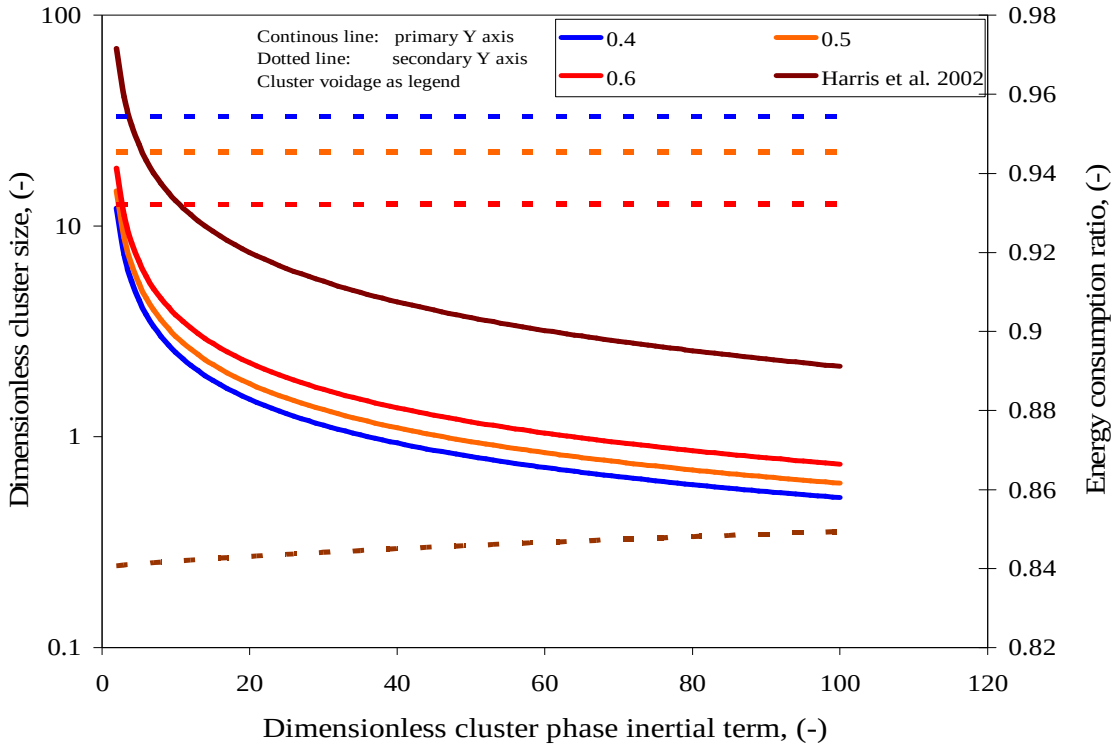

Figure 2.24: Variation of fitted dimensionless cluster size and corresponding energy consumption ratio with cluster phase inertia at different cluster voidage for Nieuwland (1994) data: u_g = 10m/s and G_s = 300 kg/m^{2}s

The dependency of the fitted cluster voidage was also ascertained with the cluster size correlation used in the model. The cluster size was obtained from either the Harris *et al.* (2002) or Li (1994) correlation. Figure 2.25 shows functionalized dependence of cluster voidage with respect to the overall solid holdup. The clusters are more loosely packed as against the clusters predicted from Harris *et al.* (2002) ε_c correlation (Equation 2.8). With the given scatter in the available literature data, the fitted cluster voidage was found not to be significantly dependent on the cluster size correlation used in the model. However the cluster phase inertia term at minimum energy consumption was dependent on the cluster size relation (Figure 2.26). The fitted cluster voidage ensured local minima in N_{st} for all the data sets tested (Figure 2.27a to 2.28b). Thus the procedure of tuning cluster voidage to match the experimental value within the extended EMMS model framework kept intact the energy minimization postulate and also showed improvement in predicting the experimental data over earlier EMMS framework without inertial terms.

The fitted cluster voidage and cluster phase inertial term computed based on Harris *et al.* (2002) cluster size, was correlated with the overall solid holdup (Figure 2.25 and 2.26) following least square algorithm as

$$\varepsilon_c = 2.0519\varepsilon_s^{\,2} - 1.9325\,\varepsilon_s + 0.9661 \qquad (2.13)$$

$$\ln\left(\frac{a_c/g}{\varepsilon_s}\right) = 3.9758\,\varepsilon_s^{\,-0.2012} \qquad (2.14)$$

Equation 2.13 and 2.14 were incorporated into the EMMS model and the pressure drop was predicted again from the extended EMMS model with these developed regression expressions. The predicted pressure drop from the model is compared with the experimental data (Figures 2.30a – 2.30f). The predictive capability of the model improved with these correlations but consistent results were not obtained at all operating conditions. Parity plot for the pressure drop computed from the extended EMMS model predictions is shown in (Figure 2.31a). It is clearly demonstrated that the EMMS model did not significantly improve the predictions in comparison with already available methods for pressure drop or solid holdup predictions (Figure 2.31b and 2.31c). Despite keeping intact the energy minimization postulate and fitting the

cluster voidage to experimental data, the percentage deviations as high as 35% were observed with the EMMS framework. With these large deviations, it might not be justifiable to employ EMMS based multi scale approach over the other available methods or correlations.

In conclusion, the extended EMMS model with inclusion of inertial term promises the attainment of distinct local minimum energy consumption for given operating condition and assumed values of cluster voidage and cluster size. These points of local minimum energy consumption could not predict the experimental pressure drop data and the model parameters require to be adjustment to predict experimental data. The dilute phase inertial term a_f can be omitted from the extended model as this was not found to have any significant effect on model predictions. Further development of extended EMMS model is required to enable to achieve minimum energy consumption on a global scale with respect to cluster voidage and/or cluster size. Attempt of fitting cluster voidage to match the experimental pressure drop data also ensured energy minimization principle of the EMMS framework. Cluster size representation plays a significant role in predicting the drag coefficient from the model. Correlation developed for fitted parameters needs further introspection for successful predictions and for reducing the large percentage deviations. Given the current state of the extended EMMS model with local minimum N_{st} and fitted cluster voidage, no significant benefit was obtained over already reported correlations. Although the EMMS approach looks promising with multiscale approach for estimating interphase momentum transfer coefficient, considering the aforementioned evaluation and observations, the usage of EMMS model in the two-fluid CFD model framework appears to be not justifiable.

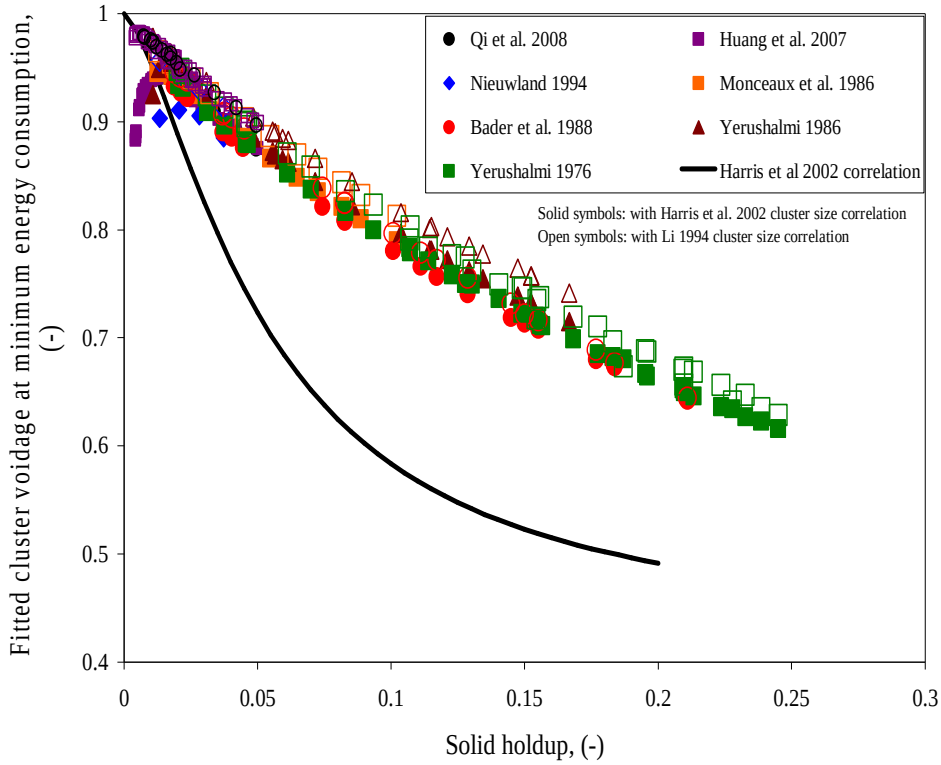

Figure 2.25: Variation of fitted cluster voidage at minimum N_{st} with overall solid holdup and with different cluster size correlations employed in EMMS framework

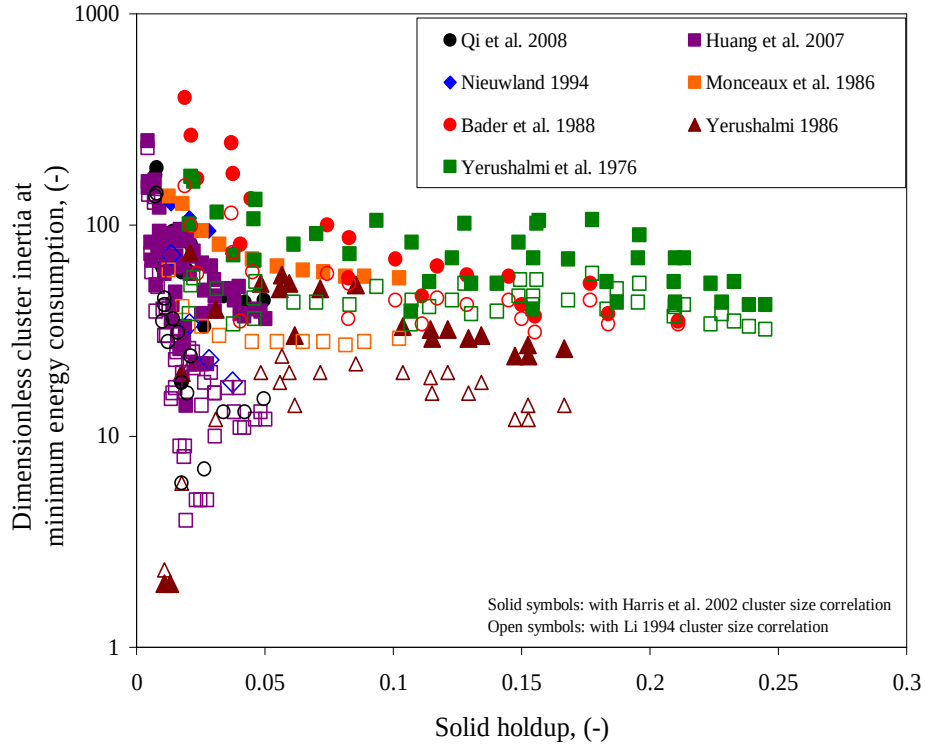

Figure 2.26: Variation of cluster phase inertia at minimum N_{st} with overall solid holdup and with different cluster size correlations employed in EMMS framework

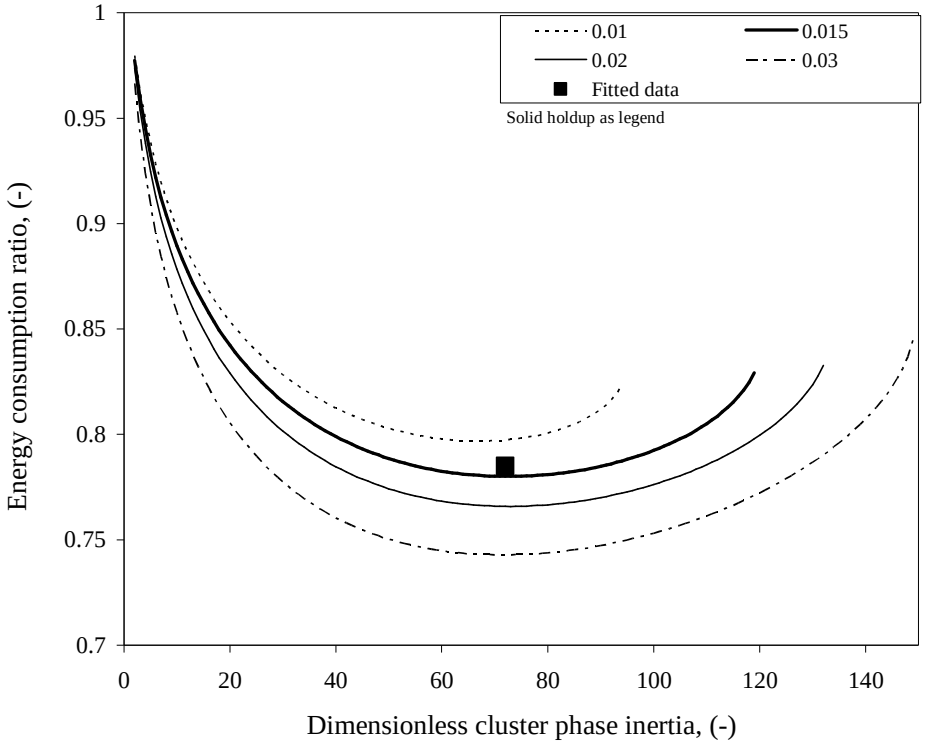

Figure 2.27a: Variation of energy consumption ratio with cluster phase inertial term at different solid holdup with Li (1994) cluster size for Nieuwland (1994) data at u_g = 10 m/s and G_s = 100 kg/m^{2}s

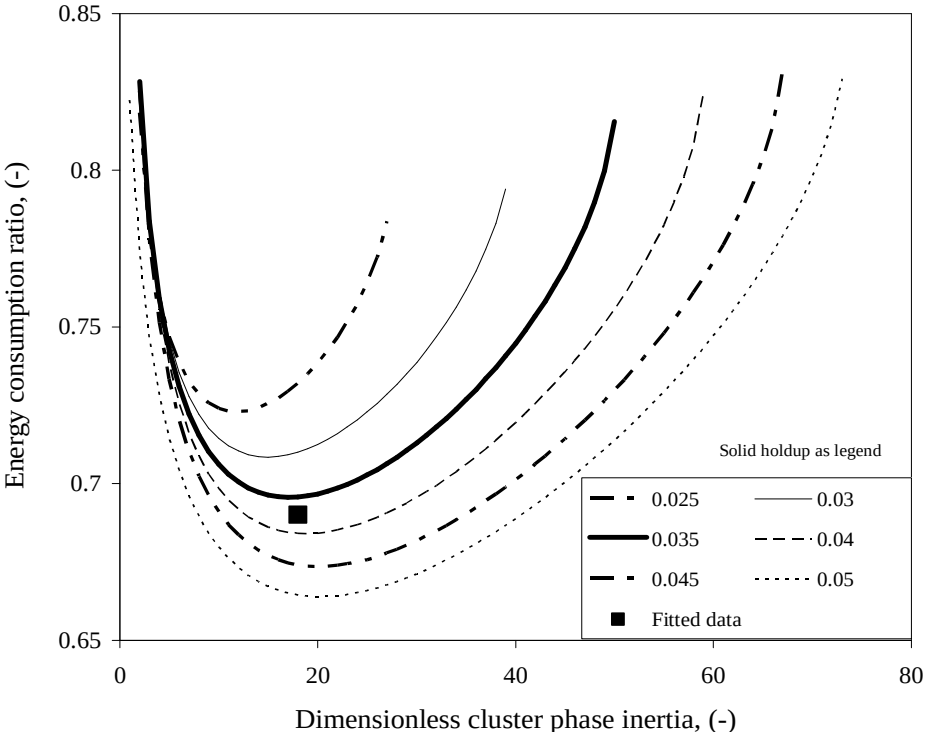

Figure 2.27b: Variation of energy consumption ratio with cluster phase inertial term at different solid holdup with Li (1994) cluster size for Nieuwland (1994) data at u_g = 10 m/s and G_s = 400 kg/m^{2}s

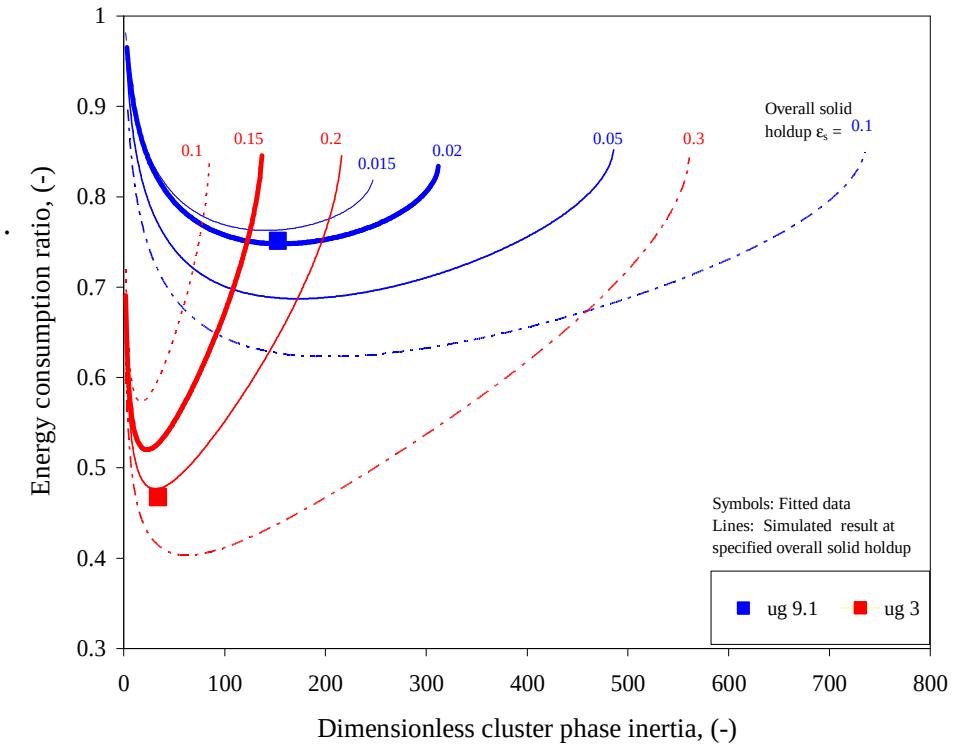

Figure 2.28a: Variation of energy consumption ratio with dimensionless cluster phase inertia at different solid holdup with Li (1994) cluster size for Bader *et al.* (1988) data at G_s = 98 kg/m^{2}s

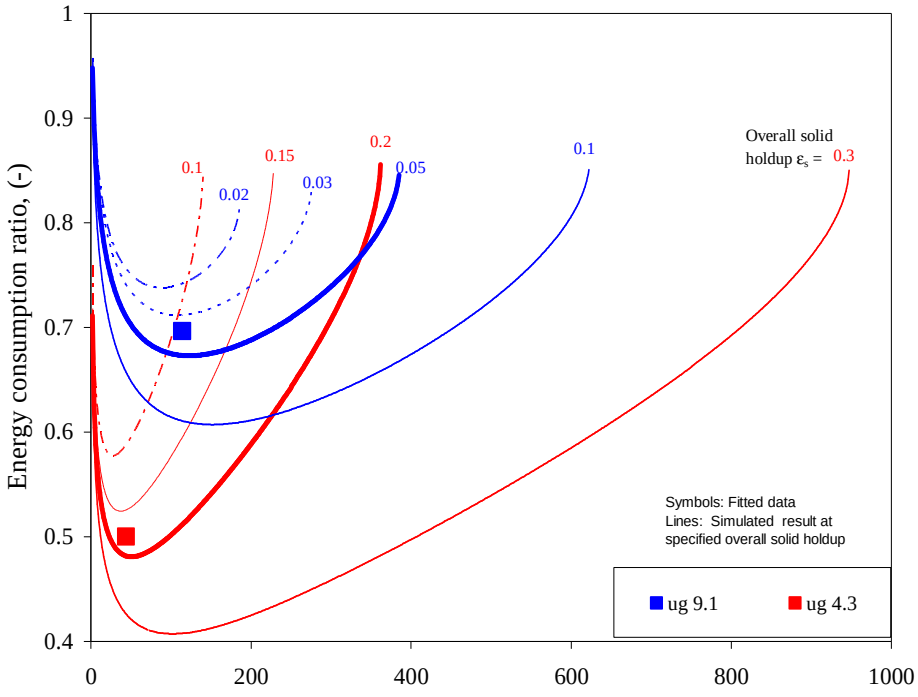

Figure 2.28b: Variation of energy consumption ratio with dimensionless cluster phase inertia at different solid holdup with Li (1994) cluster size for Bader *et al.* (1988) data at G_s = 147 kg/m^{2}s

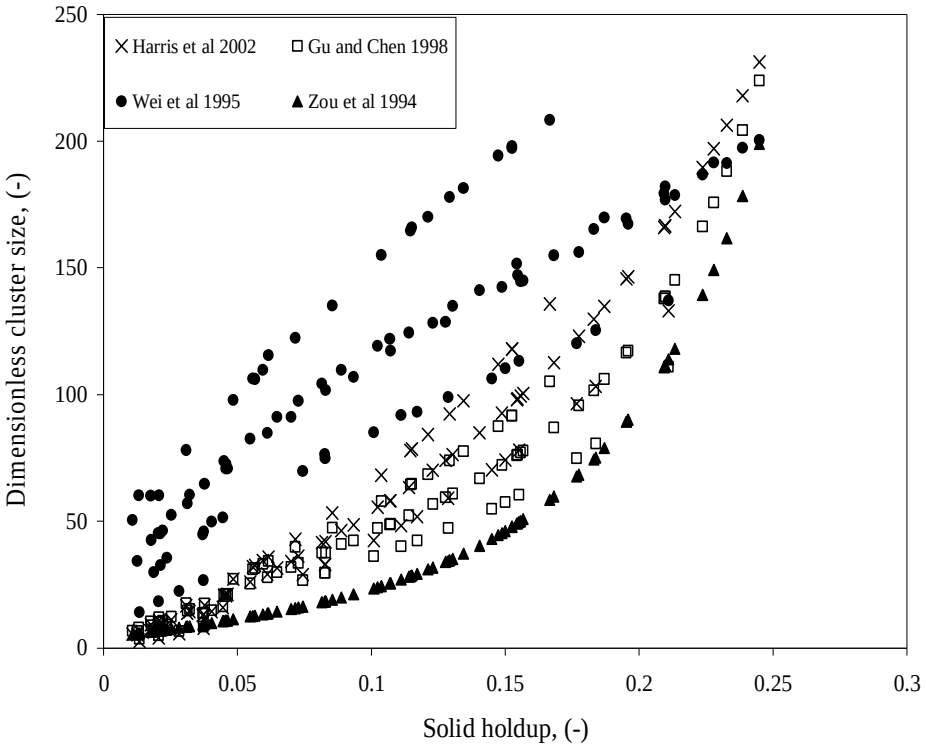

Figure 2.29: Dimensionless cluster size as function of overall solid holdup for the experimental data sets

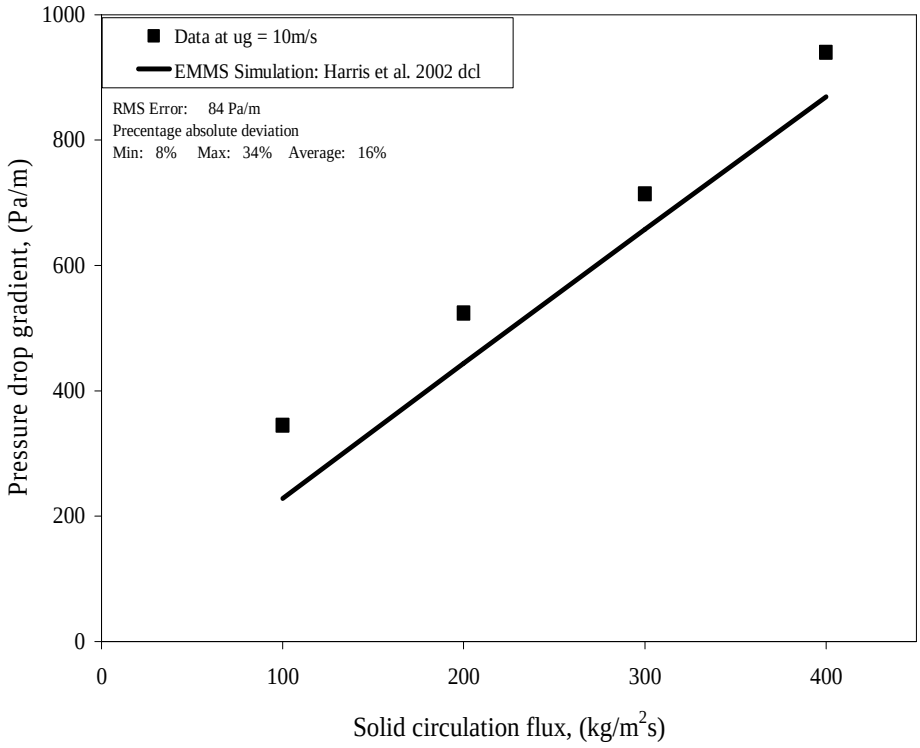

Figure 2.30a: Pressure drop gradient as function of solid circulation flux computed from EMMS model with Harris *et al.* (2002) cluster size and developed a_c and ε_c correlations for Nieuwland (1994) data at u_g = 10 m/s

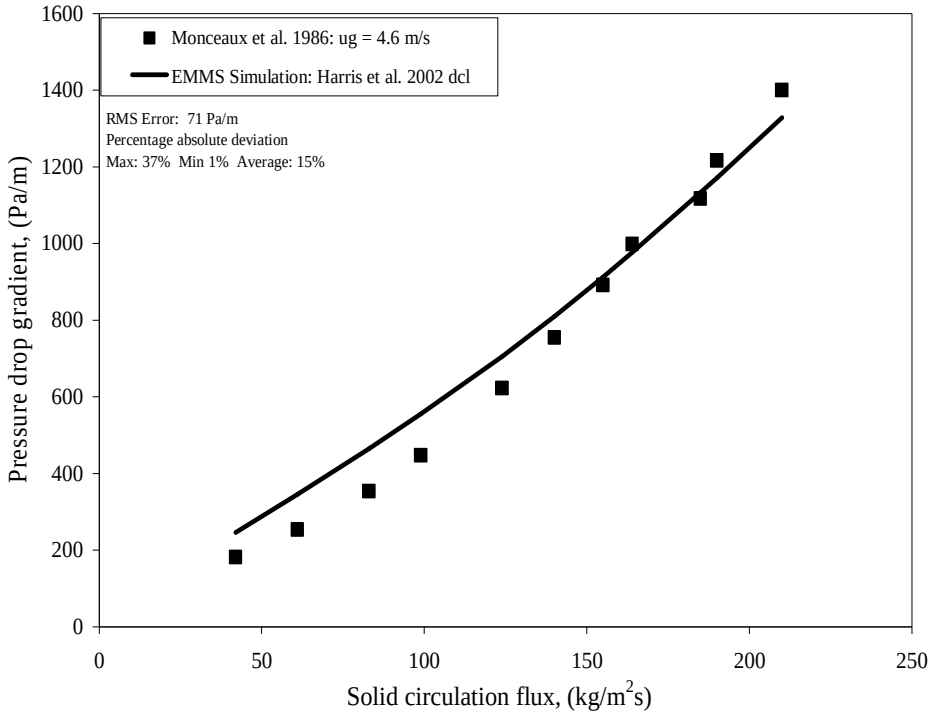

Figure 2.30b: Pressure drop gradient as function of solid circulation flux computed from EMMS model with Harris *et al.* (2002) cluster size and developed a_c and ε_c correlations for Monceaux *et al.* (1986) data at u_g = 4.6 m/s

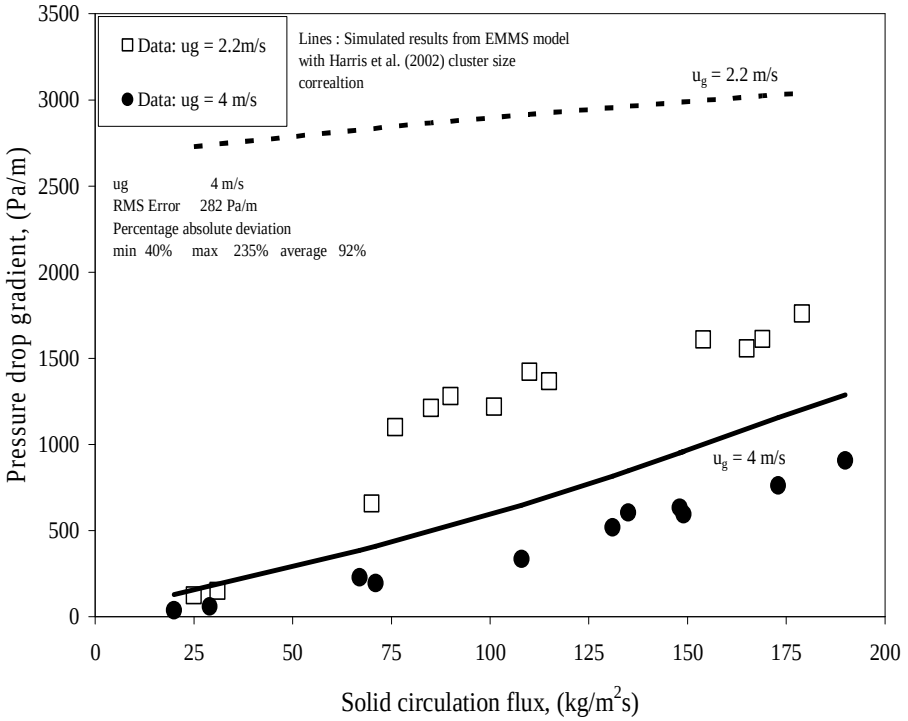

Figure 2.30c: Pressure drop gradient as function of solid circulation flux computed from EMMS model with Harris *et al.* (2002) cluster size and developed a_c and ε_c correlations for Yerushalmi (1986) data at u_g = 2.2 and 4 m/s

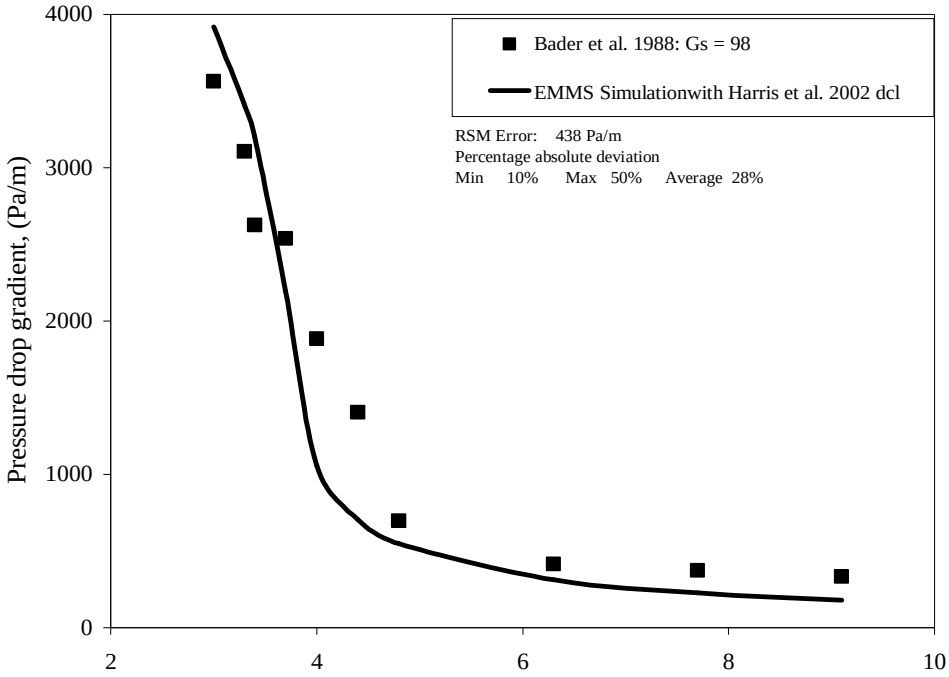

Figure 2.30d: Pressure drop gradient as function of solid circulation flux computed from EMMS model with Harris *et al.* (2002) cluster size and developed a_c and ε_c correlations for Bader *et al.* (1988) data at G_s = 98 kg/m^{2}s

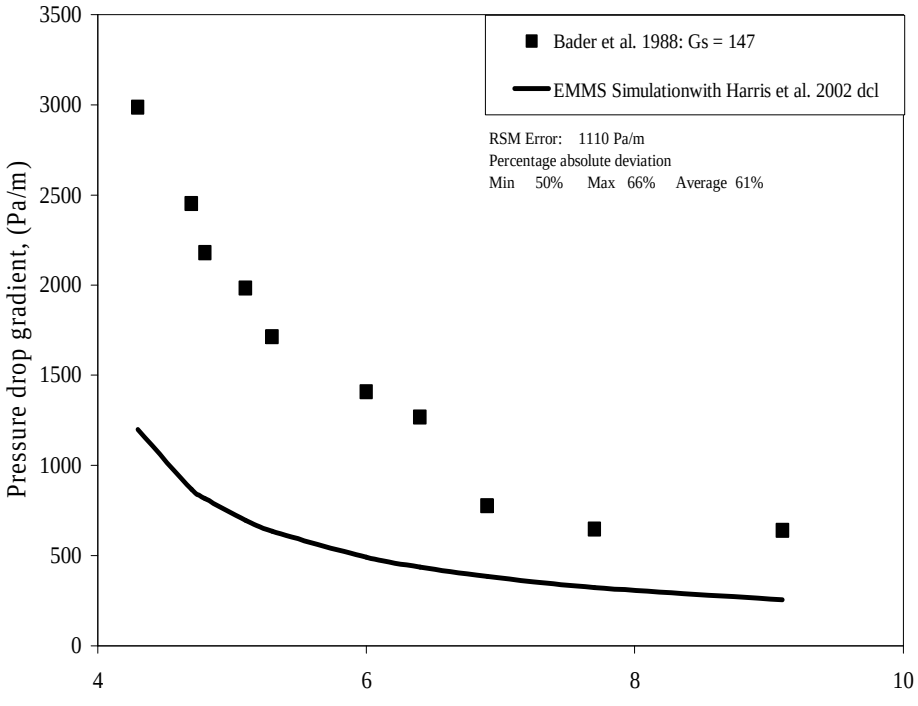

Figure 2.30e: Pressure drop gradient as function of solid circulation flux computed from EMMS model with Harris *et al.* (2002) cluster size and developed a_c and ε_c correlations for Bader *et al.* (1988) data at G_s = 147 kg/m^{2}s

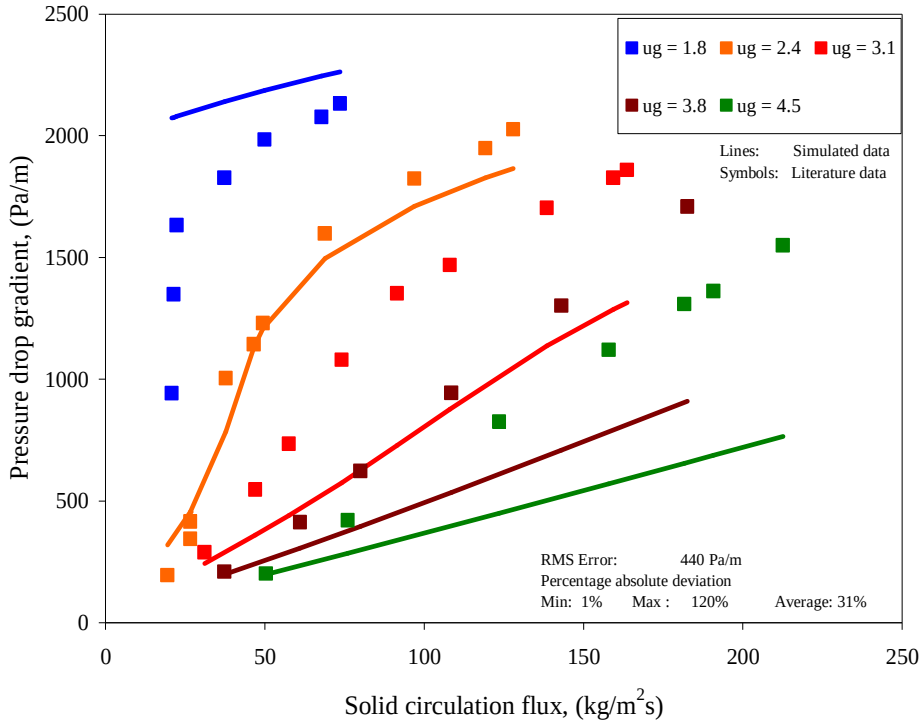

Figure 2.30f: Pressure drop gradient as function of solid circulation flux computed from EMMS model with Harris *et al.* (2002) cluster size and developed a_c and ε_c correlations for Yerushalmi *et al.* (1976) data

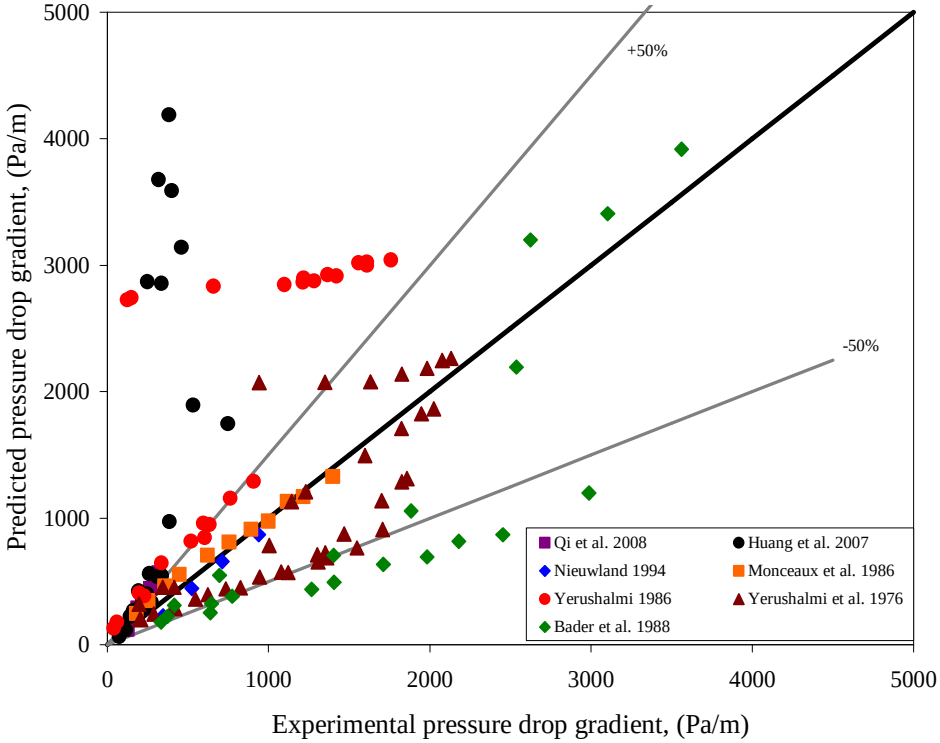

Figure 2.31a: Parity plot showing experimental and predicted pressure drop gradient from EMMS model with Harris *et al.* (2002) cluster size and developed correlations for ε_c and a_c

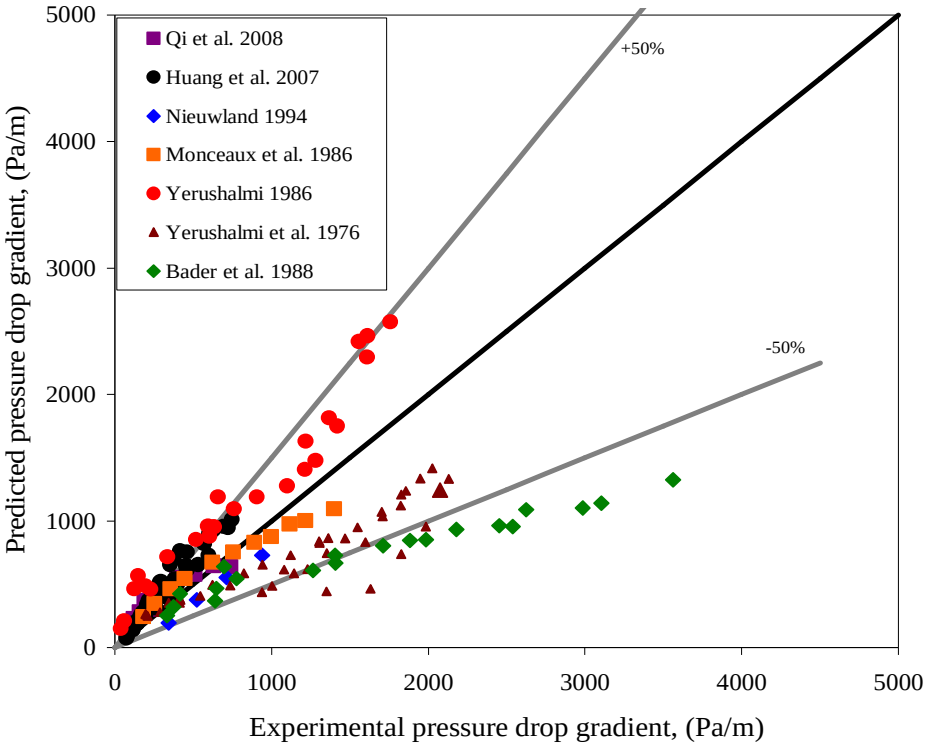

Figure 2.31b: Parity plot showing experimental and predicted pressure drop gradient from Patience *et al.* (1992) correlation for slip factor

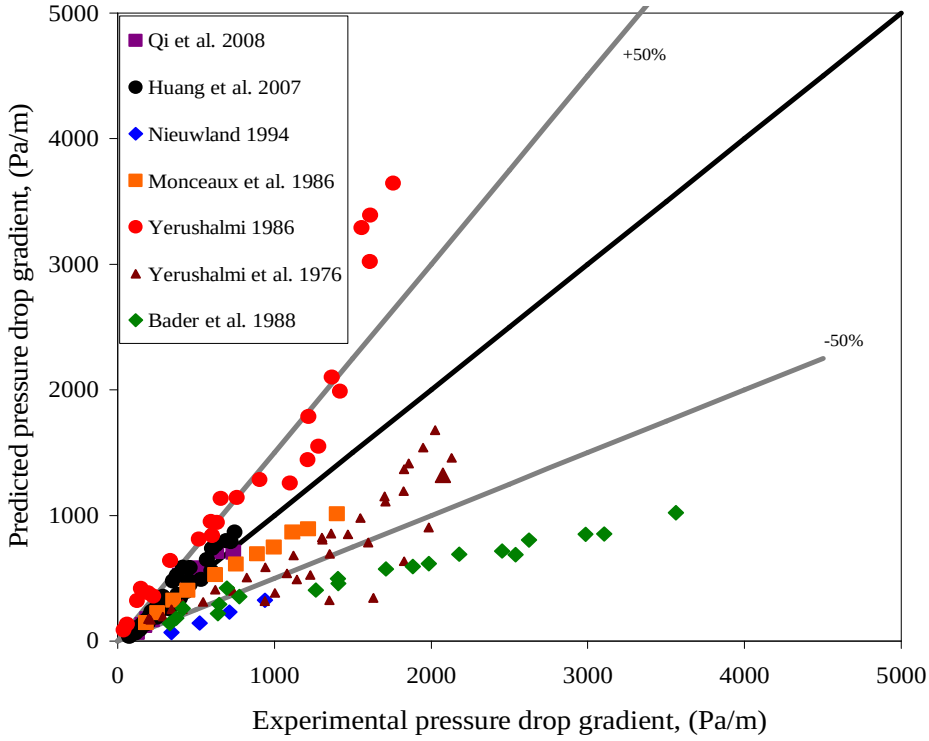

Figure 2.31c: Parity plot showing experimental and predicted pressure drop gradient from Qi *et al.* (2008) correlation

2.4. CONCLUSIONS

EMMS approach is computationally investigated for possible development of drag closures for high solid flux riser models. The conclusions of the present study are as follows:

The drag coefficient correction factor from the EMMS approach was less than unity signifying the decrease in the effective drag due to the formation of clusters in gas – solid flow. This qualitatively captured high slip velocities observed in the experiments. The extended EMMS model with the inertial term predicts distinct local minimum energy consumption for given operating condition and assumed values of cluster voidage and cluster size. However, the model parameters require adjustment to predict the experimental pressure drop data. The dilute phase inertial term can be omitted from the extended model, as this was not found to have any significant effect on model predictions. The cluster voidage was fitted to predict the experimental pressure drop keeping the energy minimization framework of the EMMS model as it was. Understanding the physics of cluster phase inertial term will help to further improve the predictive capability of extended EMMS model with the minimization of energy consumption for suspension and transport.

In light of these conclusions, it can be said that the present frame work of the EMMS model is not very useful to simulate the drag coefficient correction factor for high solid flux gas – solid flows. Improvement in terms of cluster phase drag force expression to account for particle – particle, cluster - particle frictional effects, better estimations of cluster phase voidage and usage of appropriate cluster size correlations may be necessary before the EMMS approach is used to develop the drag force correction factors.

ANNEXURE 2A: EMMS MODEL EQUATIONS

The basic EMMS model framework and the extended EMMS model equations are listed below. Most of the material presented here follows Wang and Li (2007), Yang *et al.* (2003) and Xu and Li (1998).

Basic Equations (Li *et al.*, 1999)

Force balance of particles in dense phase:

$$m_c F_c f + m_i F_i - f(1 - \varepsilon_c)(\rho_p - \rho)g = 0 \tag{2A.1}$$

Force balance of particles in the dilute phase

$$m_f F_f (1 - f) - (1 - f)(1 - \varepsilon_f)(\rho_p - \rho)g = 0 \tag{2A.2}$$

Upon simplification

$$m_f F_f - (1 - \varepsilon_f)(\rho_p - \rho)g = 0 \tag{2A.3}$$

Pressure balance between dense and dilute phase

$$m_f F_f + \frac{m_i F_i}{(1 - f)} - m_c F_c = 0 \tag{2A.4}$$

Mass balance Equations:

$$u_g = u_{gf}(1 - f) + u_{gc} f \tag{2A.5}$$

$$u_p = u_{pf}(1 - f) + u_{pc} f \tag{2A.6}$$

$$\varepsilon = \varepsilon_f (1 - f) + \varepsilon_c f \tag{2A.7}$$

Cluster size:

$$d_{cl} = \frac{d_p \left[\frac{u_p}{(1 - \varepsilon_{max})} - \left(u_{mf} + \frac{u_p \varepsilon_{mf}}{1 - \varepsilon_{mf}} \right) \right] g}{\frac{N_{st} \rho_p}{(\rho_p - \rho)} - \left(u_{mf} + \frac{u_p \varepsilon_{mf}}{1 - \varepsilon_{mf}} \right) g} \tag{2A.8}$$

Additional stability criteria of EMMS model

$$N_T = \frac{(\rho_p - \rho) u_g g}{\rho_p} \quad (2A.9)$$

$$N_{st} = \frac{1}{(1-\varepsilon)\rho_p} \left[m_c F_c u_{gc} f + m_f F_f u_{gf} (1-f) + m_i F_i u_{gf} (1-f) \right] \quad (2A.10)$$

$$= \text{min, for PFC – Fluidization} \quad (2A.11)$$

$$= \text{max, for FD – Transport} \quad (2A.12)$$

Non negativity constraints:

$$u_{sc} \geq 0 \qquad u_{sf} \geq 0 \qquad u_{si} \geq 0 \quad (2A.13)$$

Relevant Parameters (Li *et al.*, 1999)

The drag force acting on single particle or cluster in suspension

$$F_c = C_{Dc} \frac{\pi d_p^2}{4} \frac{\rho}{2} u_{sc}^2 \quad (2A.14)$$

$$F_f = C_{Df} \frac{\pi d_p^2}{4} \frac{\rho}{2} u_{sf}^2 \quad (2A.15)$$

$$F_i = C_{Di} \frac{\pi d_{cl}^2}{4} \frac{\rho}{2} u_{si}^2 \quad (2A.16)$$

Superficial slip velocity

$$u_{sc} = \frac{u_{gc}}{\varepsilon_c} - \frac{u_{pc}}{(1-\varepsilon_c)} \quad (2A.17)$$

$$u_{sf} = \frac{u_{gf}}{\varepsilon_f} - \frac{u_{pf}}{(1-\varepsilon_f)} \quad (2A.18)$$

$$u_{si} = \frac{u_{gf}}{\varepsilon_f} - \frac{u_{pc}}{(1-\varepsilon_c)} \quad (2A.19)$$

Characteristic Reynolds Number:

$$Re_c = \frac{\rho d_p u_{sc}}{\mu} \qquad Re_f = \frac{\rho d_p u_{sf}}{\mu} \qquad Re_i = \frac{\rho d_{cl} u_{si}}{\mu} \quad (2A.20)$$

No of clusters or particles in unit volume

$$m_c = \frac{(1 - \varepsilon_c)}{\pi/6\, d_p^3} \qquad m_f = \frac{(1 - \varepsilon_f)}{\pi/6\, d_p^3} \qquad m_i = \frac{f}{\pi/6\, d_{cl}^3} \tag{2A.21}$$

C_{Dc}, C_{Df} , C_{Di} is the drag coefficient for particle or cluster in suspension. Appropriate expressions in terms of Reynolds number are used for drag coefficients.

Derivation of simplified equations

Solving eq (2A.1) –(2A.4) for $m_c F_c$, $m_f F_f$ and $m_i F_i$

$$m_i F_i = f(1 - f)(\varepsilon_f - \varepsilon_c)(\rho_p - \rho)g \tag{2A.22}$$

$$m_c F_c = (1 - \varepsilon)(\rho_p - \rho)g \tag{2A.23}$$

Extended model equations

Wang and Li (2007) introduced additional terms in the force balance equations to account for the inertial loss as

$$m_c F_c = (1-\varepsilon)(\rho_p - \rho)(a_c - g) \tag{2A.24}$$

$$m_i F_i = f(\varepsilon - \varepsilon_c)(\rho_p - \rho)(a_i - g) \tag{2A.25}$$

$$m_f F_f = (1-\varepsilon_f)(\rho_p - \rho)(a_f - g) \tag{2A.26}$$

From the pressure balance equation between the phases (eq. 4) , the expression for a_i is obtained as

$$a_i = \frac{(1-f)[(1-\varepsilon)(a_c - g) - (1-\varepsilon_f)(a_f - g)]}{f(\varepsilon - \varepsilon_c)} + g \tag{2A.27}$$

Equation for Re_c

From eq. (2A.24)

$$m_c F_c = (1-\varepsilon)(\rho_p - \rho)(a_c - g) \qquad \text{eq (2A.24)}$$

Substituting eq. (2A.14) and eq. (2A.21) in eq. (2A.24) and then using eq (2A.20) we get,

$$C_{Dc}\, Re_c^2 = Ar_c \left[\frac{1-\varepsilon}{1-\varepsilon_c}\right] \frac{(a_c - g)}{g} \tag{2A.28}$$

$$Ar_c = \frac{4}{3}\frac{\rho d_p^3(\rho_p - \rho)g}{\mu^2} \qquad (2A.29)$$

Equation for Re_i:

From eq.(2A.25)

$$m_i F_i = f(\varepsilon - \varepsilon_c)(\rho_p - \rho)(a_i - g) \qquad \text{eq (2A.25)}$$

Substituting eq (2A.16) and eq.(2A.21) in eq. (2A.25) and then simplifying using eq.(2A.20) we get

$$C_{Di}\, Re_i^2 = Ar_i(1-f)(\varepsilon_f - \varepsilon_c)\frac{(a_i - g)}{g} \qquad (2A.30)$$

$$Ar_i = \frac{4}{3}\frac{\rho d_{cl}^3(\rho_p - \rho)g}{\mu^2} \qquad (2A.31)$$

Equation for Re_f:

From eq (2A.26)

$$m_f F_f = (1-\varepsilon_f)(\rho_p - \rho)(a_f - g) \qquad \text{eq (2A.26)}$$

Now substituting eq (2A.15). and eq (2A.21). in eq.v(26) , and using eq. (2A.20)

$$C_{Df}\, Re_f^2 = Ar_f \frac{(a_f - g)}{g} \qquad (2A.32)$$

$$Ar_f = \frac{4}{3}\frac{\rho\ d_p^3(\rho_p - \rho)g}{\mu^2} \qquad (2A.33)$$

Substituting appropriate expression for the drag coefficients in eq (2A.28), eq. (2A.30) and eq. (2A.32) in terms of respective Reynolds number, and solving, we get the values of Re_c, Re_f and Re_i. Once the Reynolds number is determined, the slip velocities are calculated from eq. (2A.20).

Fluidization regime: Particle Fluid Compromise (PFC) mechanism of EMMS model

Assumptions: (Xu and Li, 1998; Li *et al.*, 1999)

$$\varepsilon_c = \varepsilon_{mf}$$
$$\varepsilon_f = \varepsilon_{max} \qquad (2A.32)$$

From eq (2A.5) eq (2A.6) eq.(2A.17) and eq(2A.18)

$$u_g = u_{gf}(1 - f) + u_{gc} f \qquad \text{eq.(2A.5)}$$

$$u_p = u_{pf}(1 - f) + u_{pc}f \qquad \text{eq.(2A.6)}$$

$$u_{sc} = \frac{u_{gc}}{\varepsilon_c} - \frac{u_{pc}}{(1-\varepsilon_c)} \qquad \text{eq (2A.17)}$$

$$u_{sf} = \frac{u_{gf}}{\varepsilon_f} - \frac{u_{pf}}{(1-\varepsilon_f)} \qquad \text{eq (2A.18)}$$

Rearranging eq (17) eq.(18) and eq. (6) we get

$$u_{gc} = \left[u_{sc} + \frac{u_{pc}}{(1-\varepsilon_c)} \right] \varepsilon_c \qquad (2A.33)$$

$$u_{gf} = \left[u_{sf} + \frac{u_{pf}}{(1-\varepsilon_f)} \right] \varepsilon_f \qquad (2A.34)$$

$$u_{pf} = \frac{u_p - u_{pc}f}{(1-f)} \qquad (2A.35)$$

Substituting eq. (2A.34) and eq. (2A.35) in eq. (2A.5) and eliminating u_{pf} using eq.(2A.35) we get expression for u_{pc} as follows

$$u_g = f\left(u_{sc} + \frac{u_{pc}}{1-\varepsilon_c} \right) \varepsilon_c + (1-f)\left(u_{sf} + \frac{u_{pf}}{1-\varepsilon_f} \right) \varepsilon_f \qquad (2A.36)$$

$$u_{pc} = \frac{\text{TMP}}{\left[\frac{\varepsilon_c f}{1 - \varepsilon_c} - \frac{\varepsilon_f f}{1 - \varepsilon_f} \right]} \qquad (2A.37)$$

$$\text{TMP} = u_g - u_{sc}\varepsilon_c f - u_{sf}\varepsilon_f (1-f) - \frac{u_p \varepsilon_f}{1-\varepsilon_f} \qquad (2A.38)$$

Summary of equations for solving fluidization regime: PFC approach

$$m_c F_c = (1-\varepsilon)(\rho_p - \rho)(a_c - g) \qquad \text{eq. (2A.24)}$$

$$m_i F_i = f(\varepsilon - \varepsilon_c)(\rho_p - \rho)(a_i - g) \qquad \text{eq. (2A.25)}$$

$$m_f F_f = (1-\varepsilon_f)(\rho_p - \rho)(a_f - g) \qquad \text{eq. (2A.26)}$$

$$a_i = \frac{(1-f)[(1-\varepsilon)(a_c - g) - (1-\varepsilon_f)(a_f - g)]}{f(\varepsilon - \varepsilon_c)} + g \qquad \text{eq. (2A.27)}$$

$$\varepsilon_c = \varepsilon_{mf}$$
$$\varepsilon_f = \varepsilon_{max}$$ eq.(2A.32)

$$Ar_c = \frac{4}{3}\frac{\rho d_p^3(\rho_p - \rho)g}{\mu^2}$$ eq. (2A.29)

$$C_{Dc}\,Re_c^2 = Ar_c\left[\frac{1-\varepsilon}{1-\varepsilon_c}\right]\frac{(a_c - g)}{g}$$ eq. (2A.28)

$$Ar_i = \frac{4}{3}\frac{\rho d_{cl}^3(\rho_p - \rho)g}{\mu^2}$$ eq. (2A.31)

$$C_{Di}\,Re_i^2 = Ar_i(1-f)(\varepsilon_f - \varepsilon_c)\frac{(a_i - g)}{g}$$ eq. (2A.30)

$$Ar_f = \frac{4}{3}\frac{\rho\ d_p^3(\rho_p - \rho)g}{\mu^2}$$ eq. (2A.33)

$$C_{Df}\,Re_f^2 = Ar_f\,\frac{(a_f - g)}{g}$$ eq. (2A.32)

$$u_{pc} = \frac{TMP}{\left[\frac{\varepsilon_c f}{1-\varepsilon_c} - \frac{\varepsilon_f f}{1-\varepsilon_f}\right]}$$ eq.(2A.37)

$$TMP = u_g - u_{sc}\varepsilon_c f - u_{sf}\varepsilon_f(1-f) - \frac{u_p\varepsilon_f}{1-\varepsilon_f}$$ eq. (2A.38)

$$u_{pf} = \frac{u_p - u_{pc}f}{(1-f)}$$ eq. (2A.35)

$$u_{gc} = \left[u_{sc} + \frac{u_{pc}}{(1-\varepsilon_c)}\right]\varepsilon_c$$ eq.(2A.33)

$$u_{gf} = \left[u_{sf} + \frac{u_{pf}}{(1-\varepsilon_f)}\right]\varepsilon_f$$ eq. (2A.34)

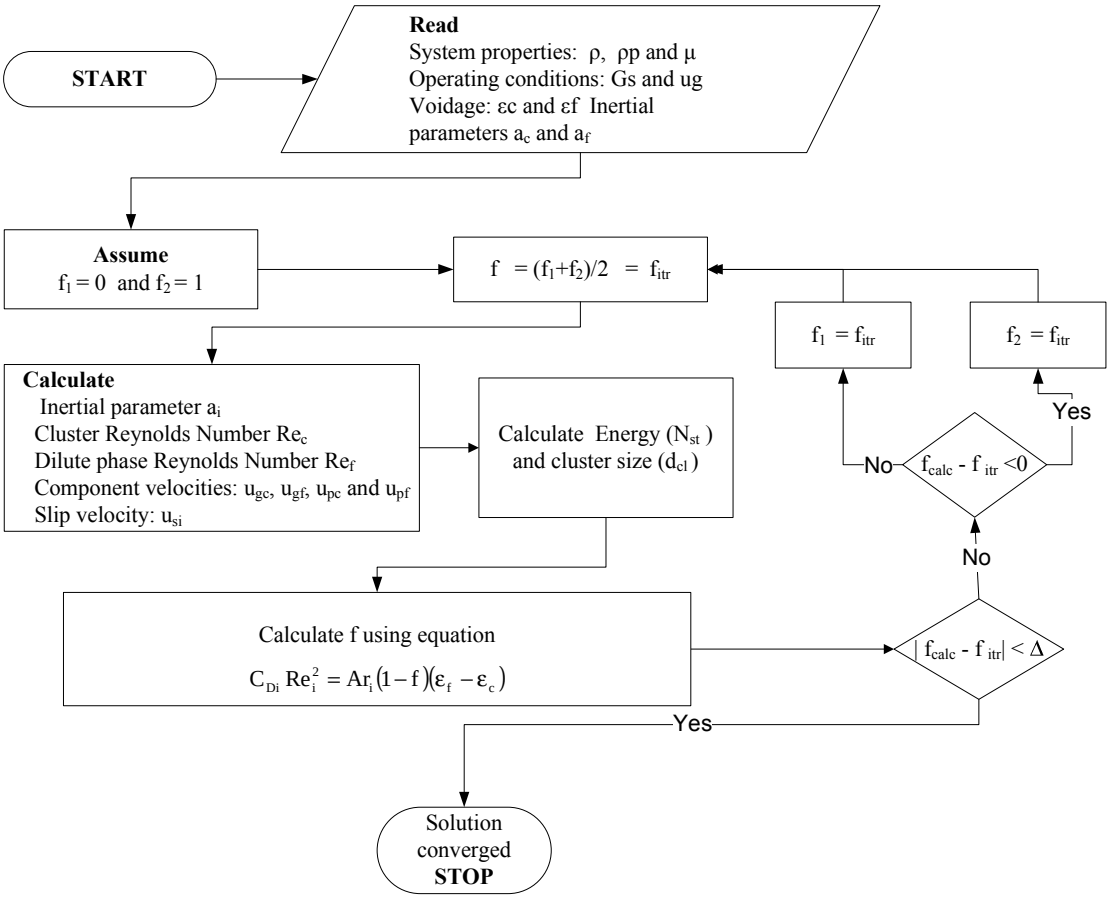

Figure 2A.1 Solution algorithm to solve the EMMS model

Drag coefficients expressions:

1. Wen and Yu (1966) drag coefficient expression

$$C_D = C_{D0}\varepsilon^{-4.7} \tag{2A.39}$$

$$\text{where } C_{D0} = \frac{24}{Re} + \frac{3.6}{Re^{0.313}} \tag{2A.40}$$

2. Modified drag coefficient of Xu and Li (1998) based on Wen and Yu (1966)

$$C_D = C_{D0}\varepsilon^{-4.7} \tag{2A.41}$$

$$\text{where } C_{D0} = \frac{B}{Re^{k}} \tag{2A.42}$$

The values of B and k are got from the Table 2A.1, read against corresponding to the value of κ. The term κ is a modified form of Archimedes number defined as follows for the different phases c, f and i respectively,

$$\kappa_c = d_p\left[\frac{(1-\varepsilon)(\rho_p-\rho)\rho g}{\varepsilon_c^{-4.7}(1-\varepsilon_c)\mu^2}\right]^{1/3} \tag{2A.43}$$

$$\kappa_f = d_p\left[\frac{(\rho_p-\rho)\rho g}{\varepsilon_f^{-4.7}\mu^2}\right]^{1/3} \tag{2A.44}$$

$$\kappa_i = d_{cl}\left[\frac{(1-f)^{5.7}(\varepsilon_f-\varepsilon_c)(\rho_p-\rho)\rho g}{\mu^2}\right]^{1/3} \tag{2A.45}$$

3. Ergun (1952) drag coefficient expression

$$C_D = \frac{4}{3\varepsilon^3}\left[\frac{150(1-\varepsilon)}{Re} + 1.75\right] \tag{2A.46}$$

Table 2A.1: Parameters for Xu and Li (1998) drag coefficient expression

κ	$C_{D0} = \frac{B}{Re^{k}}$
$\kappa \leq 1.75$	$C_{D0} = \frac{24}{Re}$
$1.75 \leq \kappa \leq 4.55$	$C_{D0} = \frac{27}{Re^{0.89}}$
$4.55 \leq \kappa \leq 12.43$	$C_{D0} = \frac{20.4}{Re^{0.69}}$
$12.43 \leq \kappa \leq 51.35$	$C_{D0} = \frac{7.8}{Re^{0.43}}$
$51.35 \leq \kappa \leq 192.95$	$C_{D0} = \frac{1.16}{Re^{0.13}}$
$192.95 \leq \kappa \leq 1234.25$	$C_{D0} = \frac{0.15}{Re^{-0.11}}$
$1234.25 \leq \kappa \leq 1530$	$C_{D0} = \frac{4.26}{Re^{0.19}}$

ANNEXURE 2B: VALIDATION OF EMMS MODEL WITH CORE – ANNULUS RISER FLOW APPROACH

The flow structure in the riser was assumed to be of core – annulus type flow (Figure 2B.1). At given operating conditions, the diameter of core and superficial gas velocity in the core were assumed. From mass balance, the superficial gas velocity in the annulus was determined (Equation 2B.1). At fully developed flow condition, the pressure drop across core is equal to pressure drop across annulus (Equation 2B.3). By trial and error procedure, the solid circulation flux through core that satisfies Equation 2B.3 was found out. Figure 2B.2 illustrates solution procedure for the core – annulus approach. The procedure was repeated for different assumed values of superficial gas velocity through core and for different values of core diameter.

$$u_g D^2 = u_{gcore} D_{core}^2 + u_{gannulus}\left(D^2 - D_{core}^2\right) \quad (2B.1)$$

$$G_s D^2 = G_{score} D_{core}^2 + G_{sannulus}\left(D^2 - D_{core}^2\right) \quad (2B.2)$$

$$\Delta P_{core} = \Delta P_{annulus} \quad (2B.3)$$

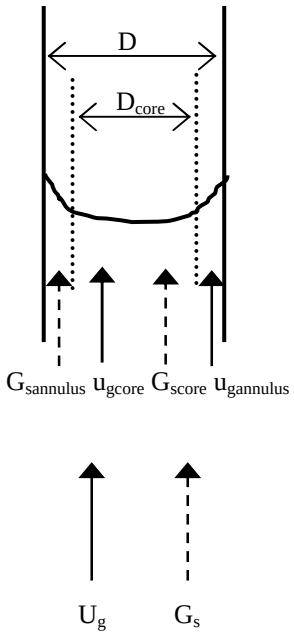

Figure 2B.1: Core annulus riser flow approach

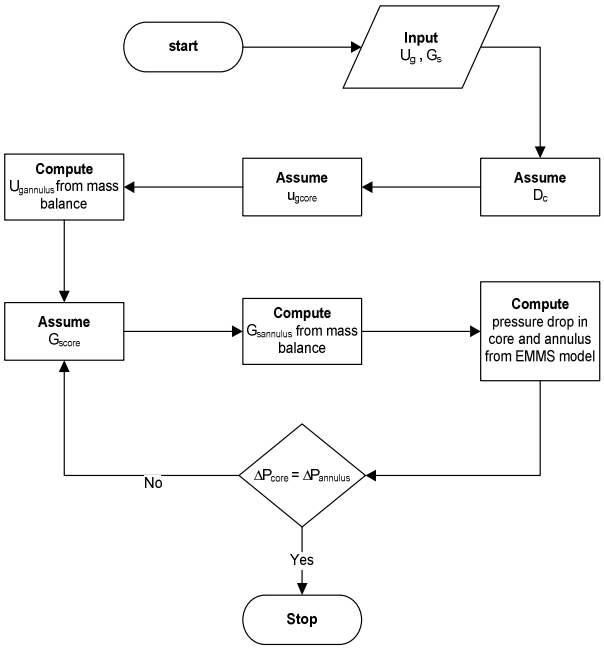

Figure 2B.2: Solution procedure for core – annulus riser flow approach

CHAPTER 3

CFD MODELING OF GAS SOLID RISER FLOWS

The chapter discusses the development of CFD model to simulate fully developed flow profiles for gas solid riser flows. The fully developed flow profiles were simulated using FLUENT™ (Ansys Inc, USA). The two fluid model equations, closures and the methodology of implementing periodic flow boundary conditions using user defined function (UDF) are discussed in the following sections. Drag coefficient was found to significantly affect the radial flow structure. Radial segregation of solids was also found to be sensitive to the value of specularity coefficient (more pronounced segregation at lower values of specularity coefficient). Some simulations were also done in 2D and 2D axis symmetric domain. Influence of grid resolution on predicted radial segregation is discussed.

3.1. BACKGROUND

Hydrodynamic flow modeling of circulating fluidized bed systems is categorized into three groups based on the outcome from the models as category I, II and III (Fan and Zhu, 1998). Type I models ignore radial flow structure and provide steady state axial flow profiles. Type II models provide both steady state radial and axial profile for riser flows based on pre-assumed radial flow pattern like core annulus, dense and dilute cluster in co-existence etc. Type III models use computational flow modeling (CFD) techniques and solve full 3D conservation equations of mass, momentum and energy. Such models provide detailed flow information in all the 3 three spatial co-ordinates as well as transient flow characteristics. The CFB modeling test exercise of Fluidization VIII conference (Berruti *et al.*, 1995) and it's follow up (Sun and Gidsapow, 1999) strongly suggested that type III models based on full conservation equations of mass, momentum and granular specification for the solid phase captured the significant trends in the riser flows. Consequently, CFD models offer an edge in modeling riser systems and are widely adopted in modeling riser flows. The CFD models for dispersed multiphase flow systems like gas solid risers and general methodology of CFD models for such complex systems can be found in Curtis and van Wachem (2004), van Wachem *et al.* (2003), Loth (2000), Crowe *et al.* (1996) etc. The CFD models are classified into different groups based on the Eulerian or the Lagrangian treatment of the primary phase (gas) and the secondary solid phase. For large industrial riser systems, models based on two fluid model approach or called the Eulerian – Eulerian model framework are more suitable.

The two fluid model equations for the risers are based on the continuum description of fluidized beds by Anderson and Jackson (1969 and 1967). In this two fluid approach, both the primary and the secondary phase (gas and solid) are treated as fluid continua. The hydrodynamics of the system are described in terms of volume averaged conservation equations for mass, momentum and energy for the pertinent phases. The interactions between the phases are modeled based on constitutive relations for interphase momentum exchange factors. The shear stress within the solid phase is modeled empirically based on experimental data or based on kinetic theory of granular flow (KTGF). The KTGF model is analogous to the kinetic theory of gases and is based on the granular temperature of the solid phase measured in terms of

fluctuations in the particle phase velocities. Table 3.1 lists some of the studies which deal with the CFD modeling of risers. More detailed information about the computational studies on riser flows can be had from Appendix I. The models based on KTGF approach offer flexibility for matching the predicted results with the data or for extending the developed model to larger systems (Ranade 2002).

Table 3.1: List of studies on gas solid riser flows based on two fluid model

Non KTGF Models	**KTGF based models**		
	Laminar – Laminar	**Turbulent – Laminar**	**Turbulent - Turbulent**
Benyahia *et al.*, 2002 Dasgupta *et al.*, 1994 Tsuo and Gidaspow, 1990	Benyahia, 2009 Lu *et al*., 2009 Almuttahar and Taghipour, 2008 Benyahia *et al.*, 2007 Vaishali *et al.*, 2007 Benyahia *et al.*, 2000 Neri and Gidaspow, 2000 Pita and Sundaresan, 1991 Sinclair and Jackson, 1989	Hadinoto and Curtis, 2009 Benavides *et al.*, 2008 Bolio and Sinclair, 1995 Bolio *et al.*, 1995 Nieuwland,1994 Louge *et al.*, 1991	Benyahia *et al.*, 2007 Benyahia *et al.*, 2005 Zhang and Reese, 2003 Zhang and Reese, 2001

Despite large amount of research publications reporting successful predictions of gas solid riser flows with two fluid model approach, general framework or guidelines for riser flow modeling are seldom visible. As noted in the Chapter 1, there are still lacunae in the basic understanding of complex flow information like predicting cluster or meso scale structures, radial segregation in solids, particle-particle interaction, usage of constituent drag laws for momentum exchange etc. A study of the reported riser flow models shows that all possible variants of model closures and model parameters have been used to model riser flows (see Appendix I). For example the value of specularity coefficient used to specify the solid wall boundary condition varied from 0.5 to 0.002 (Benyahia *et al.*, 2007; Benyahia *et al.*, 2005; Bolio *et al.*, 1995; Nieuwland, 1994; Sinclair and Jackson, 1989). In many of the studies, simulations of experimental circular cross section riser have been performed in 2D Cartesian framework (Almuttahar and Taghipour, 2008; Vaishali *et al.*, 2007;

Benyahia *et al.*, 2002; Neri and Gidaspow, 2000 etc.). Such a representation might destroy the basic flow physics of cylindrical riser systems. Quantitative predictions in some cases were poor and required proper investigation into constituent closure relations used in such two fluid models. For instance, Benavides *et al.* (2008) simulated rise flow at u_g = 5 m/s and G_s = 40 kg/m^{2}s in 3D computational domain with transient two fluid model approach and KTGF closures for the solid phase. Better prediction of radial solid holdup profile was found at higher axial locations. Almuttahar and Taghipour (2008) performed transient simulations in 2D computational domain. Their simulation results captured the quantitative trends but qualitative match required improvement of the model. Similar results can be obtained from work of Vaishali *et al*. (2007). They compared their 2D transient simulation results with the data obtained of Bhusarapu (2005). Though the drag closures from Syamlal *et al.* (1993) improved the model prediction for certain selected experimental data, no generalization can be made of the model. For example, inverse segregation of solid holdup towards the axis was observed for riser operated at dense flowing conditions of u_g = 4.5 m/s and G_s = 37 kg/m^{2}s. Similar inverse segregation was also found from the work of Benyahia *et al.* 2005. Further, though many investigators employed 1D model with periodic boundary conditions, not all effects like gas phase turbulence, particle – particle interactions, a separate granular energy conservation equation were accounted together.

The importance of periodic flow models in simulating gas solid riser flows is briefed in Chapter 1. The two fluid model equations are capable of predicting the meso-scale structures provided the spatial grid resolution is fine enough to capture them. Agarwal *et al.* (2001) noted that with grid size of the order of 10 particle diameters, one can simulate the meso-scale structures in two dimensional and three dimensional periodic computational domains. Recently, Igci *et al.* (2008) predicted the existence of meso-scale structure and heterogeneity in gas solid vertical flows through use of filtered two fluid model equations. These filtered equations were obtained by averaging results obtained over small domain, size of which is in the range of few centimeters (2 - 4 cm). Apart from increased understanding of the gas solid interactions, periodic flow simulations also find use in development of fully developed flow profiles. The fully developed flow profiles are useful in development of engineering scale performance models for process industries. Moreover, typical riser reactors are with H/D ratio of

30 and above. Computation of the entire riser reactor without jeopardizing the grid resolution demands enormous computational resources. This demand for large computational requirements can be partially avoided if fully developed flow profiles were simulated with periodic flow boundaries across the region of interest.

Given this background, a systematic study was undertaken to evaluate a two fluid model for gas solid riser flows using commercial CFD software FLUENT^{TM} (v 6.3.26, Ansys Inc, USA). However, commercial CFD tools like FLUENT^{TM} (v 6.3.26, Ansys Inc, USA) do not have the in-built facility to simulate fully developed flow profile with mass flow rate specification for multiphase flow models. In the present work, the user defined functions (UDF) of FLUENT^{TM} were used to enable periodic boundary condition for the computational domain and thereby simulations were performed to predict fully developed flow profiles. With this periodic boundary condition methodology, the domain size in the stream wise direction was considerably reduced. This reduction in stream wise domain size requirement was utilized to have significantly finer grid resolution in the span wise flow direction. Consequently, attempt was made to employ the UDF based periodic model to simulate fully develop flow profiles for gas solid riser flows. The mathematical framework of the two fluid model for risers is discussed in the next section.

3.2. MATHEMATICAL MODEL

The gas solid two phase riser flow was modeled with the two fluid approach (Anderson and Jackson, 1967), wherein the two phases were considered to be interpenetrating continua coupled with momentum exchange coefficient. Both the fluids were considered to be incompressible and Newtonian. Reynolds averaged mass and momentum conservation equations were solved to compute the gas solid flow in the vertical riser.

Conservation equations for mass, momentum and turbulent quantities are given in Table 3.2. For more details the one can refer to FLUENT 6.3 user manual and Ranade (2002). The gas phase shear stress was given as sum contribution of the molecular transport mechanism (laminar shear stress) and of the turbulent transport arising out of Reynolds averaging. The turbulent stresses were modeled following Boussinesq's eddy viscosity hypothesis. The turbulent shear stresses were computed

from the turbulent kinetic energy and turbulent dissipation rate. Only gravity and interphase drag force were considered. Other forces like lift and virtual mass were found not very significant in gas solid vertical flows (Armenio and Fiorotto, 2001). The drag coefficient C_D was calculated based on the standard drag coefficient of a single particle falling through an infinite stagnant medium (C_{D0}) and correction factor to account for the presence of other particles and/or clusters. Wen and Yu (1966) was employed as default drag coefficient to develop the base case CFD model for riser flows.

For the solid phase, the kinetic theory of granular flow (Jenkins and Savage, 1983) was employed to compute the shear stress. The stress tensor for the solid phase was composed of three terms, namely, due to solid pressure (p_s), shear viscosity ($\mu_{s,s}$) and bulk viscosity ($\mu_{b,s}$) of the solid phase. These constituent terms in the stress tensor were calculated from the reported literature correlations (Table 3.3).

Table 3.2: Two fluid model equations

Overall continuity	$\sum \varepsilon_q = 1$
Continuity for each phase	$\frac{\partial \varepsilon_q \rho_q}{\partial t} + \mathrm{div}(\varepsilon_q \rho_q \mathbf{U_q}) = 0$
Gas phase momentum balance	$\frac{\partial (\varepsilon \rho \mathbf{U})}{\partial t} + \mathrm{div}(\rho \mathbf{U}\mathbf{U}) = -\varepsilon\, \mathrm{grad}\, \mathbf{p} + \mathrm{div}(\boldsymbol{\tau}) + \mathbf{S_M}$
Solid phase momentum balance	$\frac{\partial (\varepsilon_s \rho_p \mathbf{V})}{\partial t} + \mathrm{div}(\rho_p \mathbf{V}\mathbf{V}) = -\varepsilon_s\, \mathrm{grad}\, \mathbf{p} + \mathrm{div}(\boldsymbol{\tau}_s) + \mathbf{S_M}$
Granular temperature	$\frac{3}{2}\left[\frac{\partial}{\partial t}(\rho_p \alpha_s \Theta) + \nabla.(\rho_p \alpha_s \mathbf{V}\Theta)\right] = \alpha_s \boldsymbol{\tau_s} \nabla \mathbf{V} + \nabla.(\kappa_{\Theta s} \nabla \Theta_s) - \gamma_{\Theta s} + \phi_{gs}$
Turbulent kinetic energy (a) Mixture model	$\frac{\partial (\rho_m k)}{\partial t} + \mathrm{div}(\rho_m \mathbf{U_m} k) = \mathrm{div}\left(\frac{\mu_{t,m}}{\sigma_k} \nabla k\right) + \mathbf{G_{k,m}} - \rho_m \epsilon$ where $\rho_m = \sum_{i=1}^{N} \varepsilon_i \rho_i \quad \mathbf{U_m} = \frac{\sum_{i=1}^{N} \varepsilon_i \rho_i \mathbf{U_i}}{\sum_{i=1}^{N} \varepsilon_i \rho_i}$
(b) Dispersed model	$\frac{\partial (\varepsilon \rho k)}{\partial t} + \mathrm{div}(\varepsilon \rho \mathbf{U} k) = \mathrm{div}\left(\varepsilon \frac{\mu_t}{\sigma_k} \nabla k\right) + \varepsilon \mathbf{G_k} - \varepsilon \rho \epsilon + \varepsilon \rho \Pi_k$

(c) Per phase model	$\frac{\partial\left(\varepsilon_q \rho_q k_q\right)}{\partial t} + \mathrm{div}(\varepsilon_q \rho_q \mathbf{U_q} k_q)$ $= \mathrm{div}\left(\varepsilon_q \frac{\mu_{t,q}}{\sigma_k} \nabla k_q\right) + \varepsilon_q \mathbf{G_{k,q}} - \varepsilon_q \rho_q \epsilon_q + \sum_{l=1}^{N} K_{lq}\left(C_{lq} k_l - C_{ql} k_q\right)$ $- \sum_{l=1}^{N} K_{lq}\left(\mathbf{U_l} - \mathbf{U_q}\right).\frac{\mu_{t,l}}{\varepsilon_l \alpha_l} \nabla \varepsilon_l + \sum_{l=1}^{N} K_{lq}\left(\mathbf{U_l} - \mathbf{U_q}\right).\frac{\mu_{t,q}}{\varepsilon_q \alpha_q} \nabla \varepsilon_q$
Turbulent dissipation rate (a) Mixture model	$\frac{\partial\left(\rho_m \epsilon\right)}{\partial t} + \mathrm{div}(\rho_m \mathbf{U_m} \epsilon) = \mathrm{div}\left(\frac{\mu_{t,m}}{\sigma_\epsilon} \nabla \epsilon\right) + \frac{\epsilon}{k}\left(C_{1\epsilon} \mathbf{G_{k,m}} - C_{2\epsilon} \rho_m \epsilon\right)$ where $\rho_m = \sum_{i=1}^{N} \varepsilon_i \rho_i$ $\mathbf{U_m} = \frac{\sum_{i=1}^{N} \varepsilon_i \rho_i \mathbf{U_i}}{\sum_{i=1}^{N} \varepsilon_i \rho_i}$
(b) Dispersed model	$\frac{\partial\left(\varepsilon \rho \epsilon\right)}{\partial t} + \mathrm{div}(\varepsilon \rho \mathbf{U} \epsilon) = \mathrm{div}\left(\varepsilon \frac{\mu_t}{\sigma_\epsilon} \nabla \epsilon\right) + \varepsilon \frac{\epsilon}{k}\left(C_{1\epsilon} \mathbf{G_k} - C_{2\epsilon} \rho \epsilon\right) + \varepsilon \rho \Pi_\epsilon$
(c) Per phase model	$\frac{\partial\left(\varepsilon_q \rho_q \epsilon_q\right)}{\partial t} + \mathrm{div}(\varepsilon_q \rho_q \mathbf{U_q} \epsilon_q)$ $= \mathrm{div}\left(\varepsilon_q \frac{\mu_{t,q}}{\sigma_k} \nabla \epsilon_q\right) + \frac{\epsilon_q}{k_q}\left(C_{1\epsilon} \varepsilon_q \mathbf{G_{k,q}} - C_{2\epsilon} \varepsilon_q \rho_q \epsilon_q\right) + \frac{\epsilon_q}{k_q} C_{3\epsilon} \sum_{l=1}^{N} K_{lq}\left(C_{lq} k_l - C_{ql} k_q\right)$ $- \frac{\epsilon_q}{k_q} C_{3\epsilon} \sum_{l=1}^{N} K_{lq}\left(\mathbf{U_l} - \mathbf{U_q}\right).\frac{\mu_{t,l}}{\varepsilon_l \alpha_l} \nabla \varepsilon_l + \frac{\epsilon_q}{k_q} C_{3\epsilon} \sum_{l=1}^{N} K_{lq}\left(\mathbf{U_l} - \mathbf{U_q}\right).\frac{\mu_{t,q}}{\varepsilon_q \alpha_q} \nabla \varepsilon_q$
Gas phase laminar shear stress	$\boldsymbol{\tau_l} = \varepsilon \mu_g\left(\nabla \mathbf{U} + \nabla \mathbf{U}^T\right) - \frac{2}{3} \varepsilon \mu_g \nabla.\mathbf{U} \bar{\bar{I}}$

Gas phase turbulent shear stress	$\boldsymbol{\tau}_{\mathbf{t}} = \rho\,\mu_t\left(\nabla\mathbf{U} + \nabla\mathbf{U}^T\right) - \frac{2}{3}\left(\,\rho k + \rho\mu_t \nabla.\mathbf{U}\right)\bar{\bar{I}}$
Gravity force	$\mathbf{F}_{\mathbf{g}} = \varepsilon\rho\mathbf{g}$
Drag force	$\mathbf{F}_{\mathbf{D}} = K_{g-s}\left(\mathbf{U} - \mathbf{V}\right)$
Interphase momentum exchange coefficient	$K_{g-s} = \frac{3}{4}\frac{\varepsilon\,\varepsilon_s\,\rho\,C_D\,\left\|\mathbf{U} - \mathbf{V}\right\|}{d_p}$
Drag coefficient	$C_D = C_{D0} f\left(\varepsilon\right)$
Solid phase shear stress	$\boldsymbol{\tau}_{\mathbf{s}} = -\mathbf{p}_{\mathbf{s}} + \mu_{s,s}\left(\nabla\mathbf{V} + \nabla\mathbf{V}^T\right) + \left(\mu_{b,s} - \frac{2}{3}\mu_{s,s}\right)\nabla.\mathbf{V}\bar{\bar{I}}$
Granular energy dissipation due to particle collision	$\gamma_{\Theta s} = \frac{12\left(1 - e_p^2\right)g_0}{d_p\sqrt{\pi}}\rho_p\alpha_s^2\Theta_s^{3/2}$
Granular energy dissipation due to interphase momentum exchange	$\phi_{gs} = -3K_{g-s}\Theta_s$

Table 3.3: Granular model specifications

Granular temperature model	Algebraic
Granular conductivity	Syamlal *et al.*, 1993
Granular bulk viscosity	Lun *et al.*, 1984
Frictional viscosity	None
Granular conductivity	Syamlal *et al.*, 1993
Solids pressure	Syamlal *et al.*, 1993
Radial Distribution	Iddir and Arastoopour, 2005
Elasticity modulus	Derived
Packing limit	0.6
Particle – Particle restitution coefficient	0.9

The solid pressure and solid phase viscosity depends on the fluctuations in the solid phase velocity given in terms of granular temperature. The granular temperature (Θ) is defined as root mean square of the solid phase fluctuating velocity (V`).

$$\Theta = \frac{1}{3}\left\langle \mathbf{V}^{'2} \right\rangle \tag{3.1}$$

Therefore, in addition to the momentum equation for the solid phase velocity, a conservation equation for the granular temperature was also solved. The granular energy flux depends on the diffusion coefficient for granular temperature ($\kappa_{\Theta s}$), collisional dissipation of granular energy ($\gamma_{\Theta s}$) due to inelastic particle-particle collision (Lun *et al.*, 1984) and the transfer of granular energy (ϕ_{gs}) between the gas phase with the solid phase (Gidaspow, 1994). The inter-particle collision ($\gamma_{\Theta s}$) was characterized by the particle – particle restitution coefficient (Table 3.3). Zero value for the particle – particle restitution coefficient denotes purely elastic collisions.

In the algebraic granular energy formulation, the accumulation, convection and the diffusion terms in the granular energy conservation equation were neglected resulting

in algebraic expression for the granular energy. In the partial differential equation (pde) formulation, the full conservation equation for the granular energy (Table 3.2) was solved to compute the granular energy.

The turbulent quantities were computed by solving the two equation k-ϵ model. FLUENT provides three formulations – mixture, dispersed and per phase of the multiphase k-ϵ model. In the k-ϵ mixture model formulation, phase weighted average quantities were employed to solve a single set of two equations, one each for the mixture turbulent kinetic energy and mixture turbulent dissipation rate. The term $G_{k,m}$ accounts for the generation of turbulent kinetic energy due to shear in the fluid.

$$\mathbf{G_{k.m}} = \mu_{t,m}\left(\nabla \mathbf{U_m} + \nabla \mathbf{U_m^T}\right) : \nabla . \mathbf{U_m} \tag{3.2}$$

The constants appearing in the equation were taken as $C_{1\epsilon} = 1.44$, $C_{2\epsilon} = 1.92$, $C_{\mu} = 0.09$, $\sigma_k = 1$ and $\sigma_{\epsilon} = 1.3$ (Launder and Spalding 1974).

The k-ϵ dispersed multiphase model solves one set of equation for the primary phase accounting for the turbulent kinetic energy production and dissipation due to interphase momentum exchange. The turbulence in the dispersed phase was computed following Tchen theory of dispersion of discrete particles by homogeneous turbulence (Hinze, 1975). The second and third term on the RHS of equation (Table 3.2) are given by Equation (3.2). The last terms in the equation signify the effect of particles on the turbulent kinetic energy and dissipation rate of primary phase (gas). The effect on turbulent kinetic energy due to the interphase momentum exchange was modeled as

$$\Pi_k = \frac{K_{g-s}}{\varepsilon \rho}\left(k_{g\cdot s} - 2k\right) \tag{3.3}$$

Where $k_{g.s}$ signifies the covariance between the gas phase and solid phase velocities. Following Elgobashi and Abou-Arab (1983), the effect of particles on turbulent kinetic energy dissipation rate was modeled as

$$\Pi_{\epsilon} = C_{3e}\frac{\epsilon}{k}\Pi_k \quad \text{with } C_{3\epsilon} = 1.2 \tag{3.4}$$

The covariance between the gas and the solid phase velocities were computed following Simonin and Viollet (1990). Detailed equations may be obtained from the FLUENT 6.3 Manual.

The per-phase k - ε multiphase model solves set of two equations for each of the Eulerian fluid phase. This model is computationally more intensive as this necessitates solving set of two additional equations for the dispersed phase also. The turbulent kinetic energy and dissipation rate for the each phase is tabulated in Table 3.2. The parameter C_{lq} = 2 and $C_{ql} = 2\left(\frac{\eta_{lq}}{1+\eta_{lq}}\right)$ and η_{lq} is the ratio of characteristic particle relaxation time scale and Lagrangian integral time scale for the particle (FLUENT 6.3 Manual).

In the present work, all three k - ε multiphase approaches were used and their relative merits in predicting the hydrodynamic profiles are discussed.

3.2.1. Boundary Conditions

Velocity inlet boundary condition was used at the inlet face. Initially at the start of the simulation, velocity for both the phases and volume fraction of sand were specified at the given operating condition. The velocity profile for each phase was assumed to be uniform across the cross section at the inlet. After the 1st time step, user defined subroutines were hooked to specify the values from outlet at the inlet boundary (to implement periodic boundary condition). Outflow condition was used for the outlet boundary face.

For the primary phase (gas), no slip condition was employed at the walls. The wall shear boundary condition for the solid phase was given by rate of axial momentum transferred to the wall by the particles in a thin layer adjacent to wall surface (Sinclair and Jackson, 1989) as

$$\tau_{s,w} = \frac{\phi \pi u_{slip} \rho_p \varepsilon_s g_0 \Theta^{1/2}}{2\sqrt{3}\varepsilon_s^{max}} \tag{3.5}$$

where ϕ is the specularity coefficient. The value of ϕ = 0 denotes free slip or specular wall and ϕ = 1 denotes diffusive transfer of particles through the wall.

Wall boundary condition for the granular energy was obtained by use of transport balance for the thin shell adjacent to solid wall surface (Johnson and Jackson, 1987). The granular energy flux can be either positive (wall as sink) or negative (wall as source) depending upon the relative magnitudes of granular energy dissipation due to inelastic collision with wall ($\gamma_{\Theta s,w}$) and generation of granular energy due to shear at the wall. Granular energy dissipation due to inelastic collisions with wall is written as

$$\gamma_{\Theta s,w} = \frac{\sqrt{3}\pi\rho_p\varepsilon_s g_0\left(1-e_w^2\right)\Theta^{3/2}}{4\varepsilon_s^{max}} \tag{3.6}$$

For the algebraic granular model, the generation of granular energy was set equal to dissipation. Hence, specifying only the specularity coefficient implicitly specifies the particle – wall restitution coefficient. A more elaborate description of the Eulerian model for gas solid flows can be had from Gidaspow (1994) and references therein.

3.2.2. 3D Computational Domain

The computational domain consisted of a small 3D differential element of the riser column (Figure 3.1) of i.d. 0.054m and height 0.005 m (~$39d_p$). The base case simulations were performed on domain with a total of 38206 hex cells at spacing of approximately 0.68 x 10^{-3}m [$5.33d_p$] and 7 cells along the periodic domain. The unimodal size distribution of the grid size based on cell volume on outflow domain is shown in Figure 3.2, wherein the linear dimension was computed as cube root of cell volume. The mean dimensionless linear dimension was approximately $5.5d_P$ and was sufficient to ensure grid independent results (Andrews *et al.*, 2005; Agrawal *et al.*, 2001).

3.2.3. User Defined Function

To simulate periodic flow profiles across the computational domain, the computed flow quantities from the outlet boundary surface were specified at the inlet boundary surface after every iteration. This was carried out by use of user defined functions and memory variables in FLUENT^{TM}. The computed flow quantities viz gas and solid phase velocities in three directions, turbulent quantities, solid volume fraction and granular energy were accessed at the outlet boundary face and stored at the corresponding inlet face boundary through user defined memory variable (UDMI). For example, face labeled as 6 in Figure 3.3 at the outlet boundary face corresponded to face labeled as 4 at the inlet boundary. In this example, the outlet and inlet face

labels differed by a constant value of 2. For 3D computational domain, the outlet and inlet face labels differed by a value of 6. The stored values from the UDMI were then accessed at the inlet boundary. Appropriate correction factors were also employed to enforce gas and solid mass flux at their specified value. The correction factor for a phase was defined as the ratio of the computed mass flux at the outlet boundary to the specified mass flux. The mass flux of a given phase at the outlet boundary was computed from the mass flow rate across each face of the outlet cell and computed using the following equation:

$$\dot{m}_q = \frac{\sum_{i=1}^{n} (\rho_q u_q \varepsilon_q A_i)_i}{\sum_{i=1}^{n} A_i} \tag{3.7}$$

The user defined function used in this study is given in Appendix II.

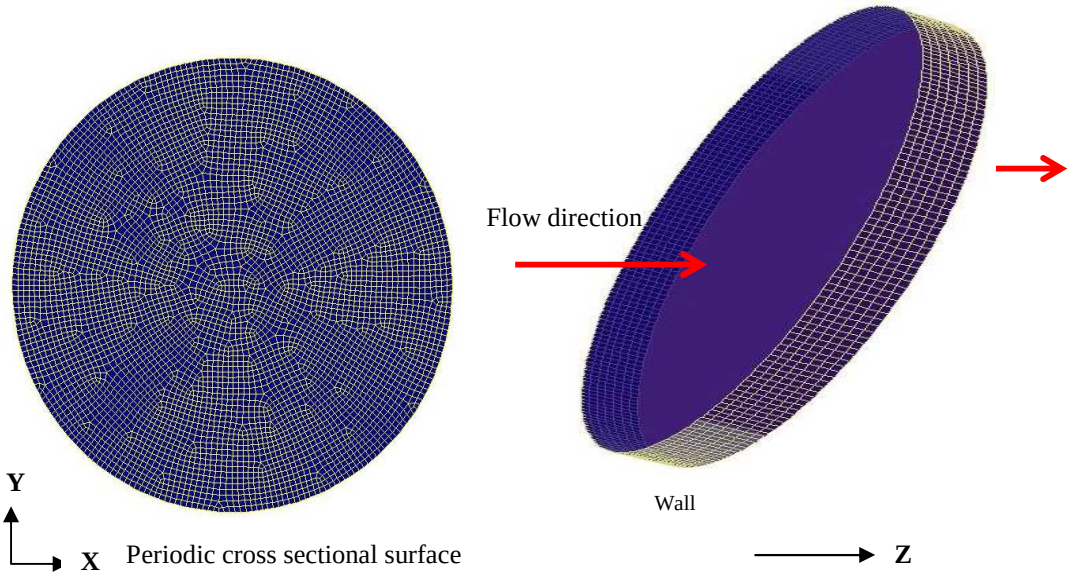

Figure 3.1: Computational domain for periodic flow simulation

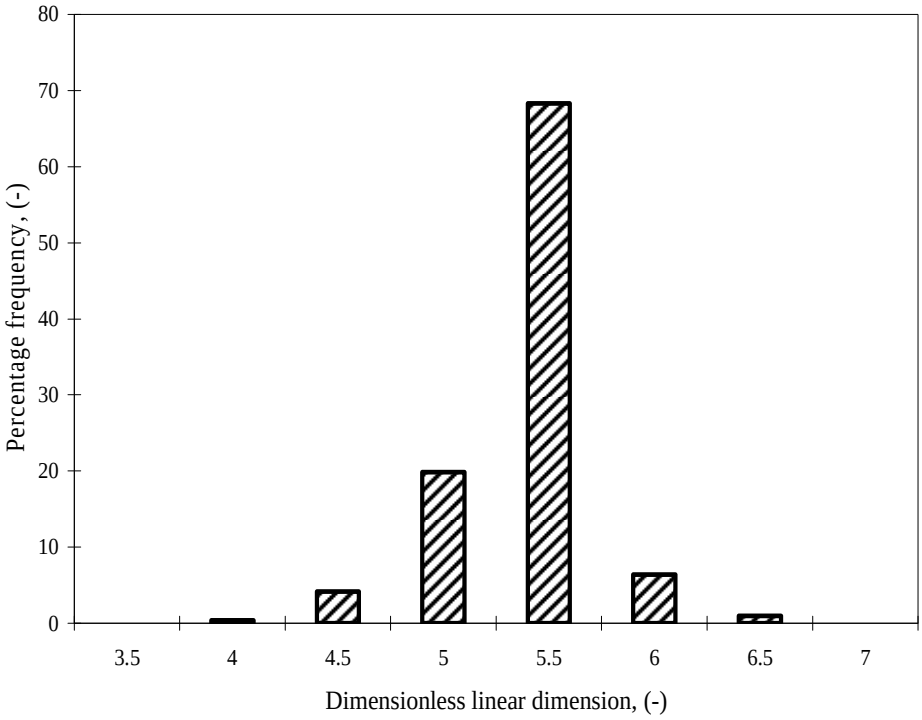

Figure 3.2: Percentage frequency distribution of cell size on the outlet face of 3D computational domain

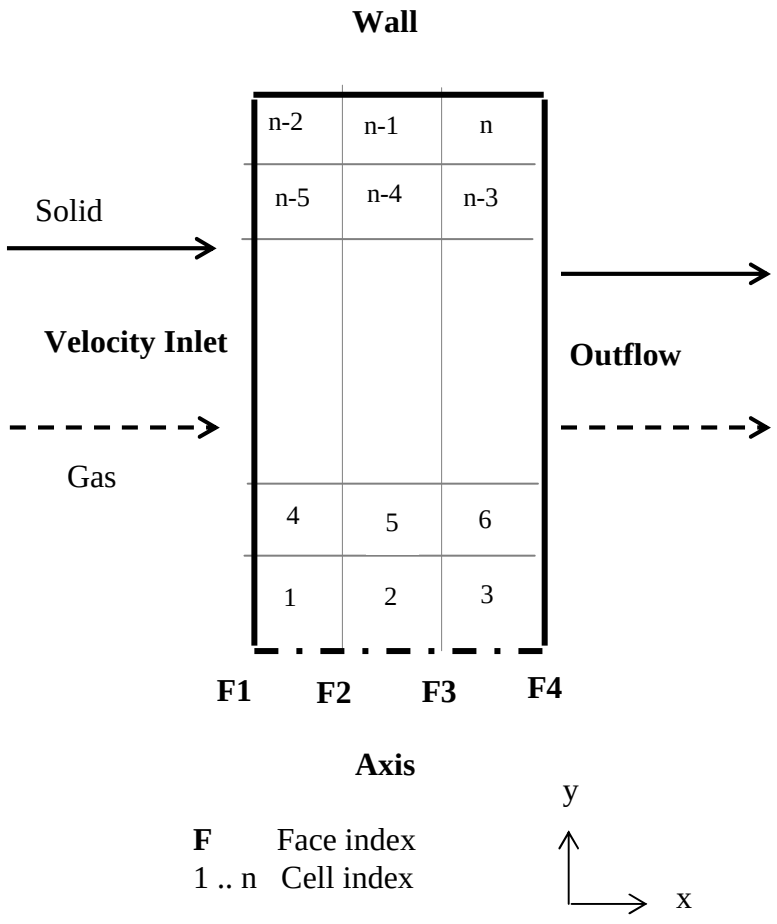

Figure 3.3: 2D-axis symmetric computational domain

3.2.4. 2D Axis Symmetric and 2D Computational Domain

Simulations were also performed with 2D axis symmetric (cylindrical) and 2D (Cartesian) computational domain for the riser of same diameter 0.054m and height of 8m.

For the 2D case, both the lateral sides were specified as wall boundary and hence would actually correspond to a channel flow in 3D. The geometry for 2D was made in Gambit^{TM} (v 2.4.6, Ansys Inc, USA). Hex meshed of two different spatial resolutions was employed. A coarse grid with spatial resolution of 0.0054m ($42d_p$) and total of 10 X 1372 hex grids along span wise y direction and stream wise x direction (flow direction) gave a total of 13720 (14k) hex cells. Fine grid geometry with spatial resolution of 0.001m (~$7.8d_p$) and total of 54 X 800 hex grids along span wise y direction and stream wise x direction (flow direction) gave a total of about 43000 hex cells (43k). Gravity was specified in the x direction as g_x = -9.81 m/s^2.

For the 2D axis symmetric domain, the riser geometry was meshed with 5 X 1600 (8k) hex cells along the radial and axial direction respectively. This corresponds to the coarse grid resolution of ~ 0.0054m ($42d_p$) with the aspect ratio of 1.08: 1 (radial: axial). Fine grid with spatial resolution of 0.0005m (~$3.8d_p$) and total of 54 X 1600 hex grids along radial direction and axial flow direction (total of about 86000 i.e., 86k hex cells) was also employed.

Unless stated otherwise, a typical gas solid particle system of particle size 129 μm and particle density 2540 kg/m^3 flowing upward at superficial gas velocity of u_g = 10 m/s and G_s 300 kg/m^{2}s was considered for all simulation studies. Air density and viscosity were taken as 1.225 kg/m^3 and 1.7894 X 10^{-5} Pa s respectively. The mixture-turbulence model and algebraic KTGF model were employed for all simulations by default. The drag coefficient was specified by Wen nd Yu (1966). Table 3.3 specifies the default granular model parameters used for the presented riser flow simulations.

3.3. RESULTS AND DISCUSSION

In the beginning, the simulations were done on the 2D and 2D axis symmetric computational domains. The equations were solved using segregated solver and second order discretization schemes for the variables. SIMPLE algorithm was employed for the pressure velocity coupling. The time step for each simulation was 1x 10^{-4} s. The simulated results were time averaged for period of about at least 20s. Solution convergence was monitored by recording the area-weighted quantities – solid circulation flux, slip velocity at the outflow boundary, static pressure drop across the domain and radial profile of flow variables obtained at different time intervals or averaging time durations.

Flow development in the 2D Cartesian geometry representing gas solid vertical channel up flow is shown in Figure 3.4a. These results were obtained with a spatial resolution of $42d_p$ across the domain and aspect ratio of ~1. The radial profile of the solid holdup was developed at distance of about 4 m from the entrance. Radial segregation of solids towards the wall was clearly captured. However, when the resolution was further increased to $7.8d_p$, the radial segregation of solids towards the wall was affected (Figure 3.4b). The peak in the radial solid holdup profile was observed at around the normalized distance of 0.9 from centre and not at the wall. Radial segregation captured at lower grid resolution may be due to the poor resolution of the computational grid near the wall. Further resolution of the grid shows inadequacy of the model to capture the radial heterogeneity. Hence, care should be taken in simulating the gas solid riser flows. Simulations reported in open literature with larger grid size (of the order of $30d_p$ and more) or with poor resolution of grids near the wall might mislead the observations. It is worth to reinforce at this point that coarse grid simulation without any sub grid closures for cluster formation could mislead observations.

Similar observation was found from the simulation results from 2d axis symmetric model with the coarse grid of ~ $42d_p$ and fine grid of $3.8d_p$ (Figure 3.5a and 3.5b).

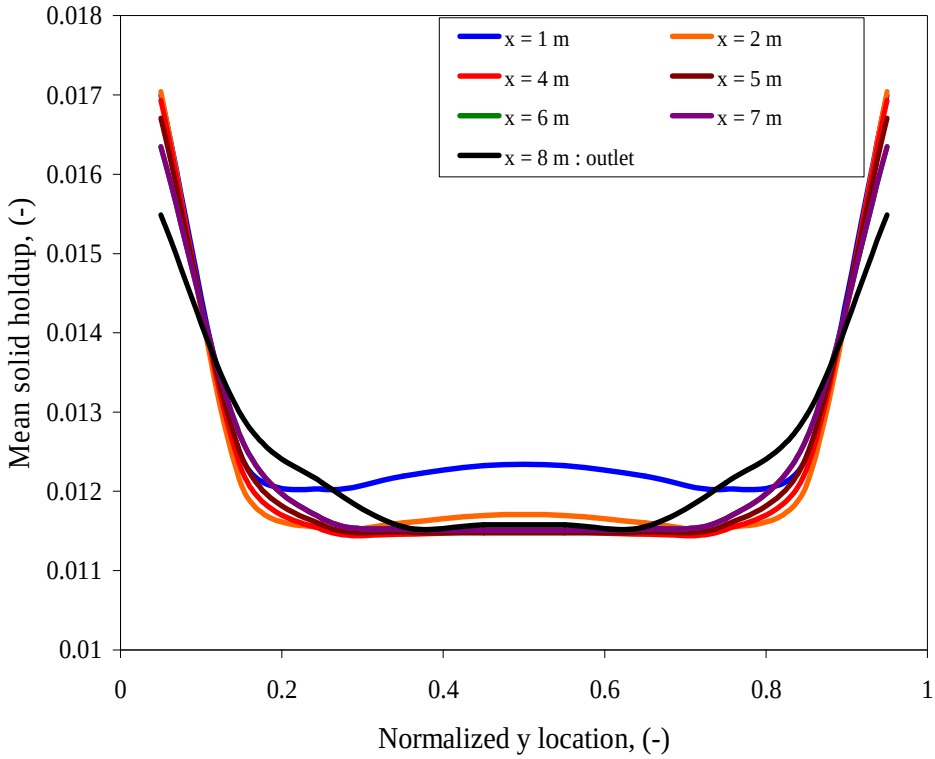

Figure 3.4a: Time averaged cross sectional profile of solid holdup at u_g = 10m/s and G_s = 300 kg/m^{2}s at planes along stream wise flow direction from 2D computational domain with spatial resolution of 42d_p

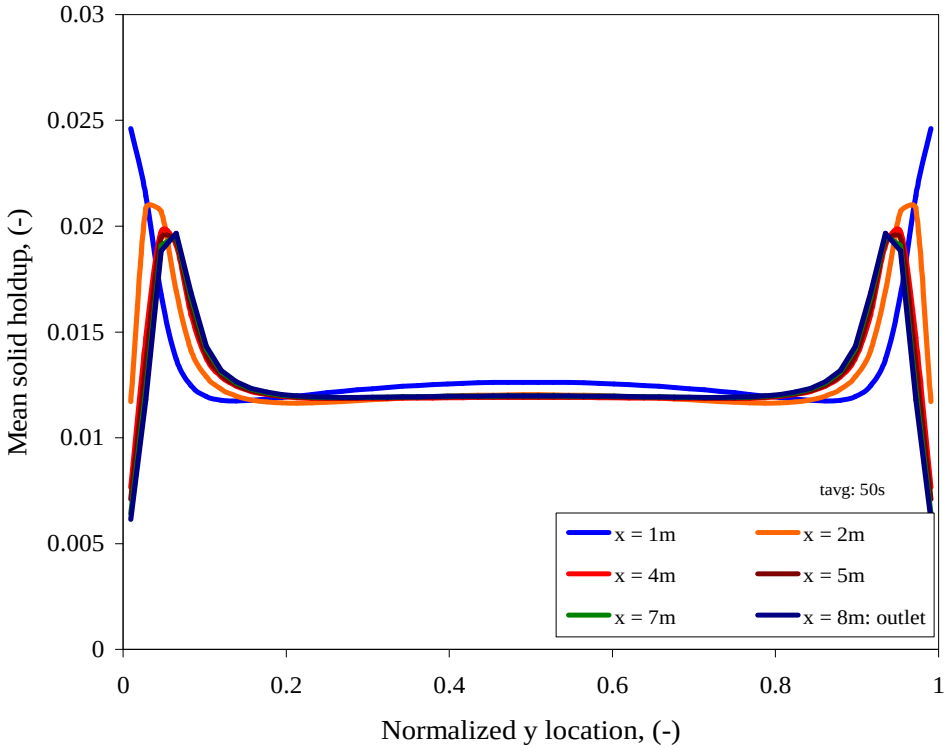

Figure 3.4b: Time averaged cross sectional profile of solid holdup at u_g = 10m/s and G_s = 300 kg/m^{2}s at planes along stream wise flow direction from 2D computational domain with spatial resolution of 7.8d_p

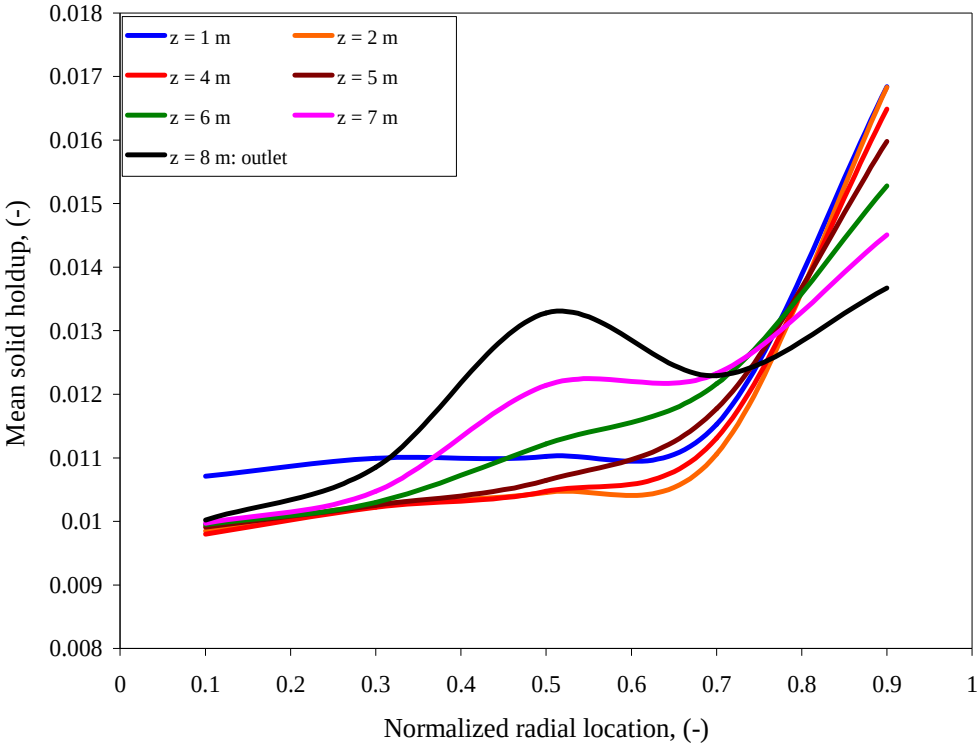

Figure 3.5a: Time averaged radial profile of solid holdup at u_g = 10m/s and G_s = 300 kg/m^{2}s at different axial locations from 2D axis symmetric computational domain with spatial resolution of 42d_p

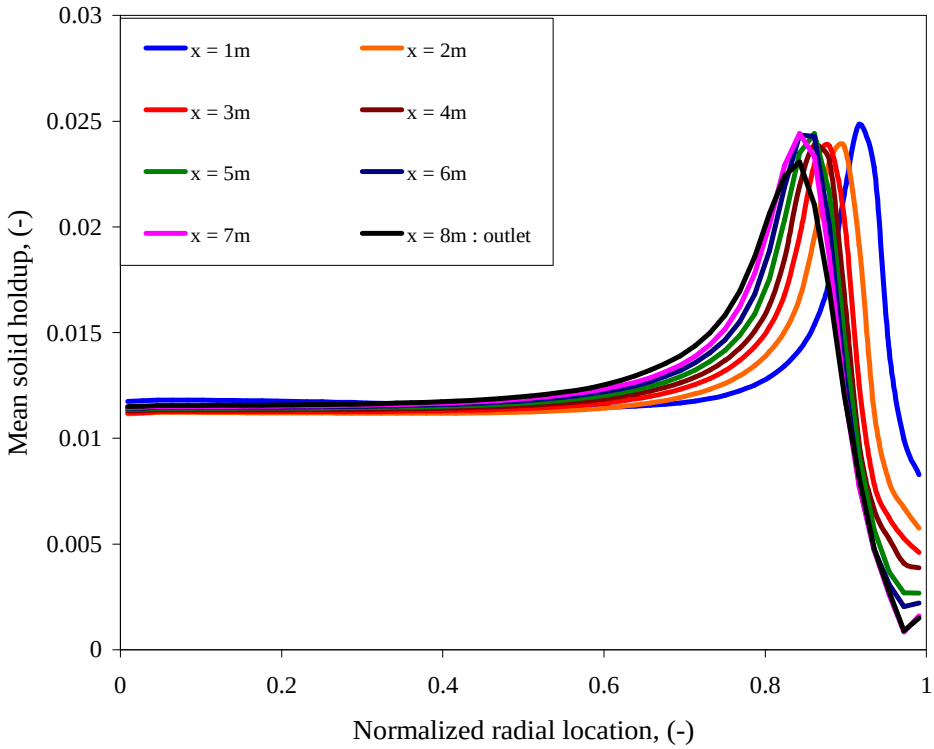

Figure 3.5b: Time averaged radial profile of solid holdup at u_g = 10m/s and G_s = 300 kg/m^{2}s at different axial locations from 2D axis symmetric computational domain with spatial resolution of 3.8d_p

3.3.1. Single Phase Flow Simulation in Periodic 3D Computational Domain

Prior to two phase gas solid periodic flow simulations, the methodology of incorporating UDF's to simulate fully developed flow was tested with single phase flow simulations on 2D axis-symmetric and 3D computational domain. For the 2D axis – symmetric test case, flow through circular cross sectional pipe was simulated on computational domain shown in Figure 3.3. No of cells across the axis (Y direction) was varied to ensure grid independent results. No of cells along the axis was kept constant at 3 in all the simulations. The result (Table 3.4) with external periodic UDF's was in coherence with the FLUENT inbuilt periodic model for single phase.

Table 3.4: Results of single phase test simulations on 2D axis symmetric domain

Simulation	**No Cells**	**Centerline velocity m/s**	**Pressure drop gradient Pa/m**
Analytical result (Assumed Darcy friction factor ~ 0.024 at Re 30117 corresponding to 10 m/s)			22.2222
54 Y cells with UDF	54	12.0251	19.3041
864 Y cells with UDF	864	12.0470	21.5634
864 Y cells with FLUENT Periodic option	864	11.7626	22.7368

For the 3D test case, the riser base case computational domain was simulated for single-phase flow through pipe. For superficial air velocity of 0.1 m/s (Re ~ 370, Laminar) through pipe of i.d. 0.054 m the simulated pressure drop gradient was 17.56 X 10^{-3} Pa/m with ~10% deviation from the analytical value. The centre line velocity was 3.45% higher than the expected analytical value. The simulated profile is shown in Figure 3.6. For 3D test case of turbulent air flow through pipe (Re ~ 37000, Turbulent flow) of i.d. 0.054m, the periodic simulation using UDF's predicted the pressure drop with 5.8% deviation from that obtained from Moody friction factor chart (f_D = 0.02). With establishing the adequate implementation of periodic boundary conditions for single-phase flows, two phase flow simulations were performed for the

base case gas solid riser system. The system falls to Geldart B classification with particle terminal velocity of 0.7914 m/s. This gives the particle relaxation time scale based on terminal settling velocity to be 0.0806 s.

Simulation was started with uniform patching of the computational domain with the operating velocities and cross sectional average solid holdup. The cross section average solid holdup was approximated based on slip factor correlation of Patience *et al.* (1992). The UDF was hooked at the inlet boundary after the 1^{st} time step. The equations were solved using segregated solver and second order discretization schemes for the variables. SIMPLE algorithm was employed for the pressure velocity coupling. The time step for each simulation was $1x\ 10^{-4}$ s. The simulated results were time averaged for period of about 30 – 50s. Radial profiles were obtained by azimuthal average of flow quantities on 50 radial bands. Solution convergence was monitored by recording the area-weighted quantities – solid circulation flux, slip velocity at the outflow boundary, static pressure drop across the domain and radial profile of flow variables obtained at different time intervals or averaging time durations. A typical time averaged radial profile of solid holdup with specularity coefficient of 0.0001 and at different averaging time duration is shown in Figure 3.7.

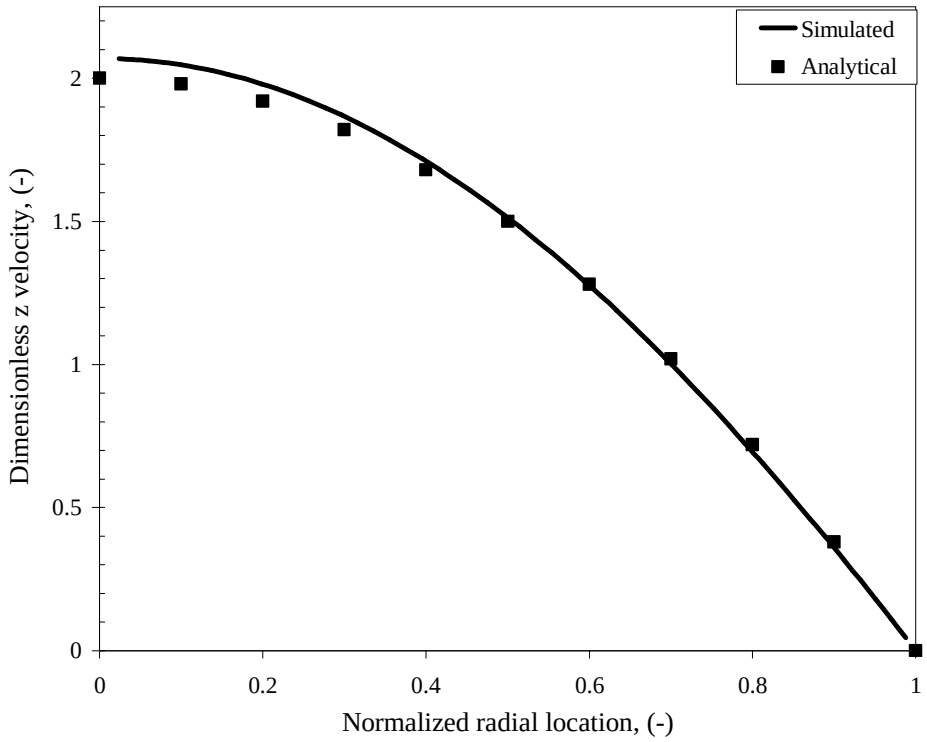

Figure 3.6: Radial profile of dimensionless z velocity for laminar flow of air through circular pipe at 0.1 m/s: 3D simulation

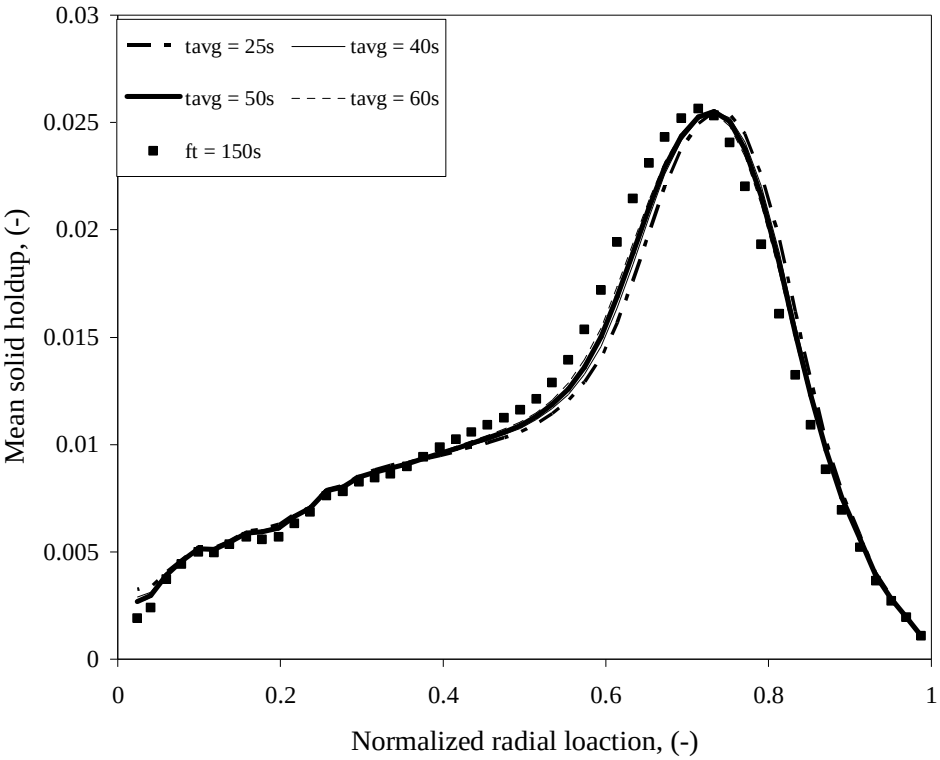

Figure 3.7: Radial profile of time averaged solid holdup at u_g = 10 m/s, G_s = 300 kg/m^{2}s, ϕ = 0.0001 and at different averaging time period duration

3.3.2. Effect of Specularity Coefficient

The effect of specularity coefficient on radial solid holdup was investigated. Specularity value of zero signifies free slip boundary for the solid phase whereas the value of 1 denotes no slip boundary. A very low value of specularity factor showed radial segregation in the solid holdup profile towards the wall (Figure 3.8a). Although, solid volume fraction profile closer to free slip condition (ϕ = 0.0001) showed solid peaking towards the wall (Figure 3.8a), simulations showed no presence of solids holdup very close the wall. Further solid tend to accumulate onto a ring rather than monotonically increasing towards the wall. At higher values of specularity coefficient, solids tend to concentrate mid-way between the centre and wall as shown in Figure 3.9. At higher values of specularity coefficient (0.01 and 0.1 show in Figure 3.9), transient motion of solid clusters were not observed in the CFD simulation. Solids were accumulated at particular location and were not significantly changing with flow time. At this juncture, no specific reason can be attributed to this anomalous behavior observed in the CFD model predictions.

Lowering the specularity coefficient reduced the overall cross sectional solid holdup in the flow domain. This is evident from the radial particle velocity profile shown in Figure 3.8b. For a specified solid circulation flux, increasing specularity coefficient resulted in decrease in average particle velocity across the domain and hence increased average solid holdup. The global hydrodynamic parameters are listed in Table 3.5. It can be observed that in all the cases, the solid hydrostatic head contributed to nearly 90% to the predicted pressure drop gradient.

The radial profile of solid holdup at different values of specularity coefficient with PDE formulation of granular energy flux is shown in Figure 3.10. It can be seen from Figure 3.8a and Figure 3.10 that the radial profiles can be easily classified into two distinct types with peak holdup near r/R ~ 0.5 or r/R = 0.8. For a given value of specularity coefficient, the difference in results predicted using algebraic and full conservation (partial differential equation formulation with convection and diffusion term) formulation of granular energy was not significant (see for example Figure 3.11 at ϕ = 0.0001). The time averaged cross sectional averaged solid holdup in both the cases was 0.75 ± 3%.

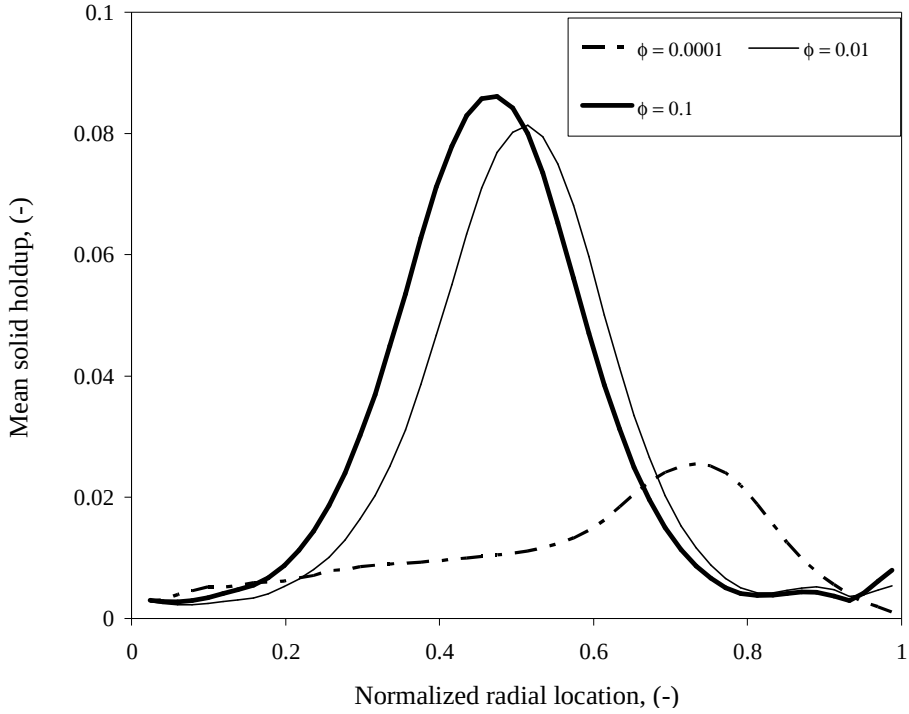

Figure 3.8a: Radial profile of time averaged solid holdup at different values of specularity coefficient for u_g = 10m/s and G_s = 300 kg/m^{2}s

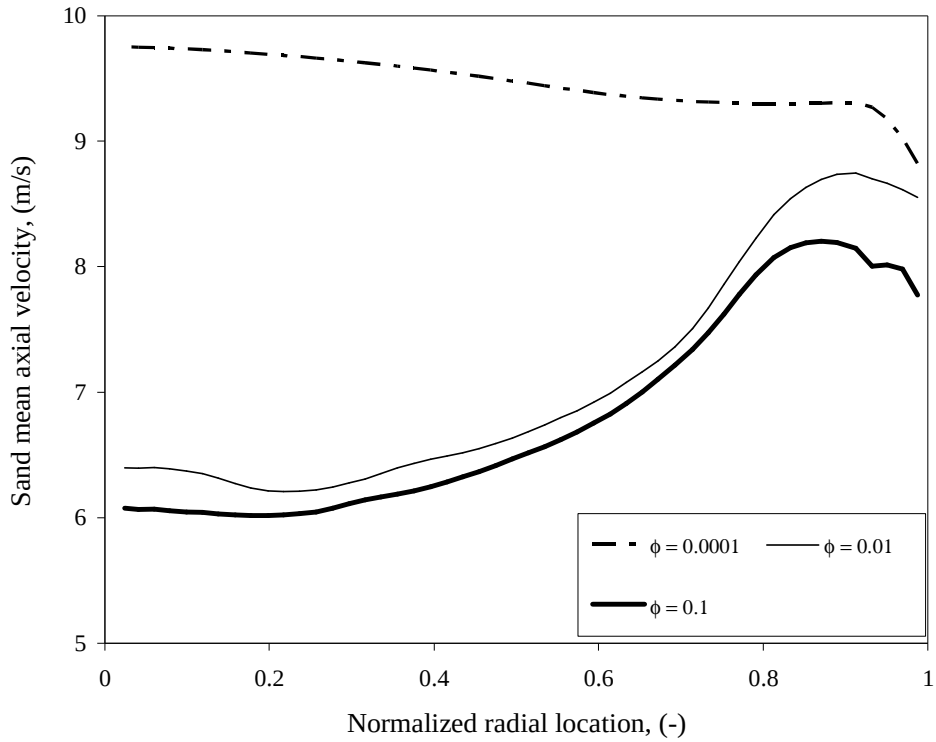

Figure 3.8b: Radial profile of time averaged axial velocity of sand at different values of specularity coefficient for u_g = 10m/s and G_s = 300 kg/m^{2}s

Table 3.5: Predicted results for u_g = 10m/s and G_s = 300 kg/m^{2}s and at ϕ = 0.0001 from periodic and full riser domain simulations

Specularity Coefficient	**Pressure drop gradient, (Pa/m)**	**Solid holdup, (-)**	**Slip velocity, (m/s)**
0.0001	340 (315)	0.01264	0.77
0.01	637 (580)	0.02327	1.9
0.1	674 (604)	0.02426	2.11

* The value in brackets denotes the contribution from solid head/gravity

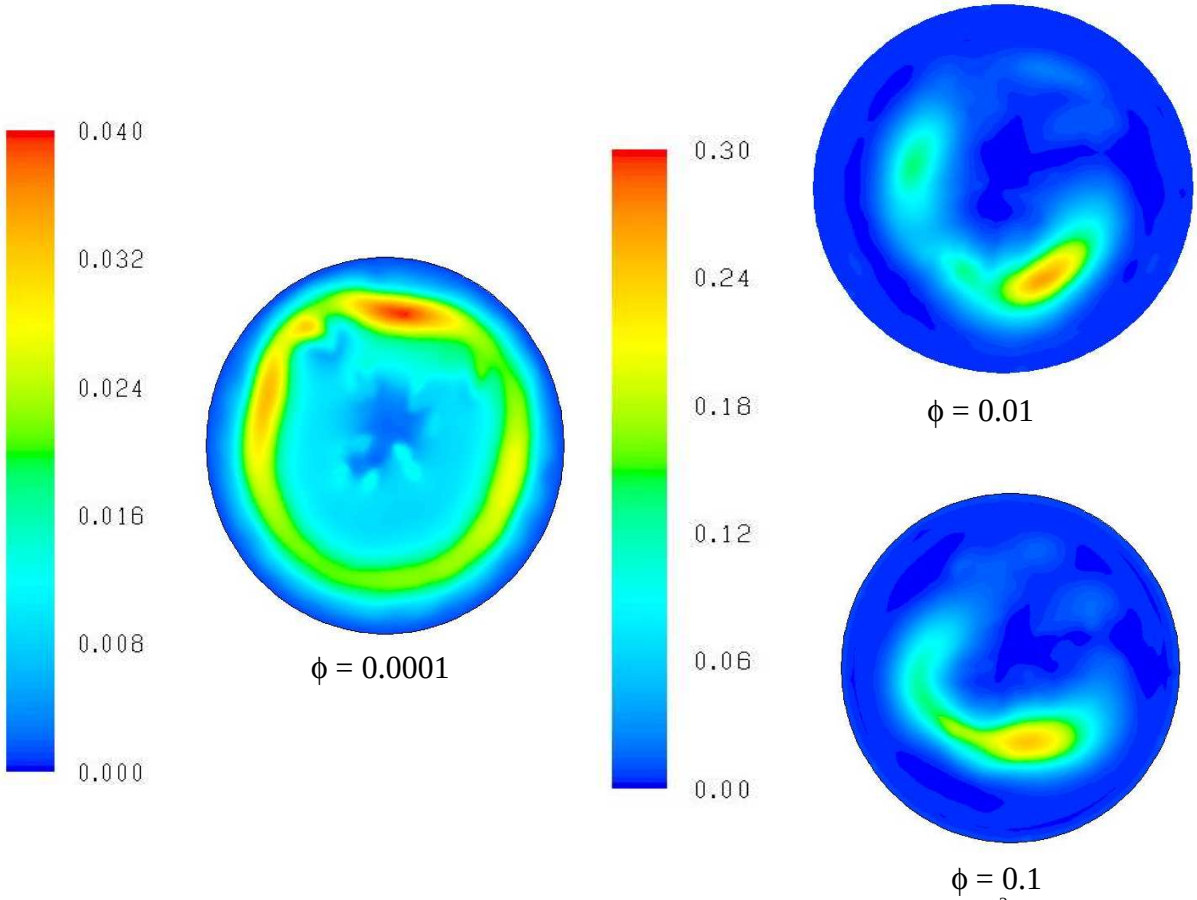

Figure 3.9: Contour of time averaged solid holdup at u_g = 10 m/s and G_s = 300 kg/m^{2}s at different values for specularity coefficient

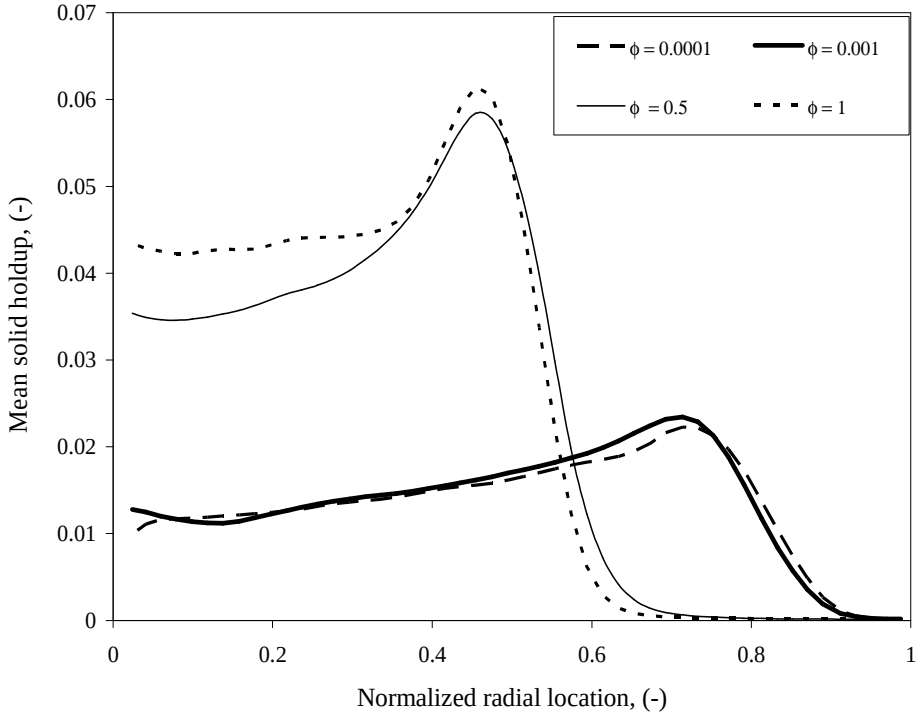

Figure 3.10: Radial profile of time averaged mean solid holdup at u_g = 10 m/s and G_s = 300 kg/m^{2}s with pde granular formulation and different values of specularity coefficient

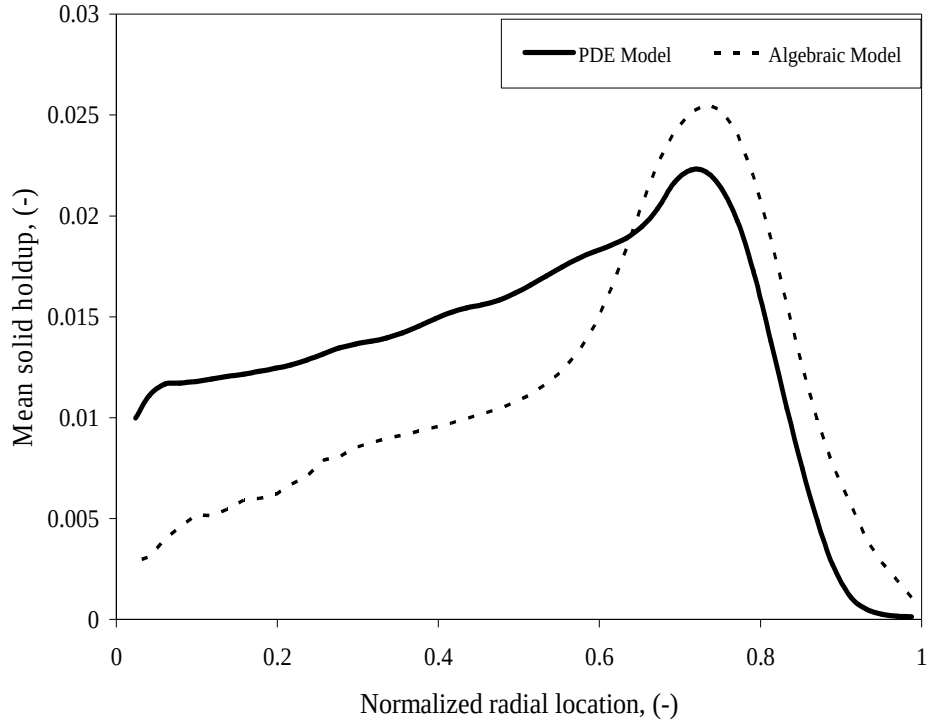

Figure 3.11: Radial profile of time averaged mean solid holdup at u_g = 10 m/s and G_s = 300 kg/m^{2}s and ϕ = 0.0001 with algebraic and pde granular formulation

3.3.3. Effect of Drag Coefficient Formulation

Considerable amount of research is devoted to the formulation of drag coefficient for gas solid riser flows in order to capture the observed increase in slip velocity in these systems (Chapter 2). Multi scale structure based drag formulation for computing the interphase exchange coefficient in high solid flux riser flows systems was assessed in Chapter 2. It was found not suitable to be implemented into the CFD framework in its current form. Hence the effect of drag coefficient formulation is demonstrated with other reported and widely used drag correlations like Wen and Yu (1966)

The time averaged radial profiles of mean gas velocity, solid velocity and solid holdup is shown in Figure 3.12a to Figure 3.12c. Helland *et al.* (2007) developed an empirical correlation for gas solid riser flows. Their correlation gives a minimum in the drag coefficient function for solid holdup values of around 0.05. Radial segregation with increased solid holdup near the wall is predicted by Helland *et al.* (2007) whereas Gidaspow (1994) Wen and Yu (1966) correlation results in lower cross sectional solid holdup and pressure drop gradient (Table 3.6). However, the simulations also predicted the presence of solids near the central core resulting in the formation of core annulus and core type profile. It should be noted here that higher solid holdup region near the center was result of time averaging of instantaneous solid holdup profiles. Contours of solid holdup at the periodic cross section (Figure 3.13) show that dense solid cluster move in random near the central core section. Such dynamics were even observed with Gidaspow (1994) drag relation but not with Wen and Yu (1966) correlation.

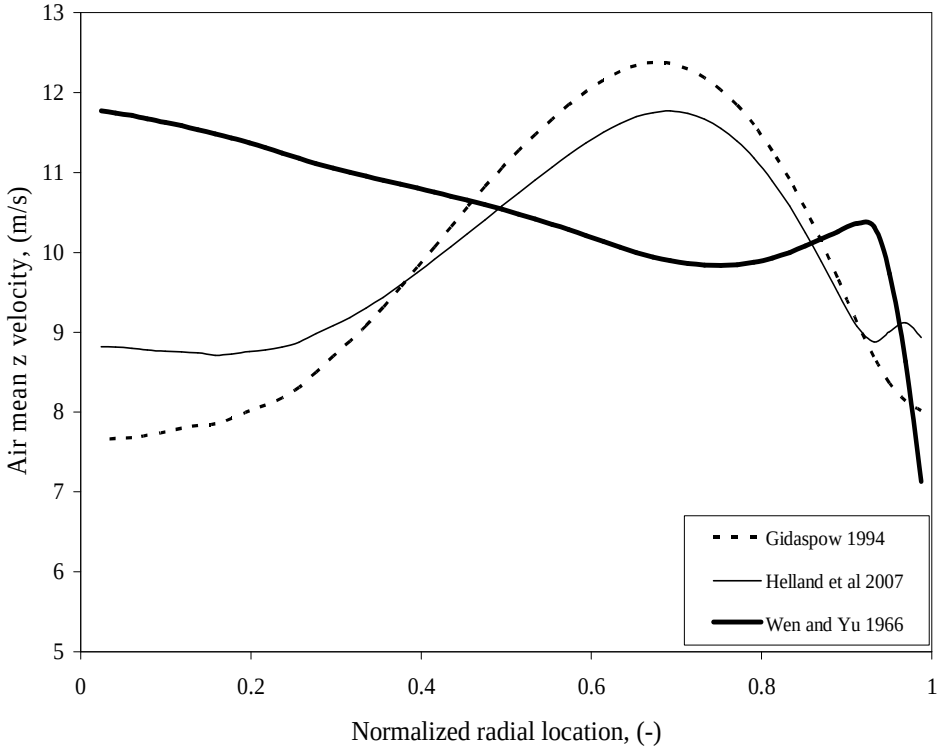

Figure 3.12a: Radial profile of time averaged air mean z velocity at u_g = 10m/s and G_s = 300 kg/m^{2}s

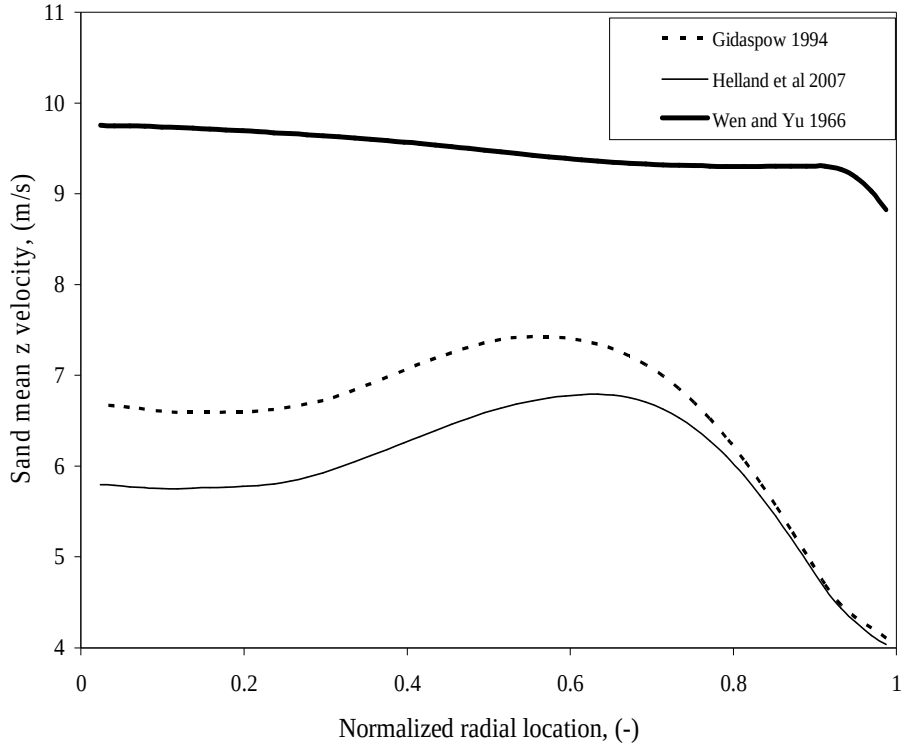

Figure 3.12b: Radial profile of time averaged sand mean z velocity at u_g = 10m/s and G_s = 300 kg/m^{2}s

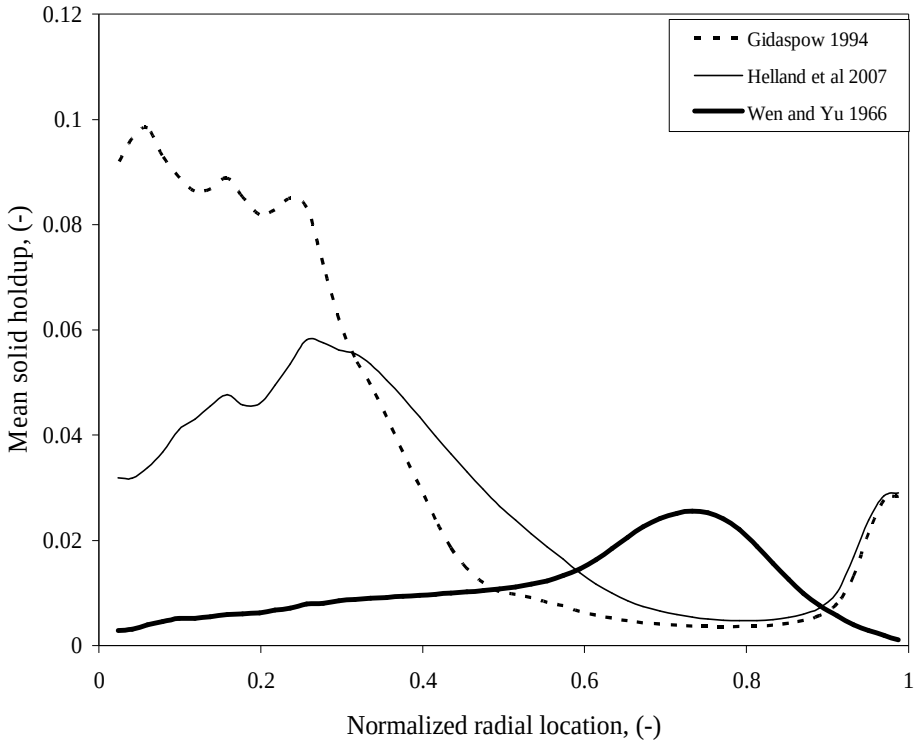

Figure 3.12c: Radial profile of time averaged mean solid holdup at u_g = 10m/s and G_s = 300 kg/m^{2}s

Table 3.6 Predicted results for u_g = 10m/s and G_s = 300 kg/m^{2}s and with different drag formulations from 3D periodic simulations

Drag	**Pressure drop gradient, (Pa/m)**	**Overall solid holdup, (-)**	**Slip velocity, (ms/)**
Wen and Yu (1966)	340 (315)	0.01264	0.77
Helland *et al.* (2007)	1913 (500)	0.0201	4.53
Gidaspow (1994)	2528 (463)	0.0186	3.839

* Pressure drop gradient given in brackets denotes the contribution due to solid head/gravity alone

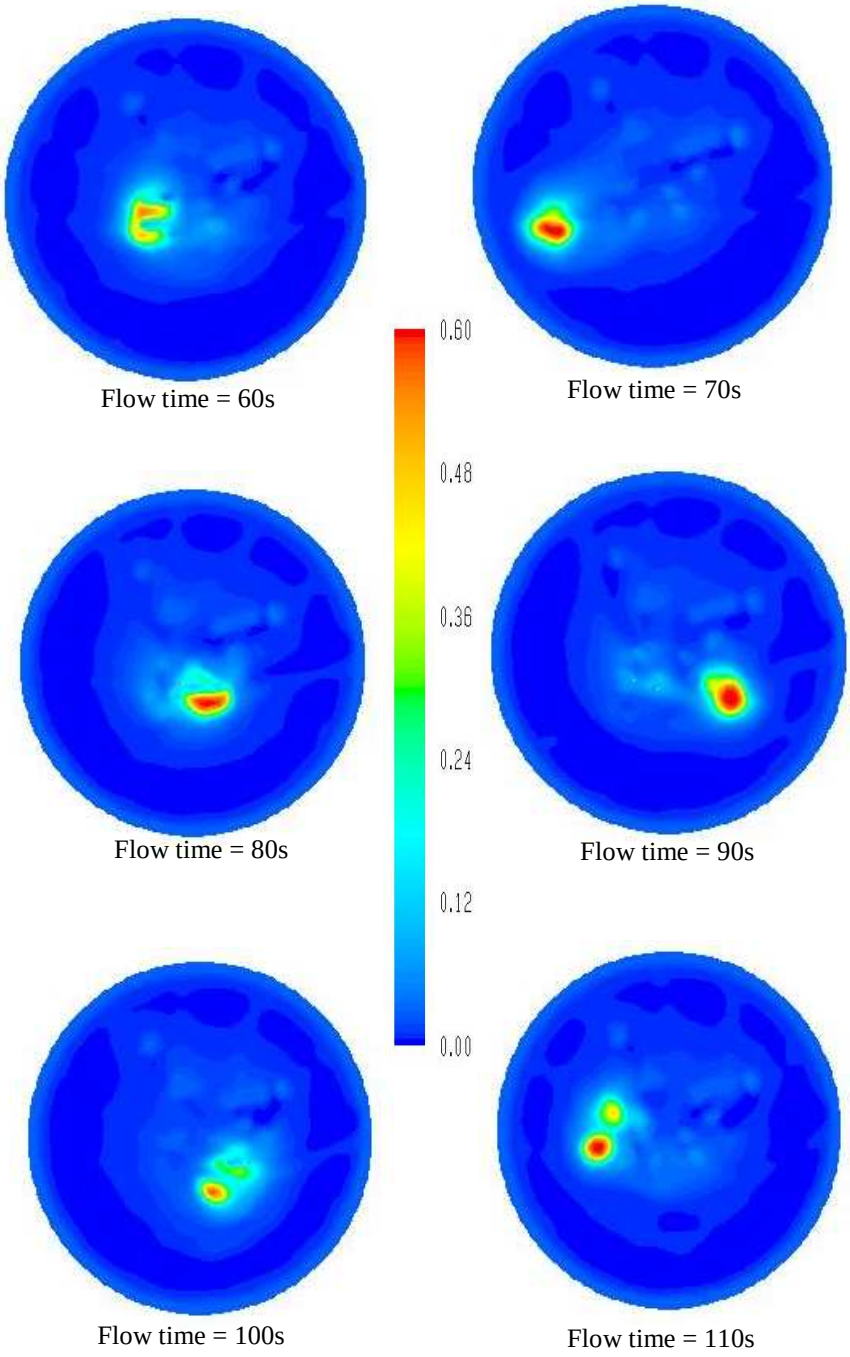

Figure 3.13: Contour plots of instantaneous solid holdup at the periodic cross section for u_g = 10m/s and G_s = 300 kg/m^{2}s with Helland *et al.*, (2007) drag correlation

The periodic flow model with the UDF was extended to study the effect of various other parameters as well like effect of particle – particle restitution coefficient, particle – wall restitution coefficient, turbulence model, operating conditions – superficial gas velocity, solid circulation flux etc. For the sake of brevity, the results from all such parametric studies are not included in the thesis. The main purpose of the research work was to develop the computational methodology to simulate fully developed flow profiles with specified mass flux for gas solid two phase flows and show the proof of concept in computing periodic flow profiles with a commercial CFD package. Additional simulation results which are not included here may be obtained from me (E-mail: naren_pr@yahoo.com)

3.4. CONCLUSIONS

Periodic boundary conditions were implemented by developing a User defined function. This was then used to carry out simulations of fully developed gas solid riser flow using a two fluid model with KTGF. The work highlighted and brought to focus the necessity of employing finer grid size in simulating gas solid riser flows. The UDF based periodic model approach developed in this work looks promising to simulate fully developed gas solid riser flow profiles without compromising on the spatial resolution. The UDF approach is helpful in judicious selection and assessment of model (turbulence, granular) parameters, which can further be employed for full domain simulations.

CHAPTER 4

RISER SCALING

The chapter deals with the evaluation of hydrodynamic scaling law for gas solid riser flows. A comprehensive analysis of literature data on pressure drop was presented. Based on this, observations are made on the development of empirical scaling laws from experimental data. Further, the 3D periodic computational model was used to perform numerical experiments and study the effect of various system and operating parameters in predicting hydrodynamic scaling in riser flows. The Qi scaling ratio ensured similarity in global parameters like overall cross sectional average solid holdup or pressure drop gradient. Similarity in local flow profiles were not observed for all the test cases.

4.1. BACKGROUND

Successful commercialization of a process from lab to industrial scale requires development of appropriate scaling laws. The scaling laws ensure proper hydrodynamic similarity between reactors at various scales or operating conditions. Scale up is an integral part of process development life cycle. Hydrodynamics of large scale industrial CFBs can be different from lab scale CFB systems. The effect of reactor scale on the prevailing flow structure has to be accounted properly. Otherwise, this might lead to performance deterioration and plant failure as well. For instance, as briefed in Chapter 1, industrial scale plant for partial oxidation of n-butane to maleic anhydride was unsuccessful owing to scaling issues (Dudukovic, 2010). Therefore, development of proper scale up criteria assumes significance.

Following Anderson and Jackson (1967), the two fluid model for gas solid riser flow is based on the conservation equation for mass and momentum transport. The scaling parameters for the hydrodynamic similarity are derived from the dimensionless form of conservation equations (Knowlton *et al.*, 2007; Xu and Gao, 2003; van der Meer *et al.*, 1999 etc.) Evaluation of scaling laws requires extensive experimentation. Performing experiments at extreme operating conditions and at larger scales may not be feasible at all times. In this context, computational fluid dynamics offers the advantage by facilitating evaluation of these scaling parameters with fewer requirements of extensive physical experiments.

Recently Qi *et al.* (2008) proposed an empirical scaling parameter based on Froude number and flow rate ratio. The proposed scaling parameter ensured both local and global hydrodynamic similarity in riser reactors. The parameter was tested with data from literature and their own experiments.

Qi empirical scaling parameter: $$Fr_D^{-0.3} G_s / \left(\rho_p u_g \right) \tag{4.1}$$

Where $$Fr_D = \frac{u_g^2}{gD} \tag{4.2}$$

For the same Qi scaling ratio, radial profiles of solid concentration, particle velocity and cluster voidage exhibited similar profile in the fully developed flow region. The

average solid holdup was shown to vary linearly with respect to the $Fr_D^{-0.3} G_s / (\rho_p u_g)$ scaling ratio.

This looks promising as a single scaling parameter ensuring hydrodynamic similitude in riser systems both at local and global level. Nevertheless, this empirical parameter cannot guarantee hydrodynamic scaling in risers beyond the tested range without rigorous validation. The parameter was tested with most of data sets obtained with air as fluid medium at ambient conditions. The proposed scaling parameter did not consider the effect of fluid density. Further, the ratio of particle size to column diameter may be significant in small diameter risers and affect the relative contribution of particle shear at wall to the overall pressure gradient (Pita and Sundaresan, 1991 and references therein). Further validation of the scaling parameter requires extensive experimental data sets of good reliability. This can be avoided to an extent, with the use of computational models, wherein the simulated profiles at different conditions can be compared to draw meaningful conclusions on scaling analogies.

With this background, work was carried out with the aim to investigate the ability of CFD models to predict scaling in riser flows. The objective was to perform numerical experiments to study the effect of parameters that were unaccounted in the Qi scaling ratio. The methodology involved simulating fully developed flow profiles in gas-solid riser flow system with imposed periodic boundary through user defined sub routines. The 3D CFD model with periodic boundary condition was developed (see Chapter 3). This was then simulated to numerically investigate the hydrodynamic similitude in gas-solid riser flows based on Qi scalng ratio.

4.2. MATHEMATICAL MODEL

The gas solid two-phase riser flow was modeled with the two-fluid approach (Anderson and Jackson, 1967), wherein the two phases were considered to be interpenetrating continua coupled with momentum exchange factors. Both fluids were assumed to be incompressible and Newtonian in nature. Reynolds averaged mass and

momentum conservation equations were solved to compute the gas-solid flow in the vertical riser.

The turbulent stresses were modeled following the Boussinesq's eddy viscosity hypothesis. The mixture k-ϵ multiphase model with standard wall functions (FLUENT 6.3 manual) was adopted for the riser scaling studies. In the k- ϵ mixture model formulation, phase weighted average quantities were employed to solve a single set of two-equations, one each for the mixture turbulent kinetic energy and mixture turbulent dissipation rate. The interphase momentum exchange between the two phases was provided through the drag coefficient. For the present case, Wen and Yu (1966) drag model was employed.

For the solid phase, the kinetic theory of granular flow (Jenkins and Savage, 1983) was employed to compute the shear stress. The constituent terms in the solid phase stress tensor were calculated from the reported literature correlations (Table 4.1). Algebraic formulation for the granular energy was used in the study, neglecting the accumulation, convection and the diffusion terms in the granular energy conservation equation.

Table 4.1: Granular model specifications

Granular temperature model	Algebraic
Granular conductivity	Syamlal et al. 1993
Granular bulk viscosity	Lun et al. 1984
Frictional viscosity	None
Granular conductivity	Syamlal et al. 1993
Solids pressure	Syamlal et al. 1993
Radial Distribution	Iddir and Arastoopour 2005
Elasticity modulus	Derived
Packing limit	0.6
Particle – Particle restitution coefficient	0.9

4.2.1. Boundary Conditions

Velocity inlet boundary condition was used at the inlet face. Initially at the start of the simulation, velocity for both the phases and volume fraction of sand were specified at the given operating condition. The velocity profile for each phase was assumed to be uniform across the cross section at the inlet. After the 1st time step, user defined subroutines were hooked to specify the values from outlet at the inlet boundary (to implement periodic boundary condition). Outflow condition was used for the outlet boundary face.

For the primary phase (gas), no slip condition was employed at the walls. The wall shear boundary condition for the solid phase was given by rate of axial momentum transferred to the wall by the particles in a thin layer adjacent to wall surface (Sinclair and Jackson, 1989) as

$$\tau_{s,w} = \frac{\phi \pi u_{slip} \rho_p \varepsilon_s g_0 \Theta^{1/2}}{2\sqrt{3}\varepsilon_s^{max}} \tag{4.3}$$

where ϕ is the specularity coefficient. The value of $\phi = 0$ denotes free slip or specular wall and $\phi = 1$ denotes diffusive transfer of particles through the wall.

Wall boundary condition for the granular energy was obtained by use of transport balance for the thin shell adjacent to solid wall surface (Johnson and Jackson, 1987). For the algebraic granular model, the generation of granular energy was set equal to dissipation. Hence, specifying only the specularity coefficient implicitly specifies the particle – wall restitution coefficient. A more elaborate description of the Eulerian model for gas solid flows can be had from Gidaspow (1994) and references therein.

4.2.2. 3D Computational Domain

The computational domain consisted of a small 3D differential element of the riser column (see Figure 3.1 of Chapter 3) of i.d. 0.054m and height 0.005 m (~$39d_p$). The base case simulations were performed on domain with a total of 38206 hex cells at spacing of approximately 0.68 x 10^{-3}m [$5.33d_p$] and 7 cells along the periodic domain.

4.2.3. User Defined Function

To simulate periodic flow profiles across the computational domain, the computed flow quantities from the outlet boundary surface were specified at the inlet boundary surface after every iteration. This was carried out by use of user defined functions (UDF) and memory variables in FLUENT^{TM}. The computed flow quantities were accessed at the outlet boundary face and stored at the corresponding inlet face boundary through user defined memory variable (UDMI). The stored values from the UDMI were then accessed at the inlet boundary. Appropriate correction factors were also employed to enforce gas and solid mass flux at their specified value. Further details are provided in Chapter 3 of the thesis.

4.3. RESULTS AND DISCUSSION

4.3.1. Investigating Scaling Law with Experimental Data on Risers

To begin with, it was envisaged to analyze the capability of Qi scaling ratio in predicting the hydrodynamic similarity in riser flows with the available data from literature. The pressure drop data (correspond to the fully developed flow region in riser) from literature was therefore consolidated and analyzed. For data wherein the axial profile of pressure drop gradient was given, the value corresponding to fully developed location was selected. The fully developed location corresponds to negligible (less than 10%) change in pressure drop gradient in the axial flow direction. Neglecting the frictional pressure drop contribution, solid holdup was calculated from the pressure drop values. Details of the data used in the study are tabulated in Table 4.2. Data used in Qi *et al.* (2008) to develop the scaling parameter are marked explicitly in the Table 4.2.

The solid holdup (cross sectional average solid holdup at fully developed conditions) as function of Qi scaling ratio is shown in Figure 4.1a and 4.1b. Figure 4.1a illustrates sample data used by Qi *et al.* (2008) to develop the empirical scaling ratio. Given the scatter, the solid holdup was found to vary linearly with Qi scaling ratio. However, when solid holdup data from other literature sources were also included in same plot (Figure 4.1b), the empirical relation fails to predict the solid holdup uniquely. Figure 4.1c illustrates the same in terms of pressure drop gradient. Thus, Qi scaling ratio,

based on Froude number and flow rate ratio, was found to be inadequate in predicting the global parameters – pressure drop gradient, solid holdup uniquely, provided the data shown were measured accurately.

In order to understand the reliability of experimental data, three data sets (Bader et al. 1988; Yerushalmi et al. 1986, 1976) from Table 4.2 were chosen to represent the pressure drop data on risers (Figure 4.2a). It is worth while to note that experimental errors bars were not directly available from the literature sources. In absence of this information, we have examined whether presence of any systematic or otherwise errors in the reported data can cause observed discrepancies. Assuming one among the chosen three data sets to be reliable at a time, the solid circulation flux and pressure drop values of the other two data sets were offset to the extent that the two data sets overlap with the first one. The offset required in terms of percentage error in solid flux (G_s) and pressure drop data (ΔP) was noted. For example, an offset of 75% and -30% in Gs and ΔP in Bader et al. (1988) data and an offset of -30% and 20% in the value of Gs and ΔP in Yerushalmi et al. (1986) data would overlap all three data sets with that of Yerushalmi et al. (1976) data line (Figure 4.2b). Similar exercise was also done with the other two data sets as shown in Figure 4.2c and 4.2d. This showed that experimental trend observed with the reported data were not unique and reliable. Lack of accuracy in the measured variable like solid flux, pressure drop may mislead the development of scaling parameters for riser flows.

It is also worth to establish that percentage errors or offset introduced into the data were not mere numerical artifacts. To illustrate and justify the same, an experimental cold CFB facility was setup and solid circulation flux was measured by manual opening of valve and collecting the solids flowing out of the riser column for known amount of time. Care was taken to see that the total inventory in the CFB system was not reduced beyond 10% of initial amount during the flux measurement. Experimental data revealed that measured solid circulation flux showed variation as high as 100%. Thus solid flux measurement by use of quick closing valves could have percentage errors as high as 100%. This justified the measurement inaccuracies incorporated in the data shown in Figure 4.2a. Details on the experimental setup, measurement procedure and solid flux data are given in Annexure 4A.

Thus it was evident from analysis of literature data and also from experimental data from present work that measurement inaccuracies were critical in data analysis and interpretation. Development of scaling laws, without taking into consideration of these experimental inaccuracies may lead to poor interpretation of riser flow data.

Table 4.2: Literature data used for evaluation of scaling law in riser flows

Sr no	**Reference**	**Riser Dimensions**	**Particle Properties**	**Superficial gas velocity m/s**	**Solid circulation flux, kg/m^{2}s**
1.	Qi *et al.* [+,*,#] (2008)	H = 15.1 m D = 0.1 m	ρ_p = 1500 kg/m^3 d_p = 67 μm	3 – 12	24 – 202
2.	Huang *et al.*[#] (2007)	H = 15.1 m D = 0.1 m	ρ_p = 1500 kg/m^3 d_p = 67 μm	2.5 - 10	38 – 220
3.	Zhang *et al.*[+] (2001)	H = 15.1 m D = 0.1 m	ρ_p = 1500 kg/m^3 d_p = 67 μm	5.5 – 8.2	23 – 201
4.	Xu *et al.*[*] (2000)	H = 3 m D = 0.097 m	ρ_p = 2222 kg/m^3 d_p = 166 μm	1.6 – 2.5	12.3 – 14.6
5.	Issangya *et al.*[#] (1999)	H = 6.1 m D = 0.0762 m	ρ_p = 1600 kg/m^3 d_p = 70 μm	4, 8	45 - 240
6.	Mastellone and Arena[*,#] (1999)	H = 5.75 m D = 0.12 m	ρ_p = 2540 kg/m^3 d_p = 89 μm	3 - 6	15 – 117
7.	Mastellone and Arena[*,#] (1999)	H = 5.75 m D = 0.12 m	ρ_p = 1700 kg/m^3 d_p = 70 μm	3	35 – 55
8.	Mastellone and Arena[*,#] (1999)	H = 5.75 m D = 0.12 m	ρ_p = 2600 kg/m^3 d_p = 310 μm	5, 6	16 – 117
9.	Nieuwland (1994)	H = 3m D = 0.03 m	ρ_p = 2900 kg/m^3 d_p = 655 μm	12.3 – 40 (1 bar), 5.4 – 12.4 (4 bar), 5.1 – 8.24 (6 bar)	98 – 312
10.	Nieuwland[+] (1994)	H = 8m D = 0.054 m	ρ_p = 2540 kg/m^3 d_p = 129 μm	10	100 – 400
11.	Nieuwland (1994)	H = 3m D = 0.03 m	ρ_p = 2900 kg/m^3 d_p = 275 μm	5.1 – 8.24 (6 bar)	86 – 300

Sr no	Reference	Riser Dimensions	Particle Properties	Superficial gas velocity m/s	Solid circulation flux, kg/m^{2}s
12.	Ouyang *et al.*,[#] (1993) [as reported in Ouyang and Potter, 1993]	H = 10 m D = 0.254 m	ρ_p = 1380 kg/m^3 d_p = 65 μm	2 – 7.5	10 - 207
13.	Arena *et al.*[#] (1991) [as reported in Ouyang and Potter, 1993]	H = 5.75 m D = 0.12 m	ρ_p = 2543 kg/m^3 d_p = 90 μm	5	92, 115
14.	Arena *et al.*[#] (1991) [as reported in Ouyang and Potter, 1993]	H = 10.5 m D = 0.4 m	ρ_p = 2543 kg/m^3 d_p = 90 μm	5	114, 251
15.	Lounge and Change [*] (1990)	H = 7 m D = 0.203 m	ρ_p = 2600 kg/m^3 d_p = 88 μm	2	40
16.	Bader *et al.*[#] (1988). [as reported in Obrien and Syamlal, 1994]	H = 12.2 m D = 0.305 m	ρ_p = 1714 kg/m^3 d_p = 76 μm	3.7 – 10 (1.5 atm)	98 and 147
17.	Li *et al.*[#] (1988) [as reported in Ouyang and Potter, 1993]	H = 10 m D = 0.09 m	ρ_p = 930 kg/m^3 d_p = 54 μm	1.5 – 2.6	14 - 193
18.	Hartge *et al.*[#] (1986) [as reported in Ouyang and Potter, 1993]	H = 3.3 m D = 0.05 m	ρ_p = 2600 kg/m^3 d_p = 56 μm	3.4 – 4	72 – 90
19.	Hartge *et al.*[#] (1986) [as reported in Ouyang and Potter, 1993]	H = 7.8 m D = 0.4 m	ρ_p = 2600 kg/m^3 d_p = 56 μm	4.2 - 5	64 – 118
20.	Monceaux *et al.* (1986) [as reported in Dasgupta *et al.*, 1998]	H = N.A. D = 0.144m	ρ_p = 1385 kg/m^3 d_p = 59 μm	4.6	50 – 210
21.	Rhodes[#] (1986) [as reported in Ouyang and Potter, 1993]	H = 6 m D = 0.152 m	ρ_p = 1800 kg/m^3 d_p = 64 μm	2.5 – 4.5	8.5 – 107

Sr no	Reference	Riser Dimensions	Particle Properties	Superficial gas velocity m/s	Solid circulation flux, kg/m^{2}s
22.	Rhodes (1986) [as reported in Ouyang and Potter, 1993]	H = 6 m D = 0.152 m	ρ_p = 2600 kg/m^3 d_p = 270 μm	6, 8	70 - 160
23.	Yerushalmi (1986) [as reported in Dasgupta *et al.*, 1998]	H = N.A. D = 0.152 m	ρ_p = 1070 kg/m^3 d_p = 49 μm	2.2 and 4	50 – 190
24.	Arena *et al.* [*] (1985) [as reported in Louge and Change, 1990]	H = 6.4 m D = 0.041 m	ρ_p = 2600 kg/m^3 d_p = 88 μm	7	199 – 600
25.	Yerushalmi and Avidan[#] (1985) [as reported in Ouyang and Potter, 1993]	H = 8.5 m D = 0.152 m	ρ_p = 1070 kg/m^3 d_p = 49 μm	1.2 – 5.1	63 – 173
26.	Weinstein *et al.*[#] (1984) [as reported in Ouyang and Potter, 1993]	H = 8.5 m D = 0.152 m	ρ_p = 930 kg/m^3 d_p = 54 μm	2.9 – 3.4	70 – 130
27.	Yang *et al.*[#] (1984) [as reported in Ouyang and Potter, 1993]	H = 8 m D = 0.115 m	ρ_p = 794 kg/m^3 d_p = 220 μm	5.3	43.5 - 160
28.	Yerushalmi *et al.* (1976)	H = 7.0104 m D = 0.0762 m	ρ_p = 881 kg/m^3 d_p = 60 μm	1.8 -4.5	20 – 220

N.A. Not Available

\+ Pressure drop obtained from axial pressure gradient profile at fully developed region.

* Pressure drop obtained from axial solid holdup profile at fully developed region, neglecting friction

\# Data used for analysis in Qi *et al.*, (2008)

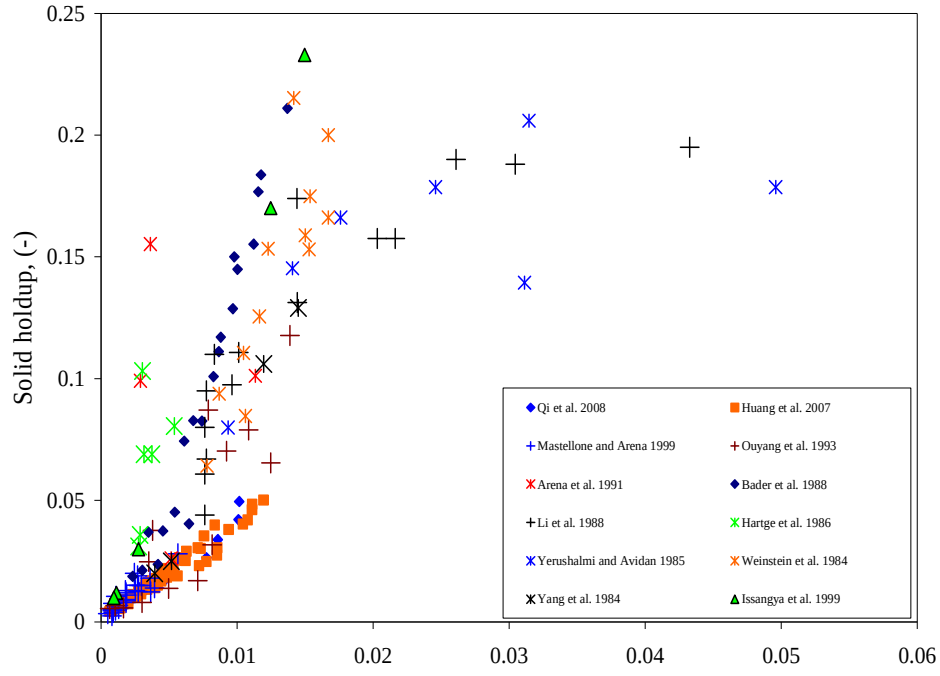

Figure 4.1a: Variation of solid holdup with Qi scaling ratio with data points used by Qi et al. 2008

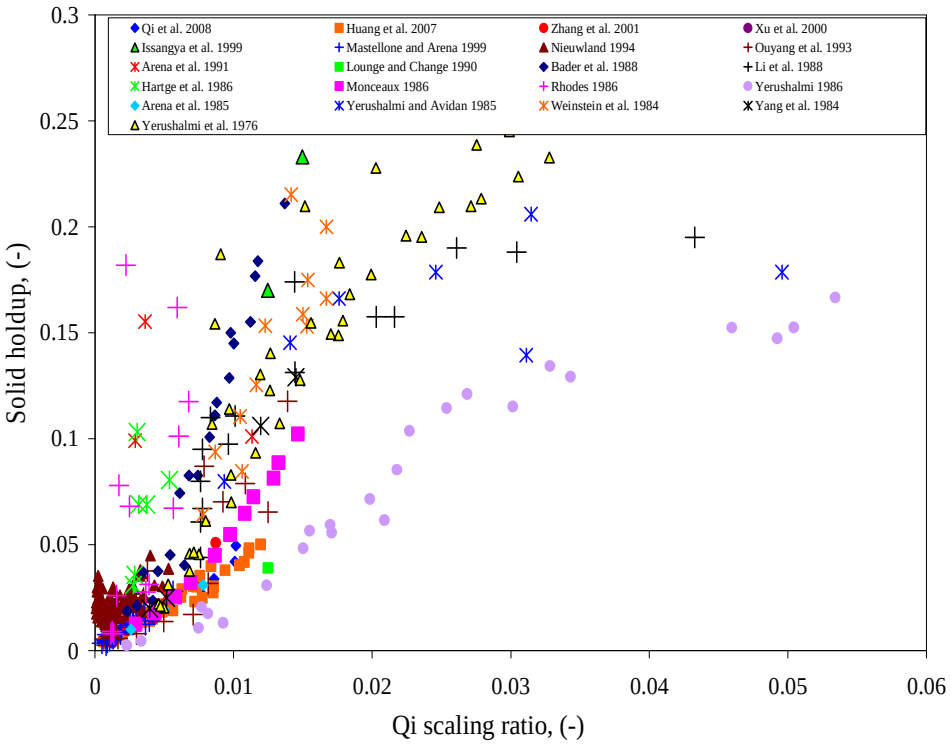

Figure 4.1b: Variation of solid holdup with Qi scaling ratio

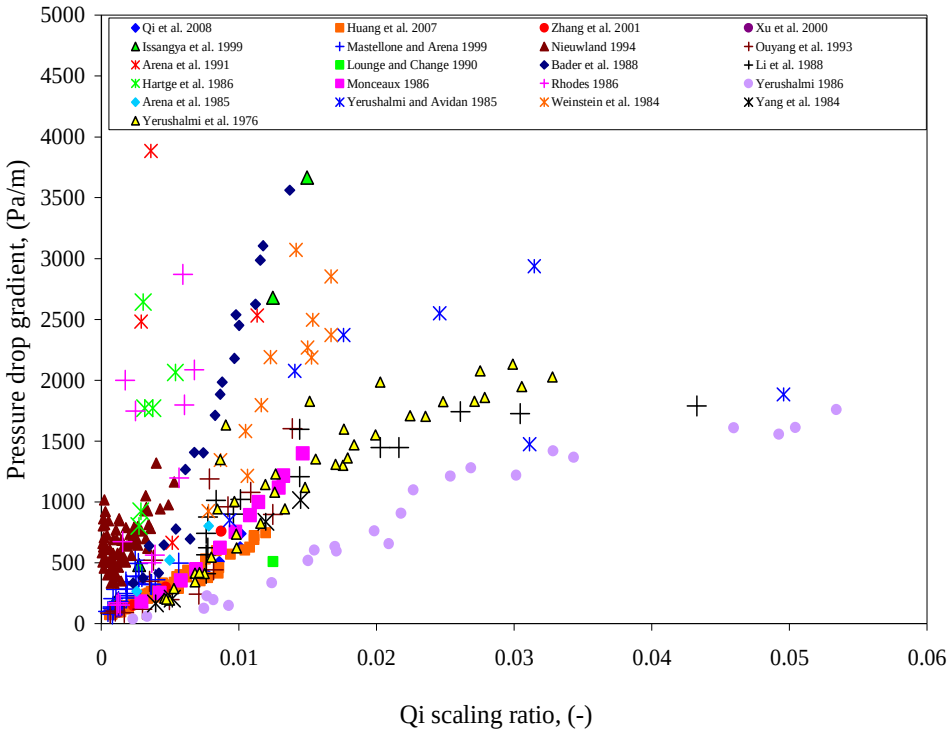

Figure 4.1c: Variation of pressure drop gradient with Qi scaling ratio

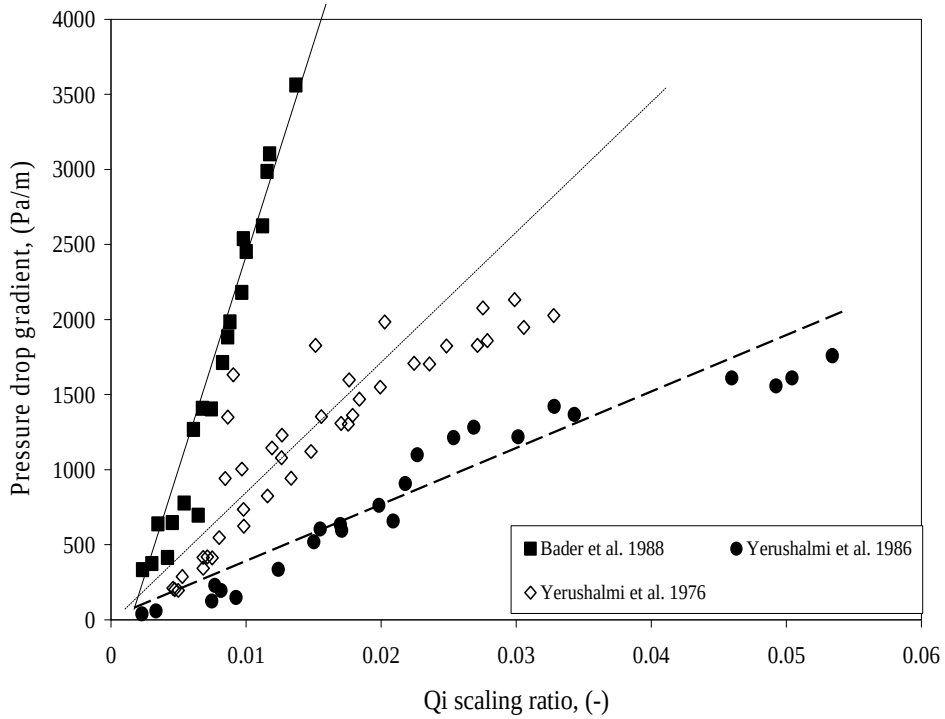

Figure 4.2a: Data sets to represent trends from consolidated data on pressure drop

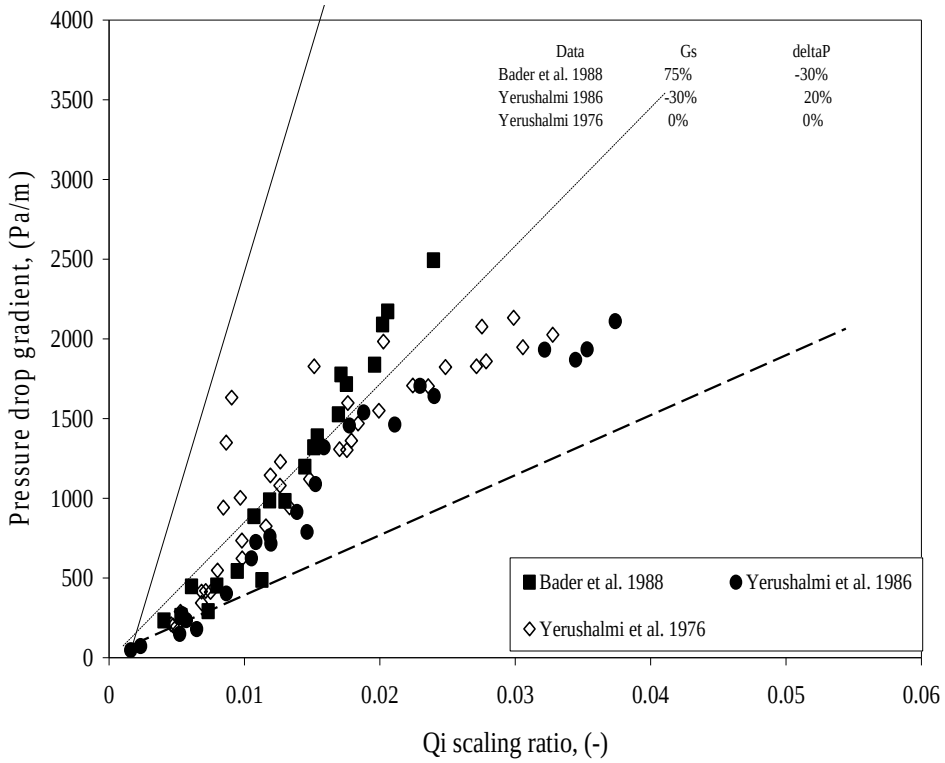

Figure 4.2b: Data sets tuned to fit Yerushalmi *et al.* (1976) trend

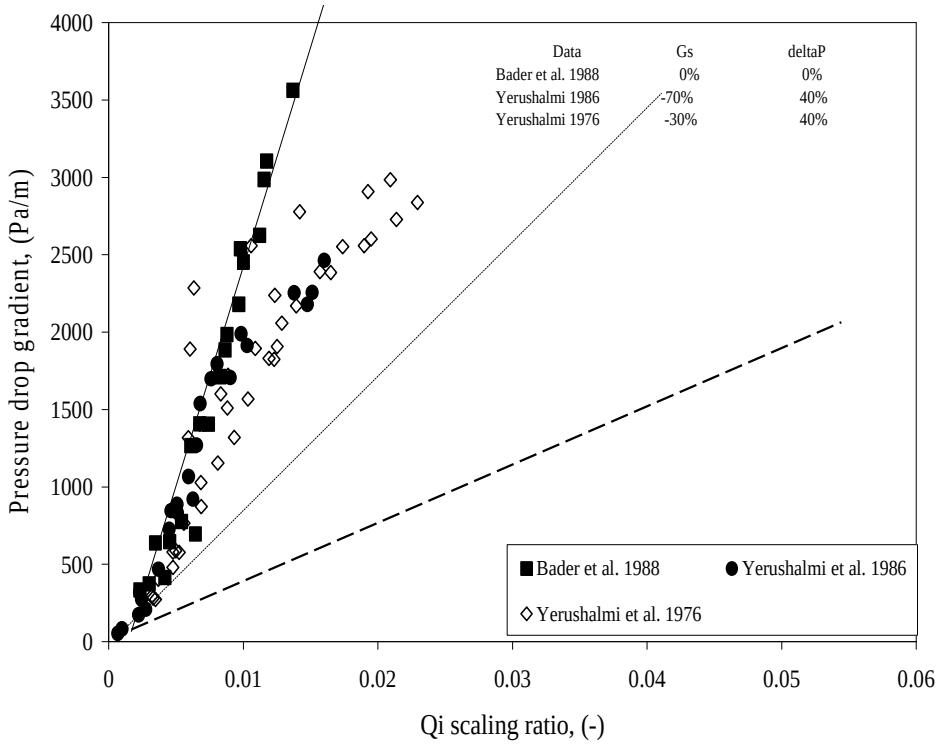

Figure 4.2c: Data sets tuned to fit Bader *et al.* (1976) trend

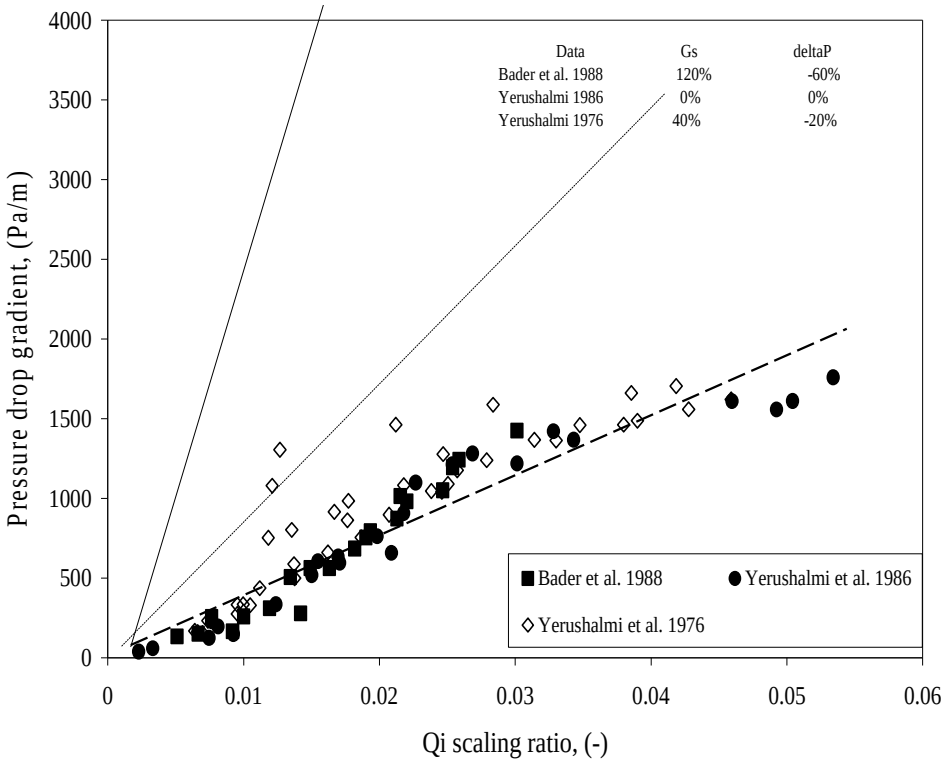

Figure 4.2d: Data sets tuned to fit Yerushalmi (1986) trend

4.3.2. Numerical Experiments to Evaluate Scaling Law

Numerical experiments were performed with the 3D computational model with imposed periodic boundary condition to assess the capability of Qi scaling ratio. The simulations were done for typical gas solid riser system of air – FCC system of d_p 129 μm and ρ_p = 2540 kg/m^3. Air density and viscosity were taken as 1.225 kg/m^3 and 1.7894 X 10^{-5} Pa s respectively. Gravity was specified as g_z = -9.81 m/s^2. Superficial gas velocity of 10 m/s and solid circulation flux of 300 kg/m^{2}s was used for base case simulations. The system belongs to Geldart B classification with particle terminal velocity of 0.7914 m/s. This gives the particle relaxation time scale based on terminal settling velocity to be 0.0806 s. The Qi scaling ratio corresponded to 0.00245 for the base case.

Simulations were started with uniform patching of the computational domain with the operating velocities and cross sectional average solid holdup. The cross section average solid holdup was approximated based on slip factor correlation of Patience *et al.* (1992). The UDF was hooked at the inlet boundary after the 1st time step. The equations were solved using segregated solver and second order discretization schemes for the variables. SIMPLE algorithm was employed for the pressure velocity coupling. The time step for each simulation was 1x 10^{-4} s. The simulated results were time averaged for period of about 30 – 50s. Radial profiles were obtained by azimuthal average of flow quantities on 50 radial bands. Solution convergence was monitored by recording the area-weighted quantities – solid circulation flux, slip velocity at the outflow boundary, static pressure drop across the domain and radial profile of flow variables obtained at different time intervals or averaging time durations.

Set of numerical experiments were performed to evaluate the effect of various parameters like particle density, particle size, operating conditions, fluid viscosity in predicting similarity in riser flows. The simulation parameters are listed in Table 4.3.

Table 4.3: Simulation details for riser scaling study

Sr no	Fluid density ρ, kg/m^3	Fluid viscosity M, Pa s	Particle density ρ_p, kg/m^3	Particle size d_p, m	Riser diameter D, m	Superficial gas velocity u_g, m/s	Solid circulation flux G_s, kg/m^{2}s	Qi scaling ratio -
1	1.225	0.000017894	2540	0.000129	0.054	10	300	0.00245192
2	1.225	0.000017894	2540	0.000129	0.054	5	99	0.002452835
3	1.225	0.000017894	2540	0.000129	0.054	15	574	0.002452172
4	1.225	0.000017894	2130	0.000129	0.03	10	300	0.0024512
5	1.225	0.000017894	2745	0.000129	0.07	10	300	0.0024525
6	1	0.000017894	2540	0.000129	0.054	10	300	0.00245192
7	2	0.000017894	2540	0.000129	0.054	10	300	0.00245192
8	1.225	0.000017894	2540	0.000075	0.054	10	300	0.00245192
9	1.225	0.000017894	2540	0.00006	0.054	10	300	0.00245192
10	1.225	0.00003	2540	0.000129	0.054	10	300	0.00245192
11	1.225	0.00001	2540	0.000129	0.054	10	300	0.00245192
12	1.225	0.000017894	2540	0.00023	0.054	10	300	0.00245192
13	1.225	0.000017894	2540	0.0001	0.054	10	300	0.00245192
14	1.225	0.000017894	2540	0.000129	0.054	10	100	0.000817307
15	1.225	0.000017894	2540	0.000129	0.054	5	33	0.000817612
16	1.225	0.000017894	2540	0.000129	0.054	10	1000	0.008173068
17	1.225	0.000017894	2540	0.000129	0.054	20	300	0.000808832
18	1.225	0.000017894	2540	0.000129	0.054	5	500	0.012388055

The effect of particle classification (Geldart type) and size over the predicted solid holdup is shown in Figure 4.3. The base case is for Geldart B system with d_p = 129 μm. The flow structure with Geldart A system (d_p = 75 and 60 μm) displays two distinct regions of higher solid holdup (Figure 4.4). Despite the difference in the local flow structure, global hydrodynamic parameter like the pressure drop gradient, cross sectional average solid holdup, slip velocity were within 5% deviation among the three cases. Hence, though the Qi scaling ratio predicted the similitude in global parameters, similarity in local flow structure was not observed in the computational model predictions.

The effect of particle size over local solid flow structure is shown in Figure 4.4. All the three particle sizes belong to Geldart B type system. At higher particle size, the radial profile was found to be more uniform than at lower particle size. The mean slip velocity (area weighted average over the periodic outflow boundary) nearly doubled from 0.66 to 1.49 m/s with particle size change from 100 μm to 230 μm. The time averaged cross sectional mean solid holdup increased from 0.0123 to 0.135 when the particle size is changed from 100 μm to 230 μm. This suggests that particle size and particle classification (Geldart type) plays significant role in determining the local flow structure and global parameters. Scaling parameters which does not account for the particle size may not be appropriate to represent the riser system.

Another set of numerical experiments with fluid density as a variable under study was performed. The radial profiles (Figure 4.6) show similar trend for all the three cases investigated. However, solid peaking or segregation was found more pronounced at gas density of 1.225 kg/m^3. Fluid density was not found to have significant influence on predicted flow structures provided the Qi scaling ratio is kept same. Further, the global quantities like pressure drop slip velocity and cross sectional average solid holdup were within 5% deviation.

Thus 3D computational model with periodic boundary was found useful in evaluating the scaling laws. The model was also used to simulate influence of parameters like fluid viscosity, riser diameter and operating conditions on predicted flow characteristics.

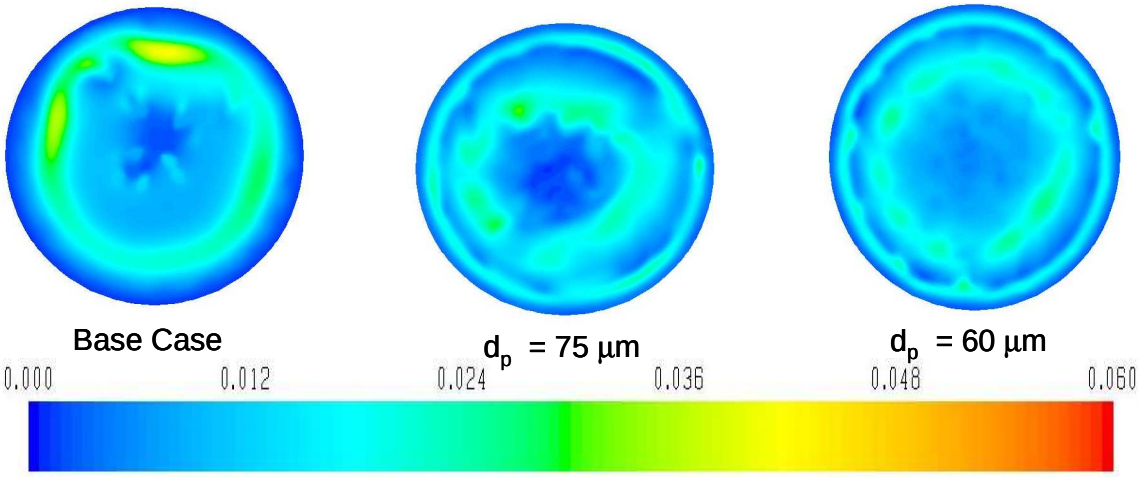

Figure 4.3: Contours of time averaged solid holdup showing the effect of particle classification

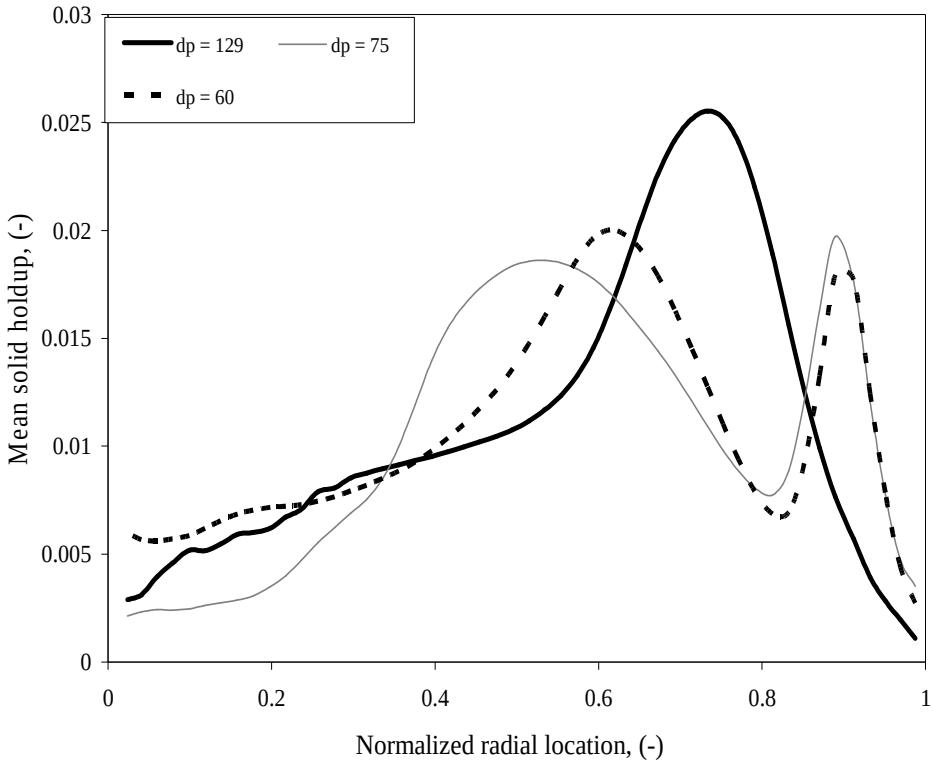

Figure 4.4: Time averaged radial profile of solid holdup showing the effect of particle classification

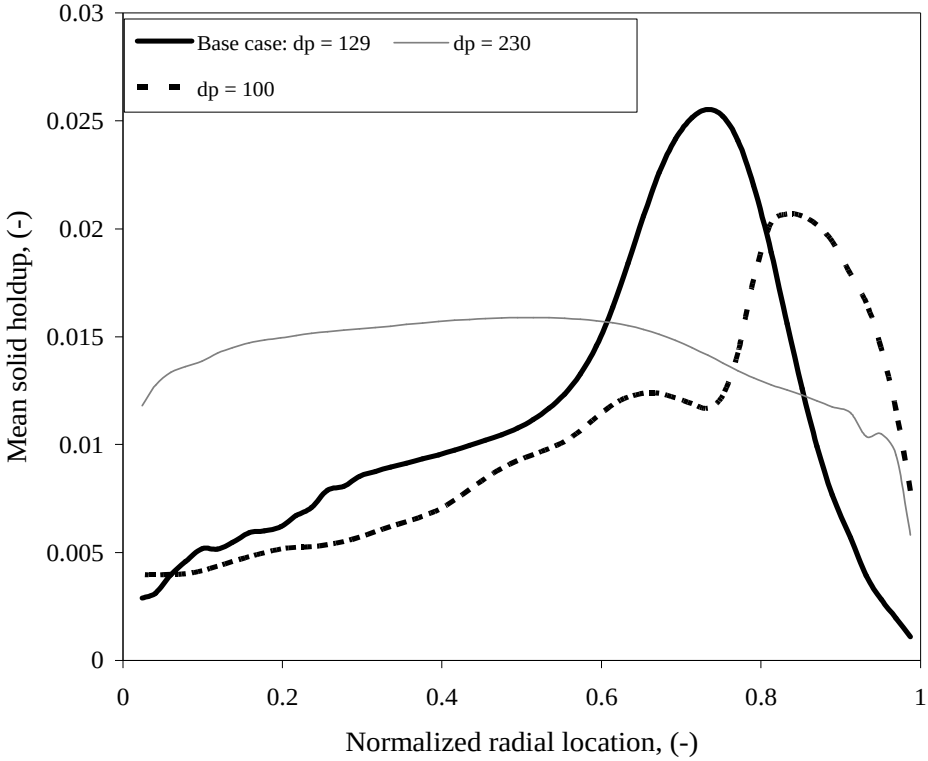

Figure 4.5: Time averaged radial profile of solid holdup showing the effect of particle size

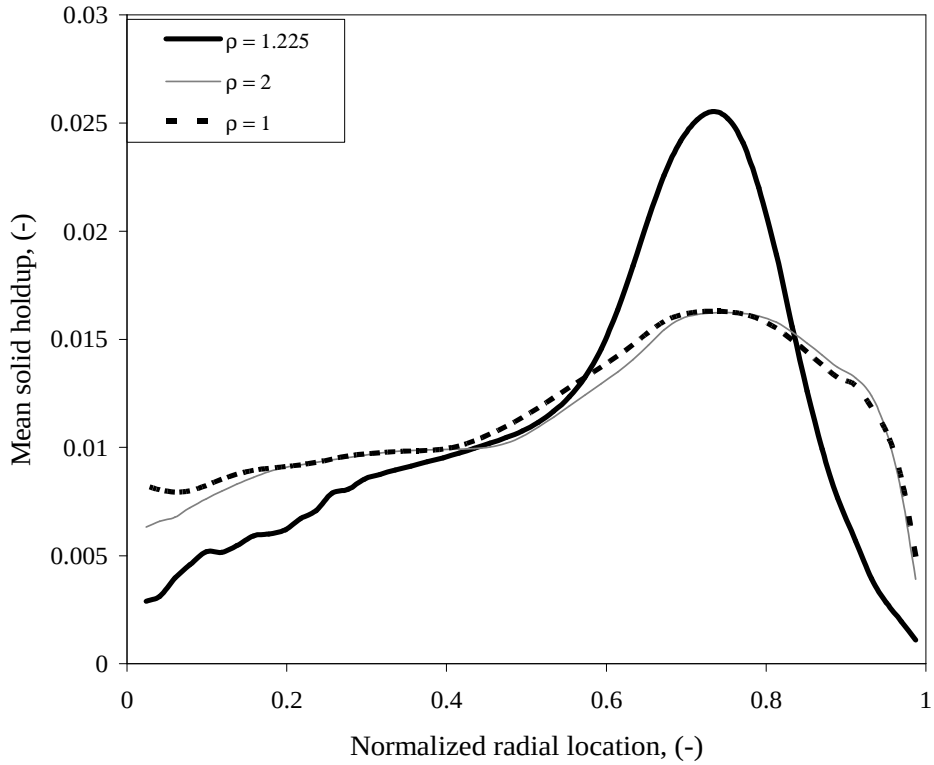

Figure 4.6: Radial profile of time averaged solid holdup showing the effect of fluid density

4.4. CONCLUSION

In conclusion, computational model with imposed periodic boundary was used to evaluate the scaling laws and study influence of various parameters on predicted local fully developed flow structures. Qi scaling ratio ensured similarity with global parameters but the similarity in local flow structure was not observed in all the simulated cases. With the Qi scaling ratio, the global quantities were predicted within an accuracy of ~5% deviation. However, in some cases, mere equivalence of Qi scaling ratio did not ensure the similarity in the local flow structure. The work consolidated the available data on pressure drop in risers. This study brought out the significance and need to incorporate error while reporting experiment data. Failure to do so may mislead the development of efficient scaling laws.

Annexure 4A: Cold Flow Experimental CFB Setup

The circulating fluidized bed setup consisted of an acrylic riser column (i.d. = 0.044 m, o.d. = 0.05 m and H = 1.5 m), a solid storage vessel (i.d. = 0.2 m, H = 0.6 m) of acrylic, a glass cyclone (d = 0.10 m, H = 0.40 m) and flexible polyethylene solid return leg (d = 0.028). The schematic sketch of the set up is shown in Figure 4A.1. Compressed air at 10bar was blown at bottom of the riser column at controlled rate. The gas velocity was measured through calibrated electronic anemometer. The riser bottom was designed for lateral entry of solids, at an angle of 45^0 to the riser axis, from the solids storage vessel through solid return leg. The solids and air travelled upward and passed through right angle exit at the riser top. The riser exit was provided with a 'T' junction and custom made quick closing solid flow control valve to divert the flowing solids through solids outlet. Solid circulation flux was measured by simultaneously operating the solid flow control valves and the diverted solids through the outlet were collected for known period of time. During normal operation, the solid control valve to the output side was kept completely closed to maintain the solids circulation between the riser and the downcomer return leg. Increased cross sectional area at the solids storage vessel provided quick separation of solids from the flowing air. The entrained solids were further separated in the cyclone separator. Solids collected in the storage vessel flow through the return leg due to gravity and were entrained into the riser at the riser bottom by the up flowing air stream. Glass beads of density 2500 kg/m^{3+} and mean diameter of 250 μm was used in the present study.

Measurement of Solid Circulation Flux

The solid circulation flux for a set superficial gas velocity was measured by weighing the amount of solids collected for measured sampling time. The solids control valves on either sides of the 'T' junction at riser top was manually operated to provide quick closing of solids flowing into the storage vessel and diverting the solids flow through the outlet valve. The measurements were taken after attainment of steady state judged by constant level of solids in the storage vessel. The leak flux, which denoted the flux of solids through the solids outlet during normal riser operation, was maintained below 1 kg/m^2s. The change in the solids level in the storage vessel was also monitored during flux measurements. Experiments were conducted at small sampling intervals and solids level/ head change in the storage vessel was not significant during these measurements. The solid circulation flux was measured for three

solids inventory of 5, 10 and 15 kg. The measured solid circulation flux as function of superficial gas velocity is shown in Figure 4A.2.

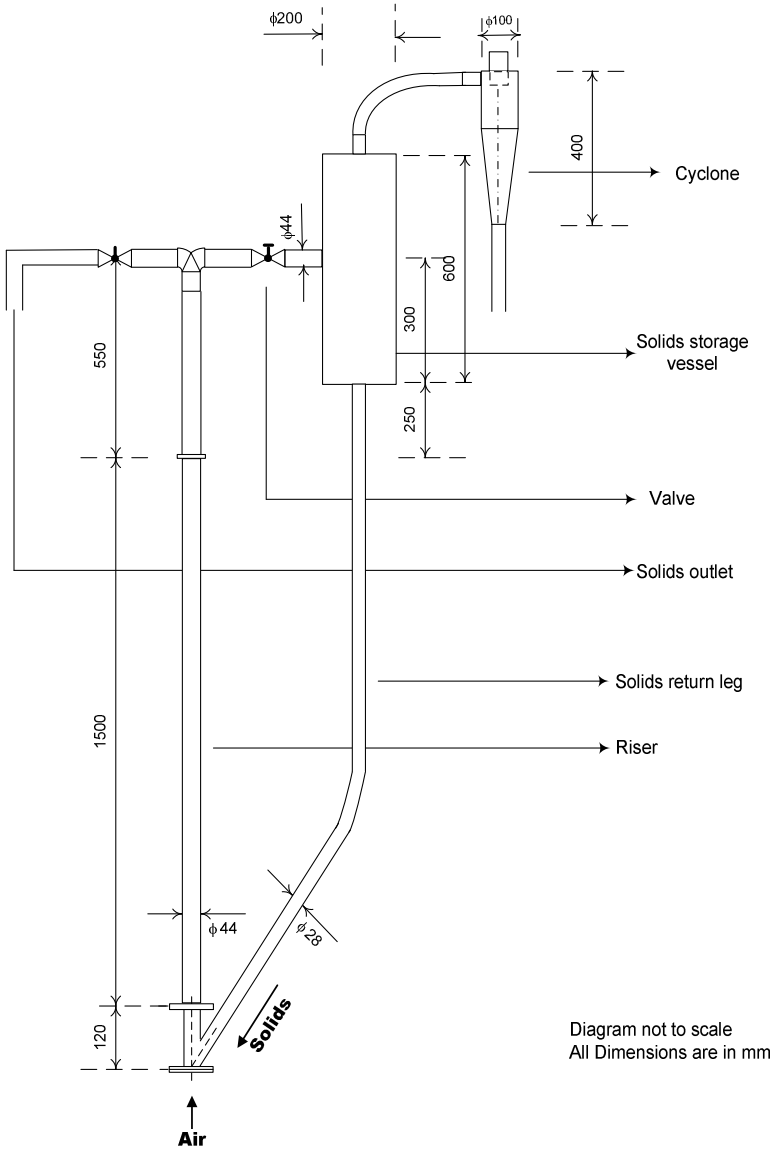

Figure 4A.1: Experimental circulating fluidized bed system

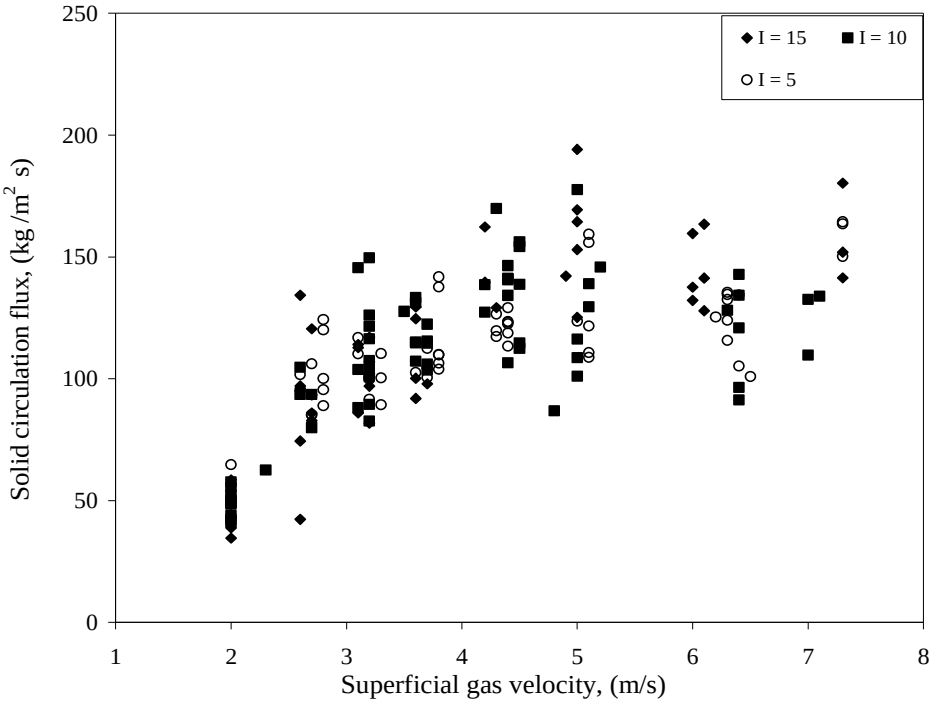

Figure 4A.2: Solid circulation flux as a function of superficial gas velocity at different values of total solid inventory in the CFB system

CHAPTER 5

CLOSURE

Summary of the research work and the areas identified for future work on modeling of gas solid riser flows are presented here.

5.1. SUMMARY

The present research work was focused on simulation of gas solid riser flows at high solid flux conditions with the two-fluid model approach. Evaluation of interphase momentum closures based on Energy Minimization Multiscale Model (EMMS) was performed to assess its applicability for riser flows. 3D CFD model with periodic boundary conditions (imposed through user defined functions) was developed to simulate fully developed flow profiles. The periodic CFD model was used to evaluate model parameters and hydrodynamic scaling laws without jeopardizing the grid resolution in gas -solid riser flows.

The specific contributions of the research work are listed as follows:

- An independent evaluation of EMMS drag model was attempted in this work. The results predicted by the EMMS model were compared with the literature data. It was found that the extended EMMS model with the inertial term predicted distinct local minimum energy consumption for given operating condition and assumed values of cluster voidage and cluster size.
- The EMMS model parameters required adjustment to predict the experimental pressure drop data. The dilute phase inertial term was not found to have significant effect on model predictions. It can be omitted from the extended EMMS model.
- Effort to fine tune the model parameters, keeping intact the energy minimization characteristic, did not improve the prediction accuracy in comparison with the predictions based on available literature correlations.
- 3D CFD model with periodic boundary conditions could shorten the time taken in evaluation of CFD model closures and parameters without jeopardizing the spatial resolution.
- In conjunction with the conventional acumen, radial segregation of solid volume fraction was predicted with 2D models at coarse grid and poor resolution near the walls. The solid holdup was found to be highest at the walls. However such maximum solid holdup at the walls was not observed with fine grid simulations.
- Through numerical experiments it was shown that the model parameters like specularity coefficient can be adjusted to match global experimental quantities like pressure drop and average solid holdup.

- The work consolidated the available data on fully developed pressure drop gradient and/or cross sectional average solid. It was shown from analysis that the experimental inaccuracies like measurement of solid circulation flux can mislead the development of hydrodynamic scaling laws for riser flows.
- Scaling law proposed by Qi *et al.* (2008) does not account system and particle characteristics and it was found to be insufficient in predicting hydrodynamic scaling in riser flows.

5.2. SUGGESTIONS FOR FURTHER WORK

With the observations from the present study, the some suggestions for further work on developing state of art computational models for riser flows are outlined in the following:

- The cluster parameters for the multi-scale EMMS drag model need more study. Development of unified correlation for cluster size based on fluid and particle properties and column diameter are in progress (Subbarao, 2009). However, currently developed correlations are based on cluster voidage as adjustable parameter. A mechanistic model to obtain the cluster parameters will help in developing the current multi-scale drag model framework.
- Effect of spatial resolution in the CFD model predictions needs to be investigated. Non occurrence of radial segregation at wall from the fine grid simulations of 3D CFD model needs to be investigated carefully.
- Proper design of riser experiments with the reporting of measurement errors is essential for further development of scaling laws.
- The 3D CFD model with imposed periodic boundary conditions can be generalized for other translationally periodic multiphase systems like slurry flow through horizontal pipes *etc*. to simulate fully developed flow profiles.

5.3. CLOSING REMARKS

In my opinion, recent works on simulating gas solid riser flows with two fluid model are not effective in predicting the experimental trends. For example, Benyahia (2009) simulated gas solid riser flows with drag coefficient obtained from filtered sub grid model and EMMS models. However, the predicted flow profiles were far from experimental data of PSRI. Despite numerous research publications on riser flows, the

predictive capability of the two fluid CFD model for riser flows did not improve significantly over the years. The present framework of the Eulerian-Eulerian models for gas solid riser flows appears to be inadequate. A fresh perspective and new approaches to re-examine the effectiveness of two fluid Eulerian Eulerian model equations for gas solid riser flows is required. Efforts are needed on identifying missing issues and enhancing understanding of complex interactions taking place in riser flows.

Nonetheless industrial relevance of riser simulations cannot be under estimated. The two fluid model is a powerful tool in evaluating novel process routes and hardware configurations (Lan *et al.*, 2009; Gao *et al.*, 2008, 2006). The effect of new hardware design on product selectivity and yields, extent of non uniformity in catalyst distribution etc can be studied qualitatively with the two fluid models. Such studies will facilitate acceleration of process innovations at industrial scale and selection of most promising configurations amongst many available options.

To sum up, simulation of gas-solid flow operating at high solid flux condition still poses challenge to chemical engineers. The development of successful state-of-art predictive models for gas-solid riser flows involves multiple tasks and requires multi-level approach. These include - understanding physics of gas-solid riser flows at high flux conditions, development of constituent models, generation of reliable and exhaustive experimental data sets and development of efficient computational models and methods to evaluate the developed gas-solid model. The present work addressed some of these issues. Despite the shortcomings reported in the work, the present computational work brought out a method for quick and reliable selection of model parameters with best possible spatial resolution. The strategy employed in the current work can be extended to provide direct one-to-one comparisons with the experimental quantities and would help in development of more effective computational models for gas solid riser flow systems.

NOMENCLATURE

NOTATIONS

Ar_c, Ar_f	Archimedes number defined as $\frac{\rho(\rho - \rho)d_p^3 g}{\mu^2}$,dimensionless
Ar_i	Archimedes number defined as $\frac{\rho(\rho - \rho)d_{cl}^3 g}{\mu^2}$,dimensionless
B	Coefficient or parameter of C_{D0}, dimensionless
C_D	Overall drag coefficient, dimensionless
C_{D0}	Standard drag coefficient of particle, dimensionless
C_{D0c}	Standard drag coefficient of particle in dense phase, dimensionless
C_{D0f}	Standard drag coefficient of particle in dilute phase, dimensionless
C_{D0i}	Standard drag coefficient of particle in interphase between dense and dilute phase, dimensionless
C_{Dc}	Drag coefficient of particle in dense phase, dimensionless
C_{Df}	Drag coefficient of particle in dilute phase, dimensionless
C_{Di}	Drag coefficient of particle in interphase, dimensionless
$\overline{d_{cl}}$	Mean cluster size, m
d_{cl}	Cluster diameter, m
d_p	Diameter of the particle, m
D	Diameter of the riser column, m
e_p	Particle – particle restitution coefficient, dimensionless.
e_w	Particle wall restitution coefficient, dimensionless
f	dense phase fraction per unit volume, dimensionless
f_t	Flow time, s
F_c	Drag Force acting on a particle in dense phase, N/particle
F_D	Overall drag force per unit volume, N/m^3
F_f	Drag Force acting on a particle in dilute phase, N/particle
F_i	Drag Force acting on a particle in interphase, N/particle
Fr_D	Froude number based on riser diameter, dimensionless
g	Acceleration due to gravity, m/s^2
g_0	Radial distribution function
G_s	Solids circulation flux, kg/m^2 s
H	Height of the riser column, m

i.d.	Internal diameter, m
k	Index of C_{D0}, dimensionless
k	Turbulent kinetic energy per unit mass, m^2/s^2
k_c	Index of C_{D0c}, dimensionless
k_f	Index of C_{D0f}, dimensionless
k_i	Index of C_{D0i} ,dimensionless
m_c	No of particles in unit volume of dense phase, /m3
m_f	No of particles in unit volume of dilute phase,/m^3
m_i	No of particles in unit volume at the interphase between dense and dilute phase, /m^3
N_{st}	Energy consumed for transportation and suspension per unit mass of particles, J/ kg s
N_T	Total energy consumed per unit mass of particles, J/ kg s
o.d.	Outer diameter, m
Re	Reynolds number, dimensionless
Re_c	Characteristic Reynolds number of particles in dense phase defined as $Re_c = \frac{d_p \rho_p u_{sc}}{\mu}$, dimensionless
Re_f	Characteristic Reynolds number of particles in dilute phase defined as $Re_f = \frac{d_p \rho_p u_{sf}}{\mu}$, dimensionless
Re_i	Characteristic Reynolds number of particles in inter phase defined as $Re_i = \frac{d_p \rho_p u_{si}}{\mu}$, dimensionless
t_{avg}	Averaging time period, s
TMP	Intermediate parameter, m/s
u_g	Superficial gas velocity, m/s
u_{gc}	Superficial gas velocity in dense phase, m/s
u_{gf}	Superficial gas velocity in dilute phase, m/s
u_{mf}	Minimum fluidization velocity, m/s
u_p	Overall superficial particle velocity defined as G_s/ρ_p, m/s
u_{pc}	Superficial particle velocity in dense phase defined, m/s
u_{pf}	Superficial particle velocity in dilute phase, m/s

u_s	Overall superficial slip velocity, m/s
u_{sc}	Superficial slip velocity of particles in dense phase, m/s
u_{sf}	Superficial slip velocity of particles in dilute phase, m/s
u_{si}	Superficial slip velocity of particles in inter phase, m/s
x	Co-ordinate axes
y	Co-ordinate axes
z	Axial location of riser, m

Greek Letters

α	Phase corresponding to c, f or i for dense, dilute and inter phase respectively, dimensionless
ε	Overall volume averaged voidage, dimensionless
ϵ	Turbulent kinetic energy dissipation rate per unit mass, m^2/s^3
ε_c	Cluster voidage, dimensionless
$\overline{\varepsilon_{cl}}$	Mean cluster voidage, dimensionless
ε_f	Dilute phase voidage, dimensionless
ε_{limit}	Limiting value of voidage, dimensionless
ε_{max}	Maximum voidage, dimensionless
ε_{mf}	Voidage at minimum fluidization conditions, dimensionless
ε_s	Solid holdup, dimensionless
ε_s^{max}	Solid holdup at maximum packing condition, dimensionless
$\overline{\varepsilon_s}$	Cross sectional averaged solid holdup, dimensionless
ϕ	Specularity coefficient, dimensionless
γ_s	Solid phase shear stress, N/m^2
$\gamma_{s,w}$	Solid phase shear stress at wall boundary, N/m^2
κ	Modified form of Archimedes number, dimensionless
μ	Viscosity of the gas phase or air, Pa s
π	Factor pi, dimensionless
Θ	Granular temperature, m^2/s^2
ρ	Density of fluid phase, kg/m^3
ρ_g	Density of primary gas phase or air, kg/m^3
ρ_p	Density of the particle, kg/m^3

REFERENCES

Agrawal, K., Loezos, P. N., Syamlal, M. and Sundaresan, S. (2001). The role of meso - scale structures in rapid gas solid flows. *Journal of Fluid Mechanics*, 445, 151 - 185.

Almuttahar, A. and Taghipour, F. (2008). Computational fluid dynamics of high density circulating fluidized bed riser: Study of modeling parameters. *Powder Technology*, 185, 11 - 23.

Anderson, T.B. and Jackson, R. (1967). A fluid mechanical description of fluidized beds. *Industrial and Engineering Chemistry Fundamentals*, 6, 527 - 539.

Anderson, T.B. and Jackson, R. (1969). A fluid mechanical description of fluidized beds. *Industrial and Engineering Chemistry Fundamentals*, 8, 137 – 144.

Andrews IV, A.T., Loezos, P.N. and Sundaresan, S. (2005). Coarse grid simulation of gas particle flows in vertical risers. *Industrial Engineering and Chemistry Research*, 44, 6022 – 6037.

Arena, U., Cammarota, A. and Pistone, L., (1985). In *Circulating Fluidized Bed Technology*, Ed., P. Basu, Pergamon Press, New York, p 119 -125

Arena, U., Malandrino, A., Manocchella, A., and Massimilla, L. (1991). Flow Structure in the Riser of Laboratory and Pilot CFB Units. In *Circulating Fluidized Bed Technology III*, Eds., P. Basu, M. Horio and M. Hasatani, M., Pergamon, Oxford, p 137-144.

Armenio, V. and Fiorotto, V. (2001). The importance of the forces acting on particles in turbulent flows. *Physics of Fluids*, 13, 2437 - 2440.

Bader, R., Findlay, J. and Knowlton, T.M. (1988). Gas/solids flow patterns in a 30.5cm diameter circulating fluidized bed. In *Circulating Fluidized Bed II*, Eds., P. Basu, and J. Large, Pergamon Press, Oxford, p123 – 137.

Bai, D., Jin, Y. and Yu, Z. (1993). Flow regimes in circulating fluidized beds. *Chemical Engineering and Technology*, 16, 307 - 313.

Bai, D.R., Jin, Y., Yu, Z. (1991). Acceleration of particles and momentum exchange between gas and solids in fast fluidized beds. In *Fluidization: Science and Technology*, M. Kwauk, D. Kunii, Eds., Science Press, Beijing, 46 – 55.

Benavides, A.G., van Wachem, B. G.M., Nijenhuis, J. and van Ommen, R. J. (2008). Comparison of experimental and simulation results for turbulent gas solid riser flow. In *9th International Conference on Circulating Fluidized Beds*, Eds., J. Werther, K. E. Wirth and W. Nowak, May 13 – 16, 2008, Hamburg, Germany.

Benyahia, S. (2009). On the effect of subgrid drag closures. *Industrial and Engineering Chemistry Research*, In press.

Benyahia, S., Arastoopour, H. and Knowlton, T.M. (2002). Two dimensional transient numerical simulation of solids and gas flow in the riser section of a circulating fluidized bed. *Chemical Engineering Communications*, 189, 510 – 527.

Benyahia, S., Arastoopour, H., Knowlton, T.M. and Massah, H. (2000). Simulation of particles and gas flow behaviour in the riser section of a circulating fluidized bed using the kinetic theory approach for the particulate phase. *Powder Technology*, 112, 24 – 33.

Benyahia, S., Syamlal, M. and O'Brien, T.J. (2005). Evaluation of boundary conditions used to model dilute, turbulent gas/solids flows in a pipe. *Powder Technology*, 156, 62 – 72.

Benyahia, S., Syamlal, M. and O'Brien, T.J. (2007). Study of the ability of multiphase continuum models to predict core- annulus flow. *AIChE Journal*, 53, 2549 – 2568.

Berruti, F., Chaouki, J., Godfroy, L., Pugsley, T.S. and Patience, G.S. (1995). Hydrodynamics of circulating fluidized bed risers: A review. *The Canadian Journal of Chemical Engineering*, 73, 579 – 596.

Bhusarapu, S.B. (2005). Solids flow mapping in gas solid risers. *PhD Dissertation*, Sever Institute of Technology, Washington University, Saint Louis, Missouri, USA.

Bi, H. T. (2002). Some issues on core-annulus and cluster models of circulating fluidized bed reactors. *The Canadian Journal of Chemical Engineering*, 80, 809 - 817.

Bi, H.T. and Grace, J.R. (1995). Flow regime diagrams for gas – solid fluidization and upward transport. *International Journal of Multiphase Flow*, 21, 1229 – 1236.

Bolio and Sinclair (1995). Gas turbulence modulation in the pneumatic conveying of massive particle in vertical tubes. *International Journal of Multiphase Flow*, 21, 985 – 1001.

Bolio, E.J., Yasuna, J.A. and Sinclair, J.L. (1995). Dilute turbulent gas-solid flow in riser with particle-particle interactions. *AIChE Journal*, 41, 1375 – 1388.

Chang, H. and Louge M. (1992). Fluid dynamic similarity of circulating fluidized beds. *Powder Technology*, 70, 259 – 270.

Cheng, Y., Wu, C., Zhu, J., Wei, F. and Jin, Y. (2008). Downer reactor: From fundamental study to industrial application. *Powder Technology*, 183, 364 - 384.

Contractor R.M. and Chaouki, J. (1991). Circulating fluidized bed as a catalytic reactor. In *Circulating Fluidized Bed Technology III*, Pergamon Press, Oxford, p 39.

Contractor, R.M. (1999). Dupont's CFB technology for maleic anhydride. *Chemical Engineering Science*, 54 5627 – 5632.

Corma, A., Melo, F. V., Sauvanaud, L. and Ortega, F. J. (2004). Different process schemes for converting light straight run and fluid catalytic cracking naphthas in a FCC unit for maximum propylene production. *Applied Catalysis A: General*, 265, 195 - 206.

Crowe, C. T., Troutt, T. R. and Chung, J. N. (1996). Numerical models for two phase turbulent flows. *Annual Reviews in Fluid Mechanics*, 28, 11 - 43.

Cruz, E., Steward, F. R. and Pugsley, T. S. (2006). New closure models for CFD modeling of high density circulating fluidized beds. *Powder Technology*, 169, 115 - 122.

Curtis, J. S. and van Wachem, B. (2004). Modeling particle laden flows: A research outlook. *AIChE Journal*, 50, 2638 - 2645.

Dasgupta, S., Jackson, R. and Sundaresan, S. (1993). Turbulent gas – particle flow in CFB – risers. In *Preprints of Circulating Fluidized Bed Technology IV*, p 448 – 453.

Dasgupta, S., Jackson, R. and Sundaresan, S. (1994). Turbulent gas particle flow in vertical risers. *AIChE Journal*, 40, 215 - 228.

Dasgupta, S., Jackson, R. and Sundaresan, S. (1998). Gas – particle flow in vertical pipes with high mass loading of particles. *Powder Technology*, 96, 6 – 23.

de Wilde, J., Marin, G. B. and Heynderickx, G. J. (2003). The effects of abrupt T-outlets in a riser: 3D simulation using the kinetic theory of granular flow. *Chemical Engineering Science*, 58, 877 - 885.

Derouin, C., Nevicato, D., Forissier, M., Wild, G. and Bernard, J.R. (1997). Industrial Engineering and Chemistry Research, 36, 4504.

Dudukovic, M. P. (2010). Reaction engineering: Status and future challenges. *Chemical Engineering Science*, 65, 3 -11.

Elgobashi S. E. and Abou-Arab T. W. (1983). A two-equation turbulence model for two-phase flows. *Physics of Fluids*, 26, 931 – 938.

Ergun, S. (1952). Fluid flow through packed columns. *Chemical Engineering Progress*, 48, 89 – 91.

Fan, L. S. and Zhu, C. (1998). *Principles of gas solid flows*. Cambridge University Press, Cambridge.

FLUENT 6.3 documentation guide, Ansys Incorporation, USA.

Gauthier, T. A. (2009). Current R&D challenges for fluidized bed processes in the refining industry. *International Journal of Chemical Reactor Engineering*, 7, A22: 21 - 70.

Ge, W. and Li, J. (2003). Macro-scale phenomena reproduced in microscopic systems – pseudo-particle modeling of fluidization. *Chemical Engineering Science*, 58, 1565 – 1585.

Gao, J., Chang, J., Lan, X., Yang, Y., Lu, C. and Xu, C. (2008). CFD modeling of mass transfer and stripping efficiency in FCCU strippers. *AIChE Journal*, 54, 1164 - 1177.

Gao, J., Xu, C. and Lin, S. (2006). Advanced reaction-terminating technique for FCC riser reactor. *Petroleum Science and Technology*, 24, 367 - 378.

Gidaspow, D. (1994). *Multiple flow and fluidization: Continuum and kinetic theory descriptions.* Academic Press Inc, California, p 314.

Gilbert, M. F., Tallman, M. J., Miller, R. B. And Niccum, P. K. (2002). FCC's role in refinery/petrochemical integration. *Grace Refining Technology Conference*, Singapore.

Glicksman, L. R. (1984). Scaling relationships for fluidized beds. *Chemical Engineering Science*, 39, 1373 - 1379.

Glicksman, L. R., Hyre, M. and Woloshun, K. (1993). Simplified scaling relationships for fluidized beds. *Powder Technology*, 77, 177 - 199.

Godefroy, A., Patience, G. S., Tzakova, T., Garrait, D. and Dubois, J. L. (2009). Reactor technologies for propane partial oxidation to acrylic acid. *Chemical Engineering and Technology*, 32, 373 - 379.

Godfroy, L., Patience, G.S. and Chaouki, J. (1999). Radial hydrodynamics in risers. *Industrial and Engineering Chemistry Research*, 38, 81 – 89.

Gu, W.K. and Chen, J. C. (1998). A Model for Solid Concentration in Circulating fluidized Beds. In *Fluidization IX*, L.S. Fan and T.M. Knowlton, Eds., Engineering Foundation, New York, pp501–508.

Hadinoto, K. and Curtis, S. J. (2009). Numerical simulation of turbulent particle-laden flows with significant fluid to particle inertia ratio. *Industrial and Engineering Chemistry Research*, 48, 5874 - 5884.

Harris, A.T., Davidson, J.F. and Thorpe, R.B. (2002). The prediction of particle cluster properties in the near wall region of a vertical riser. Powder Technology, 127, 128 – 143.

Hartge, E. U., Li, Y. and Werther, J. (1986). Analysis of the Local Structure of the Two Phase Flow in a Fast Fluidized Bed. In *Circulating Fluidized Bed Technolog*, Ed., P. Basu, P., Pergamon, Oxford, p153 - 160

Helland, E., Bournot, H., Occelli, R. and Tadrist, L. (2007). Drag reduction and cluster formation in a circulating fluidized bed. *Chemical Engineering Science*, 62, 148 - 158.

Herbert, P.M., Gauthier, T.A., Briens, C.L. and Bergougnou, M.A. (1998). Flow study of a 0.05 m diameter downflow circulating fluidized bed. *Powder Technology*, 96, 255 – 261.

Hinze, J. O. (1975). *Turbulence*, Mcgraw Hill Publishing Co., New York.

Horio, M. and Kuroki, H. (1994). Three dimensional flow visualization of dilutely dispersed solids in bubbling and circulating fluidized beds. *Chemical Engineering Science*, 49, 2413 – 2421.

Huang, W. X., Zhu, J. X. and Parssinen, J. H. (2006). Comprehensive study on the solids acceleration length in a long cfb riser. *Chemical Engineering and Technology*, 29, 1197 - 1204.

Huang, W., Yan, A. and Zhu, J. (2007). Hydrodynamics and flow development in a 15.1m circulating fluidized bed riser. *Chemical and Engineering Technology*, 30, 460 – 466.

Huilin, L., Gidaspow, D., Bouillard, J. and Wentie, L. (2003). Hydrodynamic simulation of gas–solid flow in a riser using kinetic theory of granular flow. *Chemical Engineering Journal*, 95, 1 - 13.

Iddir, H. and Arastoopour, H. (2005). Modeling of multitype particle flow using the kinetic theory approach. *AICHE Journal*, 51, 1620 – 1632.

Igci, Y., Andrews, A. T., Sundaresan, S., Pannala, S. and O'Brien, T. J. (2008). Filtered two fluid models for fluidized gas particles suspensions. *AIChE Journal*, 54, 1431 - 1448.

Issangya, A.S., Bai, D., Bi, H.T., Lim, K.S., Zhu, J. and Grace, J.R. (1999). Suspension densities in a high – density circulating fluidized bed riser. *Chemical Engineering Science*, 54, 5451 – 5460.

Jenkins, J.T. and Savage, S.B. (1983). A theory for the rapid flow of identical, smooth, nearly elastic spherical particles. *Journal of Fluid Mechanics*, 130, 187.

Jiradilok, V., Gidaspow, D., Damronglerd, S., Koves, W.J. and Mostofi, R. (2006). Kinetic theory based CFD simulation of turbulent fluidization of FCC particles in a riser. *Chemical Engineering Science*, 61, 5544 – 5559.

Johnson, P.C. and Jackson, R. (1987). Frictional collisional constitutive relations for granular materials with applications to plane shearing. *Journal of Fluid Mechanics*, 176, 67 -93.

Knowlton, T. M., Reddy Karri, S. B. and Smith, J. S. (2007). Hydrodynamic scale up of circulating fluidized beds. *The 12th International Conference on Fluidization - New Horizons in Fluidization Engineering*, Vancouver, Canada, 1 – 14.

Kolbitsch, P., Proll, T., Bolhar-Nordenkampf, J. and Hofbauer, H. (2009). Design of a chemical looping combustor using a dual circulating fluidized bed reactor system. *Chemical Engineering and Technology*, 32, 398 - 403.

Koornneef, J., Junginger, M. and Faaij, A. (2007). Development of fluidized bed combustion - an overview of trends, performance and cost. *Progress in Energy and Combustion Science*, 33, 19 - 55.

Kronberger, B., Lyngfelt, A., Loffler, G. and Hofbauer, H. (2005). Design and fluid dynamic analysis of a bench scale combustion system with CO_2 separation - chemical looping combustion. *Industrial and Engineering Chemistry Research*, 44, 546 - 556.

Lackermeier, U., Rudnick, C., Werther, J., Bredebusch, A. and Burkhardt, H. (2001). Visualization of flow structures inside a circulating fluidized bed by means of laser sheet and image processing. *Powder Technology*, 114, 71 – 83.

Lan, X., Xu, C., Wang, G., Wu, L. and Gao, J. (2009). CFD modeling of gas-solid flow and cracking reaction in two-stage riser fcc reactors. *Chemical Engineering Science*, 64, 3847 - 3858.

Launder, B. E. and Spalding, D. B. (1974). The numerical computation of turbulent flows. *Computer Methods in Applied Mechanics and Engineering*, 3, 269 – 289.

Li, J. (2000). Compromise and resolution – exploring the multiscale nature of gas solid fluidization. *Powder Technology*, 111, 50 – 59.

Li, J., and Kwauk, M. (2003). Exploring complex systems in chemical engineering – the multiscale methodology. *Chemical Engineering Science*, 58, 521 – 535.

Li, J., Cheng, C., Zhang, Z., Yuan, J., Nemet, A., Fett, F.N. (1999). The EMMS model – its application, development and updated concepts. *Chemical Engineering Science*, 54, 5409 – 5425.

Li, J., Tung, Y., Kwauk, M. (1988). Axial Voidage Profiles of Fast Fluidized Beds in Different Operating Regions. In *Circulating Fluidized Bed Technology II*, Eds., P. Basu and J. F. Large, Pergamon, Oxford, p 193-203.

Li, J., Wen, L., Ge, W., Cui, H., and Ren, J. (1998). Dissipative structure in concurrent –up gas – solid flow. *Chemical Engineering Science*, 53, 3367 – 3379.

Li, Y. (1994). Hydrodynamics. Advances in chemical Engineering, 20, 85 – 146.

Li, Y., Chen, B., Wang, F. and Wang, Y. (1982). Hydrodynamic correlations for fast fluidization. In *Fluidization: Science and Technology*, Science Press, Beijing, p124 – 133.

Loth, E. (2000). Numerical approaches for motion of dispersed particles, droplets and bubbles. *Progress in Energy and Combustion Science*, 26, 161 - 223.

Louge, M. and Chang, H., (1990). Pressure and voidage gradients in vertical gas solid risers. *Powder Technology*, 60, 197- 201.

Louge, M.Y., Mastorakos, E. and Jenkins, J.K. (1991). The role of particle collisions in pneumatic transport. *Journal of Fluid Mechanics*, 231, 345 – 359.

Lu, B., Wang, W. and Li, J. (2009). Searching for a mesh-independent sub-gridmodel for CFD simulation of gas–solid riser flows. *Chemical Engineering Science*, 64, 3437 - 3447.

Lun, C.K.K., Savage, S.B., Jeffrey, D.J. and Chepurniy, N. (1984). Kinetic theories for granular flow: inelastic particles in couette flow and slightly inelastic particles in a general flow field. *Journal of Fluid Mechanics*, 140, 223 – 256.

Lyngfelt, A., Leckner, B. and Mattisson, T. (2001). A fluidized bed combustion process with inherent CO_2 separation: Application of chemical looping combustion. *Chemical Engineering Science*, 56, 3101 - 3113.

Makkawi, Y.T., and Wright P.C. (2003). Macro scale phenomena reproduced in microscopic systems – pseudo particle modelling of fluidization. Chemical Engineering Science, 58, 2305 – 2351.

Mastellone, M.L. and Arena,U. (1999). The effect of particle size and density on solids distribution along the riser of a circulating fluidized bed. *Chemical Engineering Science*, 54, 5383 – 5391.

Matsen, T.M. (1982). Mechanisms of choking and entrainment. Powder Technology, 32, 21-33.

Mei, J. S., Shadle, L. J., Yue, P. C. and Monazam, E. R. (2007). Flow regime study in a high density circulating fluidized bed riser with an abrupt exit. *The 12th International Conference on Fluidization - New Horizons in Fluidization Engineering*,Vancouver, Canada,63 – 70.

Monazam, E., R. and Shadle, L. J. (2008). Analysis of the acceleration region in a circulating fluidized bed riser operating above fast fluidization velocities. *Industrial and Engineering Chemistry Research*, 47, 8423 – 8429.

Monceaux, L., Aziz, M., Molodtsof, Y. and Large, J. (1986). Particle mass flux profiles and flow regimes characterization in a pilot scale fast fluidized bed. In Fluidization V, M.A. Sorenson and J.R. Ostergaard, Eds., Engineering Foundation, New York, p 337.

Muller, P. and Reh, L. (1994). Particle drag and pressure drop in a accelerated gas solid flow. In Circulating Fluidized Bed Technology IV, A.A. Avidan, Eds., AIChE, New York, 159 – 166.

Nakamura, K. and Capes, C.E. (1973). Vertical pneumatic conveying: A theoretical study of uniform and annular particle flow models. *Canadian Journal of Chemical Engineering*, 51, 39 – 46.

Neri, A. and Gidaspow, D. (2000). Riser hydrodynamics: Simulation using kinetic theory. *AIChE Journal*, 46, 52 – 67.

Nieuwland J.J. (1994). Hydrodynamic modelling of gas – solid two phase flows. *PhD Dissertation*, Twente University, Enschede, The Netherlands.

Nieuwland, J.J., Van Sint Annaland, M., Kupiers, J.A.M and van Swaaij, W.P.M. (1996). Hydrodynamics modelling of gas/particle flows in riser reactors. *AIChE Journal*, 42, 1569 – 1582

O'Brien, T.J. and Syamlal, M. (1994). Particle cluster effects in the numerical simulation of a circulating fluidized bed. In *Circulating Fluidized Bed Technology IV*, p345 – 350.

Ouyang, S. and Potter, O. E. (1993). Consistency of circulating fluidized bed experimental data. *Industrial and Engineering Chemistry Research*, 32, 1041 - 1045.

Ouyang, S., Lin, J., Potter, O. E. (1993). Ozone Decomposition in a 0.264 m Diameter Circulating Fluidized Bed Reactor. *Powder Technology*, 74, 73 - 78

Patience, G.S., Chaouki, J., Berruti, F. and Wong, R. (1992). Scaling Considerations for circulating fluidized bed risers. *Powder Technology*, 72, 31 – 37.

Peirano, E. and Leckner, B. (1998). Fundamentals of turbulent gas solid flows applied to circulating fluidized bed combustion. *Progress in Energy and Combustion Science*, 24, 259 - 296.

Pita, J.A. and Sundaresan, S. (1991). Gas – solid flow in vertical tubes. *AIChE Journal*, 37, 1009 – 1018.

Pugsley, T.S., Berruti, F., Godfroy, L., Chaouki, J. and Patience, G.S. (1993). A predictive model for the gas – solid flow structure in circulating fluidized beds. In *Preprints of circulating Fluidized Bed Technology IV*, p 41.

Qi, H., You, C., Boemer, A. and Renz, U. (2000). Eulerain simulation of gas solid two-phase flow in a CFB riser under consideration of cluster effects. In Fluidization 2000: Science and Technology, D. Xu and Mori, S. Eds., Xi'an Publishing House, Xi'an, 231 – 237.

Qi, X.-B., Huang, W.-X. and Zhu, J. (2008). Comparative study of flow structure in circulating fluidized bed risers with FCC and sand particles. *Chemical Engineering and Technology*, 31**,** 542 - 553.

Qi, X.-B., Zhu, H. and Zhu, J. (2009). Demarcation of a new circulating turbulent fluidization regime. *AIChE Journal*, 55, 594 - 611.

Qi, X.-B., Zhu, J. and Huang, W.-X. (2008). Hydrodynamic similarity in circulating fluidized bed risers. *Chemical Engineering Science*, 63**,** 5613 - 5625.

Ranade, V.V. (1999). Modelling of gas – solid flows in FCC riser reactors: Fully developed flow. Second International Conference on CFD in Minerals and Process Industries, CSIRO, Melbourne, Australia, 77 – 82.

Ranade, V.V. (2002). *Computational Flow Modeling for Chemical Reactor Engineering*, Academic Press, New York.

Reh, L. (1986). The circulating fluid bed reactor – its main features and applications. *Chemical Engineering and Processing*, 20, 117 – 127.

Rhodes, M. J. (1986). High Velocity Circulating Fluidized Beds. *Ph.D. Dissertation*, University of Bradford.

Shan, H., Zhang, J.-f., Yang, C. H. and Ye, Z. G. (2006). Improving FCC product distribution with two-stage riser technology. *Petroleum Science and Technology*, 24, 379 - 387.

Simonin, C. and Viollet, P.L. (1990). Predictions of an oxygen droplet pulverization in a compressible subsonic coflowing hydrogen flow. *Numerical Methods for Multiphase Flows*, FED 91, 65 – 82.

Sinclair, J.L. and Jackson, R. (1989). Gas – particle flow in a vertical pipe with particle – particle interactions. *AIChE Journal*, 35, 1473 – 1486.

Subbarao, D. (2009). A model for cluster size in risers. *Powder Technology*, In Press.

Sun, B. and Gidaspow, D. (1999). Computation of circulating fluidized-bed riser flow for the fluidization viii benchmark test. *Industrial and Engineering Chemistry Research*, 38, 787 - 792.

Syamlal, M., Rogers, W. and O'Brien T. J. (1993). *MFIX Documentation: Volume 1, Theory Guide*. National Technical Information Service, Springfield, VA.

Tsuo, Y.P. and Gidaspow, D. (1990). Computation of flow patterns in circulating fluidized beds. *AIChE Journal*, 36, 885 – 896.

Vaishali, S., Roy, S., Bhusarapu, S., Al-Dahhan, M. H. and Dudukovic, M. P. (2007). Numerical simulation of gas solid dynamics in a circulating fluidized bed riser with Geldart group B particles. *Industrial Engineering and Chemistry Research*, 46, 8620 – 8628.

van Breugel, J.W., Stein, J.J.M. and Buurman C. (1969). Vertical gas solids flow, Internal report Shell Laboratory, Amsterdam, The Netherlands.

van der Meer, E.H., Thorpe, R. B. and Davidson, J. F. (1999). Dimensional groups for practicable similarity of circulating fluidized beds. *Chemical Engineering Science*, 54, 5369 – 5376.

van Wachem, B. G. M. and Almstedt, A. E. (2003). Methods for multiphase computational fluid dynamics. *Chemical Engineering Journal*, 96, 81 - 98.

Wang, G., Gao, J.-S. and Xu, C.-M. (2004). Evolutionary design on FCC reactors driven by the high temperature and short contact time demands. *Petroleum Science and Technology*, 22, 1581 - 1594.

Wang, W. and Li, J. (2007). Simulation of gas – solid two phase flow by a multi scale CFD approach – Extension of the EMMS model to the sub-grid level. *Chemical Engineering Science*, 62, 208 – 231.

Wei, F., Yang, G.Q., Jin, Y. and Yu, Z.Q. (1995). The characteristics of cluster in a high density circulating fluidized bed. The Canadian Journal of Chemical Engineering, 73, 650 – 655.

Weinstein, H., Graff, R. A, Meller, M. and Shao, M. J. (1984). The Influence of imposed pressure drop across a fast fluidized bed. In *Fluidization*, Eds., D. Kunii, and R. Toei, Engineering Foundation, New York, p 299 - 306.

Wen, C.Y. and Yu, Y.H. (1966). Mechanics of fluidization. *Chemical Engineering Progress Symposium Series*, 66, 100 – 111.

Wirth, K.E. (1988). Axial pressure profile in circulating fluidized beds. Chemical Engineering Technology, 11, 11.

Wu, B., Zhu, J. X. and Briens, L. (2007). A comparison of flow dynamics and flow structure in a riser and a downer. *Chemical Engineering and Technology*, 30, 448 - 459.

Xu, G. and Gao, S. (2003). Necessary parameters for specifying the hydrodynamics of circulating fluidized bed risers - a review and reiteration. *Powder Technology*, 137, 63 - 76.

Xu, G. and Li, J. (1998). Analytical solution of the energy – minimization multi – scale model for gas – solid two – phase flow. *Chemical Engineering Science*, 53, 1349 – 1366.

Xu, G., Nomura, K., Nakagawa, N. and Kato, K. (2000). Hydrodynamic dependence on riser diameter for different particles in circulating fluidized beds. *Powder Technology*, 113, 80 – 87.

Yang, G. L., Huang, Z. and Zhao, L. Z. (1984). Radial gas dispersion in a fast fluidized bed. In *Fluidization*, Eds., D. Kunii, and R. Toei, Engineering Foundation, New York, p 145-152.

Yang, N., Wang, W., Ge, W. and Li, J. (2003a). Analysis of flow structure and calculation of drag coefficient for concurrent up gas solid flow. *Chinese Journal of Chemical Engineering*, 11, 79 – 84.

Yang, N., Wang, W., Ge, W. and Li, J. (2003b). CFD simulation of concurrent up gas solid flow in circulating fluidized beds with structure dependent drag coefficient. *Chemical Engineering Journal*, 96, 71 – 80.

Yang, N., Wang, W., Ge, W., Wang, L. and Li, J. (2004). Simulation of Heterogeneous structure in a circulating fluidized bed riser by combining the two fluid model with the energy minimization multiscale approach. *Industrial Engineering and Chemistry Research*, 43, 5548 – 5561.

Yang, W. C. (2003). *Handbook of fluidization and fluid particle systems*. Marcel Dekker, Inc., New York.

Yang, Y.L., Jin, Y., Yu, Z.Q. and Wang, Z.W. (1992). Investigation on slip velocity distributions in the riser of dilute circulating fluidized bed. *Powder Technology*, 73, 67 – 73.

Yasuna, J. A., Moyer, H. R., Elliott, S., and Sinclair, J. L. (1995). Quantitative predictions of gas-particle flow in a vertical pipe with particle-particle interactions. *Powder Technology*, 84, 23.

Yerushalmi, J. (1986). Gas Fluidization Technology, Wiley, New York, p 174.

Yerushalmi, J. and Squires A.M. (1977). The phenomenon of fast fluidization. *AIChE Symposium Series*, 72, 44 – 47.

Yerushalmi, J. and Avidan, A. (1986). High-Velocity Fluidization. In *Fluidization*, Eds., J. F. Davidson, R. Clift, R. and Harrison, Academic Press, New York, p 225-289.

Yerushalmi, J., Turner, D.H. and Squires, A.M. (1976). The fast fluidized bed. *Industrial Engineering Chemistry Process Design and Development*, 15, 47 – 53.

Zhang, D.Z. and VanderHeyden, W.B. (2001). High-resolution three-dimensional numerical simulation of a circulating fluidized bed. *Powder Technology*, 116, 133 – 141.

Zhang, H., Huang, W.X. and Zhu, J.X. (2001). Gas – solids flow behavior: CFB riser vs downer. *AIChE Journal*, 47, 2000 - 2011.

Zhang, Y. and Reese, J.M. (2001). Particle-gas turbulence interactions in a kinetic theory approach to granular flows. *International Journal of Multiphase Flow*, 27, 1945 – 1964.

Zhang, Y. and Reese, J.M. (2003). Continuum modelling of granular particle flow with inelastic inter – particle collisions. *Chemical Engineering Research and Design*, 81, 483 – 488.

Zhu, H. P., Zhou, Z. Y., Yang, R. Y. and Yu, A. B. (2007). Discrete particle simulation of particulate systems: Theoretical developments. *Chemical Engineering Science*, 62, 3378 - 3396.

Zhu, J.X. and Bi, H.T. (1995). Distinctions between low density and high density circulating fluidized beds. *The Canadian Journal of Chemical Engineering*, 73, 644 – 649.

Zou, B., Li, H., Xia, Y. and Ma, X. (1994). Cluster structure in a circulating fluidized bed. *Powder Technology*, 78, 173 – 178.

"Remember that all models are wrong, the practical question is how wrong do they have to be to not be useful"

- **Prof. George E. P. Box**

SYNOPSIS

INSTITUTE OF CHEMICAL TECHNOLOGY

UNIVERSITY OF MUMBAI

SYNOPSIS

OF THE THESIS TO BE SUBMITTED TO THE

UNIVERSITY OF MUMBAI

IN THE PARTIAL FULFILLMENT OF THE REQUIREMENTS

FOR THE DEGREE OF

DOCTOR OF PHILOSOPHY (TECHNOLOGY)

IN THE FACULTY OF CHEMICAL ENGINEERING

Research Scholar	:	**Naren P.R.**
Name and Designation of Research Supervisor	:	**Prof. Arvind M. Lali** **Professor, Chemical Engineering Department**
Title of the Thesis	:	**MODELING OF HIGH SOLID FLUX CIRCULATING FLUIDIZED BED REACTORS**
Degree	:	**Doctor of Philosophy (Technology)**
Institute	:	**Institute of Chemical Technology,** **University of Mumbai, Matunga,** **Mumbai 400 019.**
Number and Date of Registration	:	**724 / 03-04-2007**
Date of submission	:	**15 – 06 - 2009**
Signature of the Candidate	:	P. R. Naren
Signature of the Research Guide:		**(Arvind M. Lali)**

MODELING OF HIGH SOLID FLUX CIRCULATING FLUIDIZED BED REACTORS

Circulating fluidized bed (CFB) refer to state of gas solid flow wherein the solids are entrained out of the system by the flowing gas at velocities far greater than particle terminal settling velocity. The solid flow into the system, in principle must be maintained externally to counterbalance the entrainment out of the system. Circulating fluidized bed applications may be broadly grouped into low density and high density circulating fluidized bed processes (Zhu and Bi, 1995). This work focuses on high density CFB processes. Typical high density CFB operates at superficial gas velocity ranging from 5 to 20 m/s with solid circulation flux greater than 100 kg/m^{2}s. Known commercial applications include fluid catalytic cracking (FCC) process, Synthol reactor for Fischer Tropsch synthesis (Contractor and Chaouki, 1991), Calcination of aluminum trihydrate to high purity alumina (Reh, 1986). Industrial processes involving CFB reactor as key element are well documented in literature (Reh, 1986., Berruti *et al.* 1995., Zhu and Bi, 1995).

The study of hydrodynamics of high solid flux circulating fluidized bed reactor assumes significance in the context of understanding the fundamentals of high flux gas – solid flow and driven by developments in current CFB technologies. For example, cracking of heavier hydrocarbon molecules, necessitates that the most advanced type of feed injection nozzles are used and catalyst be well distributed across the riser cross – section. The milli-second riser reactors also require high catalyst/oil ratio. Increase of solid circulation flux and suspension density will be very useful for other applications requiring even higher solids/gas feed ratios and higher solid concentration. There is significant scope for development of new processes and realizing improvements in existing process technologies through thorough investigation and understanding of high solid flux risers. Quantitative understanding and predicting the performance of CFBs rely on the ability to capture and model inherently complex hydrodynamics of gas – solid flow in these systems.

Computational fluid dynamics (CFD) facilitates and shortens development time cycles of new and/or improvements of existing process know-how to cater future

demands. Recent years saw increasing usage of CFD models to understand fluid dynamics of high solid flux systems like those in commercial FCC riser and to evaluate alternate hardware configuration for better process output.

Several attempts were made in the past to understand the hydrodynamics of gas – solid flows in vertical pipes or risers. Models of varying degree of complexity like two fluid models (the Eulerian-Eulerian framework), the Eulerian-Lagrangian framework and Direct numerical simulations were attempted in the past to understand the underlying dynamics of gas solid flows. However, the two-fluid based continuum models offer computational edge over other models especially in case of systems operating with high solid holdup and with those involving large/ complex geometry. The present research work is focused on development and use of two-fluid computational models for simulating flow in gas solid riser reactors.

The two-fluid continuum model description for fluidized bed is based on the mass, momentum and energy conservation law as given by Anderson and Jackson (1967). These models can be broadly classified into CFD based computational models (Sun and Gidaspow, 1999., Nieuwland 1994., Dasgupta *et al.* 1993 and 1994., Sinclair and Jackson, 1989. etc) and semi-empirical based hydrodynamic models (Godfroy *et al.* 1999., Nieuwland, 1994., Pugsley *et al.* 1993., Nakamura and Capes, 1973). The Eulerian – Eulerian two-fluid CFD based computational model is adopted here to investigate gas solid two-phase flow in high solid flux riser systems. The computational models require less ad-hoc adjustments and/or facilitate in generalization of the empirical/semi-empirical correlations developed through actual physical experiments to wide operating conditions.

The solid phase is modeled as a fluid continuum with shear stress tensors computed using kinetic theory of granular flows (KTGF). The KTGF, analogous to the kinetic theory of gases, is characterized by the granular temperature. The solid phase pressure and the viscosity, which resists the motion of the particles, are defined in terms of granular temperature. The models based on KTGF require less ad- hoc adjustments and are widely used (Ranade, 2002 and references therein).The constitutive expressions of the KTGF model involves number of parameters like specularity coefficient, particle – particle restitution coefficient, angle of internal friction etc. In

addition, prediction of high solid holdup near the walls requires appropriate specification of the wall boundary conditions for the solid phase. The shear at the wall for the solid phase is specified through an adjustable specularity coefficient parameter in the KTGF model.

Several attempts were made in the past to simulate, understand and develop state of art computational two fluid models for gas solid riser flows. In spite of such sustained efforts, most of these works that dealt with the gas solid riser flow were faced with issues like:

a) Approximating the gas solid flow in cylindrical risers as flow through channels and simulating the flow in 2D Cartesian domain.
b) Most studies addressed effects of model parameters on few selected quantities like either holdup or solid velocity or only turbulent quantities. Consistent and complete experimental data measured on a single riser system is rarely available.
c) Simulations were mainly concerned at low solid flux conditions or low mass loadings
d) Parametric analysis in some cases was coupled with complex flow geometry like risers with two inlets, abrupt exit etc and hence pose difficulty in independent parametric evaluation.

Thus, there is a need to evaluate the two-fluid model for simulating gas solid riser flow operating at high solid flux conditions and bring out the salient features and capabilities of the constituent closures in predicting the riser flow features. In the present work, the Eulerian – Eulerian two-fluid model was developed to simulate gas solid flow profile at typical high solid flux flow conditions and an attempt was made to investigate the model parameters in simulating the riser flow features. Although, work lays more emphasis on the numerical experiments pertaining to gas-solid riser flows, comparisons with available experimental data were also made and meaningful conclusions drawn thereof. The overall research work is divided into three sections as discussed below:

Part 1: Evaluation of structure dependent drag model

The flow in riser at high solid flux conditions is accompanied by pronounced radial segregation and cluster formation (Yerushalmi and Squires, 1977., Horio and Kuroki, 1994., Lackermeier *et al.* 1994). The clusters are dynamic entities and result in enhanced slip velocities observed in riser flows. The cluster formation result in decreased inter phase momentum drag experienced by the particles and modeling the interphase momentum exchange coefficient assumes significances in capturing these key features of gas solid flows. Further, the interphase momentum exchange provided by drag plays an important part than the solid phase stress tensor (Agrawal *et al.* 2001., Yasuna *et al.* 1995, Ranade, 2002 and references cited therein).

Attempts were made in the past to evaluate the momentum exchange closures in modeling the gas solid flow in high flux risers. The drag correction factors based on empirical correlations were seldom valid for range of high solid conditions existing in riser reactors and were not able to predict the observed increase in slip velocities in these systems. Nieuwland (1994) developed empirical correlation to correct the slip velocity at high solid flux flows from the data of van Breugel *et al.* (1969). At solid holdup greater than 10%, the correction factor was about 30. The correlation of Nieuwland (1994) showed improved predictability of the model with experimental data of van Breugel *et al.* (1969). But evaluation with Yang *et al.* (1992) showed not so good results. O'Brien, and Syamlal, (1994) used experimental solid volume fraction data to empirically adjust the drag coefficient in simulating gas solid riser flows. However, the model had serious limitation, as the proposed relation was not generalized for all operating conditions.

To overcome the shortcomings of the conventional drag correlation, Li (2000) developed Energy Minimization Multiscale Model (EMMS), a structure specific model to represent interaction between gas and solid phases. The model addressed the heterogeneity at different scales existing in gas solid flows and the average drag coefficient was obtained as sum contribution of the component drags at different scales of interaction. The EMMS model accounts for cluster formation and captures the effective increase in slip velocity. The model was further extended to incorporate inertial effects by Wang and Li (2007). The EMMS framework appears to be a promising approach for simulating high solid flux riser flows. However, the use of the

EMMS model at high solid flux conditions existing in FCC riser systems is yet to be ascertained. There is a lacuna in the literature regarding the applicability of EMMS approach to high flux flows.

In the first part of this work, the EMMS based drag model for interphase momentum transfer was simulated for typical high solid flux flow conditions and improvements of existing EMMS framework in terms of predicting published pressure drop data was investigated. Unlike earlier studies wherein EMMS drag correlation was incorporated into CFD and results from computational model was compared with experimental data, direct comparison of EMMS model output with available data was attempted in this work. This assumes significances as it enables evaluation of constituent expressions of computational models. Prediction of explicit occurrence of minimum energy consumption conditions, comparison of predicted cluster size with reported values from literature, sensitivity of predicted drag with EMMS parameters etc were also addressed as part of this exercise.

It was found that the extended EMMS model with the inertial term predicts distinct local minimum energy consumption for given operating condition and assumed values of cluster voidage and cluster size. However, the model parameters required adjustment to predict the experimental pressure drop data. The dilute phase inertial term can be omitted from the extended model, as this was not found to have any significant effect on model predictions. The cluster voidage was fitted to predict the experimental pressure drop keeping the energy minimization framework of the EMMS model as it was. However, the global minimum in energy consumption was not observed in the EMMS framework.

The present work brought out an independent evaluation of EMMS drag model. Assessment of model predictions with global hydrodynamic parameters brought the salient features of the structure specific EMMS model. The issues identified in the work needs to be addressed further for successful development of cluster based drag model. Once successful, this structure specific drag model can then be incorporated into the computational model to study the fluid dynamics of gas solid riser flows.

Part 2: 3D Periodic computational model for simulating fully developed riser flows

Developing state of art engineering model with reactions requires basic flow information such as fully developed flow profiles (velocity and solid volume fraction) and/or dispersion coefficients etc. Though empirical correlations are available, they do not offer predictive flexibility over wide operating conditions. This necessitates development of hydrodynamic model for gas solid riser flows to predict fully developed flow profiles. Further, to study the effect of operating parameters and model closures, simulating fully developed riser flow proves to be beneficial. Simulation of actual risers with H/D > 50, without jeopardizing the spatial resolution, to obtain fully developed flow profiles, demands enormous computational cost and time. One-way to alleviate huge computational requirement without compromising on the spatial resolution is by use of periodic flow domains to simulate fully developed flow profiles. The computational tools like FLUENT^{TM}, CFX^{TM} do not have in-built periodic model for simulating fully developed flows for multiphase systems. This can be overcome by use of user-defined functions (UDF) to make the computational domain translationally periodic along the flow direction explicitly. In this research work, periodic 3D CFD model based on two-fluid approach was developed for simulating fully developed hydrodynamic flow profiles (holdup, local velocities) through external user defined functions.

The gas solid two-phase flow was modeled in the Eulerian framework. The Wen and Yu (1966) drag model was employed for interphase momentum exchange for the base case simulations. Both the phases were considered incompressible. Solid phase shear stress was computed from kinetic theory of granular flow. Turbulence was modeled via the two-equation k - ε model with standard wall functions. The computational model was developed in FLUENT^{TM} (Version 6.3, Ansys Inc, USA). The computational domain consisted of a small differential element of the riser column of i.d. 0.054 m. User Defined Functions (UDF's) were hooked at the velocity inlet boundary to render the model periodic explicitly. The simulations were done for typical gas solid riser system of air – FCC of 129 μm and 2540 kg/m^3. The methodology of incorporating UDF's to simulate fully developed flow was tested with single phase flow simulations on 2D axis-symmetric and 3D domains. With

proof of implementation from single phase flow simulations two phase flow simulations were done for the riser operating conditions of u_g = 10m/s and G_s = 300 kg/m^{2}s. The time step for each simulation was in the range of 1x 10^{-4} to 1x 10^{-5} s. Solution convergence was monitored by recording the area-weighted quantities – solid circulation flux, slip velocity at the outflow boundary and the static pressure drop across the domain. The simulated results were time averaged for period of about 30 – 50s.

Numerical experiments were performed with this periodic computational model and conclusions drawn accordingly on the effect of various model closures and tuning parameters like specularity coefficient, granular model formulation and so on. The results from the UDF based 3D periodic model were also compared with the 2D axis-symmetric full riser domain simulations. This UDF framework provided flexibility in quick screening of model parameters that could further be used for full-scale simulations.

Part 3: Numerical simulation of scaling laws for riser flow

Successful design of such systems from lab scale to industrial scale necessitates scaling parameters that ensure proper hydrodynamic similarity between reactors at various scales or across operating conditions. Extensive efforts have gone into establishment of scaling laws based on governing equations of continuity and momentum of Anderson and Jackson (1967). Different sets of scaling laws established involves dimensionless groups such as Reynolds number, Froude number, flow rate ratio, particle diameter to column diameter ratio etc. Glicksman (1984); Chang and Louge (1992); Glicksman *et al.* (1993); van der Meer *et al.* (1999) had dealt with these scaling parameters under different flow assumptions.

Recently Qi *et al.* (2008) analyzed the available literature and own experimental data and suggested an empirical scaling parameter based on Froude number and flow rate ratio to ensure local and global hydrodynamic similarity in riser reactors. This empirical scaling parameter was shown to ensure both local and global hydrodynamic similarity under different operating conditions. For the same Qi scaling ratio, radial profiles of solid concentration, particle velocity and cluster voidage exhibited similar

profile in the fully developed flow region. The average solid holdup was shown to vary linearly with respect to the $Fr_D^{-0.3} G_s / (\rho_p u_g)$ scaling ratio.

This looks promising as a single scaling parameter ensuring hydrodynamic similitude in riser systems at both, local and global, levels. Nevertheless, this empirical parameter cannot guarantee hydrodynamic scaling in risers beyond their range without rigorous validation. The parameter was tested with most of data sets obtained with air as fluid medium at ambient conditions. The proposed scaling parameter did not consider the effect of fluid density. Further, the ratio of particle size to column diameter may be significant in small diameter risers and affect the relative contribution of particle shear at wall to the overall pressure gradient (Pita and Sundaresan 1991 and references therein). Further validation of the scaling parameter requires extensive experimental data sets of good reliability. This can be avoided to an extent, with the use of computational models, wherein the simulated profiles at different conditions can be compared to draw meaningful conclusions on scaling analogies. The periodic computational model with UDF developed earlier was employed to address this issue. A set of operating conditions, all having the same Qi scaling ratio (Qi *et al.* 2008) was simulated following the periodic 3D computational model. The solid phase stresses were computed through algebraic KTGF formulation. The computational parameters were set in accordance to the 3D periodic model developed earlier. The simulated results were time averaged for period of about 30 – 50s. Despite the same scaling ratio adopted for the simulation sets, hydrodynamic similarity was not observed for all of the simulation cases considered in this work. For example, particle size significantly affected the computed flow profiles and did not exhibit scaling as per Qi et al. (2008) parameter. It should be noted that the work investigated numerical prediction of hydrodynamic similarity at high solid flux operating conditions. With this, work on further understanding of the physics of gas-solid flows at high flux conditions is required to developed computational models to predict hydrodynamic scaling in such systems.

Despite these shortcomings, the present computational work brought out a method for quick and reliable selection of model parameters with best possible spatial resolution. The strategy employed in the current work can be extended to provide direct one-to-

one comparisons with the experimental quantities. However, it should be noted that mere numerical adjustment of model parameters tuned to fit only certain physical quantities or for particular experimental set up might not be very helpful in developing efficient computational models.

Conclusions

Simulation of gas-solid flow operating at high solid flux condition still poses challenge to chemical engineers. The development of successful state-of-art predictive models for gas-solid riser flows involves multiple tasks and requires multi-level approach. These include - understanding physics of gas-solid riser flows at high flux conditions, development of constituent models, generation of reliable and exhaustive experimental data sets and development of efficient computational models and methods to evaluate the developed gas-solid model. The present work addresses some of these issues. The work highlighted the significance of independent evaluation of constituent closures used in gas-solid fluid dynamic models. The multi scale based EMMS model was found to be not very useful in its present form. The user defined function based periodic computational approach could shorten the time taken in evaluation of CFD model closures without jeopardizing the spatial resolution. However, it should be noted that not much importance were given to actual comparisons of CFD model predictions with experimental data. Rather, the work addressed the significance of model parameters through numerical experiments. In addition, the present research brought out the model capabilities in predicting hydrodynamic similarity observed with experimental data. The methods adopted in this work and the inferences drawn would serve to fine-tune the model parameters to match model predictions with actual experimental data. Further, this will help in development of state-of-art computational models for circulating fluidized bed reactors operating at high solid flux conditions.

References

Agrawal, K., Loezos, P.N., Syamlal, M. and Sundaresan, S. (2001). The role of meso scale structures in rapid gas solid flows. *Journal of Fluid Mechanics*, 445, 151 – 185.

Anderson, T.B. and Jackson, R. (1967). A fluid mechanical description of fluidized beds. *Industrial and Engineering Chemistry Fundamentals*, 6, 527 - 539.

Berruti, F., Chaouki, J., Godfroy, L., Pugsley, T.S. and Patience, G.S. (1995). Hydrodynamics of circulating fluidized bed risers: A review. *The Canadian Journal of Chemical Engineering*, 73, 579 – 596.

Chang, H. and M. Louge (1992). Fluid dynamic similarity of circulating fluidized beds. *Powder Technology*, 70, 259 – 270.

Contractor R.M. and Chaouki, J. (1991). Circulating fluidized bed as a catalytic reactor. In *Circulating Fluidized Bed Technology III*, Pergamon Press, Oxford, p 39.

Dasgupta, S., Jackson, R. and Sundaresan, S. (1993). Turbulent gas – particle flow in CFB – risers. In *Preprints of Circulating Fluidized Bed Technology IV*, p 448 – 453.

Dasgupta, S., Jackson, R. and Sundaresan, S. (1994). Turbulent gas – particle flow in vertical risers. *AIChE Journal*, 40, 215 – 228.

Glicksman, L. R.(1984). Scaling relationships for fluidized beds. *Chemical Engineering Science*, 39, 1373 - 1379.

Glicksman, L. R., Hyre, M. and Woloshun, K.(1993). Simplified scaling relationships for fluidized beds *Powder Technology*, 77, 177 - 199.

Godfroy, L., Patience, G.S. and Chaouki, J. (1999). Radial hydrodynamics in risers. *Industrial and Engineering Chemistry Research*, 38, 81 – 89.

Horio, M. and Kuroki, H. (1994). Three dimensional flow visualization of dilutely dispersed solids in bubbling and circulating fluidized beds. *Chemical Engineering Science*, 49, 2413 – 2421.

Lackermeier, U., Rudnick, C., Werther, J., Bredebusch, A. and Burkhardt, H. (2001). Visualization of flow structures inside a circulating fluidized bed by means of laser sheet and image processing. *Powder Technology*, 114, 71 – 83.

Li, J. (2000). Compromise and resolution – exploring the multiscale nature of gas solid fluidization. *Powder Technology*, 111, 50 – 59.

Nakamura, K. and Capes, C.E. (1973). Vertical pneumatic conveying: A theoretical study of uniform and annular particle flow models. *Canadian Journal of Chemical Engineering*, 51, 39 – 46.

Nieuwland J.J. (1994). Hydrodynamic modelling of gas – solid two phase flows. *PhD Dissertation*, Twente University, Enschede, The Netherlands.

O'Brien, T.J. and Syamlal, M. (1994). "Particle cluster effects in the numerical simulation of a circulating fluidized bed". In *Circulating Fluidized Bed Technology IV*, p345 – 350.

Pita, J.A. and Sundaresan, S. (1991). Gas – solid flow in vertical tubes. *AIChE Journal*, 37, 1009 – 1018.

Pugsley, T.S., Berruti, F., Godfroy, L., Chaouki, J. and patience, G.S. (1993). A predictive model for the gas – solid flow structure in circulating fluidized beds. In *Preprints of circulating Fluidized Bed Technology IV*, p 41.

Qi, X.-B., Zhu, J. and Huang, W.-X.(2008). Hydrodynamic similarity in circulating fluidized bed risers. *Chemical Engineering Science*, 63**,** 5613 - 5625.

Ranade, V.V. (2002). *Computational Flow Modeling for Chemical Reactor Engineering*, Academic Press, New York.

Reh, L. (1986). The circulating fluid bed reactor – its main features and applications. *Chemical Engineering and Processing*, 20, 117 – 127.

Sinclair, J.L. and Jackson, R. (1989). Gas – particle flow in a vertical pipe with particle – particle interactions. *AIChE Journal*, 35, 1473 – 1486.

Sun, B. and Gidaspow, D. (1999). Computation of circulating fluidized bed riser flow for the fluidization VIII benchmark test. *Industrial and Engineering Chemistry Research*, 38, 787 – 792.

van Breugel, J.W., Stein, J.J.M. and Buurman C. (1969). Vertical gas solids flow, Internal report Shell Laboratory, Amsterdam, The Netherlands.

van der Meer, E.H., R. B. Thorpe and J. F. Davidson (1999). Dimensional groups for practicable similarity of circulating fluidized beds. *Chemical Engineering Science*, 54, 5369 – 5376.

Wang, W. and Li, J. (2007). Simulation of gas solid two phase flow by a multi scale CFD approach – Extension of the EMMS model to the sub-grid level. *Chemical Engineering Science*, 62, 208 – 231

Wen, C.Y. and Yu, Y.H. (1966). Mechanics of fluidization. *Chemical Engineering Progress Symposium Series*, 66, 100 – 111.

Yang, Y.L., Jin, Y., Yu, Z.Q. and Wang, Z.W. (1992). Investigation on slip velocity distributions in the riser of dilute circulating fluidized bed. *Powder Technology*, 73, 67 – 73

Yasuna, J. A., Moyer, H. R., Elliott, S., & Sinclair, J. L. (1995).Quantitative predictions of gas-particle flow in a vertical pipe with particle-particle interactions. *Powder Technology*, 84, 23.

Yerushalmi, J. and Squires A.M. (1977). The phenomenon of fast fluidization. *AIChE Symposium Series*, 72, 44 – 47.

Zhu, J.X. and Bi, H.T. (1995). Distinctions between low density and high density circulating fluidized beds. *The Canadian Journal of Chemical Engineering*, 73, 644 – 649.

APPENDIX

APPENDIX I: TWO FLUID CFD MODEL STUDIES ON GAS SOLID RISER FLOWS

Notation	Detail	Notation	Detail
	Model		**Wall boundary condition for solid**
Type A	Hydrostatic pressure shared by both the phases – gas and solid	SWBC1.	No slip
Type B	Hydrostatic pressure shared only by the gas (primary) phase.	SWBC2.	Shear stress zero
	Gas phase turbulence	SWBC3.	Specified shear stress
GPT1.	Eddy viscosity model based on Prandtl mixing length	SWBC4.	Johnson and Jackson (1987)
GPT2.	Eddy viscosity model based on Prandtl mixing length with correction for solid volume fraction		**Gas density**
GPT3.	Turbulent viscosity as scalar multiple of molecular viscosity	GRHO1.	Gas density specified
GPT4.	k-ϵ model	GRHO2.	Density computed form incompressible ideal gas law
GPT5.	k model – One equation turbulence model with □ correlated with turbulent length scale		**Gas viscosity**
GPT6.	No model for gas phase turbulence	GNU1.	Gas viscosity specified
	Solid phase turbulence	GNU2.	Molecular viscosity of gas corrected for presence of solid particles
SPT1.	k-ϵ model		**Drag coefficient**
SPT2.	KTGF based expression for turbulent momentum diffusivities &/ granular diffusivities	D1.	Wen and Yu (1966)
SPT3.	No model for solid phase turbulent momentum transport	D2.	Ergun (1952) and Wen and Yu (1966)
	Wall boundary condition for gas	D3.	Ding and Gidaspow 1990
GWBC1.	No slip	D4.	Syamlal and O'Brien 1987
GWBC2.	Shear stress zero	D5.	Arastoopur 1990
GWBC3.	Sinclair and Jackson 1989 – Force balance on the fluid in layer of thickness δ close to wall.	D6.	Zhang and Reese 2000
		D7.	Richardson and Zaki 1954

Reference	Model	Drag coefficient	Turbulence model	Wall BC	Model parameters	Riser system	Particle system	Operating conditions	Grid details	Simulation parameter	Notes
Almuttahar and Taghipour , 2008	Type: A 2D Unsteady KTGF pde form	D4	GPT6 SPT3	GWBC1 SWBC4	$\phi = 0$ $e_w = 0.95$ $e_p = 0.99$	a) Liu 2001 D = 0.076m H = 6.1m H/D ~ 80	a) Air ρ: GRHO1, μ: GNU1 FCC $\rho_p = 1600$ kg/m^3 $d_p = 70$ μm Ar = 2.74 u_{ter} =0.21 m/s	a) $u_g = 4 – 8$ m/s $G_s = 94 – 555$ kg/m^{2}s	r: 75 z: 308 non uniform	$t_s = 5$ X 10^{-4} – 1 X 10^{-3} s $T_s = 45$s	- Model simulated in Fluent 6.2 - Granular energy dissipation (only) through momentum exchange accounted - Frictional viscosity also accounted in the solid phase shear viscosity apart from collosional and kinetic components - Radial profiles of solid volume fraction and axial solid velocity compared with experimental data - Radial solid flux profiles are derived from local velocity and holdup data and then compared with simulations - The model was validated over a range of operating conditions covering dilute, dense and FFB regime. - The model qualitatively predicted the flow profiles for FFB regime but qualitative predictions were poor - The model could not predic the upflow of solid particles near wall for dense upflow CFB regime - Large deviations were also found in near wall predictions
Benavides *et al*., 2008	Type: A 3D unsteady KTGF pde form	N.A.	GPT4 SPT3	GWBC1 SWBC2	$\phi = 0.008$ $e_w = 0.9$ $e_p = 0.8$	Expt setup D = 0.083m H = 4m H/D ~ 48	Air ρ: GRHO1, μ: GNU1 Sand $\rho_p = 2600$ kg/m^3 $d_p = 410$ μm Ar = u_{ter} = m/s	u_g : 5 m/s G_s: 40 kg/m^2	-	$t_s = 10^{-4}$ s $T_s = 18.5$ s $\Delta T_{s,avg} = 6$ s	- Simulated in FLUENT 6.3.21 - Granular dissipation (only) through momentum exchange accounted - Turbulent kinetic energy generation and dissipation accounted via Simonin 1996 - At lower z/H (0.4, 0.53) model underpredicted the radial solid holdup profile. Near wall solid holdup underpredicted by ~30% and predicted inverse radial segregation towards the centre of pipe - At z/H ~ 0.6558 predictions were better with experimental data. - Axial holdup profile was also compared with expeirmtnal data. Fully developed cross sectional average over predicted. Also developing region (z/H < 0.2) underpredicted by more than ~50%
Benyahia *et al*., 2007	Type: A Fully developed 1D Unsteady KTGF pde form	D1	i) GPT4 SPT2 ii)GPT6 SPT3	GWBC1 SWBC4	$\phi = 0.003$, 0.001 $e_w = 0.7$ $e_p = 0.95$ $e_{w,fr} = 0.3$, 0.2	D = 0.1m	Air ρ: GRHO1, μ: GNU1 Solid $\rho_p = 2400$ kg/m^3 $d_p = 120$ μm Ar = 5.38 u_{ter} =0.68 m/s	$u_g = 5.5$ m/s $\varepsilon_s = 0.03$	r: 80 uniform $Dr/d_p \sim 10$	$t_s \sim 10^{-4}$ s $T_s = 60$s	- Model simulated in MFIX - Three k- ϵ and KTGF flavors were used in this model. – **A**grawal et al. (2001), **B**alzer et al. (1996), **C**ao and Ahmadi (1995) – Model **A** does not include gas phase turbulence where model **C** is dry granular model - Combinations of granular energy productin and dissipation due to interphase exchange and turbulent gas phase energy production and dissipation due to particles employed - Wall BC modeled using both Johnson and Jackson and Jenkins model - Standard and modified wall functions employed as well - No concrete discretion with respect to turbulent models as all **A, B** and **C** give similar core annulus result and also similar gas, particle and holdup profiles – rest of sensitivy analysis with wall BC coefficients done primarily with model **A** - Oscillatory pattern in solid holdup and gas velocity profiles shown. The frequency of oscillations were reported ~0.188 Hz. - Core annulus flow structure is result of time averaging of transient cluster motion. - Free slip WBC and lower specualrity coeff predict higer solid holdup near walls. Clusters tend to move away from wall at higher specularity or friction coeff. Wall friction coeff or specualrity coeff dictate the granular flux at wall and hence holdup at wall - Modified wall functions prevents dicontinuity of k near walls for gas phase but no significant change is observed in gas velocity profile - Core annulus observed at all e_p values from 0.9 – 0.999 - Lower particle particle restitution coefficient (highly inelastic) giver higher solid holdup at walls – In constrast steady state simulations show higher holdup at higer particle particle restitution coefficient(highly elastic). - Lower e_p increases granular dissipation and in turn causes more denser clusters and more void dilute phase regions for a fixed solid holdup

Reference	Model	Drag coefficient	Turbulence model	Wall BC	Model parameters	Riser system	Particle system	Operating conditions	Grid details	Simulation parameter	Notes
											causing core annulus or pronocunced radial segregation
Vaishali *et al.*, 2007	Type: A 2D unsteady KTGF pde form	a) D1 b) D4	GPT6 SPT3	GWBC1 SWBC4	ϕ = N.A. e_w = 0.9 e_p = 0.95	Bhusarapu 2005 D = 0.152 m H = 7.9 m H/D ~ 52	Air ρ: GRHO1, μ: GNU1 Solid ρ_p = 2550 kg/m^3 d_p = 150 μm Ar = 6.85 u_{ter} =0.974 m/s	u_g = 3.2, 3.9, 4.5 m/s G_s = 26.6, 33.7, 36.8 kg/m^{2}s	x: 15 y: 350 uniform	t_s = 1e-4 s	- Model simulated in FLUENT 6.2 - Expressions for granular energy dissipation through inelastic collisions and granular energy dissipation & production with fluid exchange not specified - Model predicted inverse solid segregation towards axis whereas experimental data shows radial segregation towards wall - Model underpredicted solid velocity, solid holdup and granular temperature - Syamlal and Obrien drag closure predicted improved solid holdup with respect to experiment only for one operating condition – could not be generalized with other conditions
Benyahia *et al.*, 2005	Type: A 2D axis symmetric unsteady KTGF pde form	D4	GPT4 SPT2	GWBC1 i)SWBC4 ii) SWBC2	ϕ = 0.02 e_w = 0.15, 0.83 e_p = 0.94 $e_{w,fr}$ = 0.125	Jones 2001 D = 0.0142 m L/D = 100	Air ρ: GRHO1, μ: GNU1 Glass beads ρ_p = 2500 kg/m^3 d_p = 70 μm Ar =3.17 u_{ter} =0.315 m/s	u_g = 14.85 m/s Solid loading 1 - 30	r: 15 z: 300	t_s ~ 50 E-6 s T_s = 1s	- Turbulent kinetic energy production and dissipation due to particles accounted - Granular energy dissipation and production due to fluid phase is accounted. - $k_2 – k_{12}$ type [granular energy – cross correlatin for gas patcile velocity fluctuation] equation is employed - Standard and modified wall functions to account for presence of particles studied - Effect of wall BC assessed in the study - Free slip, low specularity coeffcient, small friction predicted experimental solid velocity profiles with reasonable aggrement. However turbulent kinetic energy of gas was underpredicted by these wall BC of solid phase. [wall BC of solids affect turbulent kinetic energy of gas through the term k_{12}] - Fully developed flow was assured with the magnitude of radial solid velocity - The wall functions do not have significant impact on the flow profiles [Flow being dilute cited as reason]
Zhang and Reese, 2003	Type: A Fully developed 1D axis symmetric steady KTGF pde form	D6	GPT2 SPT2	GWBC1 SWBC4	ϕ = 0.3 e_w = 0.9 e_p = 0.98	a) Nieuwland 1994 D = 0.054m	a) Air ρ: GRHO1, μ: GNU1 FCC ρ_p = 2540 kg/m^3 d_p = 129 μm Ar = 5.89 u_{ter} = 0.7869 m/s	a) ug =10, 14.4 m/s G_s = 200 – 400kg/m^{2}s	-	-	- Gravity term neglected for the ga sphase - Stand wall functions of Louge *et al.* (1991). - Granular energy production and dissipation due to interaction with gas phase/momentum exchange included. Modified form of Koch (1990) expression for gas phase contribution in granular energy equation incorporated in the model - Radial solid holdup and solid velocity profile found be in good agreement with Nieuwland 1994 data. Model is in better ageement than that Nieuwland 1994 model - Predicted dimensionless radial profile of local solid flux shows minima near wall [i.e, from r= 0 to r= R, local flux decreases and then increases and then decrease towards wall] - Sensitivity of results with KTGF parameters not reported
Benyahia *et al.*, 2002	Type: B 2D unsteady	D5	GPT6 SPT3	GWBC1 Custom equation for solid phase	–	a) Knowlton *et al.* 1995 D = 0.2m H = 14.2m H/D ~ 71	a) Air ρ: GRHO2, μ: GNU1 FCC ρ_p = 1712 kg/m^3 d_p = 76 μm Ar = 3 u_{ter} =0.26 m/s	a) P = 1 bar T = 300K u_g =5.2 m/s G_s = 489 kg/m^{2}s	(i) r: 27 z:280 non uniform (ii) r: 18 z: 210 non uniform	t_s = 5 X 10^{-4} s T_s = 45s	- Model simulated in CFX 4.1 - Solid phase viscosity taken as μ_s = 0.5Pas - The model validated with the results with the PSRI, Chicago experimental fluidization challenge problem of Fluidization VIII - Solid pressure modeled as $p_s = G\nabla\varepsilon_s$ with $G = 10^{-8.5\varepsilon+5.43}$ - Solid wall BC given as $u_t = -\varepsilon_s^{-1/3} d_p \nabla_n u_t$ where u_t is the solid tangential velocity at the wall - The model predicted core- annulus flow strucutre with solid downflow near walls - The downflow of solids/annulus region oscillated between the two walls (one side to another) - Time averaged (t_{avg} = 20s, 27s) profiles of solid flux, concentration compared with expt data. Predictions were poor. The model predicted

Reference	Model	Drag coefficient	Turbulence model	Wall BC	Model parameters	Riser system	Particle system	Operating conditions	Grid details	Simulation parameter	Notes
											smaller core region than expts and were not symmetric - Axial pressure drop profile was in good aggrement than radial flow profiles - Averaging time,2D computational domain, wall boundary conditions for solid cited as probable reasons for the poor predictions
Zhang and Reese, 2001	Type: A Fully developed 1D axis symmetric steady KTGF pde form	D6	GPT5 SPT2	GWBC1 SWBC4	ϕ = N.A. e_w = 0.9 e_p = 0.75	a) Tsuij *et al.* 1984 D = 0.0305m	a) Air ρ:GRHO1 μ: GNU1 ρ_p = 1020 kg/m^3 d_p = 200,500, 1000 and 3000 μm Ar = 6.7,16.8, 33.7, 101 u_{ter} =0.7,2, 3.94 , 8.72 m/s	a)Mass loading: 0.9 – 4.2			- Gravity term neglected for the ga sphase - Turbulent dissipation rate ϵ given in terms of turbulent length scale. Louge e*t al.* (1991) length scale of pure gas (l) and Kenning and Crowe (1997) modified length scale (l_h) which accounts for the presence of particles used in the present work - Turbulent diffusivites for the particles adopted from Peirano and Leckner (1998) - Louge *et al.* (1991) and Crowe and Gillandt (1998) version for turbulent kinetic energy k employed. - Turblent kinetic energy generation due to presence of particles accounted - Granular energy generation and dissipation due to interaction with gas also accounted - For larger particles of 500μm, 1000μm Crowe and Gillandt (1998) k model with length scale l_h quantitatively predicted enhancement in gas velocity fluctuations with increaseing loading ratio, increased gas velocity flucitations with respect to single phase low on particle addition and flattening of gas velocity profiles at higer mass loadings - Predictions were good at higer mass loadings. However vlaues near wall were underestimated largely - Sensitiviy of e studied over range from 0.7 – 1 Predicted particle fluctuation velocity profiles were found to be sensitive to value of e. The fluctuating velocity varies upto 40% and upto 25% at the axis for the particles and gas respectively for the change in e from 1 to 0.7.
Neri and Gidaspow, 2000	Type: B 2D unsteeady KTGF pde form	D2	GPT6 SPT3	GBWBC1 SWBC4	ϕ = N.A. e_w = 0.96, 0.8 e_p = 0.999	Miller and Gidaspow 1992 D = 0.075 m H = 6.58 m H/D ~ 88	Air ρ: GRHO2, μ: GNU1 Solid ρ_p = 1654 kg/m^3 d_p = 75 μm Ar = 2.96 u_{ter} =0.25 m/s	u_g =2.61 m/s G_s = 20.4 kg/m^{2}s P = 118.6 kPa	Δx = 0.00375 m Δy = 0.0484 m $\Delta x/d_p$ ~50 $\Delta y/d_p$ ~ 645 ar ~ 13	Ts = 50 s $Ts_{,avg}$ = 20 – 50 s	- Production and dissipation of granular energy due to interaction with fluid phase not accounted - Simulation were also performed with symmetry boundary condition in Cartesian co ordinate system - The simulations (2D wall - wall BC) showed existence of core –annulus flow in riser with down flow near walls. The flow oscillated between the walls at frequency of 0.2 Hz. The bottom section of riser wwas denser and downflow was pronounced at the top. Quantitative comparisons with experimental data were poor. Model did not show a flatter holdup profile with steep increase in holdup near walls as observed in experiments. Velocity/Flux profiles predictions were also poor. - 2D – symmetry – Wall model showed solid segregation near wall and also near the symmetry boundary. Solids were found to accumulate at riser top than at bottom. - Addition of cohesive forces (Solid pressure expression) increased the holdup near walls - 2D axis symmetric simulations were also performed but results of the same were not reported in the paper
Benyahia *et al.*, 2000	Type: A 2D unsteady KTGF pde form	D5	GPT6 SPT3	GWBC1 SWBC4	ϕ = N.A. e_w = 0.9 e_p = 0.95	a) D = 0.2m H = 14.2m H/D ~ 71	a) Air ρ: GRHO1, μ: GNU1 FCC ρ_p = 1712 kg/m^3 d_p = 76 μm Ar = 3 u_{ter} =0.263 m/s	a) P = 1 bar T = 300K u_g =5.2 m/s G_s = 489 kg/m^{2}s	r: 18 z: 210 non uniform	t_s = 5 X 10^{-4} s T_s = 40s	- The model validated commercial FLUENT 4.4 code with the results with the PSRI, Chicago experimental fluidization challenge problem of Fluidization VIII - Granular energy generation and dissipation through interphase momentum exchange not accounted. - Different form of expression for granular energy dissipation through inelastic particle collisions used - The model captured the essential core- annulus structure of the gas solid flow with solids down flow near wall. - Axial pressure drop reasonably well predicted. - Model was simulated to show that initial conditions do not affect the predicted results upon long term averaging.

Reference	Model	Drag coefficient	Turbulence model	Wall BC	Model parameters	Riser system	Particle system	Operating conditions	Grid details	Simulation parameter	Notes
											- Position of inlet/outlet and feed location affected the predicted profiles and flow patterns. - The model captured the general trend of increase in granular temperature at dilute regions (low ε_s) but values were order of magnitude lesser from those quantified experimentally. - Power spectrum analysis of solid density fluctuations helps to identify the minimum time required for obtaining time averaged profiles
Bolio *et al.*, 1995	Type: B 1D fully developed axis symmetric steady KTGF pde form	D3	GPT4 SPT3	GWBC1 SWBC4	ϕ = 0.002 e_w = 0.7, 0.94 e_p = 0.9, 0.94	a)Maeda *et al.* 1980 D = 0.056m b) Lee and Durst 1982 D = 0.0418m c) Tsuij *et al.* 1984 D = 0.0305m	a) Air ρ:GRHO1 μ: GNU1 ρ_p = 2590 kg/m^3 d_p = 45, 136 μm Ar = 2, 6.25 u_{ter} =0.154, 0.87 m/s b) Air ρ:GRHO1 μ: GNU1 ρ_p = 2590 kg/m^3 d_p = 100,200, 400 μm Ar = 4.6,9.19,18.4 u_{ter} =0.56,1.4,3.1 m/s c) Air ρ:GRHO1 μ: GNU1 ρ_p = 1020 kg/m^3 d_p = 200,500 μm Ar = 6.7,16.8 u_{ter} =0.7,2 m/s	a)Mass loading: 0.3 b)Mass loading: 1.25,1.3, 1.55 c)Mass loading: 0.9 – 3.2	r: 60 non uniform	-	- Gravity term neglected for the fluid term - Myong and Kasagi 1990 low Re k-ϵ model used. - Turbulence generation and dissipation in gas phase due to interaction with particles accounted. Turbulent generation due to particles given by Louge *et al.* (1991) and Koch (1990) - Granular energy generation and dissipation due to interaction with turbulent gas phase eddies/interphase momentum exchange is also accounted - Model not sensitive to k - ϵ model coefficients. - Model not sensitive to specularity coefficient. Results change by 10% for order of magnitude change in specularity coefficient. Value adjusted to match experimental slip at wall - Model captured the quantitative increase in slip with in increase in d_p at same operating conditions. - Simplified model without particle phase stress was found not satisfactory in predicting expt results. But for systems with smaller particles, gas phase acts as buffer and particle shear stress can be neglected. - Model predictions are more satisfactory for larger particles. - Model results show that kinetic energy contribution to solid phase viscosity significant. - Modeling gas phase turbulence significantly affects the total pressure drop prediction. Ignoring the turbulent gas phase contribution did not predict the overall expt pressure drop. - Presence of particles dampened the gas velocity fluctuations & flattened the mean gas velocity profiles but model overestimated the experimentally observed results significantly. Probable reason could be that model does not account for turbulent generation due to vortex shedding and wakes behind particles.
Bolio and Sinclair, 1995	Type: B Fully developed 1D axis symmetric steady KTGF pde form	D3	GPT4 SPT3	GWBC1 SWBC4	ϕ = 0.002 e_w = 0.94 e_p = 0.94	a) Tsuij *et al.* 1984 D = 0.0305m	a) Air ρ:GRHO1 μ: GNU1 ρ_p = 1020 kg/m^3 d_p = 200,500 μm Ar = 6.7,16.8 u_{ter} =0.7,2 m/s	a)Mass loading: 0.9 – 3.2	-	-	- Gravity term neglected for fluid phase - Myong and Kasagi 1990 low Re k-ϵ model used. (No requirement of wall functions) - Gas phase turbulent generation and dissipation due to particles accounted. Turbulent generation due to particle wake accounted on lines of Yuan and Michaelides (1992). Improved form for wake volume also given in the work - Granular energy production and dissipation due to exchange with fluid phase accounted - Increase in gas velocity fluctuations/k with larger particles quantitatively predicted. Also for larger particles, increase in mass loading ratio increases gas phase fluctuations/flattens the mean velocity profile - For small particles, gas velocity fluctuations/k first decreases and then begins to increase with loading ratio. However, model did not predict increase in gas velocity fluctuations at higher loading ratios as observed in experiment
Dasgupta *et al.*, 1994[#]	Type: B 1D axis symmetric Fully developed	D7	GPT4 SPT1	GBWC1 SWBC1	N.A.	D = 0.3 m	Air ρ: GRHO2 μ: GNU1 Solid ρ_p = 1500 kg/m^3 d_p = 100 μm	u_g : 5 m/s G_s: 100 kg/m^{2}s	–	-	- [#] The model is written for the suspension velocity without any distinction between $u_s \sim u_p$ and slip velocity ~ 0 and turbulent fluctuations are due to particle motion. Therefore equivalent key words are given for both gas and solid phase headings - Solid phase viscosity pressure are expressed in terms of solid fraction in

Reference	Model	Drag coefficient	Turbulence model	Wall BC	Model parameters	Riser system	Particle system	Operating conditions	Grid details	Simulation parameter	Notes
	steady						Ar = 3.83 u_{ter} = 0.35 m/s				functional form analogous to KTGF expressions without the use of granular energy - Turbulent k and ϵ are written for the suspension scale and k and ϵ due to particle – gas interaction are subsumed in the expressions employed - Effect of radial dispersion of particles (turbulent dispersion) also accounted - Model predicted radial segregation towards wall with 25% increase in holdup towards wall than average value. However model exhibited slight increase in holdup values near centre/axis. Velocity profile were closer to parabolic – Presence of particles alters the near flat velocity profile of homogeneous gas phase - Radial solid dispersion flattens the solid holdup profile esp. at centre and induces more parabolic nature to velocity profile. - Model predictions were not sensitive to turbulent model parameters. Change in k profile did not alter the profile of velocity/holdup.
Nieuwland, 1994	Type: A 2D axis symmetric unsteady KTGF pde form	D2	GPT2 SPT3	GWBC1 SWBC4	ϕ = 0.5 e_w = 0.9 e_p = 1	a) Expt setup D = 0.0536m H = 8m H/D ~ 150 b) Bader et al.,1988 D = 0.304m H=10m H/D ~ 33	a)Air ρ: GRHO2 μ: GNU1 Sand ρ_p = 2540 kg/m^3 d_p = 129 μm Ar = 5.89 u_{ter} = 0.7869 m/s b) Air ρ: GRHO2 μ: GNU1 FCC ρ_p = 1714 kg/m^3 d_p = 76 μm Ar = 3 u_{ter} =0.2579 m/	a)u_g = 10, 14.4 , 15m/s G_s = 300, 350 kg/m^{2}s z = 2.5m b)u_g = 3.7m/s G_s = 98 kg/m^{2}s z = 9m	$\Delta r = 10^{-3}$ m Δz = 1m $\Delta r/d_p$ ~ 8	$t_s = 10^{-5}$ s	- Production and dissipation of granular energy due to interphase exchange neglected - No dissipation of granular energy due to inelastic particle particle collisions - Model evaluated with own experimental data obtained on 0.0536m i.d. riser with optical probes - Model slightly under predicted the experimental radial solid segregation profile. - Parabolic radial profile for the axial solid velocity was inferred from model simulations with solid velocity being under predicted near centre. - Kinetic transport mechanism due to particles was found significant in the absence of gas phase turbulent radial momentum transfer. - Model also simulated for Bader *et al.* (1988). The model qualitatively predicts solids down flow near wall but over estimate in value.
Louge *et al.*, 1991	Type: B 1D axis symmetric fully developed steady KTGF GT2	D1	GPT5 SPT3	GWBC1 SWBC4	e_w = 0.9 e_p = 0.7 $e_{w,fr}$ = 0.2	a) Tsuij *et al.* 1984 D = 0.0305m	a) Air ρ:GRHO1 μ: GNU1 Polystyrene ρ_p = 1020 kg/m^3 d_p = 200 - 500 μm Ar = 6.7 – 16.84 u_{ter} =0.6962 – 2.0406 m/s	a)Mass loading: 1 – 4.2	–	-	- Gravity term neglected for the gas phase - Production and dissipation of turbulent kinetic energy due to particles is accounted - Granular energy production and dissipation due to momentum exchange with gas also accounted - The model predicted the qualitative trend (mean gas velocity and rms gas velocity profiles) for lower mass loadings but at higher loadings the model over predicts the damping of velocity fluctuations at centre - Also at higher loadings the model predicts monotonic increase in velocity fluctuations towards wall. However, experimental data shows minimum in the profile - Pressure drop predictions were within 15% with experimental data. Contribution to pressure drop from hydrostatic head and particle phase stress were ~20% and ~8%. - Model without particle phase stress was found not to predict experimental trend in particle velocity profile.
Pita and Sundaresan, 1991	Type: A 1D fully developed	D3	GPT6 SPT3	GWBC3 SWBC4	ϕ = 0.5 e_w = 0.9 e_p = 1	a)Numerical expts: D= 1m	a) Air ρ:GRHO1 μ: GNU2 ρ_p = 1500 kg/m^3	a)u_g = 3 - 15m/s G_s = 5 -1000	–		- Production and dissipation of granular energy due to interphase exchange/gas turbulent interactions neglected - No dissipation of granular energy due to inelastic particle particle

Reference	Model	Drag coefficient	Turbulence model	Wall BC	Model parameters	Riser system	Particle system	Operating conditions	Grid details	Simulation parameter	Notes
	axis symmetric steady KTGF pde form					b) Bader *et al.* 1988 D = 0.304m H=10.2 H/D ~ 34	b) Air ρ: GRHO1 μ: GNU2 FCC ρ_p = 1714 kg/m^3 d_p = 76 μm Ar = 3 u_{ter} =0.2579 m/	kg/m^{2}s b)u_g = 3.7, 4.6 m/s G_s = 98, 147 kg/m^{2}s			collisions - The model showed existence of multiplicity with Δp/L, u_g and G_s, gas and solids downflow near wall, sharp transition in the recirculation at certain u_g for a given G_s. Multiple steady state were observed over wide u_g range as G_s is lowered - As riser diameter increased, multiple steady state solution were found to occur over wide range of u_g and at higher G_s. Multiple solutions are also obtained for G_s ~ 0 in very small diameter risers. Scale up of risers not straightforward. - Δp/L decreases to a minimum and then begins to increase with change in riser diameter/particle size with possible occurrence of multiple solutions at certain operating conditions. - The model exhibited high sensitivity to particle particle restitution coefficient. A small change in value of e destroys the fit with expt data of Bader *et al.*, 1988. Higher the value of particle particle restitution coefficient higher the solid holdup at walls - Addition of sink term for granular energy due to interphase momentum exchange also changed model results appreciably.
Tsuo and Gidaspow, 1990	Type: B 2D unsteady	D3	GPT6 SPT3	GWBC1 SWBC3	N.A.	a) Luo 1987 D = 0.0762m H=5.5 m H/D ~ 73 b) Bader *et al.* 1988 D = 0.305 m H= 11.2 m H/D ~ 37	a) Air ρ:GRHO1 μ: GNU1 Solid ρ_p = 2620 kg/m^3 d_p = 520 μm Ar = 23.9 u_{ter} = 3.98 m/s b) Air ρ:GRHO1 μ: GNU1 Solids ρ_p = 1714 kg/m^3 d_p = 76 μm Ar = 3 u_{ter} =0.2579 m/s	a)u_g = 5 m/s G_s = 25 kg/m^{2}s b)u_g = 3.7 m/s G_s = 98 kg/m^{2}s	a)Δx = 0.00762 m Δy = 0.0762 m Δx/d_p ~15 Δy/d_p ~ 147 Ar ~ 10 b)Δx = 0.010167 m Δy = 0.305 m Δx/d_p ~134 Δy/d_p ~ 4013 ar ~ 30	a)t_s = 5 X 10^{-4} s T_s = 18s $T_{s,avg}$ = 10 – 15 s b)t_s = 5 X 10^{-4} s T_s = 18s $T_{s,avg}$ = 10 – 15 s	- Solid shear stress at walls specified following Soo (1967). - Solid phase viscosity was taken as a) 0.509 Pas and b) 0.724 Pas - Solid pressure modeled as $p_s = G\nabla\varepsilon_s$ with $G = 10^{-8.76\varepsilon+5.43}$ - Model quantitatively predicted the trends for gas and solid velocity and holdup, formation of clusters, down flow near wall - Model also showed increased cluster formation/solid holdup with increase in G_s, , increase in d_p, decrease in u_g and decrease in pipe diameter - Predictions were compared with experimental data (holdup, gas and solid axial velocity) - A simplified one dimensional axial model was also simulated. This model under-predicted the experimentally measured fully developed solid holdup data of Luo 1987 (~ 44%)
Sinclair and Jackson, 1989	Type: B 1D axis symmetric fully developed steady KTGF pde form	D7	GPT6 SPT3	GWBC3 SWBC4	ϕ = 0.5 e_w = 0.9 e_p = 1	a)Numerical expts: D= 0.03 m	a) Air ρ:GRHO1 μ: GNU2 ρ_p = 2500 kg/m^3 d_p = 150 μm Ar = 6.8 u_{ter} = 0.953 m/s		-	-	- Gravity term neglected for the gas phase - Inelastic particle collisions neglected - Contours plots for constant dp/dz and solid holdup were generated - Existence of multiple steady state predicted – upflow, counter current and down flow regions identified - Solid segregation towards wall was observed in all the flow regimes - Model exhibited sensitivity with respect to particle particle restitution coefficient.

REFERENCES

Agrawal, K., Loezos, P.N., Syamlal, M. and Sundaresan, S. (2001). The role of meso scale structures in rapid gas solid flows. *Journal of Fluid Mechanics*, 445, 151 – 185.

Almuttahar, A. and Taghipour, F. (2008). Computational fluid dynamics of a circulating fluidized bed under various fluidization conditions. *Chemical Engineering Science*, 63, 1696 – 1709.

Arastoopour, H., Pakdel, P., Adewumi, M. (1990). Hydrodynamic analysis of dilute gas solids flow in a vertical pipe. *Powder Technology*, 62, 163 – 170.

Bader, R., Findlay, J. and Knowlton, T.M. (1988). Gas/solids flow patterns in a 30.5cm diameter circulating fluidized bed. In *Circulating Fluidized Bed II*, Eds., P. Basu, and J. Large, Pergamon Press, Oxford, p123 – 137.

Balzer, G., Simonin, O., Boelle, A. and Lavieville, J. (1996). Unifying modelling approach for the numerical prediction of dilute and dense gas solid twophase flow. In *CFB5*, *5th International Conference on Circulating Fluidized Beds*, Beijing, China, 1996.

Benavides, A.G., van Wachem, B. G.M., Nijenhuis, J. and van Ommen, R. J. (2008). Comparison of experimental and simulation results for turbulent gas solid riser flow. In *9th International Conference on Circulating Fluidized Beds*, Eds: Werther, J., Wirth, K.E. and Nowak, W., May 13 – 16, 2008, Hamburg, Germany.

Benyahia, S., Arastoopour, H. and Knowlton, T.M. (2002). Two dimensional transient numerical simulation of solids and gas flow in the riser section of a circulating fluidized bed. *Chemical Engineering Communications*, 189, 510 – 527.

Benyahia, S., Arastoopour, H., Knowlton, T.M. and Massah, H. (2000). Simulation of particles and gas flow behaviour in the riser section of a circulating fluidized bed using the kinetic theory approach for the particulate phase. *Powder Technology*, 112, 24 – 33.

Benyahia, S., Syamlal, M. and O'Brien, T.J. (2007). Study of the ability of multiphase continuum models to predict core- annulus flow. *AIChE Journal*, 53, 2549 – 2568.

Bolio and Sinclair (1995). Gas turbulence modulation in the pneumatic conveying of massive particle in vertical tubes. *International Journal of Multiphase Flow*, 21, 985 – 1001.

Bolio, E.J., Yasuna, J.A. and Sinclair, J.L. (1995). Dilute turbulent gas-solid flow in riser with particle-particle interactions. *AIChE Journal*, 41, 1375 – 1388.

Cao, J. and Ahmadi, G. (1995). Gas particle two-phase turbulent flow in vertical duct. *International Journal of Multiphase Flow*, 21, 1203 – 1228.

Crowe, C.T. and Gillandt, I. (1998). Turbulence modulation of fluid particle flows – A basic approach. In *Third International Conference on Multiphase Flows, ICMF' 98*, Lyon, France.

Dasgupta, S., Jackson, R. and Sundaresan, S. (1994). Turbulent gas particle flow in vertical risers. *AIChE Journal*, 40, 215 - 228.

Dasgupta, S., Jackson, R. and Sundaresan, S.(1994). Turbulent gas particle flow in vertical risers. *AIChE Journal*, 40**,** 215 - 228.

Ergun, S. (1952). Fluid flow through packed columns. *Chemical Engineering Progress*, 48, 89 – 91.

Foerster, S.F., Louge, M. Y., Chang, H. and Allia, K. (1994). Measurements of the collision properties of small spheres. *Physics of Fluids*, 6, 1108 – 1115.

Hrenya, C.M. and Sinclair, J.L. (1997). Effects of particle phase turbulence in gas solid flows. *AIChE Journal*, 43, 853 – 869.

Jones, N. E. (2001). An experimental investigation of particle size distribution effect in dilute phase gas solid flow. *PhD Dissertation*, Purdue University.

Kenning, V.M. and Crowe, C. T. (1997). Effect of particle on carrier phase turbulence in gas particle flows. *International Journal of Multiphase Flow*, 23, 403 – 408.

Koch, D.L. (1990). Kinetic theory for a mono disperse gas solid suspension. *Physics of Fluids A*, 2, 1711 – 1723.

Koch, D.L. and Sangani, A.S. (1999). Particle pressure and marginal stability limits for a homogeneous mono disperse gas fluidized beds: Kinetic theory and numerical simulations. *Journal of Fluid Mechanics*, 400, 229 – 263.

Lee, S. and Durst, F. (1982). On the motion of particles in turbulent duct flows. *International Journal of Multiphase Flow*, 8, 125.

Louge, M.Y., Mastorakos, E. and Jenkins, J.K. (1991). The role of particle collisions in pneumatic transport. *Journal of Fluid Mechanics*, 231, 345 – 359.

Luo, K.M. (1987). Dilute, Dense phase and maximum solid gas transport. *PhD Dissertation*, Illinois Institute of Technology, Chicago.

Maeda, M., Hishida, K. and Furutani, T. (1980). Optical measurements of local gas and particle velocities in an upward flowing dilute gas solid suspensions. *Polyphase Flow and Transport Technology Century 2- ETC*, 211.

Myong, H. and Kasagi, N. (1990). A new approach to the improvement of k - ε turbulence model for wall bounded shear flows. *Japanese Society of Mechanical Engineers International Journal Series II*, 33, 63.

Neri, A. and Gidaspow, D. (2000). Riser hydrodynamics: Simulation using kinetic theory. *AIChE Journal*, 46, 52 – 67.

Nieuwland J.J. (1994). Hydrodynamic modelling of gas – solid two phase flows. *PhD Dissertation*, Twente University, Enschede, The Netherlands.

Peirano, E. and Leckner, B. (1998). Fundamentals of turbulent gas solid flows applied to circulating fluidized bed combustion. *Progress in Energy and Combustion Science*, 24, 259 – 296.

Pita, J.A. and Sundaresan, S. (1991). Gas – solid flow in vertical tubes. *AIChE Journal*, 37, 1009 – 1018.

Richardson, J. and Zaki, W. (1954). Sedimentation and Fluidization: Part I. *Transactions of Institution of Chemical Engineers*, 32, 35.

Sinclair, J.L. and Jackson, R. (1989). Gas – particle flow in a vertical pipe with particle – particle interactions. *AIChE Journal*, 35, 1473 – 1486.

Soo, S. L. (1967). *Fluid dynamics of multiphase systems*. Blaisdell publishing company, Waltham MA.

Tsuji, Y., Morikawa, Y. and Shiomi, H. (1984). LDV measurements of air solid two phase flow in a vertical pipe. *Journal of Fluid Mechanics*, 417.

Tsuo, Y.P. and Gidaspow, D. (1990). Computation of flow patterns in circulating fluidized beds. *AIChE Journal*, 36, 885 – 896.

Vaishali, S., Roy, S., Bhusarapu, S., Al-Dahhan, M. H. and Dudukovic, M. P. (2007). Numerical simulation of gas solid dynamics in a circulating fluidized bed riser with Geldart group B particles. *Industrial Engineering and Chemistry Research*, 46, 8620 – 8628.

Wen, C.Y. and Yu, Y.H. (1966). Mechanics of fluidization. *Chemical Engineering Progress Symposium Series*, 66, 100 – 111.

Yuan, Z. and Michaelides, E. (1992). Turbulence modulation in particulate flows – A theoretical approach. *International Journal of Multiphase Flow*, 18, 779 – 785.

Zhang, Y. and Reese, J. M. (2003). Continuum modelling of granular particle flow with inelastic inter – particle collisions. *Chemical Engineering Research and Design*, 81, 483 – 488.

Zhang, Y. and Reese, J.M. (2001). Particle-gas turbulence interactions in a kinetic theory approach to granular flows. *International Journal of Multiphase Flow*, 27, 1945 – 1964.

APPENDIX II: USER DEFINED FUNCTION (UDF) FOR PERIODIC RISER FLOW SIMULATIONS

UDF1

```
#include "udf.h"

#define OUT_ID        4        /*  ID FOR THE OUTLET BOUNDARY - FROM FLUENT BOUNDARY CONDITION MENU */

#define IN_ID 5                /* ID FOR THE INLET BOUNDARY - FROM FLUENT BOUNDARY CONDITION MENU */

#define UG 10                  /* Specify the superficial gas velocity  */

#define GS 300                 /* Specify the solid circulation flux */

#define RHO 1.225              /* Density of gas */

#define GRID_WIDTH 6       /* No of (z cells - 1 ) along the axis  */

/* UDF TO CALCULATE CORRECTION FACTOR FOR SOLID AND GAS AXIAL VELOCITY BASED ON OUTFLOW VALUES AND ASSIGN THE VALUES AT OUTFLOW TO UDM's */
/* THE UDF IS FOR A 3D GEOMETRY WITH VELOCITY SPECIFIED IN CARTESEAN CO-ORDINATE SYSTEM OF X,Y AND Z. */

DEFINE_ADJUST(PERIODIC_MAIN,mixture_domain)
{


        Thread *mixture_thread1;
        Thread *mixture_thread2;
        Thread **pt_out;
        Thread **pt_in;

        face_t face_in;
        face_t face_out;

        cell_t cell_in;
        cell_t cell_out;

        real A_out[ND_ND];
        real total_area_out = 0;
        real solid_flux_out = 0;
        real mass_flow_rate_solid_out = 0;
        real flow_rate_solid_out = 0;
        real avg_velo_solid_out = 0;
        real gas_flux_out = 0;
```

```
        real mass_flow_rate_gas_out = 0;
        real flow_rate_gas_out = 0;
        real avg_velo_gas_out = 0;
        real correction_factor_solid_out =0;
        real correction_factor_gas_out =0;

        mixture_thread1 = Lookup_Thread(mixture_domain,OUT_ID);
        mixture_thread2 = Lookup_Thread(mixture_domain,IN_ID);

/* DETERMINATION OF CORRECTION FACTOR FOR AXIAL VELOCITY
BASED ON SOLID FLUX AND GAS FLUX CONTUINITY AT
OUtmass_flow_rate_gasTLET BOUNDARY */

        begin_f_loop(face_out,mixture_thread1)
        {

                pt_out = THREAD_SUB_THREADS(mixture_thread1);
                cell_out = F_C0(face_out,mixture_thread1);
                F_AREA(A_out,face_out,mixture_thread1);

                mass_flow_rate_solid_out = mass_flow_rate_solid_out + (
                                        F_VOF(face_out,pt_out[1]) *
                                        F_W(face_out,pt_out[1]) *
                                        F_R(face_out,pt_out[1]) *
                                        A_out[2] );

                mass_flow_rate_gas_out = mass_flow_rate_gas_out +  (
                                        F_VOF(face_out,pt_out[0]) *
                                        F_W(face_out,pt_out[0]) *
                                        F_R(face_out,pt_out[0]) *
                                        A_out[2] );

                flow_rate_solid_out = flow_rate_solid_out + (
                                        F_VOF(face_out,pt_out[1]) *
                                        F_W(face_out,pt_out[1]) *
                                        A_out[2] );

                flow_rate_gas_out = flow_rate_gas_out +  (
                                        F_VOF(face_out,pt_out[0]) *
                                        F_W(face_out,pt_out[0]) * A_out[2] );

                total_area_out = total_area_out + A_out[2];

        }
        end_f_loop(face1,mixture_thread1)


        solid_flux_out = mass_flow_rate_solid_out/total_area_out;

        avg_velo_solid_out = flow_rate_solid_out/total_area_out;
```

```
        correction_factor_solid_out = GS/solid_flux_out;

        gas_flux_out = mass_flow_rate_gas_out/total_area_out;

        avg_velo_gas_out = flow_rate_gas_out/total_area_out;

        correction_factor_gas_out = (UG*RHO)/gas_flux_out;

/* TO STORE OUTLET QUANTITIES TO UDM AT CORRESPONDING FACES
LOCATIONS */

        begin_f_loop(face_out,mixture_thread1)
        {
                pt_out = THREAD_SUB_THREADS(mixture_thread1);
                cell_out = F_C0(face_out,mixture_thread1);
                begin_f_loop(face_in,mixture_thread2)
                {
                        pt_in = THREAD_SUB_THREADS(mixture_thread2);
                        cell_in = F_C0(face_in,mixture_thread2);
                        if ( ((cell_in - cell_out) == GRID_WIDTH) &&  (cell_out <
cell_in) )

/* CELL  NUMBERS AT THE INLET AND OUTLET DIFFER BY VALUE OF
GRID WIDTH */
/* CORRECTION FACTOR GIVEN  TO ADJUST AXIAL VELOCITY OF SOLID
AND GAS TO  MATCH THE CONTINUITY AT INLET (SPECIFIED Gs AND ug)
*/
                        {

        F_UDMI(face_in,pt_in[1],0) = F_VOF(face_out,pt_out[1]);
        F_UDMI(face_in,pt_in[0],1) = F_U(face_out,pt_out[0]);
        F_UDMI(face_in,pt_in[0],2) = F_V(face_out,pt_out[0]);

        F_UDMI(face_in,pt_in[0],3) = correction_factor_gas_out *
                                     F_W(face_out,pt_out[0]);

        F_UDMI(face_in,pt_in[1],4) = F_U(face_out,pt_out[1]);
        F_UDMI(face_in,pt_in[1],5) = F_V(face_out,pt_out[1]);
        F_UDMI(face_in,pt_in[1],6) = correction_factor_solid_out *
                                     F_W(face_out,pt_out[1]);

        F_UDMI(face_in,mixture_thread2,7) = F_K(face_out,mixture_thread1);
        F_UDMI(face_in,mixture_thread2,8) = F_D(face_out,mixture_thread1);
        F_UDMI(face_in,pt_in[1],9) = F_GT(face_out,pt_out[1]);
                        }

                }
                end_f_loop(face_in,mixture_thread2)
        }
```

```
        end_f_loop(face_out,mixture_thread1)

}
```

UDF2

```
#include "udf.h"

/* THIS UDF FILE INCLUDES SET OF 10 DEFINE PROFILE UDF MACROS TO
ASSIGN THE UDM VARIABLES TO FACE CENTRED QUANTITIES */

DEFINE_PROFILE(volf_solid,thread,i)
{

        face_t face_in;
        begin_f_loop(face_in,thread)
        {
                F_PROFILE(face_in,thread,i) = F_UDMI(face_in,thread,0);
        }
        end_f_loop(face_in,thread)

}

DEFINE_PROFILE(x_velocity_gas,thread,i)
{
        face_t face_in;
        begin_f_loop(face_in,thread)
        {

                F_PROFILE(face_in,thread,i) = F_UDMI(face_in,thread,1);

        }
        end_f_loop(face_in,thread)

}

DEFINE_PROFILE(y_velocity_gas,thread,i)
{
        face_t face_in;
        begin_f_loop(face_in,thread)
        {
                F_PROFILE(face_in,thread,i) = F_UDMI(face_in,thread,2);
        }
        end_f_loop(face_in,thread)
}


DEFINE_PROFILE(z_velocity_gas,thread,i)
{
        face_t face_in;
```

```
	begin_f_loop(face_in,thread)
	{
		F_PROFILE(face_in,thread,i) = F_UDMI(face_in,thread,3);
	}
	end_f_loop(face_in,thread)
}

DEFINE_PROFILE(x_velocity_solid,thread,i)
{
	face_t face_in;
	begin_f_loop(face_in,thread)
	{
		F_PROFILE(face_in,thread,i) = F_UDMI(face_in,thread,4);
	}
	end_f_loop(face_in,thread)
}


DEFINE_PROFILE(y_velocity_solid,thread,i)
{
	face_t face_in;
	begin_f_loop(face_in,thread)
	{
		F_PROFILE(face_in,thread,i) = F_UDMI(face_in,thread,5);
	}
	end_f_loop(face_in,thread)

}

DEFINE_PROFILE(z_velocity_solid,thread,i)
{
	face_t face_in;
	begin_f_loop(face_in,thread)
	{
		F_PROFILE(face_in,thread,i) = F_UDMI(face_in,thread,6);
	}
	end_f_loop(face_in,thread)

}

DEFINE_PROFILE(turb_ke,thread,i)
{
	face_t face_in;
	begin_f_loop(face_in,thread)
	{
		F_PROFILE(face_in,thread,i) = F_UDMI(face_in,thread,7);
	}
	end_f_loop(face_in,thread)

}
```

```
DEFINE_PROFILE(turb_rate,thread,i)
{
	face_t face_in;
	begin_f_loop(face_in,thread)
	{
		F_PROFILE(face_in,thread,i) = F_UDMI(face_in,thread,8);
	}
	end_f_loop(face_in,thread)

}

DEFINE_PROFILE(granular_temp_solid,thread,i)
{
	face_t face_in;
	begin_f_loop(face_in,thread)
	{
		F_PROFILE(face_in,thread,i) = F_UDMI(face_in,thread,9);
	}
	end_f_loop(face_in,thread)
}
```